The Role of Innate Immune Triggers for the Induction of Poxviral Vectored Cytotoxic T Cell Responses

Inaugural-Dissertation

zur Erlangung des Doktorgrades
der Mathematisch-Naturwissenschaftlichen Fakultät
der Heinrich-Heine-Universität Düsseldorf

vorgelegt von

Cornelia Isabella Barnowski
aus Bergheim

Düsseldorf, Januar 2022

aus dem Institut für Virologie
der Heinrich-Heine-Universität Düsseldorf

Gedruckt mit der Genehmigung der
Mathematisch-Naturwissenschaftlichen Fakultät der
Heinrich-Heine-Universität Düsseldorf

Berichterstatter:

1. Prof. Dr. Ingo Drexler

2. Prof. Dr. Henrike Heise

Tag der mündlichen Prüfung: 20.05.2022

Table of Contents

1. SUMMARY

Modified vaccinia virus Ankara (MVA) is currently being investigated as a promising vaccine vector, due to its high safety profile and its ability to induce efficient $CD8^+$ T cell responses. Since MVA infection is accompanied by massive apoptosis, the time available for efficient stimulation of $CD8^+$ T cells by directly infected dendritic cells (DCs) is limited, and cross-presentation of antigens by uninfected DCs gains more and more relevance over the course of infection. However, the innate immune trigger leading to the functional activation of cross-presenting DCs during MVA infection remains elusive. Apart from investigation of the underlying mechanisms of cross-presentation in presenter cells, little attention has been paid to the role of feeder cell signaling in the licensing of cross-presenting DCs in general, and in particular during infection with MVA. It is clear that detailed knowledge of the mechanisms that stimulate DCs to induce efficient $CD8^+$ T cell responses would contribute to the development of MVA-based vaccines. Thus, this study aims to investigate the particular innate immune signaling pathways in MVA-infected feeder cells that trigger the activation of cross-presentation by DCs for the stimulation of poxvirus-specific $CD8^+$ T cell responses.

Using Cytarabine (AraC) to study MVA replication, I observed that cross-presentation of early expressed antigens by bone marrow derived dendritic cells (BMDCs) is abolished following AraC treatment, despite intact protein synthesis in the MVA-infected and AraC-treated feeder cells. By analyzing the transcriptome of these feeder cells, as well as of BMDCs derived from feeder cell-BMDC-cocultures, I was able to obtain candidate target genes that might be involved in the activation of BMDCs for antigen cross-presentation. After silencing several target genes in feeder cells using the gene-editing technology CRISPR/Cas9, these genetically modified cells were characterized for their ability to functionally activate cross-presentation competent BMDCs. I also studied the relevance of stimulator of interferon genes (STING) in the feeder as well as presenter cell to stimulate antigen cross-presentation, because of the crucial role of the cGAS-STING pathway in the detection of MVA (1).

Here, I demonstrate that STING signaling during infection with MVA was not only of remarkable importance in the directly infected BMDC for the induction of type I interferons (I IFNs) and subsequent BMDC maturation but also relevant in the cross-presenting BMDC. However, STING has rather a supportive role for the stimulation of antigen cross-presentation in cross-presentation competent BMDCs. Despite the

essential role of STING in the induction of I IFNs in directly infected and cross-presenting BMDCs, my findings suggest that feeder cell signaling might also be critical for the activation of antigen cross-presentation. Surprisingly, I observed a striking resemblance between AraC-treated feeder cells, and those deficient in toll-like receptor adaptor molecule 2 (TRIF)-, purinergic receptor P2X, ligand-gated ion channel 7 (P2RX7) or apoptosis-associated speck-like protein containing a CARD (ASC), in that all were unable to stimulate cross-presentation by BMDCs during infection with MVA. My data further support the idea that P2RX7- or ASC-deficient, as well as AraC-treated feeder cells, fail to activate a shared pattern recognition receptor (PRR) or innate immune signaling pathway, resulting in the inability to attract phagocytes. As a result, these feeder cells are unable to properly activate cross-presentation by BMDCs, and neither are the poxviral $CD8^+$ T cell responses stimulated. Due to the importance of signaling by TRIF, P2RX7 and ASC in the ability of feeder cells to activate cross-presentation competent BMDCs during MVA infection, the inflammasome is most likely to be involved in this process. Since I was able to show that the feeder cell phenotype is clearly of importance for the functional activation of cross-presentation competent BMDCs, a more detailed analysis is required to fully understand the exact mechanisms of feeder cell signaling during MVA-infection. Most importantly, this research should contribute to a better understanding of poxvirus-vectored $CD8^+$ T cell responses. Furthermore, this study hopes to highlight the importance of feeder cell signaling for the efficient induction of antigen cross-presentation by DCs during viral infections and extend our knowledge beyond the well-known role of DCs.

2. INTRODUCTION

2.1. Modified Vaccinia Virus Ankara

The greatest achievement of mankind in the field of vaccination is arguably the worldwide eradication of smallpox, a lethal disease caused by variola virus. Following the success of the development of an effective vaccine and a strict eradication program, the World Health Organization (WHO) declared the world to be smallpox free in 1980. Both the replication-competent vaccinia virus strain as well as MVA were used as vaccines. Vaccinia virus infection caused only mild symptoms but induced cross-protective immunity against variola virus (2).

Although there are several theories, the origin of vaccinia virus remains unknown (3). MVA originated from the vaccinia virus strain Ankara, which was named Chorioallantois vaccinia virus Ankara (CVA) after cultivation on the chorioallantois membranes (CAM) of embryonated chicken eggs by Herrlich and Mayr at the Institute for Infectious Diseases and Tropical Medicine at the University of Munich (LMU) in 1953.

2.1.1. Immune Evasion

MVA represents a highly attenuated virus obtained after 516 serial passages of CVA in chicken fibroblast tissue culture. During the attenuation process, MVA lost approximately 15 % of the parental genome, resulting in 6 major deletions and mutations in many immunomodulatory genes (4-6). The genome of MVA comprises approximately 200 open reading frames (ORFs) that encode proteins and can be divided into early, intermediate and late genes based on the time of their transcription. In most cases, early genes code for enzymes and factors crucial for DNA replication. In contrast, intermediate genes encode transcription factors and modulators of host defense, but also factors important for late gene transcription. Late genes and their products comprise early transcription factors as well as major membrane and core components of the virus particle (7).

Immunomodulatory genes, classified as virostealth proteins, viromimetics and virotransducers, target the cellular host defense and enable viral replication (8). Virostealth proteins mask viral infection to counteract the clearance of infected cells by the cellular immune response. Viromimetics are divided into virokines and viroceptors and mimic host cytokines or receptors. Virokines are normally secreted and mimic host

molecules like cytokines, complement regulators or their inhibitors. Viroceptors can be either secreted or attached to the cell surface and block cellular signaling by competing for ligands that would normally bind to the corresponding cellular receptor and activate antiviral immunity (9). Virotransducers are encoded by host range genes and function intracellularly to block innate immune pathways that mediate host range. Virotransducers interfere with the sensing of pathogens, signal transduction, cell cycle or the progression to apoptosis and therefore determine whether the virus is able to infect and replicate in a variety of mammalian species. For example, the variola virus has a narrow host range due to the restricted replication in humans, whereas the vaccinia virus can replicate naturally in almost all mammalian species. Although most of the host range and immunomodulatory genes are mutated in the MVA genome, some genes remained unaltered (4, 5). MVA is still able to synthesize some intact viroceptors, including receptors for IL-1β and IL-18. For this reason, IL-1β can only be detected in cultures of primary murine myeloid dendritic cells infected with MVA IL-1βR deletion mutants, which are not able to capture produced IL-1β (5, 10). Hence, these proteins function to abrogate the host's innate immune response by inhibiting the production of interferons (IFNs), chemokines and proinflammatory cytokines. Falivene and colleagues demonstrated that deletion of the viral IL-18 receptor from MVA resulted in enhanced $CD8^+$ and $CD4^+$ T-cell responses (11). Additional immunomodulatory genes that remain intact in the MVA genome are for example C7, K3, E3, F1 and B18. In vaccinia virus, C7 is known to control virus replication by regulating viral gene expression in mammalian cells (12-14). However, the deletion of C7 in vaccinia virus does not impair virus replication, suggesting that other or additional viral factors are involved, which remain as yet undiscovered (15-17). Interestingly, the deletion of C7 in MVA results in a block of viral late gene expression in cells of human or murine origin (15). K3 and E3 are well known to inhibit IFN signaling in the host cell (18, 19). K3 is the viral homologue of eukaryotic initiation factor 2 alpha (eIF2α), which is phosphorylated by protein kinase double-stranded RNA-dependent (PKR) in response to double-stranded RNA (dsRNA) or IFN to control the translational activity (20). E3 prevents phosphorylation of eIF2α by sequestering dsRNA and therefore inhibits activation of PKR. Moreover, E3 has been reported to impair the induction of type I interferons (I IFNs) by blocking the phosphorylation of the transcription factors IRF-3 as well as IRF-7 (21, 22). In addition to the abolished production of I IFNs, E3 is able to inhibit apoptosis and is therefore essential for intact late protein synthesis by

MVA in CEF cells (23). F1L encodes an anti-apoptotic protein that inhibits apoptosis by blocking the activation of Bax, Bak or Noxa as well as cytochrome c release (24, 25). Therefore, the deletion of F1L from the MVA genome results in increased apoptosis in HeLa cells and mouse embryonic fibroblasts (26). The 68 kDa ankyrin-like protein, the vaccinia virus homolog of the B18R gene, is important for the efficient transcription of intermediate and late genes as well as late protein synthesis in human and murine cells (27). In general, ankyrin repeat motifs containing poxviral regulatory proteins prevent the activation of NF-κB signaling but are also involved in cellular transcription, cell cycle control and cellular differentiation (28, 29).
However, the existence of an ORF does not necessarily mean that the encoded protein is functional, as there may be mutations in the amino acid sequence (30). For instance, the B8R gene of MVA is fragmented and therefore encodes a truncated, soluble and consequently non-functional viroceptor, mimicking a cellular IFN-γ receptor (4). Other fragmented immunomodulatory genes in MVA are for example the IFN-α/β receptor B19 and the TNF receptor crmB (4). Hence, MVA infection is able to trigger the activation of different transcription factors, including IRF3/7 and NF-κB, which results in the transcription of different chemokines and cytokines (31). Compared to MVA, vaccinia virus is able to inhibit host intracellular signaling via various immune evasion strategies, resulting in an abolished chemokine and cytokine response (31).

2.1.2. MVA as Vaccine and Vaccine Vector

The attenuation of MVA resulted in the abrogation of most immune evasion mechanisms and rendered the virus replication-deficient in most cells of mammalian origin (16, 32, 33). In contrast to other DNA viruses, MVA replicates exclusively in the cytoplasm. Consequently, the risk of insertion of viral genetic sequences into cellular genomic DNA is small (6). In addition to intact expression of early, intermediate and late genes, MVA features a large capacity for packaging heterologous DNA, and the expression of inserted recombinant genes is strictly virus-specifically controlled (34). As well as the high safety profile of MVA, another advantage of the use of MVA as a vaccine vector is the ease by which recombinant MVA (recMVA) and vaccine can be produced under biosafety level 1 conditions (35). Consequently, MVA is considered to be a potent vector for vaccines against different infectious diseases as well as cancer (36-38). Several prophylactic as well as therapeutic recMVA vaccines have been already tested in clinical trials, among them vaccines against HIV, malaria, cervical

cancer and melanoma (35, 39). The presence of a limited number of immunomodulatory genes probably has the advantage of an enhanced induction of innate and adaptive immunity following infection with MVA. However, the influence of these viral regulators on the immunogenicity of MVA as a vaccine remains unclear and further deletion of immune evasion genes may also result in impaired viral replication and gene expression (40).

2.1.3. I IFN during MVA infection

In contrast to vaccinia virus, MVA lacks most immunomodulatory genes and is well-known to induce a robust I IFN response (1, 41, 42). Since the discovery of I IFNs in 1957, there has been a great deal of interest in their role in the induction of innate immune responses and their antiviral function (43, 44). I IFNs represent a large family of seven members, including various IFN-α subtypes. Surprisingly, all I IFNs bind to the ubiquitously expressed interferon-α/β receptor (IFNAR), which is composed of both IFNAR1 and IFNAR2 (45). The binding of I IFNs to IFNAR results in the expression of approximately 300 interferon-stimulated genes (ISGs). These ISG-induced proteins are mainly pattern recognition receptors (PRRs) and proteins with direct antiviral activity, inclucing RNase L and protein kinase R (PKR) (44, 45).

During infection with MVA the induced I IFN response is dependent on stimulator of interferon genes (STING), due to the cytoplasmic replication of this virus (1). Despite the importance of the cGAS-STING signaling pathway for the intrinsic induction of I IFNs, STING can also be activated in an extrinsic manner by the intercellular transfer of cGAMP (46). Furthermore, STING signaling is crucial for the functional activation of cross-presentation competent $CD103^+/CD8^+$ DCs involved in the induction of antitumor immunity following intratumoral injection of heat- or UV-inactivated MVA (47). In addition to the extracellular transfer of cGAMP to neighboring cells, tumor DNA can be taken up by conventional DCs (cDCs) and activate STING-IRF3 signaling following the cytosolic sensing of DNA (48). In line with the crucial role of cross-presenting DCs in stimulating efficient $CD8^+$ T cell responses, bystander DCs are of relevance during infection with MVA. On the one hand, these non-infected bystander cells show a progressed maturation phenotype, characterized by the elevated expression of major histocompatibility complex (MHC) I/II and costimulatory molecules. On the other hand, these bystander cells are more efficient than infected DCs in activating cytotoxic $CD8^+$

T cells for the expression of the cytokine IFN-γ, which is vital for cytotoxic T cell functions (49, 50).

2.1.4. Cytotoxic T cell responses during infection with MVA

Because MVA is not dependent on a specific cellular receptor for binding and entry during infection, it is able to infect any target cell. However, APCs such as macrophages and DCs are preferentially infected by MVA (51, 52). For this reason, infected APCs induce potent $CD4^+$ and $CD8^+$ T cells as well as humoral responses, by presenting antigens via MHC-II and -I. Moreover, MVA does not impair antigen processing and presentation pathways and therefore induces strong adaptive immune responses (35). Furthermore, intact viral replication (albeit without the generation of viral progeny) results in more potent immune responses compared to the use of antigen-adjuvant combinations. However, the $CD8^+$ T cell responses induced by MVA as well as by vaccinia virus are dominated by $CD8^+$ T cells specific for early expressed antigens because late antigens remain trapped inside viral factories, which are the compartments where viral DNA replication takes place. This viral immune evasion strategy prevents the efficient processing and presentation of late antigens by direct- as well as cross-presenting DCs (53, 54). This drawback of late expressed antigens can be overcome by using strong viral early/late promoters for the expression of recombinant antigens (55).

For the induction of an efficient $CD8^+$ T cell response, both direct and cross-presentation of antigens are important during MVA infection (56-59). Since MVA infection is accompanied by massive apoptosis, the time available for the efficient stimulation of $CD8^+$ T cell responses by directly infected DCs is limited and cross-presentation of antigens by non-infected DCs gains more and more relevance during the course of infection. During the classical MHC-I presentation pathway, primary $CD8^+$ T cell responses are stimulated following the processing, loading and presentation of endogenous antigens on MHC-I molecules. In contrast, for antigen cross-presentation, primary $CD8^+$ T cells are activated by specialized DCs that present internalized and processed exogenous antigens loaded on MHC-I molecules (60). In general, the efficient induction of $CD8^+$ T cell responses requires three signals. The first signal is based on the recognition of peptides loaded on MHC-I molecules by the T cell receptor (TCR) (61). However, the interaction between TCR and peptide/MHC-I molecules alone is unable to initiate $CD8^+$ T cell responses. Therefore, two additional signals are

required: costimulatory molecules (e. g. CD40, CD80 and CD86) and cytokines (62, 63). *In vivo* the activation of $CD8^+$ T cell responses is more complex and requires a particular environment and interaction of T cells, cytokines and different DC subsets. Indeed, the recognition of antigens by antigen-experienced $CD8^+$ T cells results in the secretion of CCL3 and CCL4 to attract other immune cells. In particular, $CCR5^+$ plasmacytoid dendritic cells (pDCs) are attracted by CCL3 as well as CCL4, and start to produce high amounts of I IFNs. In addition to CCL3 and CCL4, activated $CD8^+$ T cells produce XCL1, attracting cross-presentation competent $XCR1^+$ cDCs. The I IFN produced in this environment boosts the already active antigen cross-presentation by activated $XCR1^+$ cDCs (64, 65).

2.2. Antigen Cross-Presentation

Cross-presentation was first described in 1976 by Bevan and colleagues, who broke the well-established paradigm that exogenous antigens are exclusively presented to $CD4^+$ T cells on MHC-II molecules (66). In contrast to the classical MHC-I presentation, which is performed by all nucleated cells, only professional antigen-presenting cells like DCs are able to cross-present antigens to $CD8^+$ T cells.

2.2.1. Classical MHC-I Presentation Pathway

The classical MHC-I presentation pathway involves the translocation, folding and loading of MHC-I molecules with peptide in the endoplasmic reticulum (ER). The association of MHC-I/peptide-complexes requires the cotranslational translocation of the MHC-I heavy chain polypeptide into the ER lumen by the Sec61 complex. The initial folding of the polypeptide chain is performed by the chaperons calnexin and immunoglobulin binding protein (BiP) and results in the assembly with β_2-microglobulin (β_2m). The resulting heterodimer is stabilized by the binding of low-affinity peptides but remains highly unstable until association with peptide-loading complex (PLC), which facilitates binding of high-affinity peptides. PLC, in turn, consists of the transporter associated with antigen processing (TAP) complex, ERp57, calreticulin and tapasin. Tapasin directly interacts with empty MHC-I molecules, and calreticulin and ERp57 help to stabilize the newly folded MHC-I molecule. TAP translocates peptides derived from cellular or viral proteins for MHC-I loading from the cytosol into the ER. However, these imported peptides require further cleavage by the ER-resident aminopeptidases ERAP1 and ERAP2 due to their length, which is suboptimal for efficient binding in the

peptide-binding groove of the MHC-I molecule. Empty and suboptimally loaded heavy-chain/β_2m dimers with low- or high-affinity peptides accumulate at ER exit sites and traffic via coat protein complex II (COPII)-coated vesicles to the ER-Golgi intermediate compartment (ERGIC) for quality control. Empty MHC-I molecules, or those loaded with low-affinity peptides, are recognized and prevented from moving to the plasma membrane. Instead, these suboptimal MHC-I molecules accumulate in the ERGIC and are recycled by completing another cycle of peptide binding in the PLC. After quality control in the ERGIC, MHC-I molecules loaded with high-affinity peptides move to the plasma membrane to be presented to $CD8^+$ T cells (67).

2.2.2. Cross-Presentation Pathways

Within the heterogeneous group of DCs, splenic BATF-dependent $CD8^+$ $XCR1^+$ $CD24^+$, as well as migratory tissue $CD103^+$ DCs, have the ability to cross-present peptides from engulfed exogenous antigens (68). Antigens can be derived from pathogens (for example viruses or microorganisms) or from dying cells (67). After antigen internalization by micropinocytosis, phagocytosis or endocytosis, processing and loading of peptide from extracellular sources can be accomplished via two different pathways: the vacuolar and the cytosolic antigen-processing pathways.

In the vacuolar pathway, the internalized antigens are degraded by proteases, mainly cathepsin S, in endosomes or phagosomes, and loaded onto MHC-I molecules within these compartments (69). Because endosomes and phagosomes are compartments distinct from the ER, components for the generation of peptide/MHC-I complexes, like PLC, need to be transported from the ER to these compartments by vesicular trafficking. The vacuolar pathway is independent of the cytosolic proteasomal machinery as well as of TAP function, because of protein degradation within the endosomal/phagosomal compartment (70). In contrast, for the degradation of antigens via the cytosolic pathway, proteins need to be translocated from endosomes or phagosomes to the cytoplasm for proteasomal degradation (71, 72). The resulting peptides are then imported back into the endosome/phagosome and further trimmed by insulin-regulated aminopeptidase (IRAP), in a mechanism comparable to the generation of small peptides within the classical MHC-I presentation pathway (73, 74). Both the vacuolar and the cytosolic pathway increase the peptide pool available for the generation of high-affinity peptide/MHC-I molecules. Furthermore, a large repertoire of

peptide/MHC-I molecules contributes to the induction of broad $CD8^+$ T cell responses (67).

2.2.3. Regulation of Cross-Presentation in DCs

Previous research has shown that in addition to DCs and pDCs, macrophages are also able to cross-present antigens (75). However, the efficiency of cross-presentation is greatly reduced in these APCs compared to that in splenic $CD8^+$ or migratory $CD103^+$ DCs (76). Cross-presentation competent DCs need to encounter their antigens in the presence of an innate immune trigger to become activated for cross-presentation (68, 77, 78). To avoid cross-presentation of self-antigens, only cargo present in the same individual phagosome as the activated innate sensor, TLR or IgG receptor shows enhanced cross-presentation (78-80). Cargo in other phagosomes inside the same DC is not efficiently cross-presented (81). In addition to the selective cross-presentation of antigens derived from specific phagosomes, DCs are also able to control cross-presentation efficiency by different mechanisms. One strategy for regulating cross-presentation efficiency is to reduce phagosome acidification to protect the antigens from degradation by lysosomal enzymes, which exhibit low pH optima (82). An important factor for regulating phagosome acidification is the lysosomal transcription factor EB (TFEB), which is expressed more highly in cross-presentation competent DCs than in macrophages (83-85). As well as TFEB, NOX2 is also able to limit antigen degradation due to ROS production, which inhibits lysosomal proteases with low pH optima and reversibly oxidizes cysteine cathepsin proteases (86-89). The reduction in vacuolar acidification rescues antigens from degradation by inhibiting low pH proteases in the lysosome. However, vacuolar proteases like cathepsin S with a pH optimum between 6 and 7.5 are not inhibited (90). Another mechanism for promoting antigen cross-presentation is the enhanced cytosolic translocation of antigens for degradation by the proteasome (91, 92). NOX2 can increase cross-presentation by inducing leakage of antigens from endosomes into the cytosol, through endosomal lipid peroxidation and disruption of the endosomal membranes (93). Another strategy to promote cross-presentation is to enhance the trafficking of MHC-I molecules or other ER proteins from the endocytic recycling compartment (ERC) to phagosomes containing TLR ligands (78, 94).

These mechanisms of controlling the efficiency of cross-presentation seem to be linked to the maturation status of the DCs. Immature DCs sample their environment in

peripheral tissue, mature upon antigen internalization in the presence of innate immune triggers, and migrate to the next lymph node to cross-present the encountered antigen to $CD8^+$ T cells (60, 95, 96). DC maturation can be divided into early, intermediate, and late phases, which affect the cross-presentation efficiency by the licensed DC. In the early phase of maturation, up to 6 h after DC activation, increased cross-presentation is controlled by reduced recruitment of active lysosomal proteases as well as increased recruitment of MHC-I molecules to endosomes to allow them to be efficiently loaded with peptide (78). In the intermediate maturation phase (7 to 20 h after activation), the phagocytic activity of DCs is still high enough to ensure efficient antigen cross-presentation. These maturating DCs control cross-presentation efficiency by reducing the fusion of phagosomes with lysosomes, and therefore ensuring slower antigen degradation (97, 98). Fully maturated DCs (late maturation phase 20-24 h after activation) show an impaired cross-presentation ability, mainly caused by increased acidification of the phagosomal/endosomal compartment controlled by TFEB (82, 83).

Moreover, the nature of the particular antigen also determines whether or not it will be exported to the cytosol and therefore cross-presented (60). Experiments with dextrans of different molecular mass indicate that antigen export to the cytosol is size-selective (99, 100). Moreover, particulate antigens are more efficiently cross-presented than soluble antigens (101). Compared to soluble antigens, particulate antigens require a low pH within the phagosomal/endosomal compartment for efficient export to the cytosol. Most often these antigens form large aggregates, which need to dissociate before they can be exported to the cytosol (60). However, an overly acidic pH may also destroy MHC-I binding epitopes, which might be more sensitive to low pH than MHC-II binding epitopes (60).

Many recent studies suggest that the cross-presentation compartment is not a fixed compartment but is created *de novo* upon encountering extracellular antigens, and is remodeled with regard to the specific interactions between cargo ligands and cellular receptors. Reorganization of this compartment is fast because it is based on transcription-independent phosphorylation, which controls communication between cellular organelles using soluble N-ethylmaleimide-sensitive-factor attachment receptor (SNARE) components such as synaptosomal-associated protein 23 (SNAP23) (67). Remodeling of the cross-presentation compartment is performed via the ERGIC, ERC, and lysosome-related organelle (LRO) vesicular trafficking

pathways, which are defined by their origins, molecular mediators, the underlying signaling pathway and the component which they deliver to the cross-presentation compartment (67).

2.3. Innate immune sensing of viruses

PRRs comprise a large group of membrane-associated and cytosolic sensors activated either by microbial pathogen-associated molecular patterns (PAMPs) or endogenous damage-associated molecular patterns (DAMPs). The activation of these PRRs results in the first defense response against the invading pathogen (Figure 1). For instance, Toll-like receptors (TLRs) belong to the membrane-associated PRRs and are located either at the plasma membrane to detect extracellular PAMPs or in

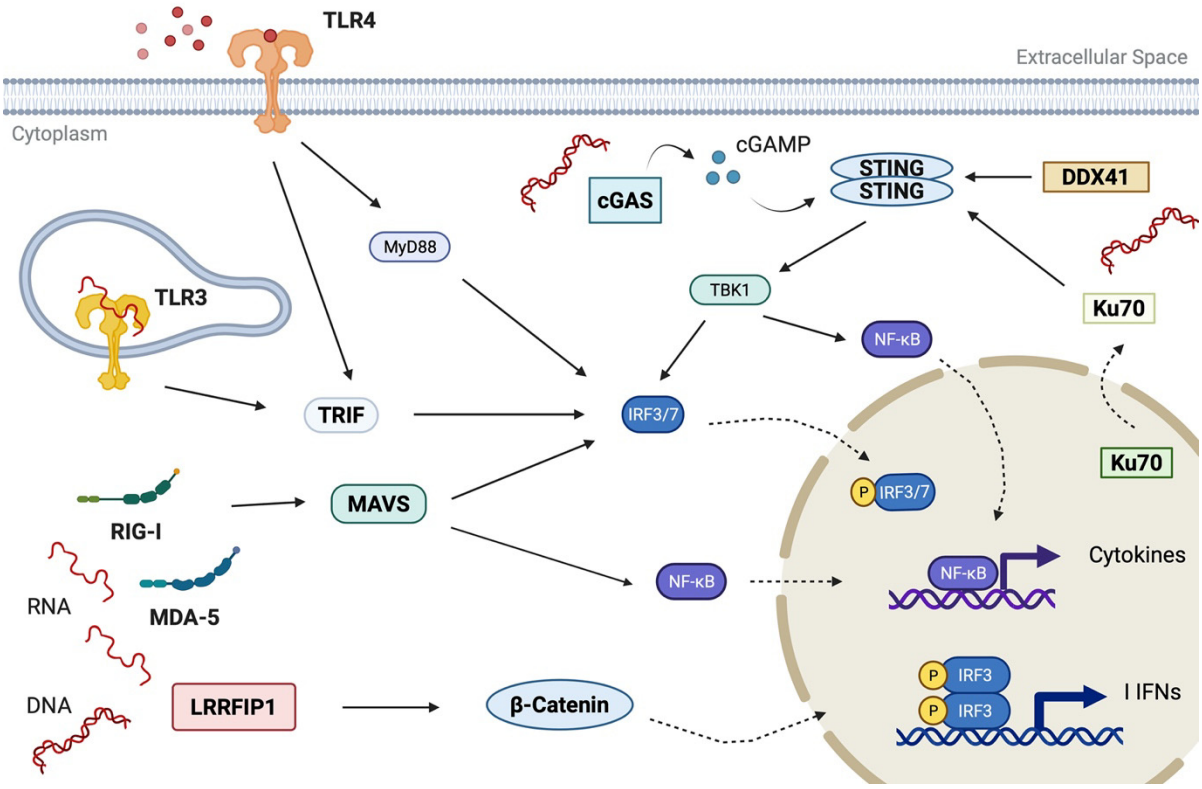

Figure 1: Innate immune sensing pathways. The recognition of PAMPs and DAMPs can be mediated by membrane-associated or cytosolic PRRs. The membrane-associated TLR3 and TLR4 specifically detect endosomal dsRNA and extracellular lipids, respectively. cGAS, DDX41, and Ku70 sense cytosolic DNA, whereas RIG-I and MDA-5 detect cytosolic ssRNA or dsRNA. LRRFIP1 can recognize both DNA and RNA, and signaling is mediated by β-catenin. One group of cytosolic sensors signals via STING, which in turn activates the transcription of I IFNs and proinflammatory cytokines via TBK1. TLR3 and TLR4 are the only TLRs which activate TRIF. However, TLR4 is also able to signal via MYD88. RIG-I and MDA-5 activate both MAVS, which enables IRF3/7 and NF-κB activation. The image was created using BioRender.com.

endosomes for the sensing of intracellular PAMPs. Together, TLRs can detect a wide range of PAMPs derived from protozoa, fungi, bacteria, and viruses. The recognition of various PAMPs can even be extended due to the association of TLRs to heteromers in addition to homomers. All TLRs represent type I transmembrane glycoproteins, consisting of a ligand-binding ectodomain, a single transmembrane helix, and a cytoplasmic Toll/interleukin-1 receptor (TIR) domain. The ligand-binding ectodomain contains 19-25 tandem leucine-rich repeat (LRR) motifs, whereas the TIR domain is required for downstream signaling. With the exception of TLR3 and TLR4, most TLRs use the adaptor protein myeloid differentiation primary response gene 88 (MYD88) for downstream signaling (102). However, TLR3 signaling depends solely on toll-like receptor adaptor molecule 2 (TRIF), and TLR4 uses both adaptor proteins. Most of the endosomal TLRs recognize all nucleic acids, however, TLR3 specifically detects dsRNA (103). In contrast, TLR4 senses LPS as well as viral products and endogenous ligands derived from apoptotic cells, for instance, high mobility group box 1 protein (HMGB1) (104-106).

The sensing of intracellular pathogens is accomplished by various cytosolic PRRs, which can detect diverse PAMPs. In general, cytosolic PRRs can be divided into two groups sensing either cytosolic DNA or RNA.

cGAS represents a crucial sensor for the detection of cytosolic DNA, especially during MVA infection. cGAS mainly binds to dsDNA, particularly to B-form DNA, and catalyzes the synthesis of the second messenger cyclic GMP-AMP (cGAMP) from ATP and GTP (107, 108). The downstream target of cGAMP is STING, which translocates from the ER to an ER-Golgi compartment and the Golgi, following a conformational change induced by cGAMP binding. Once in its active conformation, STING can activate TBK1-IRF3 and NF-κB signaling for the expression of I IFN and inflammatory cytokines including TNF, IL1-β and IL-6. Although dsRNA can also bind to cGAS, it is not able to activate the synthesis of cGAMP by cGAS (109).

In addition to cGAS, several other cytosolic DNA sensors can activate STING. Among these sensors are DEAD-box helicase 41 (DDX41) and IFN-γ-inducible protein 16 (IFI16). One function of helicases is to unwind dsRNA during RNA metabolism, however, some helicases are also relevant to the innate immune sensing of cytosolic RNA or DNA. DDX41 belongs to the family of DEAD-box helicases and recognizes cytosolic DNA via its second helicase domain. After binding to DNA, DDX41 dissociates from TRIM21 and is activated by Bruton’s tyrosine kinase (BTK) (110-112).

Furthermore, DDX41 has been shown to become activated by cyclic di-GMP and cyclic diAMP (113). DDX41 is able to bind directly to DNA and has also been reported to associate with STING (110). The DDX41-STING interaction results in subsequent activation of transcription factors including IRF3 and NF-κB for the expression of I IFNs as well as proinflammatory cytokines, including TNF and IL-6 (112). However, the role of DDX41 in the induction of I IFN remains controversial, and whether DDX41 is also able to function alone or whether it only plays a role upstream of STING is currently unknown. Previous studies tend to suggest a STING-dependent function of DDX41 since IFN-β expression was not abrogated following DNA stimulation or viral infection in the absence of DDX41 (114, 115).

Similarly, X-ray repair complementing defective repair in Chinese hamster cells 6 (Ku70) was shown to have a double function as a protein involved both in the DNA damage response and in cytosolic DNA sensing. Ku70 is part of the heterotrimeric protein complex DNA-dependent protein kinase (DNA-PK), which, additionally to Ku70, is composed of Ku80 and the DNA-dependent protein kinase catalytic subunit (DNA-PKcs). After stimulation with DNA or infection with vaccinia virus, DNA-PK activates the STING-TBK1-IRF3 pathway and leads to cytokine production (116). However, Ku70 is usually localized in the nucleus and needs to translocate to the cytoplasm to interact with STING (117). Furthermore, Ku70 seems to be crucial for the expression of IFN-λ1, which belongs to the type III interferon (III IFN) group and, in contrast to I IFNs, binds to the IFN-λ receptor to activate STAT signaling (118, 119).

Despite the crucial role of the cGAS-STING signaling pathway for the sensing of MVA and subsequent induction of I IFNs, cytosolic RNA detection mediated by retinoic acid inducible gene I (RIG-I) and MDA-5 has also been shown to be of importance during MVA infection (1, 41). Both RIG-I and MDA-5 belong to the RIG-I-like receptor (RLR) family, and are DExD/H box RNA helicases. Both RLRs consist of two caspase activation and recruitment domains (CARDs), a helicase domain and a repressor domain, which keeps the particular sensor under resting conditions in its inactive form (120). After activation by viral RNA, both RLRs change their conformation and form homodimers. The dimerized RLRs activate the adaptor protein mitochondrial antiviral-signaling protein (MAVS) via CARD-CARD interactions, which mediates downstream signaling through IRF3 and NF-κB to induce I IFN expression (121). While RIG-I recognizes cytosolic 5′-triphosphate uncapped ssRNA, MDA-5 identifies its substrate rather by the length of transcribed RNA than by the appearance of the 5’ end (122). In

particular, MDA-5 becomes activated by long dsRNA. Moreover, RIG-I is able to recognize short dsRNA, which is usually not present in the host but may be produced during viral replication (123-125). However, RLRs can also detect DNA viruses using RNA polymerase III (RNA Pol III), which recognizes AT-rich dsDNA and transcribes it into dsRNA containing a 5′-triphosphate motif that is able to activate RIG-I (126, 127). PKR is another cytosolic sensor for the detection of dsRNA and has been shown to be crucial for the sensing of vaccinia virus in the absence of E3L (21). In fact, PKR regulates protein synthesis by phosphorylating eIF2α at serine residue 51, which in turn results in the sequestration of the limiting guanine-nucleotide exchange factor eIF2β (128). As a result, GDP is not recycled and consequently translation is impaired. As well as its role in the regulation of transcription, PKR is able to activate NF-κB and stimulate subsequent cytokine and I IFN production (129). Furthermore, previous studies have suggested that PKR might be activated by TLR signaling, particularly by TLR4 and TLR3 (130).

Instead of recognizing either DNA or RNA as the above described PRRs do, leucine rich repeat (in FLII) interacting protein 1 (LRRFIP1) can sense cytosolic dsRNA, and B and Z form dsDNA. Surprisingly, the recognition of dsRNA is not dependent on RNA Pol III. Compared to other cytosolic RNA or DNA sensors, LRRFIP1 is not located directly upstream of IRF3, NF-kB or mitogen-activated protein (MAP) kinase in the signaling cascade required for I IFN production. In contrast, β-catenin is phosphorylated by LRRFIP1 and translocates into the nucleus, where it can either bind to IRF3 or acetyltransferase p300, leading to IFN-β production (118, 131).

Nucleotide-binding and oligomerization domain (NOD)-like receptors (NLRs) represent another huge and diverse family of cytosolic PRRs. NLRs become activated through the action of various microbial molecules, toxins, and DAMPs such as ATP, potassium efflux, or uric acid crystals. All NLRs exhibit the same structure, and are composed of a leucine-rich repeat domain (LRR), a nucleotide-binding oligomerization domain (NOD or NACHT), and a variable protein-protein interaction domain. This variable protein-protein interaction domain either consists of a caspase recruitment and activation domain (CARD), a pyrin domain (PYD), or a baculovirus inhibitor of apoptosis repeat domain (BIR). Despite the similar structure, NLRs differ not only in their domain structure but also in their function. In cases where the NLR has a PYD domain, it can form a multiprotein complex together with the adaptor protein apoptosis-

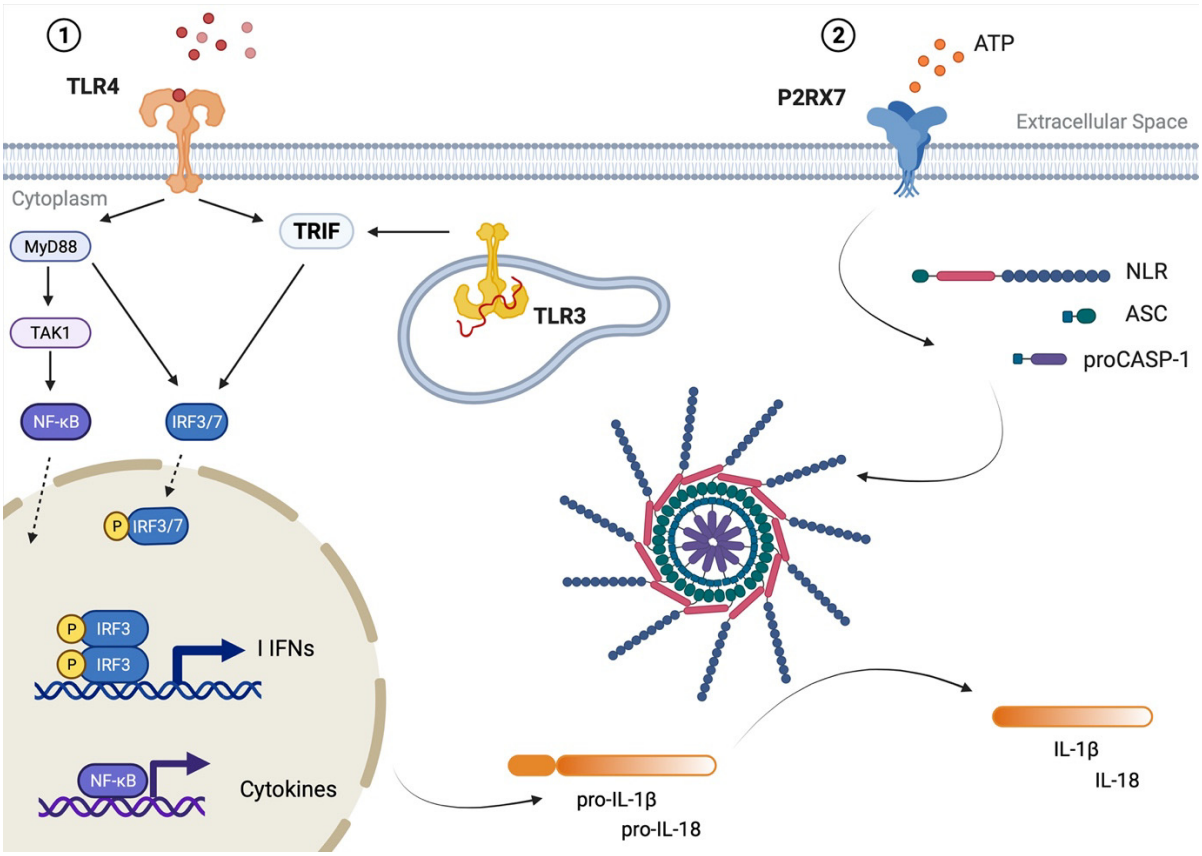

Figure 2: Inflammasome activation. Two signals are required for the full activation of the inflammasome. First, the transcription of pro-IL-1β and pro-IL-18 is initiated after the recognition of PAMPs by TLRs. A second signal (P2RX7-mediated recognition of extracellular ATP) results in the oligomerization of PYD-containing NLRs, proCASP-1 and ASC, and the formation of the multiprotein complex (also known as the inflammasome), as well as the autocatalytical cleavage of proCASP-1 to CASP-1. Once activated, CASP-1 can cleave pro-IL-1β and pro-IL-18 to its mature counterparts IL-1β and IL-18. The image was created using BioRender.com.

associated speck-like protein containing a CARD (ASC), which causes cellular apoptosis after activation by a specific PAMP/DAMP. This multiprotein complex is also known as an inflammasome. The subsequent recruitment of procaspase-1 (proCASP-1) to the inflammasome via the CARD domain of ASC results in the cleavage of pro-IL-1β and pro-IL-18 as well as gasdermin D (GSDMD), generating the mature counterparts. The cleavage of CASP-1 substrates to their active forms leads to the initiation of pyroptosis, an inflammatory cell death, which is accompanied by the release of active IL-1β and IL-18 into the extracellular space (132, 133). However, the synthesis, processing, and release of these proinflammatory cytokines are tightly controlled. First, the inflammasome has to be primed on the transcriptional level. The best-studied PRRs, which initiate the transcription of pro-IL-1β and pro-IL-18, are TLRs. Indeed, the molecular mechanisms that control the transcription of these cytokines are still under investigation, but the involvement of NF-κB and MAP kinase

signaling has been suggested. The second signal can be mediated by the ATP-gated P2X7 receptor (P2RX7), leading to the assembly and activation of the inflammasome (134). Since the recruitment of proCASP-1 to ASC via a CARD-CARD interaction brings proCASP-1 proteins into close proximity, proCASP-1 is autocatalytically cleaved to CASP-1. Active CASP-1 is able to cleave pro-IL-1β and pro-IL-18 to generate their mature counterparts (Figure 2).

However, not all NLRs exhibit a PYD domain and those lacking PYD domain are not able to form an inflammasome. Furthermore, some NLRs exhibit inhibitory functions and can, for instance, impair the induction of I IFN or the production of other cytokines (135).

2.4. Aim of this study

As the cross-presentation of antigens is important for the stimulation of efficient $CD8^+$ T cell responses during infection with MVA, the aim of this study is to explore the innate immune trigger crucial for the functional activation of cross-presenting BMDCs, with particular emphasis on the ability to present antigen on MHC-I, to express costimulatory molecules and to activate poxviral cytotoxic T cells (58). To date, only a few studies have used MVA as vaccine vector to investigate the underlying mechanisms that favor the induction of $CD8^+$ T cell responses by cross-presentation of antigens. Even less attention has been paid to the impact of different innate immune pathways within the infected feeder cell on the ability to activate cross-presentation by BMDCs.

In this thesis, I will analyze the role of different PRRs and signaling pathways involved in the sensing of MVA in cross-presentation competent BMDCs. I will also investigate whether the recognition of MVA in the infected feeder cell impacts the licensing of cross-presentation competent BMDCs. Due to the surprising effect of AraC on MVA-infected feeder cells, which lack the ability to activate BMDCs for cross-presentation of early expressed antigens, I will investigate how AraC impacts feeder cell signaling and MVA sensing. Using RNA sequencing to analyze the transcriptome of infected feeder cells and cross-presenting BMDCs, I aim to determine the target genes that are potentially involved in the stimulation of cross-presentation. By gene-editing these target genes and genes involved in crucial innate immune pathways in feeder cells, I will determine whether the encoded molecules might be relevant for the licensing of BMDCs for antigen cross-presentation. Furthermore, I will investigate whether a

particular feeder cell phenotype influences further BMDC functions, for instance, phagocytic activity or chemokine and cytokine production. As well as the impact of the feeder cell phenotype on the activation of BMDCs for antigen cross-presentation, this study will also address how the genetic modification affects the feeder cell itself regarding cytokine and chemokine production and cell death.

The results obtained from this study should contribute to the understanding of MVA-based vaccines and instigate further research focusing on the precise mechanisms which license DCs for the efficient induction of cytotoxic T cell responses during infection with MVA.

3. MATERIAL

3.1. Nucleic acids

3.1.1. Plasmids

RP-557 is a selectable 3rd generation lentiviral pSicoR-CRISPR vector encoding a nuclear-localized codon-optimized S. pyogenes-derived Cas9 gene, which is N-terminally fused to a puromycin resistance gene (PuroR) via a T2A ribosome-skipping sequence and expressed from an EF1A-short promoter. The 18-20 bp long gRNA (CRISPR RNA fused to the trans-activating crRNA) is expressed by a U6 promoter and a terminator sequence (136, 137).

psPAX is a 2nd generation lentiviral packaging plasmid (gift from Didier Trono (Addgene plasmid # 12260 ; http://n2t.net/addgene:12260 ; RRID:Addgene_12260))

pMD2.G is a VSV-G envelope expressing plasmid (gift from Didier Trono (Addgene plasmid # 12259 ; http://n2t.net/addgene:12259 ; RRID:Addgene_12259))

TMEM173 CRISPR/Cas9 KO is a plasmid encoding a 20 nt gRNA sequence targeting TMEM173 (protein name: STING), expressed by a U6 promoter. Both GFP and a nuclear-localized SpCas9 ribonuclease are expressed by a chicken β-actin hybrid promoter (sc-428364; Santa Cruz).

TMEM173 HDR is a plasmid, which ensures, in combination with the TMEM173 CRISPR/Cas9 KO plasmid, the efficient knockout of TMEM173 by homology-directed repair of double strand breaks induced by Cas9. The plasmid encodes red fluorescent protein and PuroR, which expression is driven by an EF1a promoter. Moreover, two 34 bp long recombination sites are encoded and recognized by the cellular Cre recombinase (sc-428364-HDR; Santa Cruz).

3.1.2. Primers

All oligonucleotides were synthesized by *Eurofins*.

Table 1: Primer sequences used for gRNA cloning, RT-PCR and sequencing.

Name	**Sequence** (5' → 3')	**Application**
Ctnnb1_2 fw	ACCGCACAACCGGATTGTAATCCG	gRNA cloning
Ctnnb1_2 rev	AAACCGGATTACAATCCGGTTGTG	gRNA cloning

DDX41_2 fw	ACCGTACCCTATGTGCCGTTG	gRNA cloning
DDX41_2 rev	AAACCAACGGCACATAGGGTA	gRNA cloning
Ku70_1 fw	ACCGCCACTTACCACCTGTGTCG	gRNA cloning
Ku70_1 rev	AAACCGACACAGGTGGTAAGTGG	gRNA cloning
LRRFIP1_1 fw	ACCGCGCCGTGGCCGATGGACAT	gRNA cloning
LRRFIP1_1 rew	ACCGCGCCGTGGCCGATGGACAT	gRNA cloning
MAVS_2 fw	ACCGCGTGGGCGCCACCCAGTTC	gRNA cloning
MAVS_2 rev	AAACGAACTGGGTGGCGCCCACG	gRNA cloning
MyD88_1 fw	ACCGCCCTTGGTCGCGCTTAACGT	gRNA cloning
MyD88_1 rev	AAACACGTTAAGCGCGACCAAGGG	gRNA cloning
P2rx7_2 fw	ACCGAATTATGGCACCGTCAAG	gRNA cloning
P2rx7_2 rev	AAACCTTGACGGTGCCATAATT	gRNA cloning
Pycard_2 fw	ACCGCTCTTGAAAACTTGTCAG	gRNA cloning
Pycard_2 rev	AAACCTGACAAGTTTTCAAGAG	gRNA cloning
RIG-1_1 fw	ACCGACTATATCAAGAAGATTC	gRNA cloning
RIG-1_1 rev	AAACGAATCTTCTTGATATAGT	gRNA cloning
TLR4_2 fw	ACCGACATAGTCCTTCCATGATAG	gRNA cloning
TLR4_2 rev	AAACCTATCATGGAAGGACTATGT	gRNA cloning
Trif_2 fw	ACCGTACATTCAACCTCGTGC	gRNA cloning
Trif_2 rev	AAACGCACGAGGTTGAATGTA	gRNA cloning
Ifna13 fw	CCTGCTGGCTGTGAGGAAAT	RT-PCR
Ifna13 rev	TCCTTGCTCAGTCTTGCCAG	RT-PCR
mt-Rnr2 fw	TGCCTGCCCAGTGACTAAAG	RT-PCR
mt-Rnr2 rev	GACCCTCGTTTAGCCGTTCA	RT-PCR
RP-557 fw seq primer	TGCAGGGGAAAGAATAGTAGAC	Sequencing

3.1.3. gRNAs sequences

Ctnnb1_2	CACAACCGGATTGTAATCCG AGG
DDX41_2	ACGTACCCTATGTGCCGTTG CGG
Ku70_1	GCCACTTACCACCTGTGTCG GGG
LRRFIP1_1	GCGCCGTGGCCGATGGACAT GGG
MAVS_2	GCGTGGGCGCCACCCAGTTC TGG
MyD88_1	CCCTTGGTCGCGCTTAACGT GGG
P2rx7_2	CGAATTATGGCACCGTCAAG TGG

Pycard_2	CGCTCTTGAAAACTTGTCAG GGG
RIG-I_1	AGACTATATCAAGAAGATTC TGG
TLR4_2	ACATAGTCCTTCCATGATAG AGG
Trif_2	CTGTACATTCAACCTCGTGC TGG

3.1.4. Additional nucleic acids

DNA-Size Standard Hyperladder I (1 kb ladder)	Bioline
100 bp DNA Ladder	NEB

3.2. Proteins

3.2.1. Antibodies

Table 2: Antibodies used for flow cytometric analysis.

Antibody	Clone	Manufacturer
α-Annexin V APC	-	Invitrogen
α-CD11c APC/Cy7	HL3	BD Pharmingen
α-CD11c PE	N418	eBioscience
α-CD16/32 antibody Fc-Block™	2.4G2	eBioscience
α-CD40 PB	3/23	Biolegend
α-CD8 PB	53-6.7	eBioscience
α-CD86 APC	GL1	BD Pharmingen
α-I-A/I-E PB	M5/114.15.2	eBioscience
α-I-A/I-E PE	AF6-120.1	BD Pharmingen
α-IFN-γ APC	XMG1.2	eBioscience
α-H2-Kb FITC	AF6-88.5	Biolegend
α-H2-Kb PE/Cy7	AF6.88.5.5.3	eBioscience
α-SIINFEKL/H-2Kb PE/Cy7	eBio25-D1.16	eBioscience
α-TNF-a PE/Cy7	MP6-XT22	Invitrogen

Table 3: Antibodies for western blot analysis.

Antibody	Clone	Host	Manufacturer
α-mouse IgG	-	goat	Jackson
α-rabbit IgG	-	goat	Jackson
α-β-actin	AC-74	mouse	Sigma
α-β-catenin	-	rabbit	Cell signaling
α-CASP-3	-	rabbit	Cell signaling
α-CASP-9	-	rabbit	Cell signaling

α-Cleaved CASP-8 (Asp387) XP®	D5B2	mouse	Cell signaling
α-DDX41	D3F1Z	rabbit	Cell signaling
α-Ku70	D10A7	rabbit	Cell signaling
α-LRRFIP1	PA5-23445	rabbit	Invitrogen
α-MAVS	4983	rabbit	Cell signaling
α-MDA-5	D74E4	rabbit	Cell signaling
α-MyD88	D80F5	rabbit	Cell signaling
α-TICAM-1 (Trif)	1H4B01	mouse	Biolegend
α-RIG-I	D14G6	rabbit	Cell signaling
α-STING	-	rabbit	Cell signaling
α-TLR4	-	rabbit	Cell signaling

3.2.2. Synthetic Peptides

All peptides were purchased from *Biosynthan*.

Table 4: Peptides used for $CD8^+$ restimulation.

Peptide	Sequence	MHC-I restriction
$A19_{47-56}$	VSLDYINTM	H2-Kb
$A3_{270-277}$	KSYNYMLL	H2-Kb
$B8_{20-27}$	TSYKFESV	H2-Kb
$D13_{118-126}$	NCINNTIAL	H2-Dd
$OVA_{257-264}$	SIINFEKL	H2-Kb

3.2.3. Enzymes

BsmBI	Thermo Scientific
Quick Ligase	NEB

3.2.4. Proteins and Proteinase Inhibitors

Bovine Serum Albumin (BSA)	Thermo Scientific
Precision Plus Protein Prestained Standard	Thermo Scientific
RiboLock™ RNase Inhibitor	Thermo Scientific

3.3. Cells

3.3.1. Bacterial cells

NEB stable (NEB)	*F' proA+B+ lacIq Δ(lacZ)M15 zzf::Tn10 (TetR)/ Δ(ara-leu) 7697 araD139 fhuA ΔlacX74 galK16 galE15 e14- Φ80dlacZΔM15 recA1 relA1 endA1 nupG rpsL (StrR) rph spoT1 Δ(mrr-hsdRMS-mcrBC)*

XL-1-Blue (Stratagene)	*recA1 endA1 gyrA96 thi-1 hsdR17 supE44 relA1 lac [F´ proAB lacIqZ∆M15 Tn10 (Tetr)]*

3.3.2. Mammalian cells

Table 5: Cell lines used in this project.

Cell line	Type	Origin	Reference
Cloudman S91	melanoma	mouse (DBA)	ATCC Nr. CCL.53.1
DF1	fibroblasts	chicken	
EL4	T-lymphocytes (lymphoma derived)	mouse	ATCC Nr. TIB-39
HEK293T	embryonic kidney cells	human	Heiner Schaal
HeLa	cervical carcinoma	human	ATCC© CRM-CCL-2TM
J774	reticulum cell sarcoma	mouse (Balb/c)	Georg Häcker
MEF	embryonic fibroblast cells	mouse (DBA)	Albert Zimmermann
WEHI3	leukemia cells	mouse (Balb/c)	

3.3.3. Mice

Mice were either used for bone marrow preparation and subsequent BMDC generation or for isolation of splenocytes to restimulate $CD8^+$ T cell lines. For experiments with genetically modified (transgenic) mice, wildtype littermates were used as controls instead of mice from *Janvier*.

Balb/c	https://www.jax.org/strain/000651
C3H	https://www.jax.org/strain/000659
C57BL/6N	https://www.jax.org/strain/005304
IFN-$\beta^{-/-}$	Zoé Waibler, PEI, Langen, Germany
IFNAR$^{-/-}$	Steffanie Scheu, HHU, Düsseldorf, Germany
STING$^{-/-}$	Lei Jin, University of Florida, Florida, USA.

3.4. Virus

All viruses were purified by Ronny Tao using two consecutive ultracentrifugation steps through a 36 % (w/v) sucrose cushion and titrated by using standard methods (35).

MVA-PK1L-OVA	Recombinant MVA expressing OVA under control of the early promoter PK1L
MVA-P11-OVA	Recombinant MVA expressing OVA under control of the late promoter P11
MVA-P7.5-eGFP	Recombinant MVA expressing eGFP under control of the early and late promoter P7.5

3.5. Kits

NucleoSpin® Gel and PCR Clean-up	Macherey-Nagel
QIAprep Spin Miniprep	Qiagen
RevertAid H Minus First Strand cDNA Synthesis	Thermo Scientific
RNase-free DNase Kit	Qiagen
RNeasy Mini Kit	Qiagen

3.6. Buffers

Annealing buffer	10 mM Tris pH 8.0
	50 mM NaCl
	1 mM EDTA
5x Loading buffer	250 mM Tris pH 6.8
	10 % SDS
	30 % Glycerol
	12.5 % 2-Mercaptoethanol (100%)
	0.5 % Bromophenol blue
10x Running buffer	250 mM Tris-base
	2 M Glycine
	1 % (w/v) SDS
10x TBS-T	0.1 M Tris/HCl pH 8.0
	1.5 M NaCl
	0.5 % (v/v) Tween- 20
10x Transfer buffer	0.5 M Tris- base
	0.4 M Glycine
1x Transfer buffer	100 ml 10x Transfer buffer
	200 ml Methanol
	700 ml dH20

Tyr-lysis buffer	50 mM Tris-HCl pH 8.0
	150 mM NaCl
	0.02 % NaN_3
	1 % Triton X-100

Additional purchased buffers used in this thesis:

DPBS	Gibco
Pharm Lyse Buffer™	BD
Quick Ligase Reaction Buffer	NEB
Tango Buffer (10x)	Thermo Scientific
TBE (10x)	Merck

3.7. Media

Culture medium	RPMI 1640 or DMEM
LB-medium	20 g on 1 l water
LB-Agar	5 % (w/v) Agar in LB-medium
M2 medium	RPMI 1640
	10 % FCS
	1 % Pen-Strep
	50 µM β-Mercaptoethanol
	10 % FCS
Selection medium	RPMI 1640
	0,5 µg/ml Puromycin

3.8. Chemical

β-Mercaptoethanol	Roth
Acetic acid	Merck
Agarose	Biozym
Ampicillin	Roth
Bacto-Agar	Fluka

BD Cytofix/Cytoperm ™	BD Biosciences
BD Perm/Wash ™	BD Biosciences
Brefeldin A	Sigma
Bromphenol Blue	Merck
Calcium chloride	Merck
Cytosine β-D-arabinofuranoside	Sigma
Dimethyl sulfoxide (DMSO)	Sigma Life Science
DTT (0,1 M)	Invitrogen
Ethanol absolute	Merck
EZ-Vision® In-Gel	VWR
FBS Superior	Merck
Fixable Viability Dye eFluor™ 506	eBioscience
Fixable Viability Dye eFluor™ 660	eBioscience
Gel loading dye purple (6x)	NEB
Glycerol	Roth
Glycine	Roth
Hydrochloric acid (32%)	Roth
Isoflurane	Piramal
Isopropanol	Merck
LB Broth (Lennox)	Roth
Magnesium chloride	Merck
Methanol	Merck
Paraformaldehyde	Merck
Pierce™ ECL western blotting substrate	Thermo Scientific
Polybrene	Sigma
Polyethylenimine, branched	Sigma
Propidium Iodide	Invitrogen
Psoralene	Sigma
Puromycin dihydrochloride	Sigma
Rotiphorese® Gel (37.5:1)	Roth
Skimmed milk powder	Sucofin
Sodium Azide	Merck
Sodium chloride	Roth
Sodium dodecyl sulfate (SDS)	Roth

Sodium hydroxide (NaOH)	Merck
SYBR™ Select Master mix	Applied Biosystems
TEMED	VWR
Tris-Base	Roth
Triton X-100	Sigma
Trypan Blue Stain (0.4 %)	Gibco
Trypsin-EDTA (0,05 %)	Gibco
Tween® 20	Merck
UltraPure ™ Distilled Water DNase/RNase free	Invitrogen

3.9. Technical equipment

Benchtop orbital shaker MaxQ™ 4000	Thermo Scientific
Centrifuge Heraeus Megafuge 16R	Thermo Scientific
Cross-Linker Bio-Link BLX 365	Peqlab
ECL imager Chemostar	Intas
Electrophoresis chambers	Neolab
FACS Canto II	BD Biosciences
Freezer Forma 88000 Series (-80 °C)	Thermo Scientific
Freezer GNP 4166 Premium NoFrost (-20 °C)	Liebherr
Freezer Herafreeze (-80 °C)	Thermo Scientific
Freezer IG 1166 Premium (-20 °C)	Liebherr
Fridge FKUv 1610 Premium (4 °C)	Liebherr
Fridge KB 4260 Premium (4 °C)	Liebherr
Fridge KUR18421 (4 °C)	Bosch
Fridge LKUv 1610 MediLine (4 °C)	Liebherr
Gammacell 1000 Elite	Nordion international
Heating plate MR Hei-Tec	Neolab
Ice machine AF124	Scotsman
Inkubator HERAcell 150i CO2	Heraeus
Laminar flow Scanlaf Mars Safety 2	Labogene
Light cycler ABI7500 Real Time PCR System	Applied Biosystems
Microcentrifuge 5810 R	Eppendorf
Microcentrifuge Fresco 21	Heraeus
Microscope CKX41	Olympus

Microwave Gn3431MA	Moulinex (Krups)
neoBlock heater I 2-2503	NeoLab
pH-meter PB-11	Satorius
Power supply MS 3AP	Major scientific
Rotor 75003624	Thermo Scientific
Rotor 75003629	Thermo Scientific
Scale AEJ 220-4M	Kern & Sohn GmbH
Scale EW 4200 2NM	Kern & Sohn GmbH
Scissors HSB 0140-11	Hammacher
Sonopuls	Bandelin
spectrophotometer NanoDrop 2000	Thermo Scientific
Thermal Cycler Biometra Trio	Analytik Jena
Thermomixer comfort	Eppendorf
Trans-Blot® Turbo™	Bio-Rad
Tweezers HSC 801-11	Hammacher
Vortex-Genie 2 shaker	Scientific Industries
Waterbath type 1083	GFL
western blot equipment	Neolab

3.10. Consumables

12-well plates	VWR
24-well plates	VWR
6-well plate	VWR
96-well plate	TPP
Cell scraper M	TPP
Cell scraper S	TPP
Cell strainer 70 µm	VWR
Falcon tube 15 ml	Cellstar
Falcon tube 50 ml	Cellstar
Filter 0.2 µm	GE Healthcare Life Sciences
Filter 0.45 µm	GE Healthcare Life Sciences
Filter tip 1000 µL XL Graduated	TipOne, Starlab
Filter tip 20 µL Bevelled	TipOne, Starlab
Nitrocellulose blotting membrane 0.45 µm	GE Healthcare Life Science

PCR tubes 0.2 ml 8-Strip	Starlab
Petri Dish 100 mm	Thermo Scientific
Stripette® 10 ml	Costar
Stripette® 25 ml	Costar
Stripette® 5 ml	Costar
Syringe 1 ml	BD Plastipak
Syringe 5 ml	BD
Tissue culture dish 100 mm (sterile)	TPP
Tissue culture dish 60 mm (sterile)	VWR
Tissue culture flask 182. 5 cm^2	VWR
Tissue culture flask 25 cm^2	VWR
Tissue culture flask 75 cm^2	Thermo Scientific
Titertube® Micro Test Tubes	Bio-Rad
Tube 1.5 ml	Sarstedt
Tubes 2.0 ml	Eppendorf
Whatman paper	GE Healthcare Life Sciences

4. METHODS

4.1. Molecular biological methods

4.1.1. Guide-RNA (gRNA) cloning

All gRNAs were designed as 18-20 mers to ensure maximal gene knockout efficiency (138). gRNAs were designed using UCSC genome browser (https://genome.ucsc.edu) as well as CRISPOR (http://crispor.tefor.net) (139, 140). Usually, gRNAs were designed to target the first exon to cause a frame-shift mutation and thus the production of a non-functional protein. All gRNAs were cloned into the pSicoR-CRISPR vector RP-557 that was kindly provided by Robert-Jan Lebbink and Emmanuel Wiertz (UMC Utrecht, Department of Medical Microbiology).

The RP-557 vector was digested overnight at 37 °C using the enzyme BsmBI from Thermo Scientific according to the manufacturer's protocol. The linearized product was purified by agarose gel electrophoresis, using 1 % agarose in 1x TBE buffer. The DNA was extracted with the *Macherey-Nagel™ NucleoSpin™ Gel and PCR clean-up Kit* according to the manufacturer's instructions. Primers for cloning of the appropriate gRNA were designed with either an ACC or AAAC overhang to facilitate efficient annealing of these primers and subsequent ligation into the digested vector. For annealing, 1 µl of 100 µM forward and reverse primers, respectively, were incubated with 23 µl annealing buffer at 95 °C for 5 min, 85 °C for 5 min, 75 °C for 5 min, 65 °C for 5 min, 5 °C for 5 min, 45 °C for 5 min, 35 °C for 5 min, 25 °C for 5 min and finally hold at 15 °C until ligation. Ligation was performed using *Quick Ligation™* Kit according to the manufacturer's protocol.

4.1.2. Transformation

Competent *Escherichia coli* bacteria (XL-1-Blue) were used for amplification and transformed with plasmid DNA by heat shock. To this end 50 µl bacteria were thawed on ice for 10 min followed by the addition of 3 µl of the ligation reaction. Samples were gently mixed and incubated for another 10 min on ice. Afterwards samples were transferred to 42 °C for 45 s and immediately placed on ice for 2 min. After adding of 400 µl lysogeny broth (LB) medium, cells were recovered at 37 °C in a shaking incubator for 30-45 min, placed on Ampicillin-containing LB plates and incubated overnight at 37 °C.

4.1.3. Preparation of plasmid DNA

Plasmid DNA was prepared from 4 ml overnight bacteria cultures using *QIAprep Spin Miniprep* Kit according to the manufacturer's instructions. Briefly, bacteria were lysed using an SDS-containing alkaline buffer for resolving the bacterial membrane and NaOH for denaturation of protein and DNA. For DNA renaturation, the solution was neutralized using guanidine hydrochloride. Subsequent centrifugation separated denaturated proteins, genomic DNA and cell debris from the plasmid DNA that was contained in the supernatant. The use of silica membrane columns enabled the purification and concentration of plasmid DNA under high-salt conditions. The plasmid DNA was eluted from the silica membrane under low-salt conditions in water.

4.1.4. DNA sequencing

To confirm annealing and insertion of the right gRNA sequence into the pSicoR-CRISPR RP-557 vector, 15 µl of 5-10 ng/µl plasmid DNA were sequenced at *Eurofins* using TGC AGG GGA AAG AAT AGT AGA C as sequencing primer.

4.1.5. RNA extraction

RNA was extracted from 2 x 10^6 MVA- and mock-infected cells, respectively, using the *RNeasy Mini* Kit according to the manufacturer's instructions. After 2-16 h post infection, cells were scraped, centrifuged at 319 xg and 4 °C and the cell pellet resuspended in 350 µl RLT-buffer supplemented with β-mercaptoethanol according to the instructions of the manufacturer. After lysis of the plasma membrane, ethanol was added to the samples, and the samples were transferred to a silica membrane column that could efficiently bind RNA. To remove DNA that might have bound to the column, an on-column digestion step using DNase I was performed. After several washing steps, RNA was eluted in 50 µl water and stored at -80 °C.

4.1.6. RNA sequencing

For RNA sequencing, feeder cells were infected with MVA-PK1L-OVA at multiplicity of infection (MOI) of 1 or mock-infected in the presence of 40 µg/ml AraC. RNA was extracted 8 h post infection as described in 4.1.5. For RNA sequencing of cross-presenting BMDCs, feeder cells were infected with MVA-PK1L-OVA at MOI 1 or mock-infected in the presence of 40 µg/ml AraC for 16 h. Feeder cells were cocultured with BMDCs either for 4 or 6 h. Afterwards, cocultures were stained with a viability dye and

for $CD11c^+$ or $CD11c^+$ as well as SIINFEKL/Kb^+ as described in 4.4.2. Cocultures were sorted for viable $CD11c^+$ and $CD11c^+$ SIINFEKL/Kb^+ DCs, respectively, using the *MoFloXDP* cell sorter from Beckman-Coulter at the Core Flow Cytometry Facility at the Institut für Transplantationsdiagnostik und Zelltherapeutika (ITZ) at the University Hospital Düsseldorf. After determining RNA concentrations using the spectrophotometer *Nanodrop 2000*, RNA was sequenced using *Illumina HiSeq3000/4000* by the Genomics and Transcriptomics Lab in the Biologisch-Medizinisches Forschungszentrum (BMFZ) of the Heinrich-Heine-University Düsseldorf.

4.1.7. Quantitative reverse transcriptase polymerase chain reaction (RT-PCR)

RNA was extracted as described in 4.1.5 and RNA concentrations determined using the spectrophotometer *Nanodrop 2000*. cDNA was synthesized from 2 µg RNA using the *RevertAid H Minus First Strand cDNA Synthesis* Kit according to the manufacturer's protocol. Briefly, RNA was mixed with random hexamer primers to a total volume of 12 µl. After adding of 5x reaction buffer, RiboLock RNase inhibitor, dNTPs and RevertAid H Minus M-MuLV Reverse Transcriptase to the reaction, samples were incubated for 5 min at 25 °C. After incubation for 1 h at 42 °C, cDNA synthesis was terminated by heating the samples at 70 °C for 5 min. The reaction mix was diluted 1:5 by adding of 80 µl water to dilute the concentration to 20 ng/µl. Samples were stored at -20 °C until analysis. Gene expression was analyzed by semi-quantitative RT-PCR using the fluorescent dye SYBR Green that bound to dsDNA by intercalation between DNA bases. Primers were designed for optimal annealing at 60 °C, but at least a temperature of 57 °C was required for efficient annealing. Furthermore, primers were calculated to amplify a PCR product between 90-150 bp using *ensemble genome browser 101* (https://www.ensembl.org/index.html) as well as *primer3web* (https://primer3.ut.ee).

Moreover, primers were designed exon-exon spanning, beginning at the 3' end of the mRNA, to avoid quantification of false-positive results from possible contaminations with genomic DNA. The analysis was performed using the reaction mix indicated in Table 6.

Table 6: Reaction mix for RT-PCR

Components	Volume [µl]
cDNA (20 ng/µl)	2
primer foward (10 µM)	1
primer reverse (10 µM)	1
SYBR-green (2x)	10
water	6
in total	**20**

Every sample was analyzed using the *ABI7500 Real Time PCR System* light cycler in two replicates according to the following program:

Table 7: PCR program

Process	**Temperature [°C]**	**Time**	
Activation	95	2 min	
Denaturation	95	15 s	40 cycles
Annealing	60	15 s	
Extension	72	1 min	

The obtained RT-PCR results were analyzed by normalization to 16S ribosomal RNA as housekeeping gene and by calculating ΔCT as well as ΔΔCT (141).

4.2. Cytological methods

4.2.1. Cell culture

Cells were cultured either in RPMI or DMEM containing 10 % heat-inactivated FCS, at 37 °C and 5 % CO_2. Cells were passaged every 3 days and cultured in new medium. Adherent cells were washed with PBS prior to trypsinization using 0,05 % Trypsin-EDTA to ensure that cells efficiently detached from the cell culture flask. After centrifugation at 319 xg for 5 min at room temperature, the supernatant was discarded, and the cell pellet resuspended in fresh medium to remove trypsin from the medium. Semi-adherent cells or in suspension cultured cells were scraped, centrifuged and resuspended in fresh medium.

4.2.2. Generation of BMDCs

Bone marrow was isolated from 12-16 weeks old wildtype C57BL/6 and STING KO C57BL/6 mice by flushing the femur and tibiae with M2 medium. Erythrocytes were

lysed using 5 ml of diluted BD Pharm Lyse buffer™ and incubated for 1 min at room temperature. Bone marrow cells were counted using a Neubauer cell counting chamber and 5 x 10^6 cells seeded in 10 ml M2 medium (containing 10 % heat inactivated FCS, 50 µM 2-mercaptoethanol) and 10 % GM-CSF (conditioned medium obtained as supernatant from B16 cells expressing GM-CSF) in 10 cm Petri-dishes. Three days after the bone marrow preparation, 10 ml of fresh GM-CSF containing medium was added to the cultures. On day six 10 ml of the cell culture medium was replaced with fresh 10 ml of M2 medium containing 10 % GM-CSF. BMDC cultures were used for experiments on day 7.

4.2.3. Isolation of Splenocytes

Spleens of naive animals were collected and processed into a single-cell suspension by mechanical disruption using a 70 µm cell strainer and a plunger. The cell suspension was centrifuged at 319 xg for 5 min at room temperature. The supernatant was discarded and the cell pellet resuspended in lysis buffer to remove erythrocytes. Lysis was performed with the Pharm Lyse Buffer™ from BD according the manufacturer's protocol and resuspended cells incubated for 1 min at room temperature. To inhibit further cell lysis of splenocytes, cells were washed with PBS and centrifuged. The cell pellet was resuspended in M2 medium and passed through a 70 µm cell strainer to remove remaining tissue from the cell suspension. Cells were counted using a Neubauer cell counting chamber and added at a concentration of 12 x 10^6 cells/ml to a 24-well plate to create a special environment for the restimulation of $CD8^+$ T cell lines by peptide-loaded EL4 (ATCC TIB-39) cells, as described in 4.2.4.

4.2.4. Restimulation of $CD8^+$ T cell lines

Prior to this project, $CD8^+$ T cell lines were generated by incubation of peptide-loaded LPS blasts from naive C57BL/6 mice with splenocytes derived from MVA-PK1L-OVA vaccinated mice as described elsewhere (Barnowski & Ciupka er al. 2020). $CD8^+$ T cell lines were weekly restimulated with peptide-loaded EL.4 cells (ATCC TIB-39), naïve splenocytes as filler cells as well as M2 medium containing 5 % TCGF (conditioned medium containing supernatant from rat splenocytes stimulated with 5µg/ml Concanavalin A) (142). EL4 cells and splenocytes were irradiated to restrict cell growth with 100 Gy and 30 Gy, respectively. EL4 cells were loaded with 1 ng/ml peptide for 30 min in serum-free medium at 37 °C and 5 % CO_2. Cells were washed twice with 10 ml M2 medium and added at a concentration of 1 x 10^5 cell/ml to $CD8^+$ T

cell lines in a 24-well plate. $A19_{47-56}$ (VSLDYINTM), $B8_{20-27}$ (TSYKFESV), $A3_{270-277}$ (KSYNYMLL), or $D13_{118-126}$ (NCINNTIAL), derived from MVA, and $OVA_{257-264}$ (SIINFEKL) peptide derived from ovalbumin were used as peptides. D13-derived peptide was H2-Db-restricted, all other peptides were H2-Kb-restricted.

4.2.5. Infection of cells with MVA

As BMDCs represent semi-adherent cells, they were scraped and counted using a Neubauer cell counting chamber. Four x 10^6 BMDCs were centrifuged at 319 xg for 5 min and resuspended in 200 µl M2 medium (RPMI 1640 containing 10 % heat inactivated FCS, 50 µM 2-mercaptoethanol). BMDCs were infected at MOI 1 and incubated overnight at 37 °C and 5 % CO_2. Infected and mock-infected BMDCs were softly shaken every 10 min to keep them in suspension and ensure a high infection efficiency. After 1 h, cells were seeded in a 6 cm Petri-dish and incubated at 37 °C and 5 % CO_2 for the remaining infection time (Figure 3).
Cloudman S91 melanoma cells were washed and trypsinized. Prior to infection, cells were counted using a Neubauer cell counting chamber. Two x 10^6 cells were infected with MVA-PK1L-OVA at MOI 1 or mock-infected. In the first hour of infection, cells were softly shaken every 10 min. In the second hour of infection, cells were softly shaken every 20 min. Afterwards, cells were incubated overnight at 37 °C and 5 % CO_2.

4.2.6. Cross presentation assay

All feeder cells, used in this project, were MHC-I mismatched to avoid direct presentation of antigen on MHC-I and subsequent T cell activation. Adherent feeder cells were trypsinized, while semi-adherent cells were scraped. All cells were counted using a Neubauer cell counting chamber and 2 x 10^6 feeder cells were centrifuged at 319 xg for 5 min. Cell pellets were resuspended in 200 µl of M2 medium (RPMI 1640 containing 10 % heat-inactivated FCS, 50 µM 2-mercaptoethanol) and infected at MOI 1, if not indicated differently. Infected feeder cells were incubated for 16 h at 37 °C and 5 % CO_2. In the first hour of infection, feeder cells were softly shaken every 10 min and in the second hour of infection, every 20 min to keep the cells in suspension and to ensure efficient infection. Afterwards, cells were plated in a 6-well plate and incubated at 37 °C and 5 % CO_2 for the remaining infection time. Infected and mock-infected cells were treated with 0,3 µg/ml psoralen for 15 min following irradiation with UVA at approximately 3000 µwatts/cm^2 (PUVA) for 15 min at room temperature. Feeder cells were washed and cocultured 1:1 with 2 x 10^6 BMDCs in a 6 cm Petri-dish

at 37 °C and 5 % CO_2. Cross-presentation competent BMDCs were analyzed 12 h post cocultivation for their ability to reactivate antigen-specific $CD8^+$ T cell lines for the production of cytokines, described below, or 20 h post cocultivation for their ability to express SIINFEKL/Kb on the cell surface and for their maturation phenotype (Figure 3).

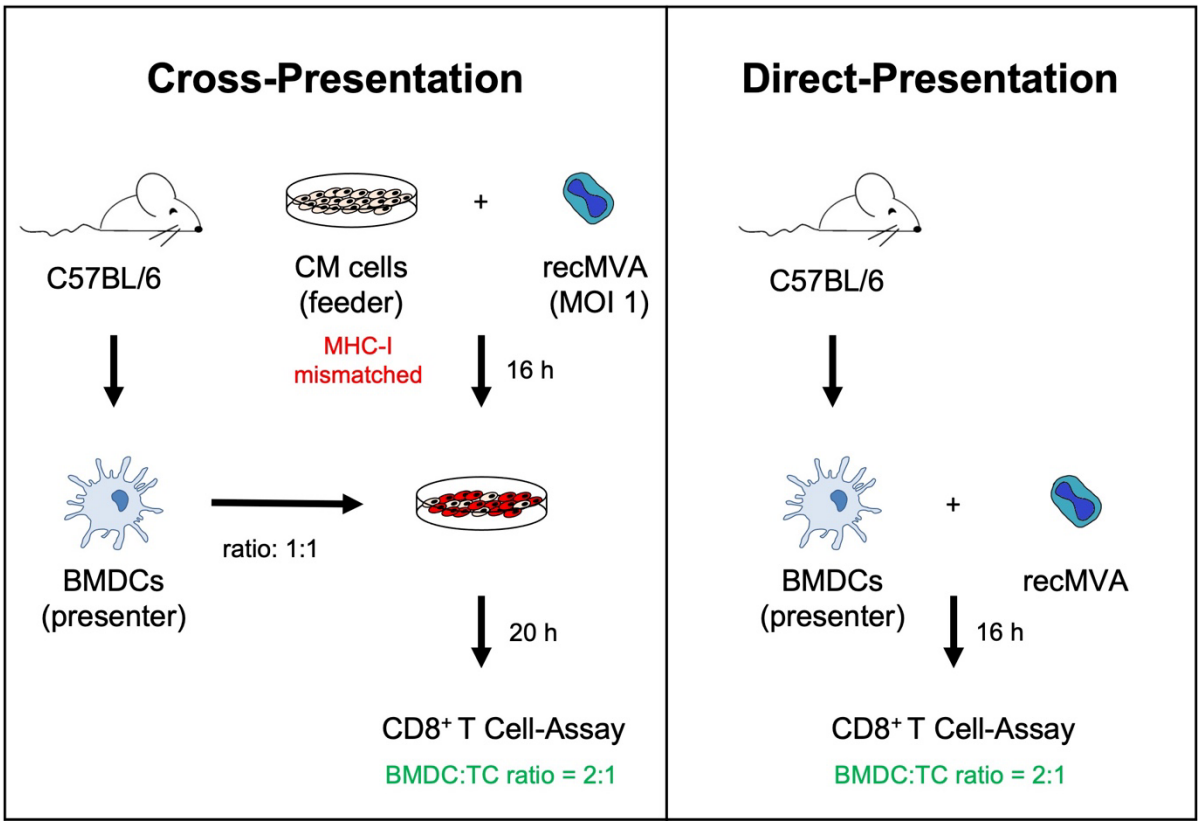

Figure 3: Cross- and direct-presentation assays. For **cross-presentation**, MHC I-mismatched feeder cells were infected with recombinant MVA (recMVA) at MOI 1 for 16 h. After washing and virus inactivation by PUVA treatment, infected feeder cells were cocultured with bone marrow-derived dendritic cells (BMDCs). For **direct-presentation**, BMDCs were infected with MVA for 16 h. In both settings, BMDCs were incubated with $CD8^+$ T cell (TC) lines for 4 h after washing. As read-out for the antigen presentation capability of cross-presenting or directly presenting BMDCs, the activation of peptide-specific $CD8^+$ T cells was determined by IFN-γ and TNF-α production using flow cytometry (143).

4.2.7. CD8+ T cell activation assay

As read-out for the capacity of infected directly presenting or non-infected cross-presenting BMDCs to present antigen, peptide-specific $CD8^+$ T cell lines were used and their ability to become activated determined by the production of cytokines analyzed by intracellular cytokine staining (ICS) as described in 4.4.3. $CD8^+$ T cells were cultured in a 1:2 ratio with BMDCs, to be precise 2 x 10^5 T cells were cocultured with 4 x 10^5 BMDCs for 4 h in the presence of 1 µg/ml brefeldin A (BFA) at 37 °C and 5 % CO_2.

4.2.8. Transfection

The day before transfection, 3,8 x 10^6 HEK293T cells were seeded in a 10 cm Petri-dish and incubated over night at 37 °C and 5 % CO_2. Lentivirus containing the particular gRNA was generated by transfection of 10 µg of transfer (pSicoR-CRISPR RP-557 containing the cloned gRNA), 5 µg envelope (pMD2.G) and 5 µg packaging (psPAX2) plasmids and 60 µg PEI were thoroughly mixed in 500 µl serum-free DMEM medium and incubated for 15 min at room temperature. Medium of HEK293T cells was replaced with 10 ml fresh serum-free DMEM and the DNA-PEI mix added. Following the incubation for 6-8 h at 37 °C and 5 % CO_2, medium was changed to DMEM containing 10 % FCS. After approximately 48 h of virus production, supernatant was harvested, centrifuged at 319 xg, filtered through a 0,45 µm filter and either directly used or stored at -80 °C.

4.2.9. Transduction

The day before transduction, 1,25 x 10^5 Cloudman S91 melanoma cells were seeded in 2 ml culture medium in a 12-well plate. The next day, the cell culture medium of the approximately 70-80 % confluent cells was replaced with 2 ml of lentivirus containing medium, supplemented with 8 µg/ml polybrene. To increase the transduction efficiency, cells were centrifuged for 1 h at 568 xg and 37 °C. Afterwards, cells were incubated over night at 37 °C and 5 % CO_2. To dilute the polybrene concentration, 2 ml of culture medium were added, and cells were incubated for another 3 days at 37 °C and 5 % CO_2. Successfully transfected cells were selected using 0,5 µg/ml puromycin for 5 days. Every second to third day the puromycin containing culture medium was renewed. After puromycin selection, cells were cultured in culture medium without puromycin and either used as bulk population or the cells were diluted to single cell clones to obtain a homogenic cell population.

4.3. Protein biochemical methods

4.3.1. Protein isolation

After infection, cells were scraped, harvested into a 1,5 ml tube and centrifuged at 319 xg for 5 min at 4 °C. After centrifugation, the supernatant was discarded and the cell pellet was washed with cold PBS. Following centrifugation at 319 xg, the cell pellet was resuspended in 80 µl TYR-lysis buffer. For separation of transmembrane proteins

from cellular membranes, cell lysates were three times frozen at -80 °C and thawed, respectively. Afterwards, cell lysates were sonified three times for 1 min on ice and centrifuged at 20.000 xg for 5 min at 4 °C to remove cell debris. Supernatants were collected and stored at -80 °C.

4.3.2. SDS-PAGE

Using sodium dodecyl sulfate polyacrylamide gel electrophoresis (SDS-PAGE) as method for electrophoretic protein separation, proteins were denaturated and separated according to their molecular weight. Protein denaturation was performed by heating the samples for 5 min to 95 °C in a SDS and β-mercaptoethanol containing buffer. Because proteins were uniformly coated with SDS, the intrinsic charge of the amino acids was shielded. As a result, the gel electrophoresis was not influenced by other properties such as protein charge and shape. The β-mercaptoethanol reduced disulfide bridges and separated oligomeric proteins into their subunits. However, the decisive step in protein denaturation represented the boiling of the sample. Acrylamide, bis-acrylamide, APS and TEMED were required to prepare the gel matrix.
The main components of the gel matrix were acrylamide and bis-acrylamide, used in a 29:1 ratio. Acrylamide formed linear polymers, while bis-acrylamide was required for the crosslinking of the polymers. The polymerization of the gel was based on a radical chain reaction, which was initiated by adding the radical chain initiator ammonium persulfate (APS) and catalyzed by N, N, N', N'-tetramethylethylenediamine (TEMED). Discontinuous gels were used to focus the protein bands within the gel. These gels are usually composed of two gel solutions that differ in pH, ionic strength and pore size. In a discontinuous SDS-PAGE, proteins are usually concentrated in the upper collection gel and then separated within the separation gel according to their molecular weight. After loading of the samples and a protein size marker on the gel, the electrophoresis was performed at 100 V for 2,5 h.

4.3.3. Western blot

After electrophoresis, the gel was removed carefully to transfer the proteins to a nitrocellulose membrane. For the protein transfer, the gel was covered with a nitrocellulose membrane, and both, the gel and the membrane, were placed between six pieces of Whatman paper, soaked in transfer buffer. Protein transfer was performed in the presence of an electric field (17 V for 1 h) and individual proteins immobilized on the membrane. These protein bands were specifically identified by antibodies. The

binding of the proteins to the membrane led to the loss of the bound SDS, resulting in a partial refolding. This partial refolding of the proteins resulted in the formation of epitopes, which were present before denaturation and were necessary for antibody-protein binding. In order to avoid unspecific binding of the antibody, the membrane was blocked in 5 % skimmed milk or BSA in TBS-T for 1 h at room temperature. For protein detection a particular primary antibody was diluted in blocking solution and incubated overnight at 4 °C under shaking. The primary antibody was detected by a secondary antibody, which was conjugated with horse radish peroxidase (HRP). After washing of the membrane three times with TBS-T, the membrane was incubated with the secondary antibody for 1 h at room temperature. Horseradish peroxidase oxidized the substrate luminol in the presence of H_2O_2 to a peroxide anion, forming the aminophthalic acid dianion. This dianion was present in an excited state and reached the ground state via chemiluminescence. The chemiluminescence could be detected using a X-ray film or a specific detector that was able to illustrate the protein bands digitally.

In order to verify a particular gene knockout in Cloudman S91 melanoma cells, the synthesis of the appropriate protein in these genetically modified feeder cells was analyzed by western blot using an ECL imager from *Intas*. Furthermore, protein levels of cleaved CASP-3, -8 and -9 were analyzed from MVA- and mock-infected feeder cells to determine the role of apoptosis during infection with MVA.

4.4. Immunological methods

4.4.1. Annexin V staining

To analyze the plasma membrane permeability and integrity and to determine healthy, early apoptotic, late apoptotic and necrotic cells the *Annexin V Apoptosis Detection Kit APC* form Invitrogen was used according to the manufacturer's instructions. Annexin V is a calcium-dependent phospholipid-binding protein, which binds to phosphatidylserine (PS). Since PS was located in healthy cells at the inner leaflet of the plasma membrane and it was exposed early during apoptosis, apoptotic and necrotic cells could be specifically recognized by phagocytes. In addition to Annexin V, cells were incubated with a viability dye to discriminate between apoptotic and necrotic cells. In contrast to apoptosis, necrosis led to the loss of plasma membrane integrity and to an increased permeability of the membrane. Therefore, unlike healthy cells, necrotic cells could be stained by a viability dye, such as propidium iodide (PI).

4.4.2. Flow Cytometry

After washing of the cells with PBS, dead cells were stained with the *Fixable Viability Dye eFluor™ 506* from eBioscience for 20 min on ice, cells were washed with PBS. Prior to the surface staining of $CD8^+$ T cells or BMDCs, cells were washed twice with staining buffer. For the analysis of activated $CD8^+$ T cells, cells were stained for CD8 using α-CD8-PB antibodies (eBioscience) for 30 min on ice. Afterwards, an intracellular staining was performed, as described below. Furthermore, BMDCs were analyzed for the surface expression of SIINFEKL/Kb using α-CD11c-PE, -I-A/I-E-PB, -Kb-PE/Cy7 and -SIINFEKL/H2-Kb-PE/Cy7 or for their maturation phenotype using α-CD11c-APC/Cy7, -CD86-APC, -I-A/I-E-PE antibodies or α-CD40-PB antibody. Antibodies were added after the blocking of Fc-receptors by CD16/32 antibodies. Following an incubation on ice for 30 min, cells were washed and fixed with 1 % paraformaldehyde and stored at 8 °C until flow cytometric analysis.

4.4.3. ICS

In order to analyze the intracellular production of cytokines, cells were washed twice and permeabilized for 15 min on ice using BD Cytofix/Cytoperm™ solution. Following an additional washing step, cells were incubated with α-IFN-γ and α-TNF-α for 30 min in the dark on ice. Finally, cells were washed and fixed with 1 % paraformaldehyde. Samples were stored until the flow cytometric analysis at 8 °C for maximum 5 days.

4.4.4. ELISA

Enzyme Linked Immunosorbent Assay (ELISA) was used for the specific detection and quantification of proteins. In the first step of ELISA, the protein was bound to a special 96-well polystyrene plate by overnight incubation of the proteins in a carbonate buffer. The adsorbed proteins could be detected with HRP conjugated antibodies and a substrate solution containing luminol to induce chemiluminescence. By using a protein standard, the chemiluminescence of the standard was used to calculate the protein concentrations of the samples.

Supernatants of MVA- or mock-infected feeder cells, BMDCs or feeder-BMDC-cocultures were collected after 16 h post infection or overnight coculturing and stored at -80 °C until analysis. IFN-α was detected by *LumiKine™ mIFN-α* and IFN-β by *LumiKineTM Xpress mIFN-β.* Both assays were performed according to the manufacturer's protocol.

4.4.5. LEGENDplex assay

The LEGENDplex™ assay was used for the simultaneous detection and quantification of several cytokines/chemokines in one sample. By using beads with two different sizes and different levels of APC fluorescence, different bead populations could be distinguished by flow cytometry. Indeed, these beads were further conjugated with capture antibodies that specifically recognized a particular cytokine or chemokine. Following cytokine/chemokine binding to the capture antibody, the antigen could be quantified using a biotinylated antibody. Because of the interaction of biotin with streptavidin, the antigen could be visualized using a fluorophore conjugated streptavidin antibody followed by flow cytometric analysis.

LEGENDplex™ assays (*Mouse Proinflammatory Chemokine Panel* and *Mouse Anti-Virus Response Panel*) were performed to quantify cytokines and chemokines in the supernatants from MVA-infected and mock-infected feeder as well as in supernatants from feeder-BMDC-cocultures. Supernatants were collected after overnight infection or after 20 h of coculturing of infected feeder with BMDCs at -80 °C. A volume of 25 µl supernatant was used for the assays according to the manufacturer's protocol. Samples were analyzed by flow cytometry and the data were analyzed using Biolegend's LEGENDplex software.

4.5. Statistical Analysis

All statistical analyses were performed using Graphpad Prism software version 7. Statistical comparisons of two groups were conducted using the unpaired, two-tailed Student's t-test. The comparison of multiple groups was performed by two-way ANOVA with Fisher's LSD multi post-hoc test. The results were depicted as mean ± standard deviation (SD) either pooled or representative from an indicated number of independent experiments. Statistical significance (P) is represented as: * = $P \leq 0.05$; ** = $P \leq 0.01$; *** = $P \leq 0.001$; **** = $P \leq 0.0001$ or ns = not significant.

5. RESULTS

5.1. AraC has different effects on directly and cross-presenting BMDCs

AraC is commonly used to study viral replication in poxviruses (144). Because AraC is an antimetabolite analog of cytidine with an arabinose sugar moiety, it competes with cytidine within the cell for incorporation into the DNA. Therefore, AraC is well known to inhibit the viral DNA polymerase and thus also viral replication. Previous research has shown that during MVA-infection, the expression of late and intermediate expressed genes in particular is inhibited by AraC (144). I investigated protein synthesis in BMDCs using two different recombinant MVA vectors expressing OVA either under the early promoter PK1L or the late promoter P11. Infected and AraC-treated BMDCs displayed unaltered protein synthesis only for the early recombinant antigen OVA and the early viral antigen B8. Furthermore, these early transcribed antigens were processed intracellularly and presented on MHC-I molecules by directly infected BMDCs, to activate antigen-specific $CD8^+$ T cells for the production of IFN-γ (Figure 4A). Activation of $CD8^+$ T cells specific for the early and late expressed viral core protein A3, and the late expressed antigens D13 and A19, showed a tendency to be reduced or were significantly reduced by directly infected and AraC-treated BMDCs (Figure 4A). Interestingly, cross-presenting BMDCs that had been cocultured with MVA-infected and AraC-treated feeder cells were unable to activate OVA- or B8-specific $CD8^+$ T cells, even though early antigen levels were not affected by AraC (Figure 4B; Supplementary Figure 1). As expected, cross-presentation of late antigens by infected BMDCs was abrogated by AraC (Figure 4B). Cloudman S91 melanoma cells (CM cells) were chosen as feeder cells due to their DBA origin and consequent MHC-I mismatch, to avoid the direct presentation of antigens from infected feeder cells to $CD8^+$ T cell lines. Moreover, MVA-infected feeder cells were treated with psoralen and irradiated with UV-light (PUVA), as described in more detail in the Materials and Methods section, to prevent the transmission of residual virus from feeder to presenter cells (BMDCs). Because T cell activation is rather an indirect effect of antigen presentation, I analyzed the effect of AraC on the processing, loading, and presentation of the MHC-I (Kb)-restricted SIINFEKL-peptide epitope of OVA using an antibody that recognizes SIINFEKL/Kb-complexes. To do this, I determined the frequencies of SIINFEKL/Kb^+ cells as well as the mean fluorescence intensities (MFIs), which describe the expression of SIINFEKL/Kb complexes at the cell surface. As can

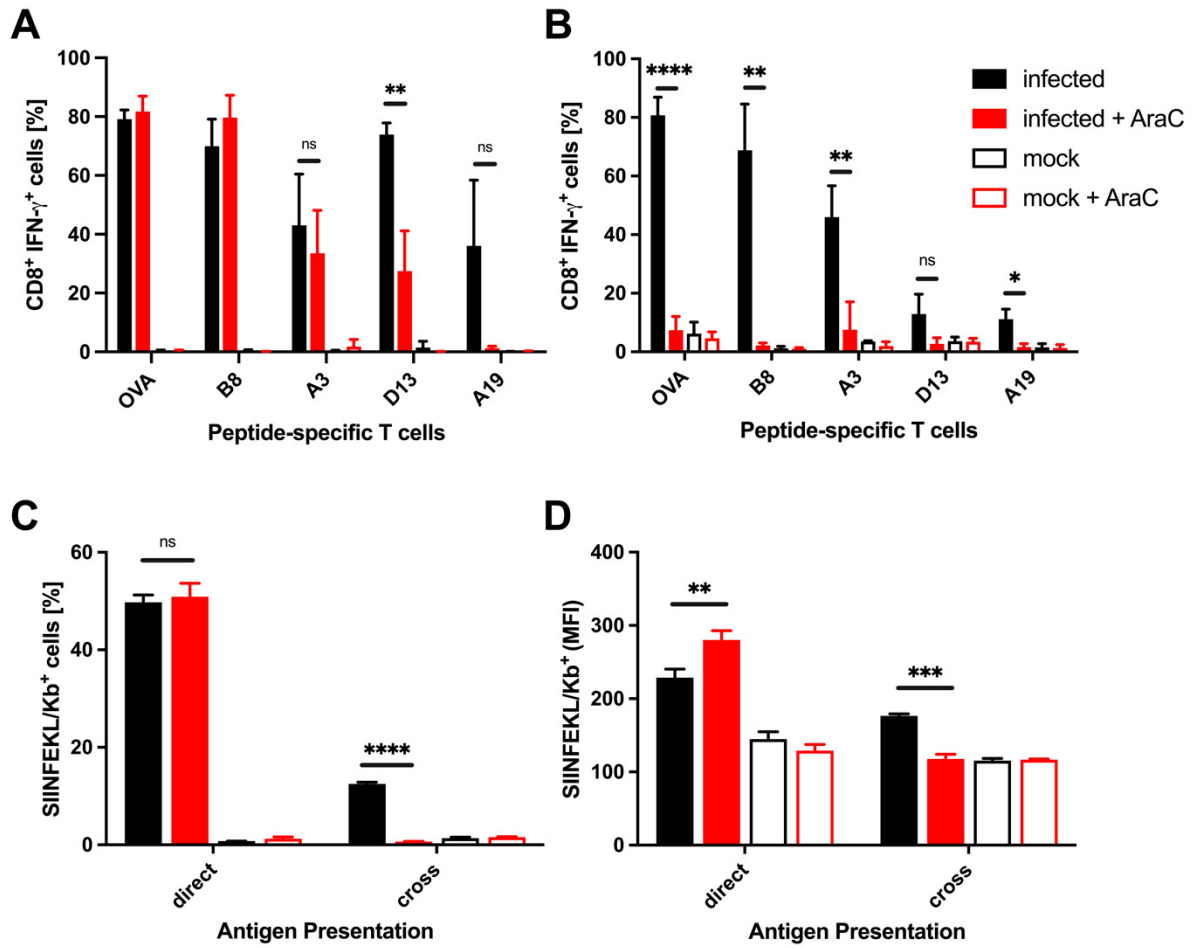

Figure 4: AraC in feeder cells abolishes T cell activation and antigen presentation by cross-presenting BMDCs. GM-CSF-BMDCs generated from C57BL/6 mice and MHC-I mismatched feeder cells (murine Cloudman S91 melanoma cells) were infected with MVA-PK1L-OVA expressing ovalbumin under the control of the early promoter PK1L at MOI 1, or mock-infected for either 16 h or 10 h in the presence or absence of 40 µg/ml AraC. For the analysis of cross-presentation infected and mock-infected feeder cells were treated with PUVA, washed and cocultured with uninfected BMDCs for 16 h. Directly infected (A) as well as cross-presenting BMDCs (B) were analyzed for their ability to activate $CD8^+$ T cells as well as for the surface expression of SIINFEKL/Kb (C, D). T cell activation was determined using flow cytometry as frequency of IFN-γ expressing T cells specific for different viral antigens or the recombinant antigen OVA (A, B). The SIINFEKL/Kb-loading ability is presented as frequency (C) and MFI (D) of $CD11c^+$ $MHC\text{-}II^{high}$ SIINFEKL/Kb^+ cells. Data are depicted as mean ± SD of three independent experiments. Statistical significance (P); * = $p \leq 0{,}05$; ** = $p \leq 0{,}01$; *** = $p \leq 0{,}001$; **** = $p \leq 0{,}0001$; ns = not significant; unpaired, two-tailed Student's t-test.

be seen in Figure 4C, a comparable number of SIINFEKL/Kb^+ cells was induced following AraC treatment and MVA infection, indicating that AraC does not affect the presentation of early antigens by directly infected cells. However, AraC appeared to confer an advantage on directly infected BMDCs, as can be seen in the significantly increased surface expression of SIINFEKL/Kb-complexes (Figure 4D). As Supplementary Figure 1 shows, early gene expression was not affected by AraC in MVA-infected feeder cells, resulting in almost similar, or slightly increased protein

levels compared to infected control cells. The transcription of early genes within the viral core is activated by its release into the cytoplasm. After transcription, these early mRNAs are released into the cytoplasm for translation (145). Since the poxviral replication is organized in a cascade-like way, early gene expression is most often terminated, when the transcription of intermediate genes has started. Because early gene expression is not shut down in the presence of AraC, early transcripts continue to be produced. This ongoing expression of early genes could be a major reason for the increased presentation of SIINFEKL/Kb-complexes on the surface of AraC-treated cells, as more early antigens are produced that can be processed and loaded on MHC-I molecules. Unfortunately, as shown in Supplementary Figure 1, I observed only slight differences, if any, in protein levels of early expressed OVA between MVA-infected and AraC-treated feeder cells and control cells. However, the difference in protein levels might be more apparent after a shorter infection time, for instance 6 or 8 h post infection.

Interestingly, cross-presenting BMDCs cocultured with feeder cells, that had been infected in the presence of AraC, showed a significantly decreased frequency of SIINFEKL/Kb$^+$ cells, as well as significantly reduced MFIs (Figure 4C, D). Taken together, these data suggest that AraC acts differently on directly presenting BMDCs, which were infected in the presence of AraC, and cross-presenting BMDCs, that never had direct contact with AraC but were cocultured with infected and AraC-treated feeder cells, regarding the ability to activate CD8$^+$ T cells as well as to process and present antigen on the cell surface. It seems that even though early antigens were abundantly synthesized by infected feeder cells in the presence of AraC, BMDCs apparently were not able to cross-present these antigens.

Because the efficiency of cross-presentation of antigens is closely connected with the maturation phenotype of the DC, I analyzed the frequency as well as the surface expression of the costimulatory molecules CD40 and CD86 as well as MHC-II as maturation markers. In agreement with the T cell activation and antigen presentation data (Figure 4), AraC had no impact on the frequencies of CD40$^+$, CD86$^+$, or MHC-II$^+$ directly infected and AraC-treated BMDCs (Figure 5A-C). However, in the presence of AraC, directly infected BMDCs showed a significantly enhanced surface expression of CD40 and a slight tendency to express increased levels of CD86 at the cell surface (Figure 5D, E). In line with the previous results, AraC-treatment also seemed to be beneficial for the surface expression of costimulatory molecules in BMDCs infected in

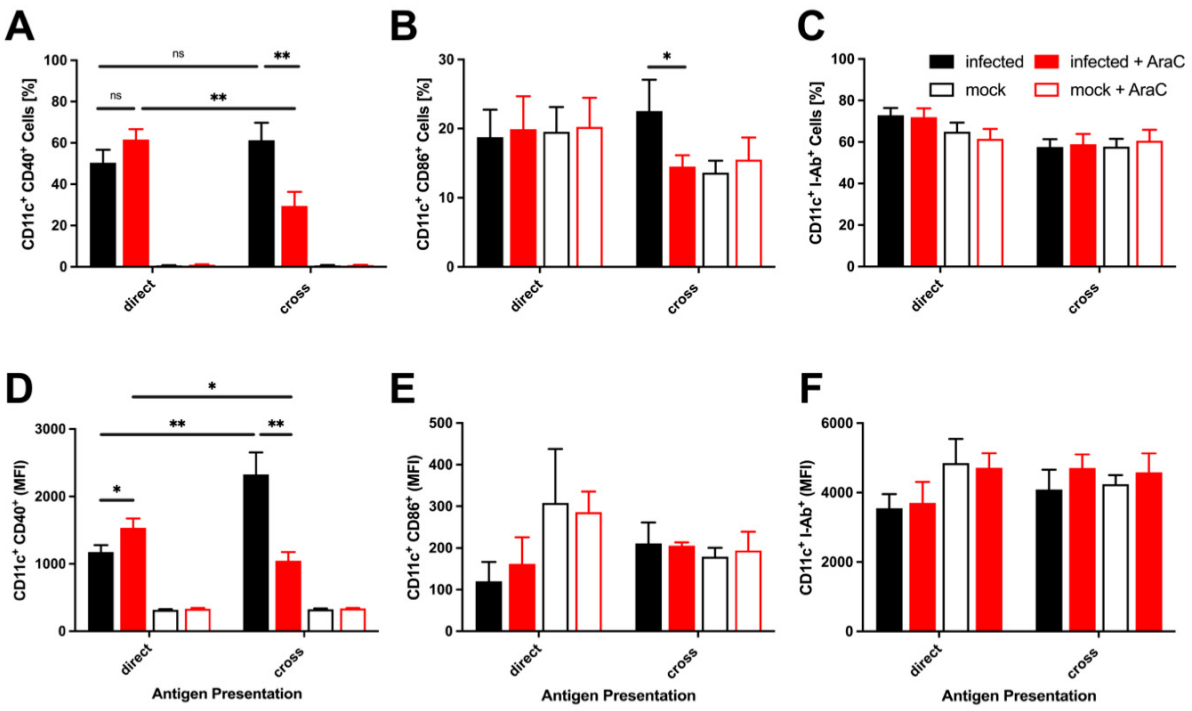

Figure 5: AraC in feeder cells impairs maturation of cross-presenting BMDCs. GM-CSF BMDCs from C57BL/6 mice and feeder cells (murine Cloudman S91 melanoma cells) were infected with MVA-PK1L-OVA at MOI 1, or mock-infected for either 16 h or 10 h in the presence or absence of 40 µg/ml AraC. For the analysis of cross-presentation MVA-infected and mock-infected feeder cells were treated with PUVA, washed and cocultured with uninfected BMDCs for 16 h. Directly infected as well as cross-presenting $CD11c^+$ $MHC\text{-}II^{high}$ BMDCs were analyzed for CD40 (A, D), CD86 (B, E) and MHC-II expression (C, F). Data are depicted as frequencies (A-C) as well as MFIs (D-F) and represent means ± SD of three independent experiments. Statistical significance (P); * = $p \leq 0{,}05$; ** = $p \leq 0{,}01$; ns = not significant; unpaired, two-tailed Student's t-test.

the presence of AraC. AraC-treated and MVA-infected BMDCs expressed only MHC-II at levels comparable to those of the control (Figure 5D). However, AraC-treatment of feeder cells in a cross-presentation setting resulted in a significant reduction in the frequency of $CD40^+$ and $CD86^+$cells (Figure 5A, B). The number of $MHC\text{-}II^+$ cells and the surface expression of MHC-II and CD86 were not affected by AraC in either directly infected or in cross-presenting BMDCs (Figure 5C, E, F). Indeed, in an earlier experiment, I had observed high steady-state expression of CD86 and MHC-II in mock-infected or mock cross-presenting BMDC controls, which is very likely to have been caused by the use of GM-CSF for the differentiation of bone marrow cells to BMDCs (146, 147). Collectively, these results suggest that the presence of AraC in feeder cells impaired the maturation of cross-presenting BMDCs, while directly infected BMDCs treated with AraC were not affected or even had a slight advantage, especially in the expression of CD40.

Because previous research has shown that MVA and vaccinia virus infection results in

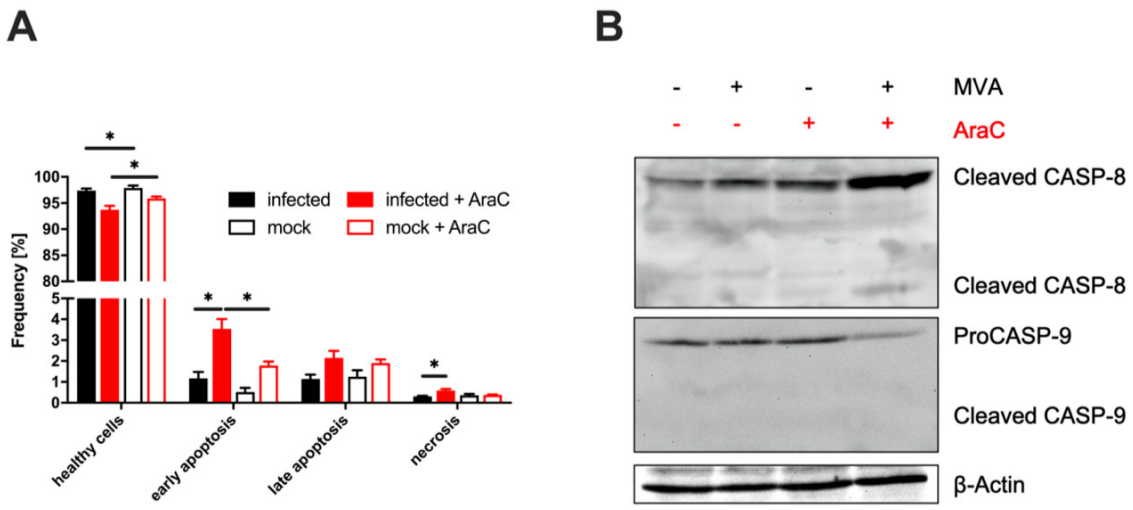

Figure 6: AraC induces apoptotic cell death. Feeder cells (murine Cloudman S91 melanoma cells) were infected with MVA-PK1L-OVA at MOI 1 or mock-infected for either 16 h in the presence or absence of 40 µg/ml AraC. The induced cell death was determined by flow cytometry (A) and western blot (B). Plasma membrane integrity and permeability were determined using annexin V and propidium iodide, and frequencies of healthy (annexin V^- PI^-), early (annexin V^+ PI^-) and late (annexin V^+ PI^+) apoptotic as well as necrotic (annexin V^- PI^+) cells determined. Data are presented as means ± SD of two independent experiments. Statistical significance (P); * = $p \leq 0{,}05$; ns = not significant; unpaired, two-tailed Student's t-test (A). For western blot analysis, protein was isolated from samples and protein levels of cleaved CASP-8 and -9 as well as proCASP-9 determined. Data represent one blot representative of three experiments (B).

massive apoptosis, I investigated whether AraC augments cell death caused by MVA. Cell death was analyzed by monitoring the plasma membrane integrity and permeability using annexin V and PI as well as western blot analysis. Annexin V and PI facilitate the use of flow cytometry in the determination of healthy, late and early apoptotic cells as well as necrotic cells. As shown in Supplementary Figure 2, healthy cells were evident in the flow cytometric analysis as annexin V^- and PI^-, due to their intact membrane integrity and insignificant PI permeability. However, apoptotic cells expose more and more phosphatidylserine (PS) as cell death advances, and therefore early apoptotic cells appeared annexin V^+ but PI^-, while late apoptotic cells were double-positive. Since necrotic cells were permeable to PI and lost membrane integrity completely, they were plotted during a flow cytometric analysis in the upper left quadrant as annexin$^-$ PI^+ cells (Supplementary Figure 2). I observed that AraC treatment in addition to MVA-infection resulted in a significantly increased frequency of early apoptotic as well as necrotic cells. MVA infection alone only tended to increase the number of early apoptotic cells (Figure 6A). By determining the levels of cleaved CASP-8 and -9 as well as proCASP-9 using western blot analysis, I observed that

MVA-infection in combination with AraC resulted in the highest level of cleaved CASP-8. However, AraC-treatment alone appeared to induce levels of cleaved CASP-8 that were comparable to cells infected only with MVA. This suggests an additive rather than synergistic effect of AraC and MVA-infection on CASP-8 levels. Besides proCASP-9, I was unable to detect cleaved CASP-9 (Figure 6B). In summary, AraC-treatment alone led to a slight increase in apoptosis, but AraC in combination with MVA-infection led to a sharp and significant rise in apoptosis as well as necrosis. Assuming an additive effect, these findings suggest that AraC and MVA-infection might impact the same signaling pathway in feeder cells. Nevertheless, the impact of AraC, especially on antigen processing and induced cell death, might be cell type-dependent. It is well known that the feeder cell line, which was chosen for my cross-presentation experiments on account of the characteristic MHC-I mismatch, has several defects in the type I interferon signaling pathway (148). To rule out the possibility that the previously described effect of AraC was exclusively specific for Cloudman S91 melanoma cells, I studied the impact of AraC on other MHC-I mismatched feeder cell lines.

5.2. The AraC-effect is cell type dependent

To gain insight into the distinct effects that AraC had on directly infected and cross-presenting BMDCs, and to exclude the possibility that MVA-infection might by a Cloudman (CM) cell-specific effect, GM-CSF-BMDCs originating from Balb/c and C3H mice were infected with MVA and used as MHC-I mismatched feeder cells for C57BL/6 presenter BMDCs. Activation of $CD8^+$ T cells specific for OVA expressed as early antigen (Figure 7A) or the viral early antigen B8 (Figure 7B) as well as late antigens D13 (Figure 7C) and A19 (Figure 7D) by cross-presenting BMDCs was tested. When CM cells were used as feeder cells, numbers of IFN-γ^+ $CD8^+$ T cells were significantly reduced for all tested T cell lines, as shown previously (Figure 4B, Figure 7). However, we observed that the stimulation of $CD8^+$ T cells by cocultures of BMDCs with MHC-I mismatched feeder cells after infection in the presence of AraC (which activated cross-presenting C57BL/6 presenter BMDCs) was similar, whether the $CD8^+$ T cells were specific for early antigens (Figure 7A, B) or late antigens (Figure 7C, D).

In addition to IFN-γ expression, TNF-α expression by $CD8^+$ T cells was determined. TNF-α is usually not as abundantly expressed in T cells as IFN-γ, and is therefore a more sensitive marker for T cell activation. However, the number of TNF-α^+ T cells was

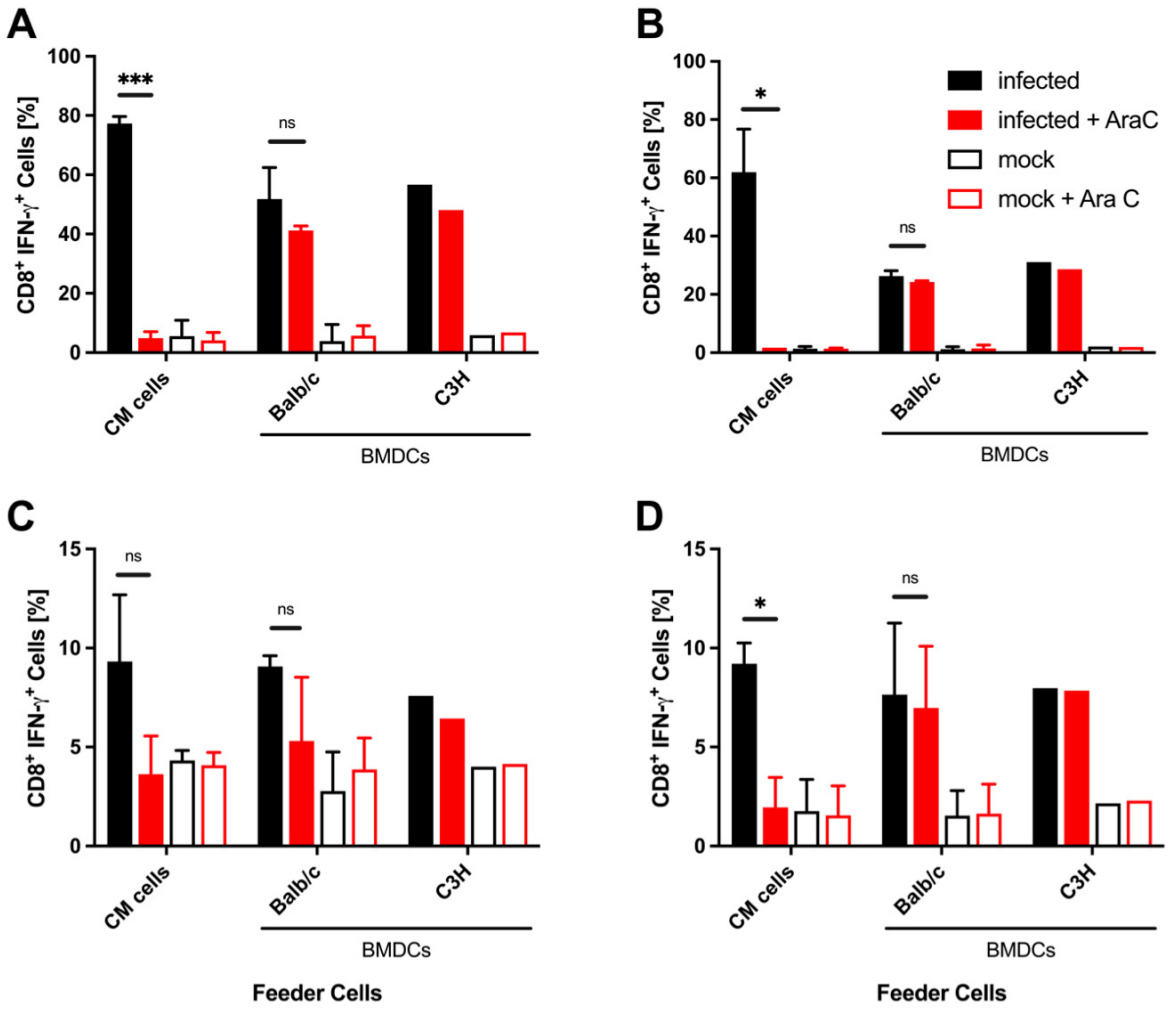

Figure 7: The effect of AraC on BMDCs as feeder cells on cross-presentation in cocultures is non-significant as compared to CM cells used as feeders. Murine Cloudman S91 melanoma cells (CM) as well as GM-CSF-BMDCs derived from Balb/c and C3H mice, both MHC-I mismatched, were infected with MVA-PK1L-OVA at MOI 1, or mock-infected for 10 h in the presence or absence of 40 µg/ml AraC. After PUVA treatment and washing, feeder cells were cocultured with cross-presentation competent BMDCs generated from C57BL/6 mice. The ability to license cross-presenting BMDCs for the activation of $CD8^+$ T cells specific for the recombinant antigen OVA (A) and the viral antigens B8 (B), D13 (C) and A19 (D) was determined using flow cytometry as frequency of IFN-γ expressing T cells. Data are depicted as mean ± SD of one (C3H) or two (CM & Balb/c) independent experiments. Statistical significance (P); * = $p \leq 0{,}05$; *** = $p \leq 0{,}001$; ns = not significant; unpaired, two-tailed Student's t-test.

also comparable between AraC-treated and -untreated infected feeder BMDCs (Supplementary Figure 3). These results suggest that when BMDCs (which are professional APCs) were used as feeder cells for cross-presenting BMDCs, the effect of AraC to prevent cross-presentation in this coculture was abolished which is in strong contrast to CM cells used as feeders.

Since it remained unclear whether the effect of AraC was CM specific, I then assessed the MHC-I mismatched cell lines J774 (reticulum cell sarcoma) as well as WEHI3 (leukemia cells) for their ability to activate cross-presenting BMDCs in the presence of

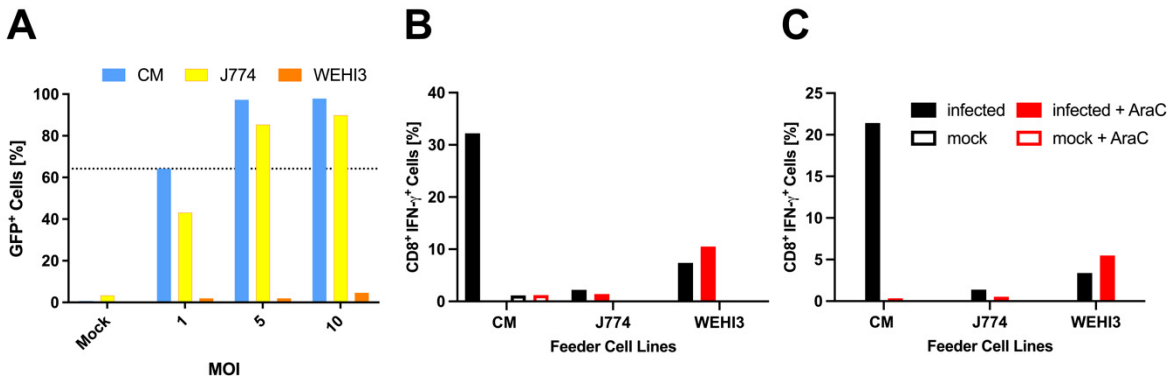

Figure 8: The effect of AraC on immune cells as feeder cells is non-significant compared to that on CM cells. Cloudman S91 melanoma (CM), reticulum cell sarcoma (J774), leukemia cells (WEHI3), all of murine origin and MHC-I mismatched, were infected with MVA-P7.5-eGFP at different MOIs for 10 h. The infection efficiency of each cell line was determined by the frequency of eGFP$^+$ cells using flow cytometry (A). All feeder cells were infected with MVA-PK1L-OVA at MOI 1, or mock-infected for 10 h in the presence or absence of 40 µg/ml AraC. Afterwards, feeder cells were PUVA-treated, washed and cocultured o. n. with C57BL/6 BMDCs. The ability of the different feeder cell lines to activate cross-presenting BMDCs for stimulation of CD8$^+$ T cells was analyzed using OVA- (B) as well as B8-specific (C) CD8$^+$ T cell lines. T cell activation was determined using flow cytometry as frequency of IFN-γ producing T cells. Data are derived from one experiment.

AraC. All cell lines were tested for their susceptibility to MVA using another recombinant MVA expressing eGFP at different MOI, to ensure equal infection. CM and J774 cells showed a comparable GFP expression, while WEHI3 cells were difficult to infect at MOI 10 (Figure 8A). There was a striking difference in the abilities of CM, J774 and WEHI3 cells to license cross-presenting BMDCs for T cell activation, as shown for OVA- (Figure 8B) and B8 specific CD8$^+$ T cells (Figure 8C).

Even though the ability to activate cross-presenting BMDCs was in general low, both the J774 and WEHI3 cell lines appeared to be resistant to the AraC-effect (Figure 8B, C). Due to the poor T cell responses obtained after coculturing of MVA-infected J774 or WEHI3 cells with cross-presenting BMDCs, my data raised the question of whether the tested cell lines were suitable for my cross-presentation assay. However, it seemed that the effect of AraC on the immune cells J774 and WEHI3 was non-significant compared to that on CM cells. Therefore, I analyzed the MHC-I mismatched non-immune cells DF1 (chicken fibroblast cells), HeLa (human cervical carcinoma cells) and MEF cells (mouse embryonic fibroblast cells) for their ability to license cross-presenting BMDCs in the presence or absence of AraC. As shown in Figure 9A, MEF cells were harder to infect with MVA than were CM, DF1 or HeLa cells. Therefore, MEF cells were infected at MOI 5, while the other cell lines, including CM cells, were infected at MOI 1 (Figure 9A). DF1 and HeLa cells showed an inability to activate cross-

presenting BMDCs for T cell stimulation in the presence of AraC comparable to that seen in CM cells (Figure 9B, C). Collectively these results show that the activation of cross-presentation by not only CM cells but also the non-immune DF1 and HeLa cells was impaired by AraC. These results suggest that AraC might inhibit a particular innate immune pathway which may be compensated by other pathways in professional APCs or immune cells.

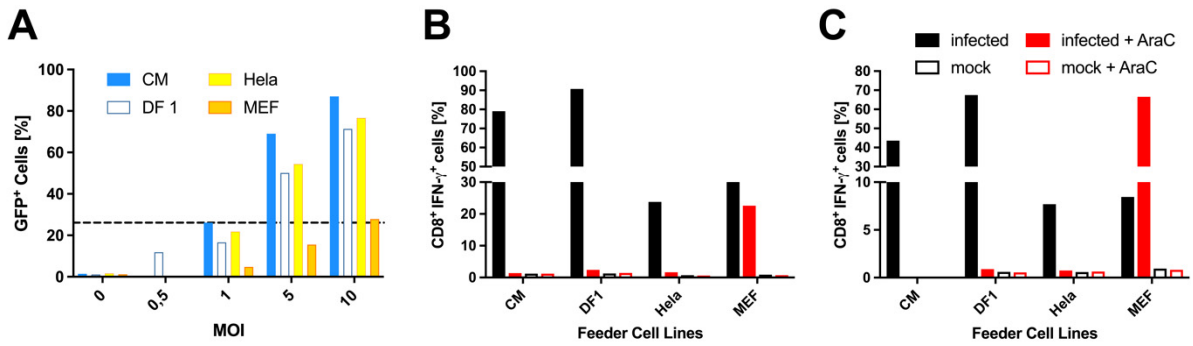

Figure 9: AraC has not only an effect on CM cells, but also affects other cell lines when those are used as feeder cells for cross-presenting BMDCs. Murine Cloudman S91 melanoma (CM), chicken fibroblast (DF 1), human cervical carcinoma (HeLa) and mouse embryonic fibroblast (MEF) cells, all MHC-I mismatched, were infected with MVA-P7.5-eGFP at different MOIs for 5 h. The infection efficiency of each cell line was determined by the frequency of eGFP$^+$ cells by flow cytometry (A). All feeder cells were infected with MVA-PK1L-OVA either at MOI 1 (CM, DF1, HeLa cells) or at MOI 5 (MEF), or mock-infected for 10 h in the presence or absence of 40 µg/ml AraC. Thereafter, feeder cells were PUVA treated, washed and cocultured o. n. with C57BL/6 BMDCs. The ability of the different feeder cell lines to activate cross-presenting BMDCs for stimulation of CD8$^+$ T cells was analyzed using OVA- (B) as well as B8-specific (C) CD8$^+$ T cell lines. T cell activation was determined using flow cytometry as frequency of IFN-γ producing T cells. Data are derived from one experiment.

5.3. Next-generation sequencing reveals new insights into the phenotype caused by AraC

To elucidate which pathway might be impaired by treatment with AraC, I sequenced RNA from feeder cells that had been either infected with MVA or mock-infected in the presence or absence of AraC and cross-presenting BMDCs. In order to determine the time post infection at which it is most appropriate to analyze gene expression and the capacity of feeder cells to license cross-presenting BMDCs for T cell activation, feeder cells were infected for between four and 12 h at MOI 1 before being cocultured with BMDCs and incubation of feeder-BMDC-cocultures with peptide-specific CD8$^+$ T cells. As shown in Figure 10A, a minimum time of 8 h of infection was necessary to achieve IFN-γ expression in about 70 % of the OVA-specific T cells. Shorter infections of less

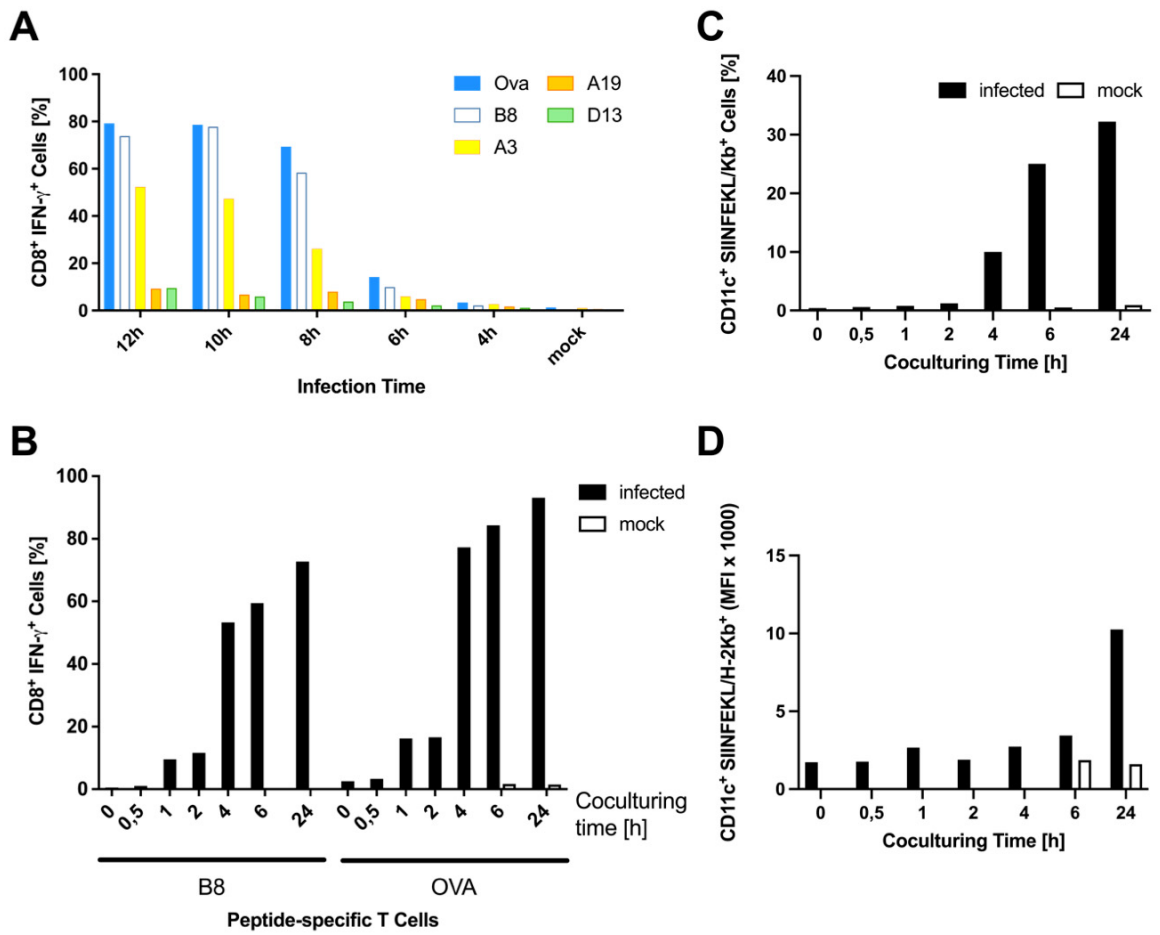

Figure 10: Feeder and presenter kinetics during cross-presentation. Murine Cloudman S91 melanoma (CM) were used as feeder cells and infected with MVA-PK1L-OVA at MOI 1 for different periods of time (A) or mock-infected. After PUVA treatment, washing and coculturing with C57BL/6 BMDCs for 10h, feeder cells were analyzed for their potential to activate BMDCs for cross-presentation and activation of $CD8^+$ T cells specific for recombinant or viral antigens. T cell activation was determined using flow cytometry as frequency of IFN-γ expressing T cells (A). Feeder cells were infected with MVA-PK1L-OVA at MOI 1, or mock-infected for 16 h. Prior to coculturing with BMDCs for different periods of time, feeder cells were treated with PUVA and washed. Using flow cytometry, the ability to cross-present antigen was shown by the activation of $CD8^+$ T cells as determined by the expression of IFN-γ (B) as well as the presentation of SIINFEKL/Kb-complexes at the cell surface of BMDCs (C, D). Data are depicted as frequencies (A, B, C) or mean fluorescent intensities (D) and are derived from one experiment.

than 8 h resulted in a dramatic drop in T cell activation to below 20 % (Figure 10A). For this reason, an infection time of 8 h was chosen for the subsequent RNA sequencing.

To analyze the impact of AraC on cross-presenting BMDCs, I determined the most suitable coculturing time by incubating MVA-infected feeder cells (16 h post infection) with BMDCs in a kinetic study for 0.5-24 h. Because this experiment was only performed once, these results should be interpreted with caution. However, this kinetic study was sufficient to determine the most appropriate infection and coculturing time in preparation for the subsequent RNA sequencing. As can be seen from Figure 10B,

there was a sharp decline in the activation of B8- and OVA-specific T cells by cross-presenting BMDCs for coculturing times lower than 4 h. In addition, staining for SIINFEKL/Kb revealed that cross-presenting BMDCs needed at least 4 h for the processing, loading and presentation of SIINFEKL/Kb-complexes at the cell surface (Figure 10C). The MFIs of SIINFEKL/Kb$^+$ cells showed only a slight increase until 24 h (Figure 10D). These results indicate that the time for which the BMDCs are cocultured with infected feeder cells should be at least 4 to 6 h before analysis of gene expression in cross-presenting BMDCs using RNA sequencing.

To determine how AraC influences the gene expression in MVA-infected feeder cells, cells were infected with MVA-PK1L-OVA or mock-infected, in the presence or absence of AraC. Eight hours post-infection, RNA was isolated from the MVA-infected feeder cells. RNA sequencing was performed using Illumina HiSeq3000/4000 in collaboration with Karl Köhrer and Patrick Petzsch from the Genomic & Transcriptomics Laboratory of the Biologisch-Medizinische Forschungszentrum (BMFZ) at the Heinrich-Heine-University in Düsseldorf. As shown in Figure 11, the comparison of MVA-infected feeder cells with or without AraC treatment revealed many genes that exhibit fold change (FC)-values greater than or equal to 1.5 or less than or equal to -2, and p-values less than or equal 0.05, indicating that AraC had an impact on the expression of various genes. Among these genes, I identified several target genes involved in important innate immune signaling pathways and DNA-sensing (Figure 11A). Furthermore, as can be seen from Figure 11, Ara-treatment in addition to MVA-infection resulted in a greater number of genes that showed upregulated expression. Interestingly, most of these upregulated genes were mapped with gene ontology (GO)-terms assigned to the biological processes antigen processing and presentation, innate immune response and cell death (Figure 11B, C). The gene expression profile of infected and AraC-treated feeder cells therefore implies that AraC might influence several innate immune signaling pathways as well as apoptosis, necrosis and cell death.

Two approaches have been chosen to analyze the impact of AraC on gene expression in cross-presenting BMDCs. In the first approach, the influence of AraC on gene expression was studied using BMDCs, which were cocultured for 4 h with MVA-infected or mock-infected feeder cells in the presence or absence of AraC. RNA sequencing was performed from CD11c$^+$ cells, which were sorted from the feeder-presenter-cocultures described above using flow cytometry. After filtering off data with

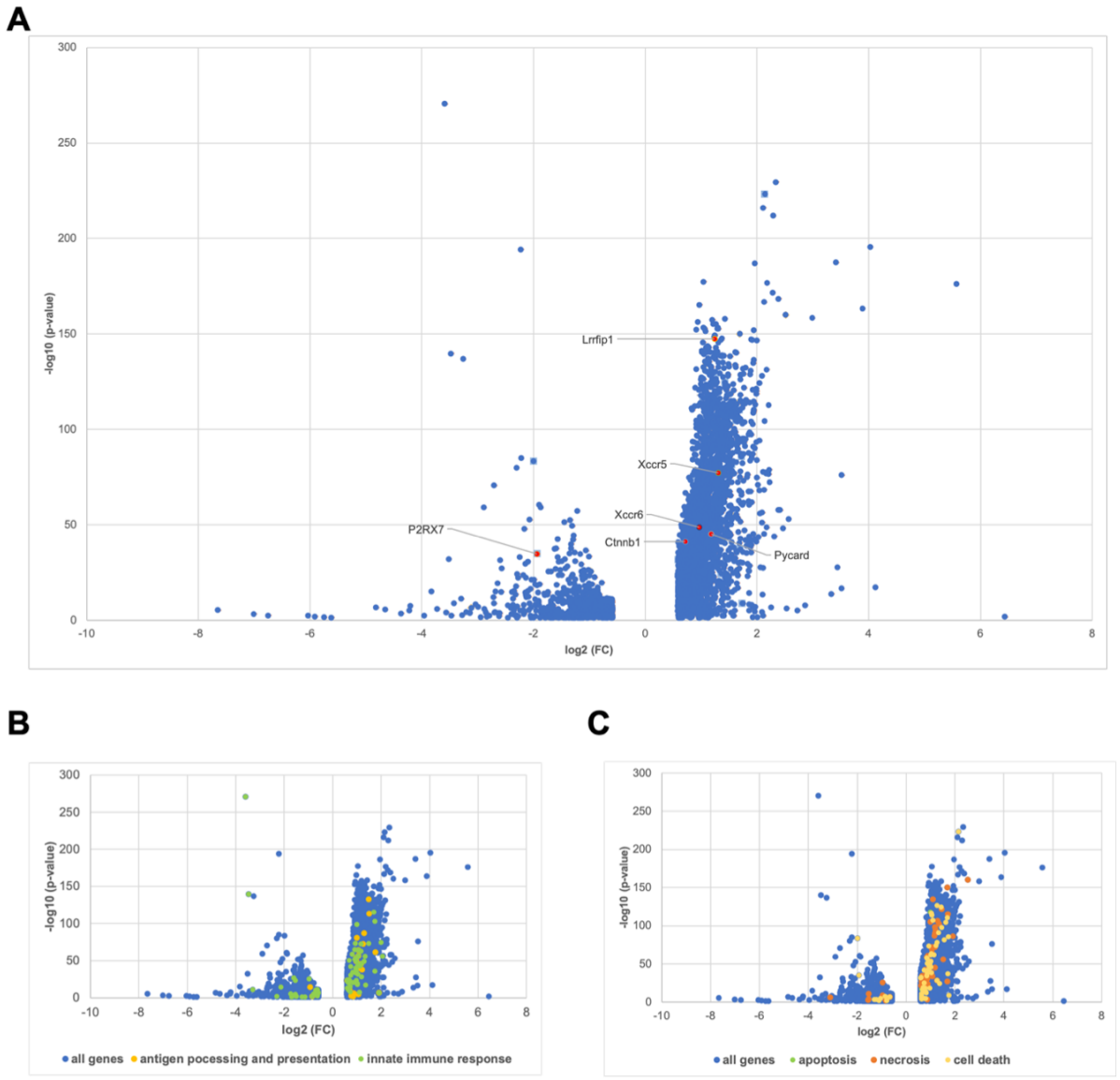

Figure 11: Comparative gene expression profiles of infected feeder cells treated with or without AraC. Feeder cells were infected with MVA at MOI 1, or mock-infected in the presence or absence of 40 µg/ml AraC. Cells were harvested at 8 h post infection and RNA was isolated for subsequent RNA sequencing using Illumina HiSeq3000/4000. Data are depicted as FC ≥ 1,5 or ≤ -1,5 and p ≤ 0,05 and > 0 from the comparison of MVA-infected with infected and AraC-treated feeder cells and are represented as means of 4 biological replicates. The volcano plots illustrate genes involved in important innate immune signaling pathways (A), antigen processing and presentation, innate immune response (B), and cell death (C).

a fold change lower than 2 and higher than -2 as well as data with insignificant p-values ($p > 0.05$), the comparison “CD11c MVA AraC ($CD11c^+$ BMDCs cocultured with MVA infected and AraC treated feeder cells) vs. CD11c MVA ($CD11c^+$ BMDCs cocultured with MVA-infected feeder cells)” only comprised data with positive FC. This was surprising and indicated that in comparison to “CD11c MVA AraC”, changes in gene expression observed in “CD11c MVA” samples were all upregulations (Figure 12A). Usually, NGS-data are more balanced and show a vast number of down- as well as

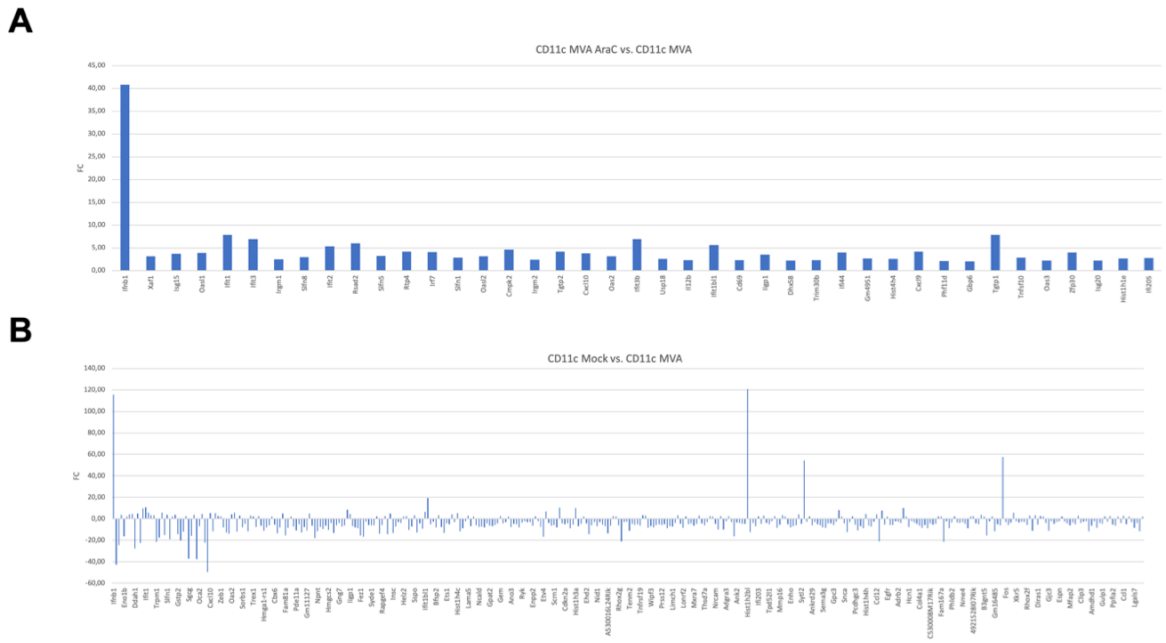

Figure 12: The comparison BMDCs cocultured with infected and AraC-treated feeder cells vs. BMDCs cocultured with feeder cells infected without AraC show in contrast to other comparisons a one-sided gene expression pattern. MHC-I mismatched feeder cells (murine Cloudman S91 melanoma cells) were infected with MVA-PK1L-OVA at MOI 1, or mock-infected in the presence or absence of 40 µg/ml AraC for 16 h. After PUVA-treatment and washing, feeder cells were cocultured with GM-CSF-BMDCs derived from C57BL/6 mice for 4 h. Viable $CD11c^+$ cells were sorted using flow cytometry and RNA isolated. RNA sequencing was performed using Illumina HiSeq300/4000. Data are depicted as FC ≥ 2 or ≤ -2 and p ≤ 0,05 and > 0 from the comparison of $CD11c^+$ cells (BMDC) cocultured with feeder cells infected in the presence of AraC and $CD11c^+$ cells cocultured with feeder cells infected in the absence of AraC (A). Similarly, the comparison of $CD11c^+$ cells cocultured with either MVA-infected or mock-infected feeder cells is shown (B). Data are presented as means of 4 biological replicates.

upregulated genes, as in the comparison “CD11c Mock ($CD11c^+$ BMDCs cocultured with mock-infected feeder cells) vs. CD11c MVA ($CD11c^+$ BMDCs cocultured with MVA-infected feeder cells)” (Figure 12B).

In the second approach to investigate the effect of AraC on gene expression in cross-presenting BMDCs, the differential gene expression in SIINFEKL/Kb^+ and SIINFEKL/Kb^- cells was analyzed using BMDCs, which were cocultured for 6 h with MVA-infected or mock-infected feeder cells. Because BMDCs cocultured with MVA-infected feeder cells do not present SIINFEKL/Kb at the cell surface following AraC-treatment, I was only able to study the gene expression of this group in the absence of AraC. In addition, a more extended coculture period of 6 h was chosen for this group, on account of the marginal and delayed presentation of SIINFEKL/Kb at the cell surface when assessed earlier. Figure 13 illustrates that I and II IFNs in particular showed differential gene expression between MVA-infected and mock-infected groups, while AraC-treatment affected the expression of genes assigned to I and II

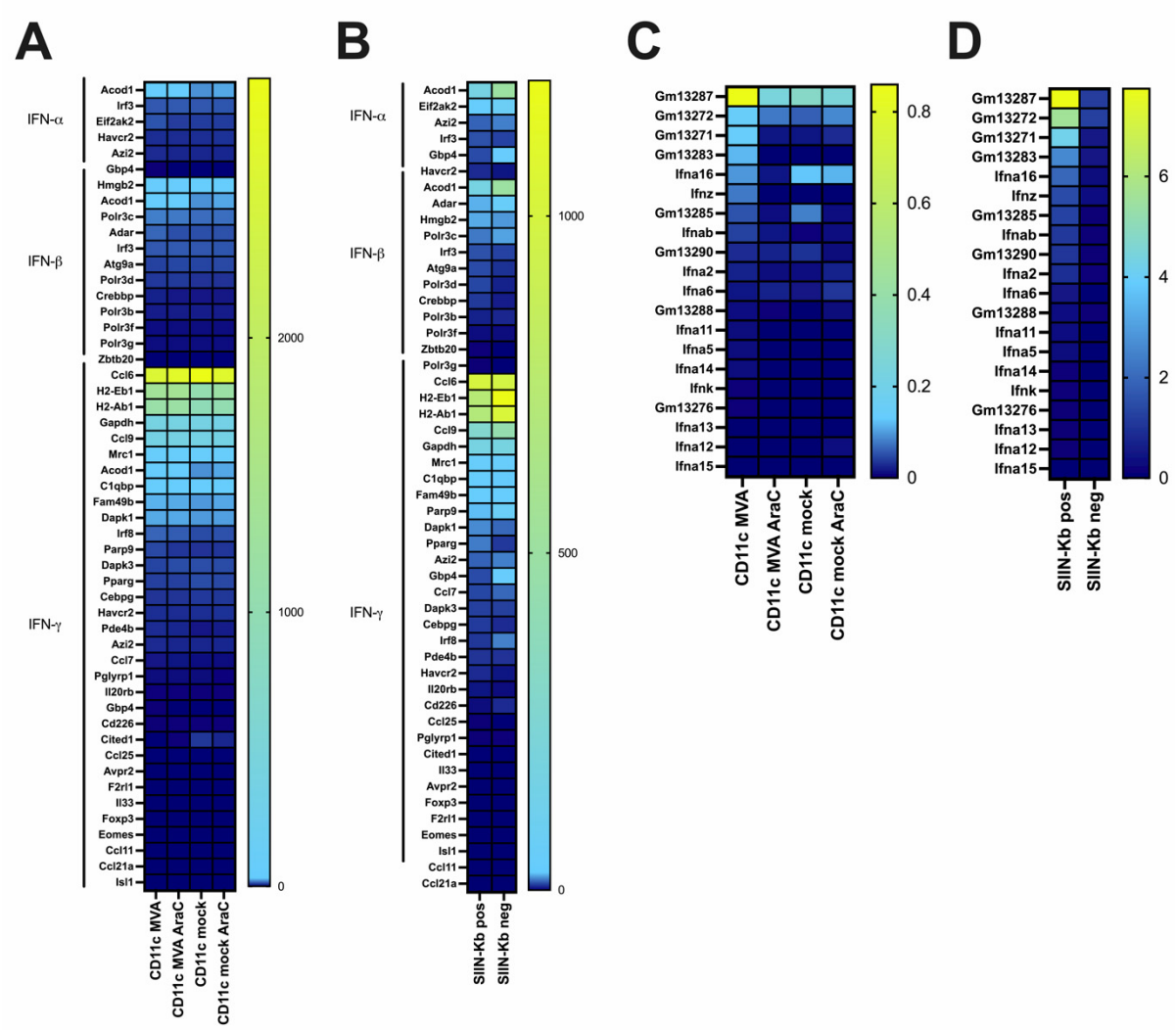

Figure 13: Genes related to IFN-β and -γ as well as exogenous dsRNA are differently expressed in cross-presenting BMDCs. MHC-I mismatched feeder cells (murine Cloudman S91 melanoma cells) were infected with MVA-PK1L-OVA at MOI 1, or mock-infected in the presence or absence of 40 µg/ml AraC for 16 h. After PUVA-treatment and washing, feeder cells were cocultured with GM-CSF-BMDCs derived from C57BL/6 mice for 4 h. Viable $CD11c^+$ cells were sorted by flow cytometry and RNA isolated (A, C). Feeder cells were infected with MVA-PK1L-OVA at MOI 1 or mock-infected for 16 h. Feeder cells were PUVA-treated and washed and cocultured with BMDCs for 6 h. Viable $CD11c^+$ SIINFEKL/Kb^+ cells were sorted using flow cytometry and RNA isolated (B, D). RNA sequencing was performed using Illumina HiSeq300/4000. Data are depicted as reads per kilobase of transcript per million mapped reads (RPKM) values and are presented as means of 4 biological replicates.

IFNs only negligibly (Figure 13A). Surprisingly, SIINFEKL/Kb^+ cells showed a lower expression of I and II IFN-related genes than the SIINFEKL/Kb^- population (Figure 13B). In addition to interferons, GO-term analysis indicated that many of the differentially regulated genes were assigned to the sensing of exogenous RNA. In line with these results, “CD11c MVA” differed considerably from AraC-treated as well as mock-infected samples (Figure 13C). Likewise, SIINFEKL/Kb^+ cells showed a higher expression of genes linked to components of the exogenous dsRNA signaling pathway

(Figure 13D). Hence, the gene expression analysis from cross-presenting BMDCs suggests that AraC mostly affects signaling pathways involved in the recognition and processing of exogenous dsRNA, rather than I and II IFN signaling. I observed robust upregulated expression of genes associated with exogenous dsRNA sensing in BMDCs cocultured with MVA-infected feeder cells, suggesting that differently regulated genes involved in I and II IFN signaling and observed in the presence of AraC, or in the absence of MVA-infection might be a consequence of the missing dsRNA sensing by cross-presenting BMDCs.

All in all, analysis of the gene expression in AraC-treated and MVA-infected feeder cells as well as cross-presenting BMDCs suggests that AraC may interfere with a signaling pathway that is activated after MVA-infection in feeder cells and is crucial for the activation of BMDCs for cross-presentation of antigen. This activated signaling pathway could be that of a PRR or adaptor protein involved in the induction of common innate immune signaling pathways during MVA-infection.

5.4. I IFNs support the licensing of cross-presenting BMDCs

Due to the important role of I IFNs during infection with MVA, I analyzed the role of IFNAR and IFN-β in the process of cross-presentation. IFNAR is expressed by almost every cell and recognizes I IFNs, resulting in the activation of JAK-STAT signaling (149, 150). IFNAR KO BMDCs were cocultured with feeder cells mock-infected or infected with one of two different MVA recombinants. The IFN-γ expression was determined in $CD8^+$ T cells specific for viral antigens (B8, A3, D13 or A19) or the recombinant antigen OVA. Feeder cells were either infected with MVA-PK1L-OVA (Figure 14A), which resulted in the expression of OVA early during viral replication, or MVA-P11-OVA (Figure 14B), which led to OVA-expression late during viral transcription in the replication cycle. As shown in Figure 14A, IFNAR KO BMDCs showed almost the same ability as wildtype BMDCs to activate $CD8^+$ T cells for the production of IFN-γ. Only IFNAR KO BMDC-feeder cocultures that were incubated with T cells specific for late antigens apparently showed a reduced ability to activate IFN-γ^+ T cells (Figure 14A). Interestingly, in feeder cells infected with MVA-P11-OVA, I observed a significantly reduced ability to license cross-presenting BMDCs for the activation of T cells specific for late antigens, including OVA, in the absence of IFNAR (Figure 14B). These results seem to suggest an essential role for IFNAR during MVA-infection in the stimulation of $CD8^+$ T cell responses for late expressed viral antigens

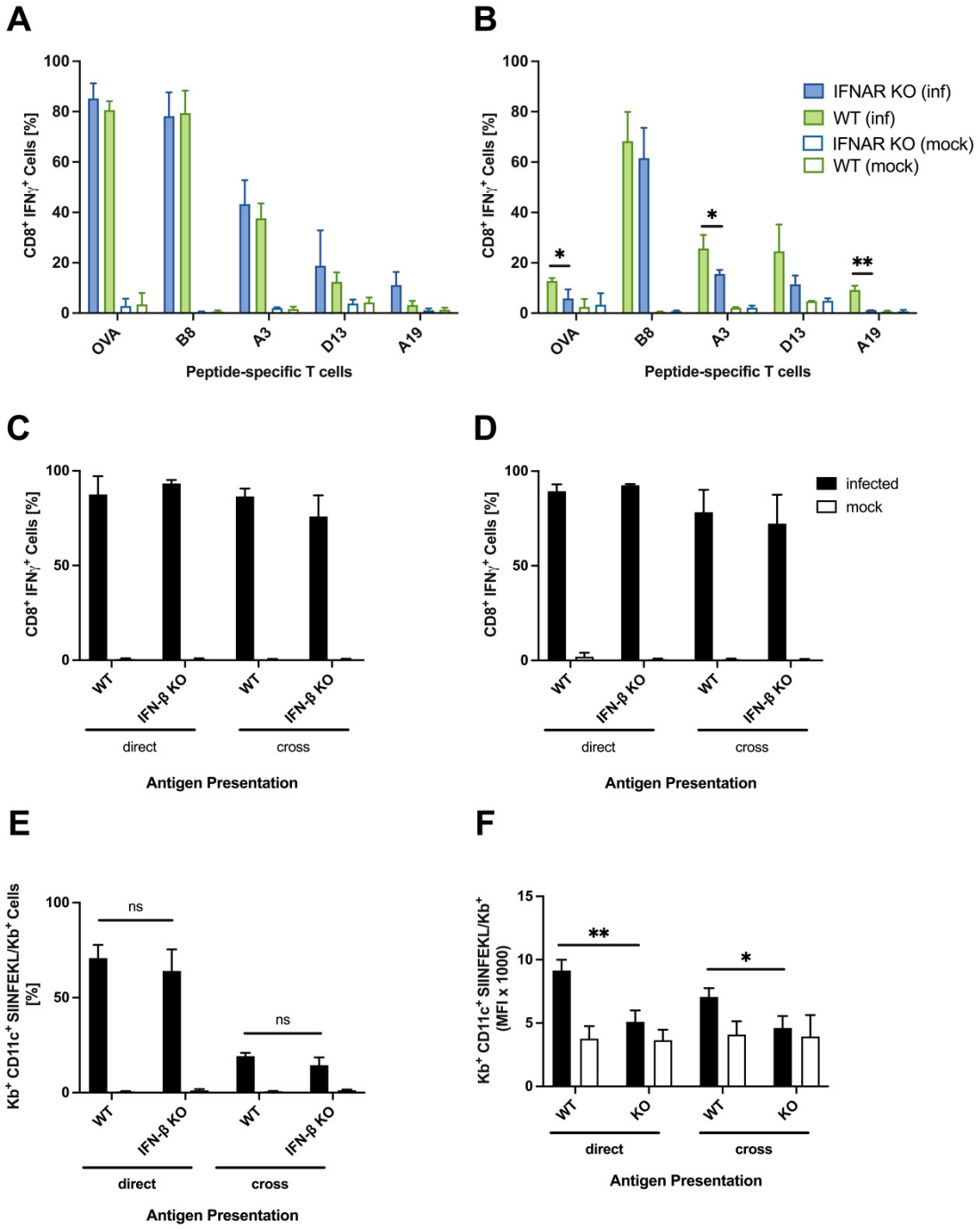

Figure 14: Type I interferon signaling is important for the activation of cross-presenting BMDCs *in vitro* during infection with MVA. MHC-I mismatched feeder cells (murine Cloudman S91 melanoma cells) were infected with MVA-PK1L-OVA (A) or MVA-P11-OVA (B) at MOI 1, or mock-infected for 10 h, respectively. After PUVA-treatment and washing, feeder cells were cocultured with uninfected IFNAR KO BMDCs for 16 h which were generated from IFNAR$^{-/-}$ mice (IFNAR KO) using GM-CSF. Cross-presenting IFNAR KO BMDCs were analyzed for their ability to activate CD8$^+$ T cells specific for the recombinant antigen OVA, expressed after infection with MVA-PK1L-OVA early (A) or MVA-P11-OVA late during viral infection (B), or for indicated viral antigens (A, B). GM-CSF-BMDCs generated from C57BL/6 IFN-β$^{-/-}$ mice (IFN-β KO) as well as MHC-I mismatched feeder cells were infected with MVA-PK1L-OVA at MOI 1, or mock-infected for either 16 h or 10 h. Directly infected as well as cross-presenting BMDCs were analyzed for their ability to activate OVA- (C) or B8-specific CD8$^+$ T cells (D) as well as for the surface expression of SIINFEKL/Kb (E, F). T cell activation was determined using flow cytometry as frequency of IFN-γ expressing T cells (A-D). The SIINFEKL/Kb-loading ability is represented as frequency (E)

and MFI (F) of CD11c$^+$ MHC II^{high} SIINFEKL/Kb$^+$ cells. Data are depicted as mean ± SD of three independent experiments. Statistical significance (P); * = $p \leq 0,05$; ** = $p \leq 0,01$; ns = not significant; unpaired, two-tailed Student's t-test.

by cross-presenting BMDCs.

In addition to the autocrine and paracrine signaling of I IFNs, I investigated the role of IFN-β produced by BMDCs during infection with MVA. Missing IFN-β production in directly infected or cross-presenting BMDCs had no impact on the ability to stimulate OVA- or B8-specific CD8$^+$ T cells (Figure 14C, D). In agreement with the T cell activation results, the frequency of SIINFEKL/Kb$^+$ cells in cultures of directly infected IFN-β KO BMDCs and cross-presenting IFN-β KO BMDCs cocultured with infected feeder cells was comparable (Figure 14E). However, the amount of SIINFEKL/Kb-complexes presented at the cell surface differed significantly between IFN-β KO and control BMDCs for directly infected DCs as well as in the cross-presentation setting (Figure 14F). Taken together, these results suggest that IFNAR, which mediates the positive feedback loop induced by I IFNs, was particularly important for the activation of CD8$^+$ T cells by cross-presenting BMDCs against antigens with low abundance. In addition, IFN-β seems to be important in the initiation of efficient surface expression of SIINFEKL/Kb-complexes by directly infected as well as cross-presenting BMDCs.

In order to investigate whether IFNAR deficiency in cross-presenting BMDCs also had an influence on the induced cytokine response during infection with MVA, I collected supernatants from feeder-BMDC-cocultures and determined the presence or absence of various cytokines. As can be seen in Figure 15A, the absence of IFNAR resulted in a steady decline in the production of IL-1α, IFN-β, and TNF-α, but the production of MCP-1 as well as IL-6 was also decreased in cross-presenting BMDCs. Interestingly, I observed a strong drop in the same cytokines produced by cross-presenting BMDCs cocultured with infected and AraC-treated feeder cells (Figure 15B). In addition to IL-1α, IFN-β, TNF-α, MCP-1 and IL-6, supernatants were tested for the content of other cytokines (Supplementary Figure 4). However, these cytokines were only produced at background levels and therefore not considered to be important. Moreover, the LEGENDplex assay was performed only once, and these results, especially IL-23 and IL-27, should therefore be interpreted with caution. In particular, cytokines that were produced at background levels need to be detected in another experiment to avoid drawing hasty conclusions (Supplementary Figure 4). In contrast to the cytokine production in the cross-presenting BMDCs, directly infected and AraC-treated BMDCs

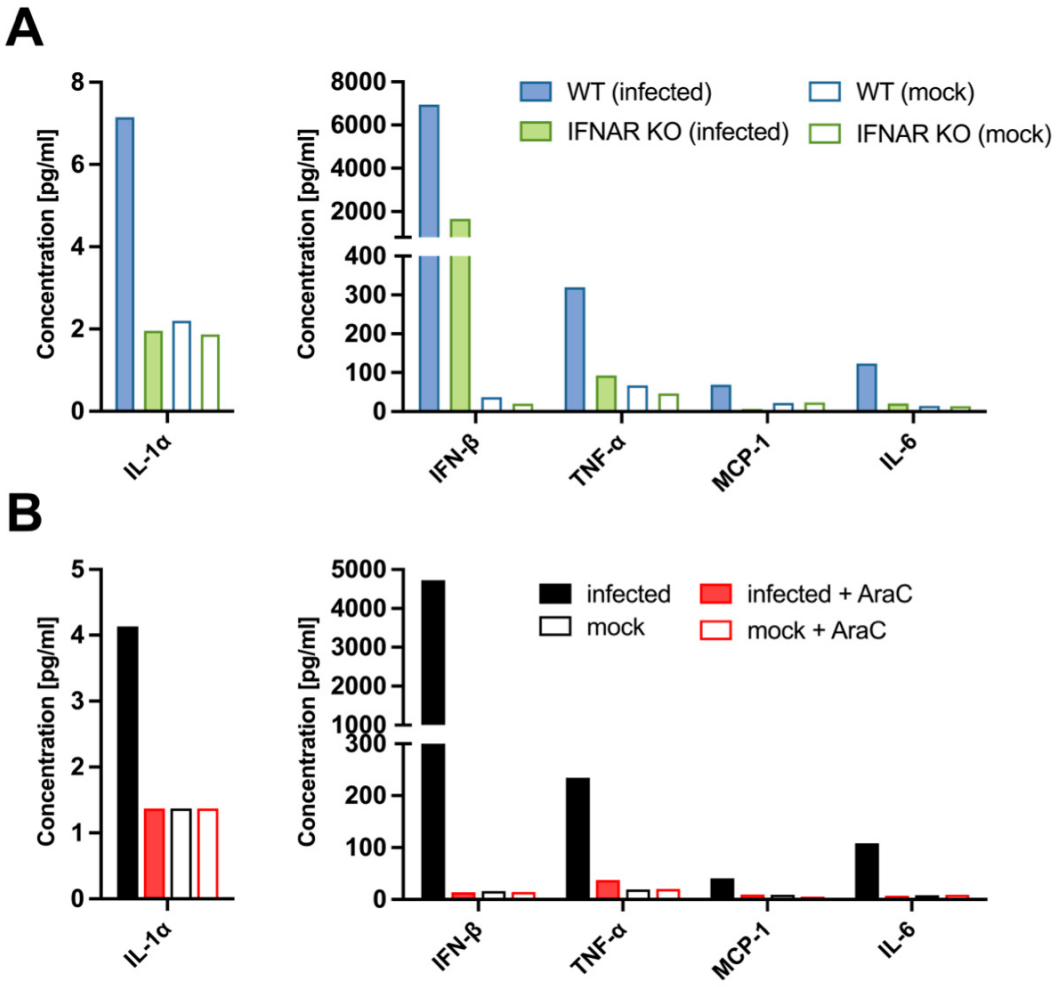

Figure 15: Cocultures of infected feeder cells with IFNAR KO BMDCs resemble the cytokine response of infected and AraC-treated feeder plus BMDC cocultures. Supernatants from cocultures of MVA-infected (MOI 1), or mock-infected feeder cells with IFNAR KO or WT BMDCs (A) or supernatants from cocultures of AraC-treated and infected feeder cells with WT BMDCs (B) were collected at 16 h post infection and cytokines were determined with LEGENDplex assays. Data are derived from one experiment.

showed only marginally decreased TNF-α levels compared to infected BMDCs (Figure 16A). IFN-β levels of AraC-treated and infected BMDCs were approximately 200 pg/ml higher than in control supernatants (Figure 16A). In addition to IFN-β and TNF-α, also IL-1α and IL-6 were detected in supernatants from infected and AraC-treated cell culture supernatants but were at levels almost comparable to those from the control supernatants (Figure 16A). Furthermore, some additional cytokines were produced at levels comparable to those from supernatants from mock-infected BMDCs (Supplementary Figure 5A). It is possible that some of the cytokines induced by MVA-infection in feeder-BMDC-cocultures were produced by feeder cells, and to rule this out, supernatants from MVA-infected and mock-infected feeder cells were analyzed for various cytokines. Most of the tested cytokines and chemokines were not produced

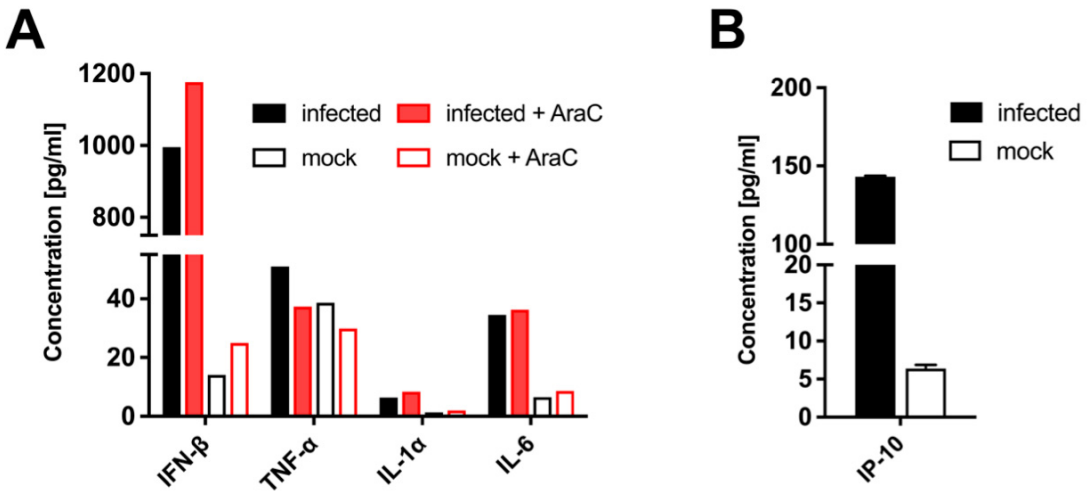

Figure 16: Cytokine response by directly infected cells. Supernatants from GM-CSF-BMDCs (A) and feeder cells (murine Cloudman S91 melanoma cells) (B), infected with MVA-PK1L-OVA at MOI 1, or mock-infected, were collected at 16 h post infection and cytokine concentrations were determined with Cytoplex assays. Data are derived from one (A) or two (B) experiments.

by infected feeder cells, with the exception of IP-10 (Figure 16B, Supplementary Figure 5B). Surprisingly, I also observed that BMDCs cocultured with infected feeder cells produced more IFN-β than directly infected BMDCs (Supplementary Figure 6). However, these results should be interpreted with caution, as the LEGENDplex and Cytoplex assays were performed only once due to their high cost. In summary, the cytokine response of IFNAR-deficient cross-presenting BMDCs resembled the cytokine pattern induced by cross-presenting BMDCs which had been cocultured with infected and AraC-treated feeder cells. These cytokines must be exclusively produced by cross-presenting BMDCs, because the only cytokine detected in supernatants from infected feeder cells was IP-10. My findings suggest that AraC might interfere with an important innate signaling pathway crucial for the cross-presentation of MVA-antigens, and is also possibly involved in the I IFN or IFNAR signaling pathway in BMDCs, as the cytokine pattern is similar in IFNAR-deficient cross-presenting BMDCs and AraC-treated feeder-BMDC-cocultures.

5.5. STING is crucial for the induction of I IFNs by directly infected and cross-presenting BMDCs

Previous research has shown that the induced type I interferon response during infection with MVA is exclusively dependent on STING (1, 47). However, the impact of STING on the stimulation of $CD8^+$ T cell responses and for the cross-presentation of

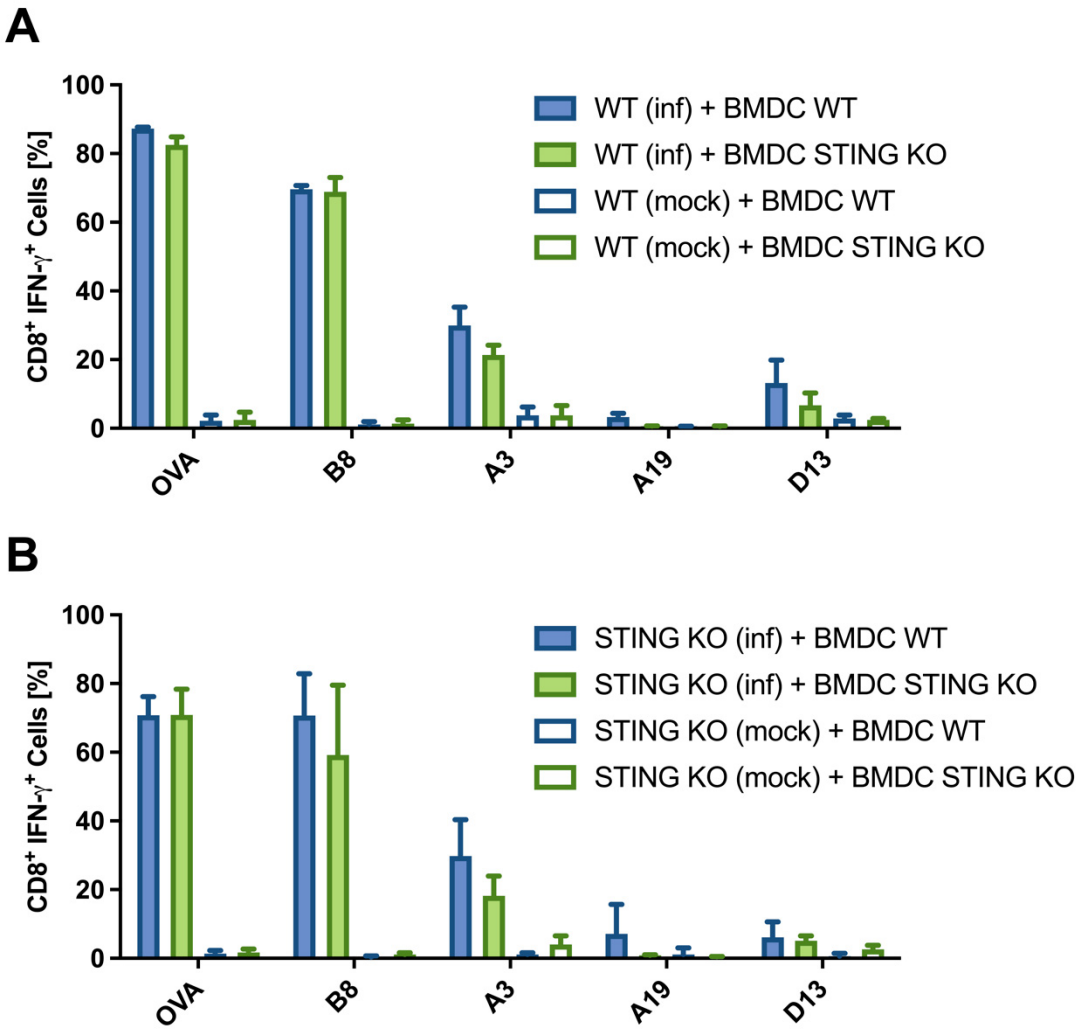

Figure 17: STING is not required in feeder nor in presenter cells for the reactivation of antigen-specific CD8$^+$ T cells by cross-presenting BMDCs. MHC-I mismatched wildtype (A) and STING KO feeder cells (B) were infected with MVA-PK1L-OVA at MOI 1, or mock-infected for 12 h, treated with PUVA, washed and cocultured with GM-CSF-BMDCs generated from either STING KO mice or WT-littermates. Cross-presentation competent BMDCs were analyzed 12 h post cocultivation for their ability to activate CD8$^+$ T cells specific for the indicated recombinant or viral antigens. T cell activation was determined using flow cytometry as frequency of IFN-γ expressing CD8$^+$ T cells. Data are depicted as mean ± SD of two independent experiments.

antigens during infection with MVA has not been addressed to date. To study the role of STING in feeder cells and BMDCs as presenter cells, I generated a feeder cell line deficient in STING, using murine Cloudman S91 melanoma cells (Supplementary Figure 7). I also investigated the effect of STING deficiency in presenter cells using GM-CSF-BMDCs generated from homozygous STING KO mice. To study the impact of STING on presenter cells, I analyzed the ability of cross-presenting BMDCs to activate CD8$^+$ T cells by coculturing either STING KO or WT BMDCs with MVA-infected feeder cells. As shown in Figure 17A, I observed a comparable ability to activate CD8$^+$

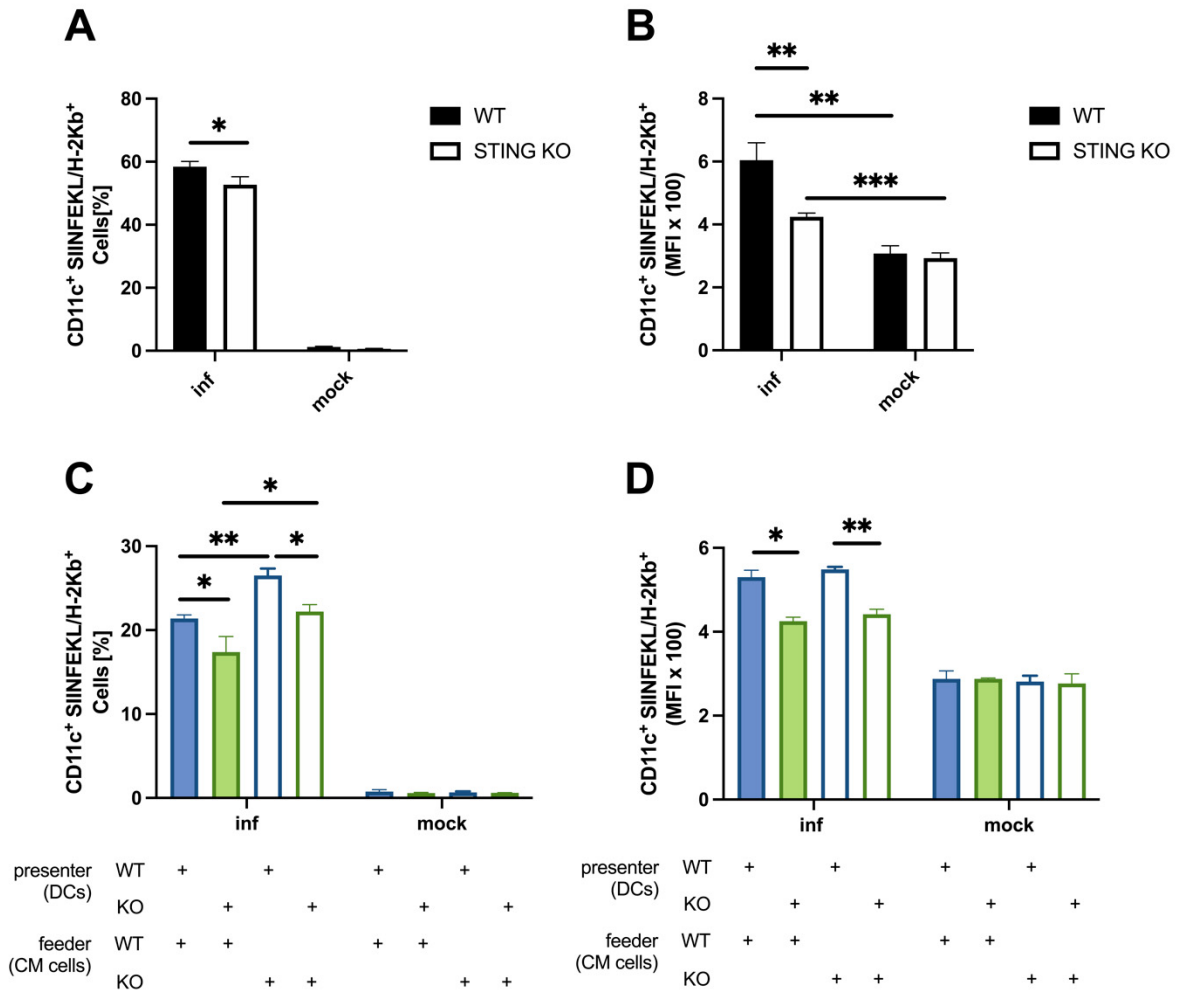

Figure 18: STING in BMDCs is crucial for efficient antigen processing and presentation, whereas STING deficiency in feeder cells has a positive effect on the loading and presentation of SIINFEKL/MHC-I complexes at the cell surface. GM-CSF-BMDCs generated from STING KO mice and WT-littermates (A, B) or feeder cells with or without STING (C, D) were infected with MVA-PK1L-OVA at MOI 1, or mock-infected for 12 h. Infected or mock-infected feeder cells were treated with PUVA, washed and cocultured with uninfected STING KO or WT BMDCs for 20 h. The SIINFEKL/MHC-I loading ability of directly infected (A, B) and cross-presenting BMDCs (C, D) was analyzed using flow cytometry. Data are presented as one experiment representative of two independent experiments as frequencies (A, C) and mean fluorescent intensities (MFI) and are depicted as mean ± SD of n=3 BMDC preparations from individual mice per group. Statistical significance (P); * = $p \leq 0,05$; ** = $p \leq 0,01$; *** = $p \leq 0,001$; unpaired, two-tailed Student's t-test.

T cell lines by STING KO and control BMDCs. Similarly, $CD8^+$ T cells showed a comparable IFN-γ production after being cocultured with either STING KO or WT feeder cells plus wildtype BMDCs (Figure 17B). Because the $CD8^+$ T cell lines used for this study represent antigen-experienced cells, which only need a low epitope density on the cell surface of antigen-presenting cells to become activated, even significant differences in the amount of peptide/MHC I-complexes presented by STING KO and control BMDCs may still result in proper T cell activation (151, 152). Therefore,

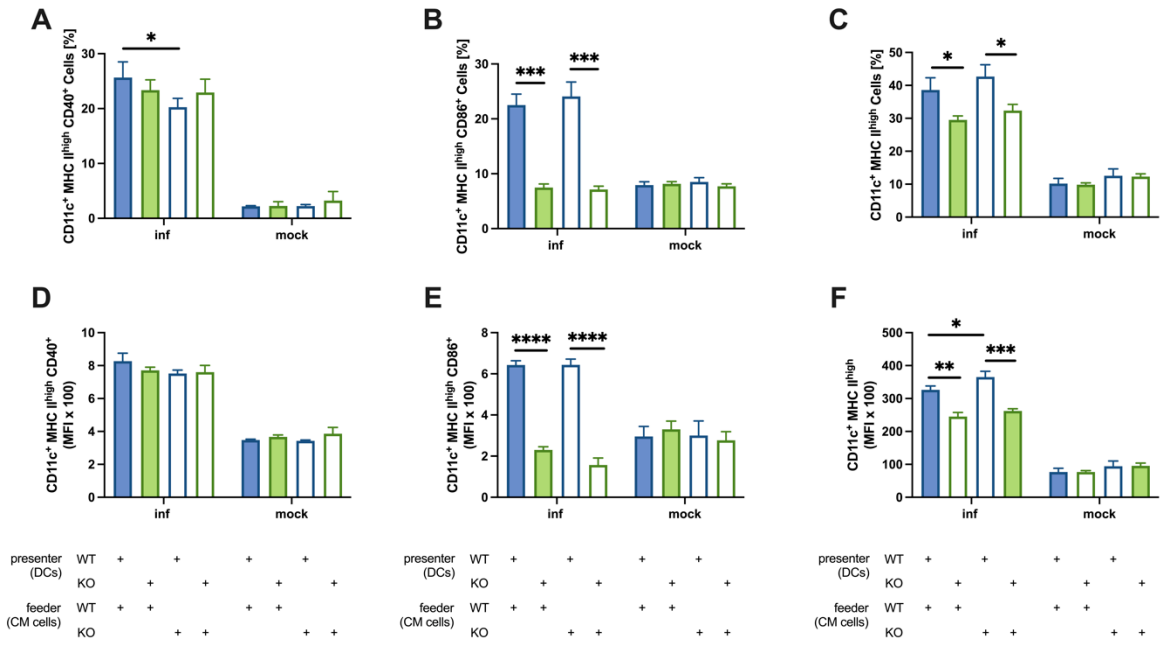

Figure 19: STING in presenter cells supports DC maturation. STING KO and WT feeder cells were infected with MVA-PK1L-OVA at MOI 1, or mock-infected for 12 h. After PUVA-treatment and washing, feeder cells were cocultured with BMDCs generated from STING KO or WT-littermates for 20 h. The maturation phenotype of cross-presenting BMDCs was analyzed for the expression of CD40 (A, D), CD86 (B, E) and MHC II (C, F) using flow cytometry. Data are presented as frequencies (A-C) or mean fluorescent intensities MFI (D-F) and depicted as one experiment representative of two independent experiments, each with n=3 BMDC preparations from individual mice per group. Statistical significance (P); * = $p \leq 0,05$; ** = $p \leq 0,01$; *** = $p \leq 0,001$; **** = $p \leq 0,0001$; unpaired, two-tailed Student's t-test.

I analyzed the role of STING in the surface expression of SIINFEKL/Kb-complexes (in addition to T cell activation) for directly infected as well as cross-presenting BMDCs. In the direct infection setting I observed a significantly reduced frequency and MFI for SIINFEKL/Kb$^+$ cells in the absence of STING compared to control BMDCs (Figure 18A, B). These results suggest that STING affects the number of SIINFEKL/Kb$^+$ cells, but is even more important for determining the amount of SIINFEKL/Kb-complexes presented at the cell surface of directly infected BMDCs.

To gain insight into the role of STING in antigen processing and presentation during cross-presentation, I studied both STING-deficient feeder and STING KO BMDCs by coculturing STING deficient BMDCs and control BMDCs with either infected or mock-infected STING KO or WT feeder cells. Consistent with the results from directly infected BMDCs, STING-deficiency in cross-presenting BMDCs resulted in a significantly decreased number of SIINFEKL/Kb$^+$ cells and reduced surface expression of SIINFEKL/Kb-complexes (Figure 18C, D). Surprisingly, infected STING KO feeder cells demonstrated a significantly improved ability to license cross-presenting BMDCs

compared to infected WT feeder cells, irrespective of the presence or absence of STING in presenter cells (Figure 18C). However, cross-presenting BMDCs cocultured with MVA-infected STING KO feeder cells showed equivalent MFIs to wildtype feeder-BMDC-cocultures, indicating that the feeder cell phenotype had no impact on the efficacy of surface expression of SIINFEKL/Kb-complexes by cross-presenting BMDCs (Figure 18D). Taken together, these data indicate that STING is important for the sensing of MVA in directly infected presenter cells but plays a minor role in the activation of cross-presenting BMDCs by infected feeder cells.

Due to the substantial number of studies that describe the association of STING with the maturation of DCs (54-57), I investigated the impact of STING on the maturation phenotype of cross-presenting BMDCs using CD40, CD86 and MHC-II expression as markers. Again, I investigated the impact of STING in feeder cells and BMDCs by coculturing cross-presenting STING-deficient or control BMDCs with either STING KO or wildtype feeder cells. As shown in Figure 19A, I observed a significantly reduced number of $CD40^+$ cells after coculturing STING KO feeder cells with wildtype BMDCs. However, the STING phenotype of feeder cells had no impact on the surface expression of CD40 by cross-presenting BMDCs (Figure 19D). Interestingly, STING-deficiency in presenter cells resulted in a significant drop in $CD86^+$, and $MHC\text{-}II^+$ cell numbers (Figure 19B, C). Consistent with these results, I observed that STING KO presenter cells showed a significantly reduced surface expression of CD86 and MHC-II (Figure 19E, F). In conclusion, these results indicate that the maturation phenotype of cross-presenting BMDCs was affected by STING in both feeder and presenter cells. On the one hand, STING in feeder cells negatively affected the number of cross-presenting BMDCs that expressed CD40, while the efficiency of CD40 expression was not affected. On the other hand, STING in presenter cells was crucial for MHC-II expression and important for the expression of CD86. Therefore, my results suggest that STING in the presenter cell supports the efficient maturation of cross-presenting BMDCs during MVA-infection.

As previously demonstrated by Dai *et al.*, the induced I IFN response during infection of BMDCs with MVA was exclusively dependent on STING (1). In agreement with this study, I observed considerably reduced IFN-α and -β levels in the absence of STING in supernatants from directly infected BMDCs (Figure 20A, B). Likewise, supernatants from cocultures of infected feeder cells and STING-deficient BMDCs showed an abrogated IFN-α and -β response, indicating that STING in presenter cells was crucial

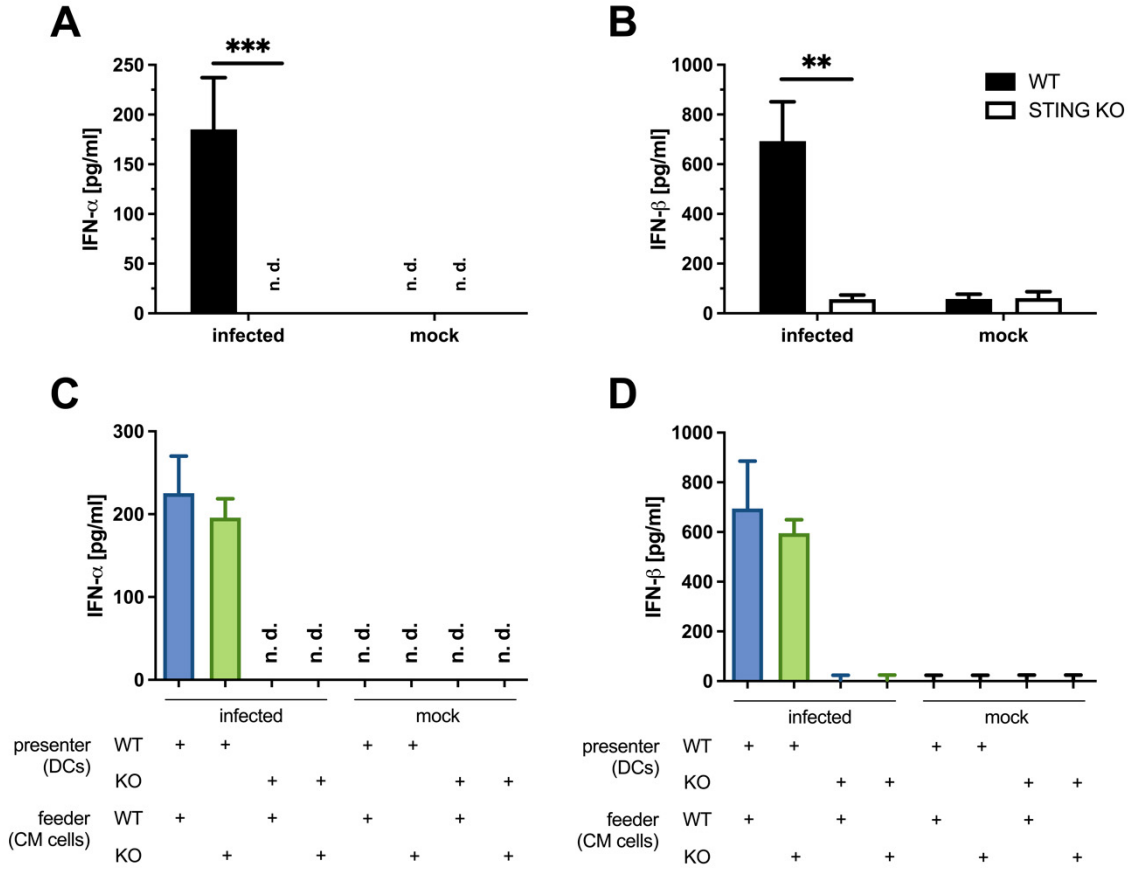

Figure 20: STING in presenter cells is essential for the induction of type I interferon. BMDCs generated with GM-CSF from STING KO mice and WT-littermates were infected with MVA-PK1L-OVA at MOI 1, or mock-infected (A, B). For the analysis of the induced type I interferon response of cross-presenting STING KO and WT BMDCs, STING KO and WT feeder cells were infected with MVA-PK1L-OVA at MOI 1 or mock-infected for 12 h, PUVA-treated, washed and cocultured with STING KO and WT BMDCs (C, D). Twelve hours post infection (A, B) or cocultivation (C, D) cell culture supernatants of directly infected cells (A, B) as well as coculture supernatants (C, D) were collected and IFN-α (A, C) and -β (B, D) concentrations determined by ELISA. Data are depicted as mean ± SD of n=4 (A, B) and n=3 (C, D) BMDC preparations from individual mice per group from three independent experiments. Statistical significance (P); ** = $p \leq 0{,}01$; *** = $p \leq 0{,}001$; n. d. = not detected.

for the induced I IFN response, and that the feeder cell phenotype was negligible (Figure 20C, D).

Taken together, these results indicate that STING has a strong impact on antigen processing and presentation, BMDC maturation, and induced I IFN response in both directly infected and cross-presenting BMDCs. However, the effects of STING deficiency on presenter and feeder cells were different. Surprisingly, my findings suggest that the absence of STING in feeder cells seems to be beneficial for antigen presentation by cross-presenting BMDCs, as I observed an enhanced number of SIINFEKL/Kb^{+} cells in feeder STING KO-BMDC-cocultures. However, STING deficiency in feeder cells appeared to reduce CD40 expression. In addition to the role

of STING in feeder cells, I demonstrated that STING in presenter cells was not only crucial for the efficient processing and presentation of SIINFEKL/Kb-complexes at the cell surface, and that STING supported BMDC maturation regarding the expression of CD86 and MHC-II, but that it was also fundamental to the induced I IFN response in directly infected as well as cross-presenting BMDCs. Despite the essential role of STING in cross-presenting BMDCs, STING is probably not the molecule or part of the signaling pathway that appears to be blocked by AraC treatment.

5.6. Characterization of genetically modified feeder cells for their ability to activate BMDCs for antigen cross-presentation

To elucidate how AraC impairs antigen presentation and the activation of cross-presenting BMDCs, I used the results obtained from the RNA sequencing of infected and AraC-treated feeder cells to narrow down some target genes which might be affected directly by AraC treatment. As well as the target genes shown in Figure 11A as red labeled dots (*Lrrfip1*, *Xccr5* (Protein name: Ku70), *Ctnnb1* (protein name: β-catenin), PYCARD (Protein name: ASC), and P2RX7), additional molecules involved in important innate immune signaling pathways or the sensing of RNA/DNA were chosen as targets for gene-editing of MHC-I mismatched murine Cloudman S91 melanoma cells (Table 8). Various feeder cell lines deficient in a particular protein were generated using CRISPR/Cas9 as described in the Material and Methods. Gene-edited polyclonal feeder cell lines were tested for the absence of the respective protein using western blot analysis and either used directly in experiments or were selected as a monoclonal cell line by limiting dilution (Supplementary Figure 8). To investigate whether the target genes chosen for gene-editing in MHC-I mismatched feeder cells have an impact on the activation of BMDCs for cross-presentation and the stimulation of $CD8^+$ T cell responses, cocultures of C57BL/6 BMDCs and MVA-infected gene-edited feeder cells were incubated with $CD8^+$ T cell lines specific for viral antigens or the recombinant antigen OVA. As can be seen from Figure 21A, only feeder cells deficient in TRIF showed a reduced ability to activate cross-presenting BMDCs for the induction of B8-specific IFN-γ^+ $CD8^+$ T cells. In addition, B8-specific T cell numbers tended to be lower in infected feeder MAVS KO-BMDC-cocultures (Figure 21A). As well as IFN-γ, the expression of the more sensitive cytokine TNF-α was analyzed. Interestingly, TNF-α^+ $CD8^+$ T cell frequencies were significantly reduced in the absence of TRIF or MAVS in feeder cells (Figure 21B), indicating that during infection

Table 8: Brief description of the targets studied in feeder cells in this project.

Protein	Function	Description
STING[1]	Adaptor	activated by cGAMP following dsDNA sensing by cGAS and the synthesis of the second messenger cGAMP (109)
DDX41[2]	PRR	detects dsDNA (112)
Ku70[3]	PRR	cytosolic DNA sensor (116)
RIG-I[4]	PRR	recognizes short dsRNA as well as cytosolic 5′-triphosphate uncapped ssRNA (122, 123)
MAVS[5]	Adaptor	activated by RIG-I or MDA-5 after dsRNA detection (121)
TLR4[6]	PRR	activated by various lipids, viral products and endogenous ligands (102, 105)
MYD88[7]	adaptor	adaptor protein which mediates signaling from all TLRs, except TLR4 (102)
TRIF[8]	Adaptor	adaptor protein which mediates TLR3/TLR4 signaling (102)
LRRFIP1[9]	PRR	sensing of dsDNA as well as dsRNA (131)
β-Catenin	Adaptor	adaptor protein as downstream target of LRRFIP1 (131)
ASC[10]	Adaptor	oligomerizes with PYD-domain containing NLRs to from an inflammasome (132, 153)
P2RX7[11]	Ion channel	ATP-gated ion channel which senses extracellular ATP, and was shown to be involved in inflammasome activation (134, 154)

[1]STING: Stimulator of interferon genes; [2]DDX41: DEAD-box helicase 41; [3]Ku70: X-ray repair complementing defective repair in Chinese hamster cells 6; [4]RIG-I: retinoic acid inducible gene; [5]MAVS: Mitochondrial antiviral-signaling protein; [6]TLR4: Toll-like receptor 4; [7]MYD88: Myeloid differentiation primary response 88; [8]TRIF: toll-like receptor adaptor molecule 2; [9]LRRFIP-1: Leucine rich repeat (in FLII) interacting protein 1; [10]ASC: Apoptosis-associated speck-like protein; [11]P2RX7: Purinergic receptor P2X, ligand-gated ion channel, 7

with MVA, TRIF as well as MAVS in feeder cells supported the licensing of cross-presenting BMDCs for the stimulation of poxvirus-specific cytotoxic T cell responses. Because T cell activation by antigen-presenting cells is a rather indirect effect of antigen processing and presentation, I also monitored the ability of cross-presenting BMDCs to express SIINFEKL/Kb-complexes at the cell surface. In line with the above

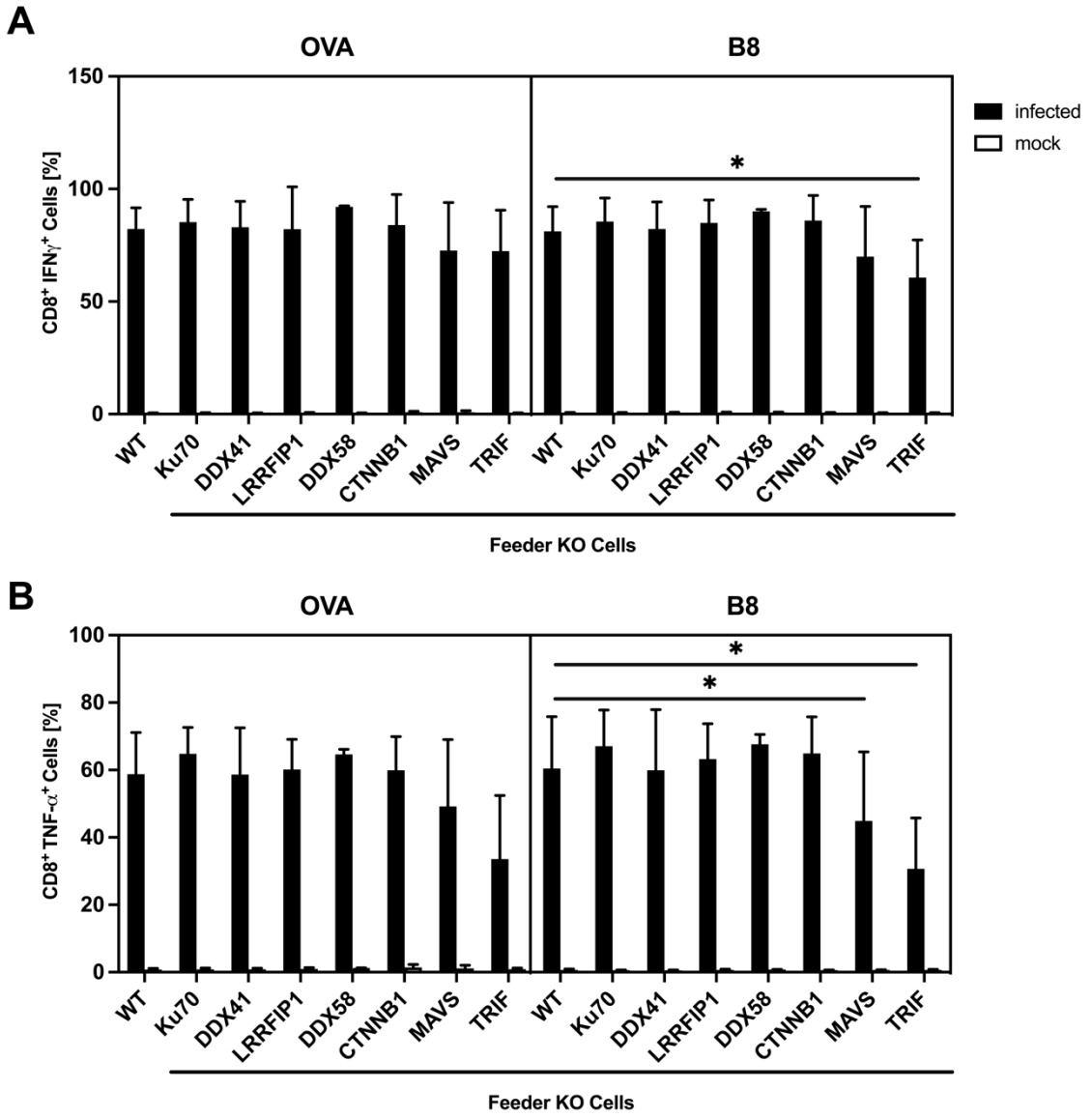

Figure 21: MAVS as well as TRIF in feeder cells appear to be important for the licensing of cross-presenting BMDCs for T cell activation. MHC-I mismatched feeder cells (murine Cloudman S91 melanoma cells) deficient in the indicated proteins were infected with MVA-PK1L-OVA at MOI 1, or mock-infected for 16 h. After PUVA-treatment cells were washed and cocultured with uninfected BMDCs for another 20 h. Cross-presenting BMDCs were analyzed for their ability to activate $CD8^+$ T cells by coculturing $CD8^+$ T cells specific for the viral antigen B8 or the recombinant antigen OVA with the feeder-BMDC-cocultures. T cell activation was determined using flow cytometry as frequencies of IFN-γ (A) or TNF-α (B) expressing $CD8^+$ T cells. Data are presented as mean ± SD of two to three independent experiments. Statistical significance (P); * = $p \leq 0{,}05$; two-way ANOVA with Fisher's LSD multiple comparison post-hoc test.

finding that TRIF and MAVS deficiency in feeder cells revealed a drop in T cell activation by cross-presenting BMDCs (Figure 21), the surface expression of SIINFEKL/Kb-complexes was even more dramatically reduced (Figure 22). Cross-presenting BMDCs cocultured with feeder cells deficient not only in TRIF and MAVS but also in LRRFIP1 showed a significant decline in numbers of SIINFEKL/Kb^+ cells as

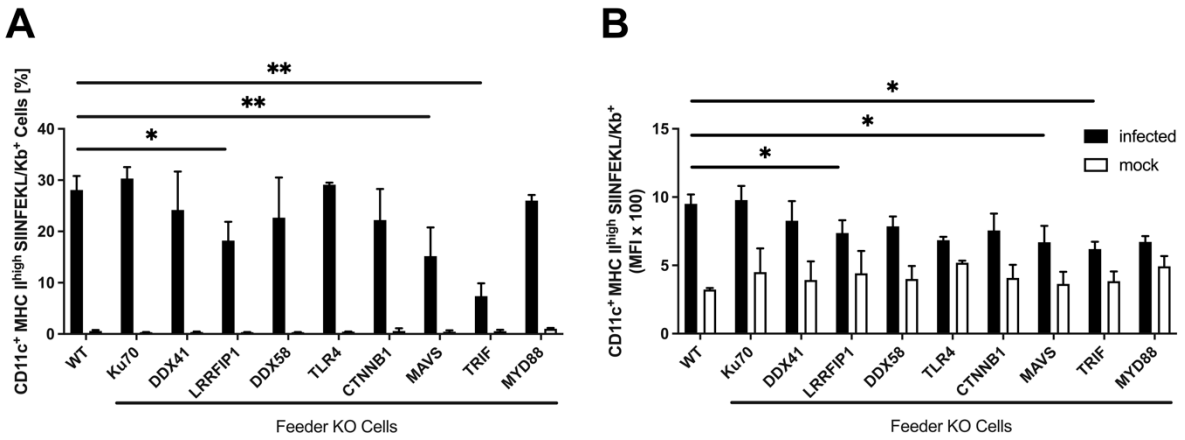

Figure 22: Cross-presenting BMDCs show a decreased antigen processing and presentation ability after coculturing with MVA-infected LRRFIP1-, MAVS- and TRIF-deficient feeder cells. MHC-I mismatched feeder cells (murine Cloudman S91 melanoma cells) deficient for the indicated proteins were infected with MVA-PK1L-OVA at MOI 1, or mock-infected for 16 h. Feeder cells were PUVA treated, washed and cocultured with uninfected BMDCs for 20 h. Cross-presenting BMDCs were analyzed for their antigen processing and presentation ability by monitoring the surface expression of SIINFEKL/Kb using flow cytometry. The SIINFEKL/Kb-loading ability is depicted as frequency (A) and MFI (B) of CD11c$^+$ MHC II^{high} SIINFEKL/Kb$^+$ cells. Data are represented as mean ± SD of two (TLR4 & MYD88) to three independent experiments. Statistical significance (P); * = $p \leq 0,05$; ** = $p \leq 0,01$; two-way ANOVA with Fisher's LSD multiple comparison post-hoc test.

well as a reduced efficiency to load and present SIINFEKL on MHC-I (Figure 22A, B). Although TLR4 KO and MYD88 KO cells showed a lower standard deviation than LRRFIP1-, MAVS- and TRIF-deficient feeder cells, the number of SIINFEKL/Kb$^+$ cells and the SIINFEKL/Kb presentation efficacy were not significantly lower in BMDC cocultures with these feeder cells. As I only examined the ability of TLR4 KO and MYD88 KO feeder cells to activate BMDCs to present SIINFEKL/Kb-complexes in only two independent experiments, the statistical power was lower compared with the other KO feeder cells. Taken together, these results suggest that TRIF and MAVS in feeder cells may be crucial for the licensing of cross-presenting BMDCs for antigen processing and presentation and consequently for the activation of antigen-specific cytotoxic T cells.

To gain insight into whether gene-edited cells, in particular, TRIF-, MAVS-, and LRRFIP1-deficient feeder cells, affect BMDC maturation, cross-presenting BMDCs were analyzed for the expression of the costimulatory molecules CD40 and CD86 as well as MHC-II. As shown in Figure 23, frequency values and MFIs for all examined markers lacked significance due to large standard deviations. However, some gene-edited feeder cells tended to be less able to activate cross-presenting BMDCs to express costimulatory molecules. For instance, CD40 expression by cross-presenting

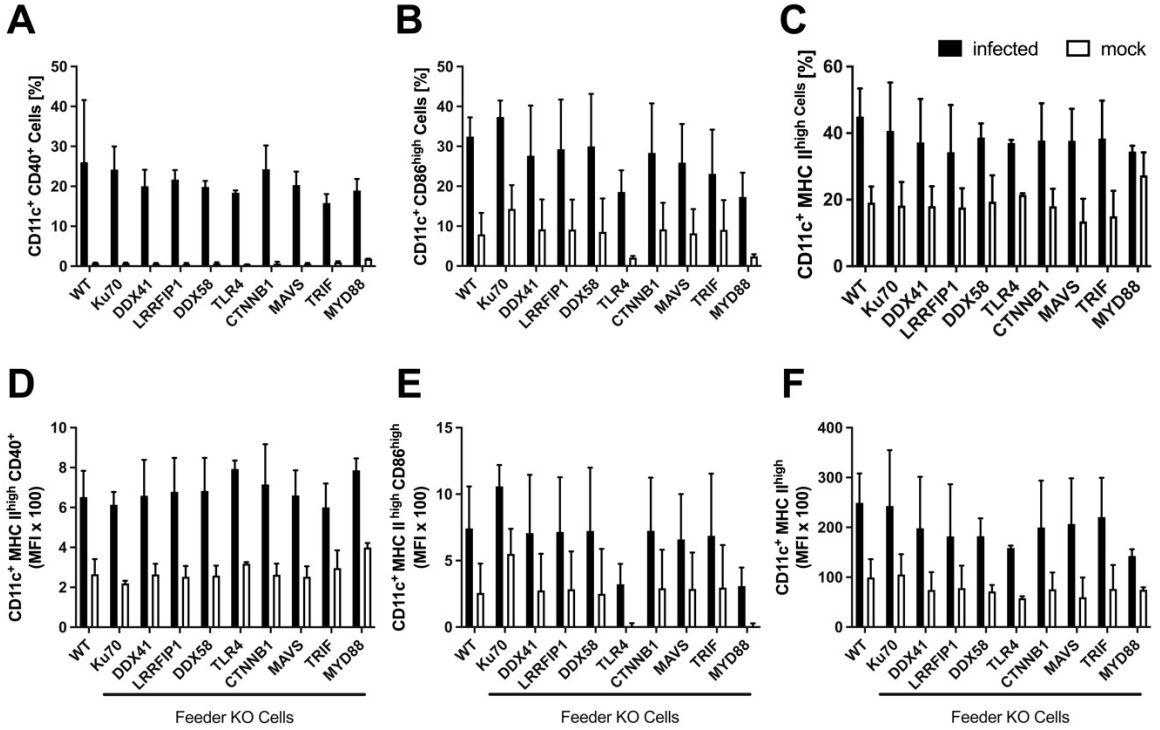

Figure 23: Maturation phenotype of cross-presenting BMDCs cocultured with MVA-infected feeder cells. Feeder cells (murine Cloudman S91 melanoma cells) deficient for the indicated proteins were infected with MVA-PK1L-OVA at MOI 1, or mock-infected for 16 h. For the analysis of cross-presentation infected and mock infected feeder cells were treated with PUVA, washed and cocultured with uninfected BMDCs for 20 h. Cross-presenting CD11c$^+$ MHC II^{high} BMDCs were analyzed for CD40 (A, D), CD86 (B, E) and MHC II expression (C, F). Data are depicted as frequencies (A-C) as well as MFI (D-F) and represent means ± SD of two to three independent experiments.

BMDCs which had been cocultured with TRIF-deficient feeder cells tended to be lower and those cells also showed a slight trend to express decreased amounts of CD40 at the cell surface (Figure 23A, D). In contrast, only TLR4- and MYD88-deficient feeder cells showed a trend for reduced CD86$^+$ cell numbers in cocultures with BMDCs and, in addition, displayed a drop in the amount of CD86 expressed on the cell surface (Figure 23B, E). The number of MHC-II expressing cross-presenting BMDCs seemed to be slightly impaired after coculture with MYD88- and LRRFIP1- deficient feeder cells (Figure 23C). The efficiency of MHC-II expression determined per cell (MFI) tended to be most affected in feeder-BMDC-cocultures composed of feeder cells deficient in MYD88 and TLR4, but deficiencies in DDX41, LRRFIP1, DDX58, CTNNB1 (also known as β-catenin), MAVS and TRIF also resulted in a slightly reduced MCH-II surface expression (Figure 23F). All in all, because of the high standard deviations, the gene knockouts tested in feeder cells gave only limited information on the maturation of cross-presenting BMDCs during infection with MVA.

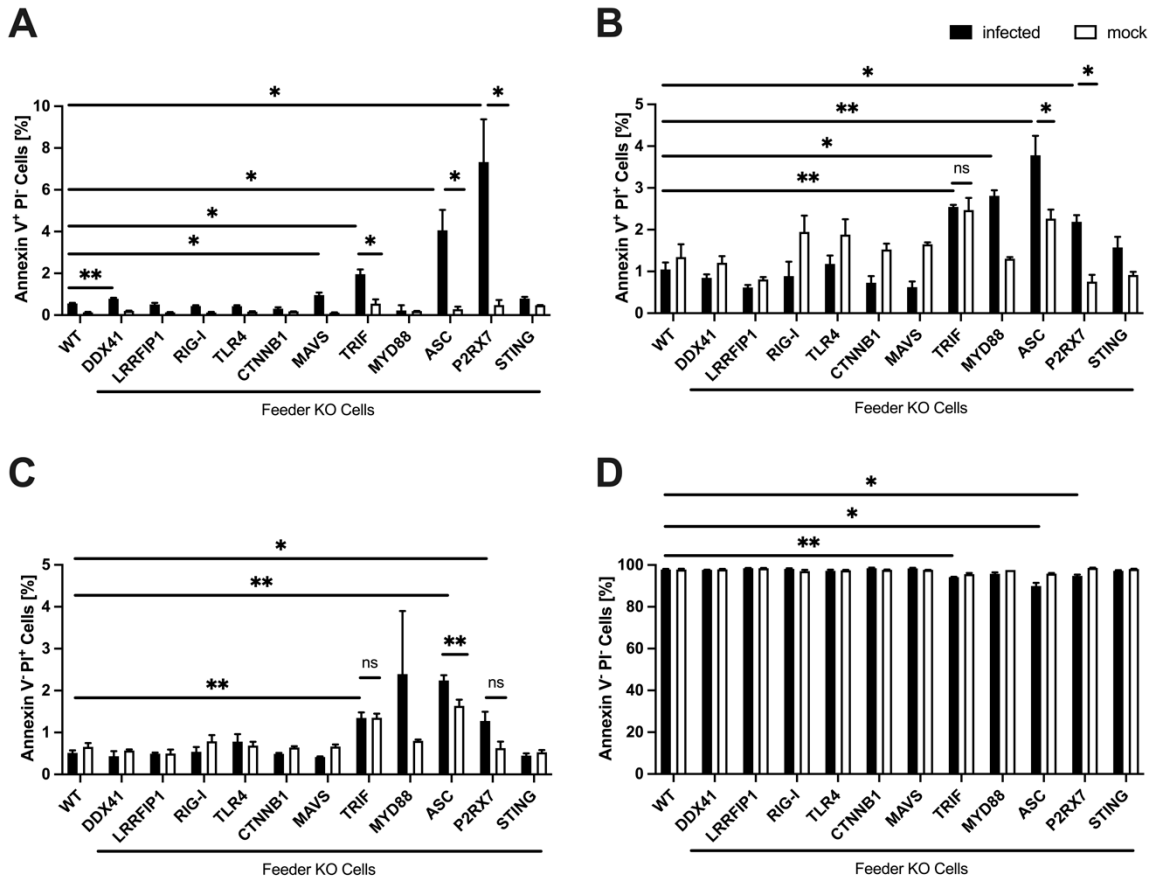

Figure 24: Apoptosis and necrosis are predominantly increased in TRIF-, ASC- and P2RX7-deficient feeder cells. MHC-I mismatched feeder cells (murine Cloudman S91 melanoma cells) deficient for the indicated proteins were infected with MVA-PK1L-OVA at MOI 1, or mock-infected for 16 h. MVA-induced cell death was analyzed by determining plasma membrane integrity and permeability using annexin V and propidium iodide. Data are depicted as frequencies of early apoptotic (**A**), late apoptotic (**B**), necrotic (**C**) and healthy cells (**D**) and represent the mean ± SD of three independent experiments. Statistical significance (P); * = $p \leq 0,05$; ** = $p \leq 0,01$; two-way ANOVA with Fisher's LSD multiple comparison post-hoc test.

Due to the observed impact of AraC on apoptosis, I further analyzed the susceptibility of the genetically modified feeder cells (Table 8) to apoptosis during infection with MVA, using plasma membrane integrity and permeability as markers for apoptosis or necrosis. In addition to the previously mentioned gene targets, ASC (PYCARD) and P2RX7-deficient feeder cells were tested for their potential to induce enhanced cell death in response to MVA-infection. These feeder cells were generated and characterized during a masters thesis project by Ylenia Longo, which I additionally supervised and which was linked to this study. P2RX7 and ASC-deficient feeder cells were analyzed for their potential to activate $CD8^+$ T cells, the SIINFEKL/Kb-loading ability, and the maturation phenotype of cross-presenting BMDCs. Interestingly, the absence of P2RX7 or ASC revealed a striking drop in T cell activation and the SIINFEKL/Kb-loading was comparable to the phenotype induced in cross-presenting

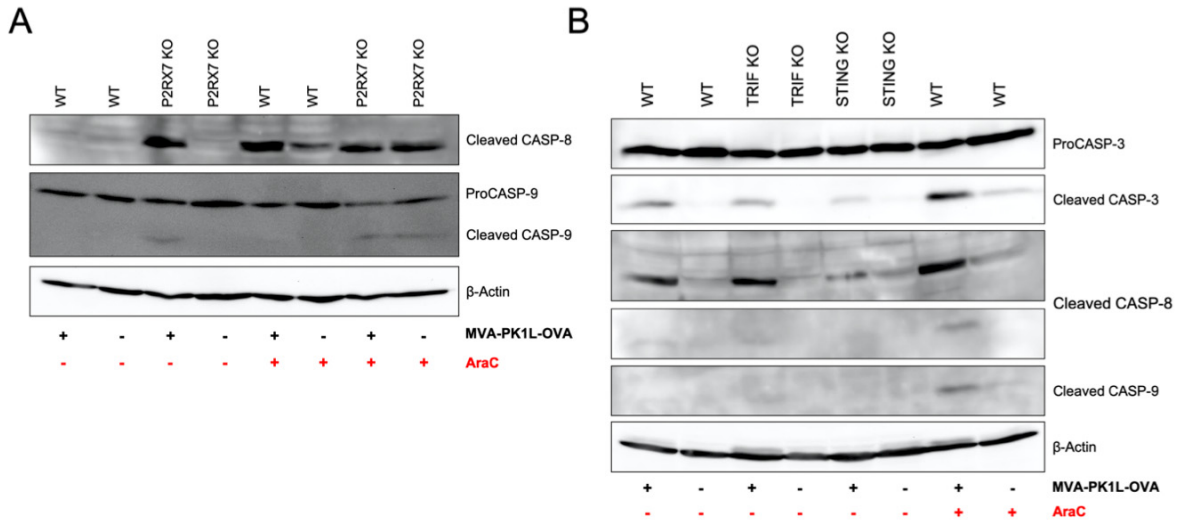

Figure 25: The enhanced apoptotic cell death observed in MVA-infected P2RX7- and TRIF-deficient feeder cells is comparable to that in infected and AraC treated feeder wildtype (WT) cells. P2RX7 KO (A) and wildtype (WT) feeder cells (murine Cloudman S91 melanoma cells) (A, B) were infected with MVA-PK1L-OVA at MOI 1, or mock-infected in the presence or absence of 40 µg/ml AraC. TRIF- and STING-deficient feeder cells (B) were infected with MVA-PK1L-OVA at MOI 1, or mock-infected. After 16 h cells were harvested, protein isolated and protein levels of cleaved CASP-8 and -9 as well as proCASP-9 (A) and cleaved CASP-3, -8 and -9 as well as proCASP-3 (B) were determined by western blot analysis. Data represent one blot representative of three independent experiments.

BMDCs by MVA-infected and AraC-treated feeder cells (data not shown, Figure 4, Figure 5). Furthermore, P2RX7 and ASC deficiency in feeder cells resulted in impaired expression of costimulatory molecules by cross-presenting BMDCs (data not shown). STING-deficient feeder cells were also analyzed and used as controls because they had no major impact on antigen cross-presentation (Figure 18). As Figure 24A illustrates, the absence of DDX41, MAVS, TRIF, ASC or P2RX7 in feeder cells resulted in a significantly enhanced number of early apoptotic cells, with the highest frequencies of early apoptotic cells seen in P2RX7 and ASC-deficient cells. In addition, feeder cells deficient in TRIF-, P2RX7-, ASC-, or MYD88- showed a significant increase in the number of late apoptotic cells after infection with MVA (Figure 24B). Interestingly, only the absence of TRIF, P2RX7, and ASC resulted in elevated necrotic cell numbers accompanied by a drop in healthy cell numbers (Figure 24C, D).

Taken together, these results indicate that MVA-infection in the absence of TRIF, P2RX7, and ASC led to an increase in apoptosis as well as necrosis. Using western blot analysis as the second method to determine the role of important innate immune signaling pathways for the induction of cell death during infection with MVA, I discovered elevated levels of cleaved CASP-8 as well as cleaved CASP-9 in cell

lysates from MVA-infected P2RX7-deficient feeder cells (Figure 25A). Surprisingly, only wildtype feeder cells infected in the presence of AraC exhibited cleaved CASP-8 at levels comparable to those in infected P2RX7-deficient feeder cells (with or without AraC). Apart from infected P2RX7-deficient feeder cells, only protein lysates from MVA-infected and AraC-treated cells or from P2RX7-deficient feeder cells with AraC-treatment alone exhibited cleaved CASP-9 with a size of 39 kDa next to proCASP-9. However, low levels of cleaved CASP-9 were also sometimes detectable in lysates of infected and AraC-treated feeder cells, suggesting that MVA-infection in combination with AraC-treatment synergistically resulted in proCASP-9 cleavage (Figure 25B). Interestingly, after infection with MVA, TRIF deficiency resulted in cleavage of CASP-3 and CASP-8 at levels comparable to those in infected wildtype feeder cells, while AraC-treatment in combination with MVA-infection showed the highest levels of cleaved CASP-8 and -9 (Figure 25B). Consistent with the results obtained for antigen presentation using STING KO feeder cell-BMDC-cocultures, infected STING-deficient feeder cells only showed low levels of cleaved CASP-3 as well as CASP-9 (Figure 25B). Collectively these results suggest that the absence of TRIF, P2RX7, and ASC signaling seems to promote apoptosis, while STING had no impact on apoptosis. Moreover, my data suggest that the ability of feeder cells to stimulate BMDCs for cross-presentation might be limited by cell death.

To gain insight into the innate pathway which might be relevant for the AraC-phenotype, namely the complete abrogation of cross-presentation by BMDCs, I analyzed the cytokine and chemokine production in gene-edited feeder cells as well as in cocultures comprising these feeder cell lines and BMDCs. In addition, cytokine and chemokine concentrations were determined in the supernatants from feeder cells that had been infected in the presence of AraC as well as supernatants from infected and AraC-treated feeder-BMDC-cocultures. The concentrations of the cytokines IFN-γ, IL-1β, IL-10, IFN-α, IFN-β, and IL-6 were determined in supernatants obtained from MVA-infected gene-edited feeder cells. As Figure 26 illustrates, infected wildtype feeder cells produced IL-1β, IL-10, and I IFNs at low levels (Supplementary Figure 9). Infected LRRFIP1-, TLR4- and STING-deficient feeder cells did not produce IL-1β, while in the absence of CTNNB1, MAVS, TRIF, PYCARD, or P2RX7 or with AraC-treatment, IL-1β production was higher in mock-infected as compared to MVA-infected cells (Figure 26). Interestingly, TRIF-deficient infected feeder cells produced 30 times more IFN-β and P2RX7- or ASC-deficient feeder cells almost 150- and 290 times more

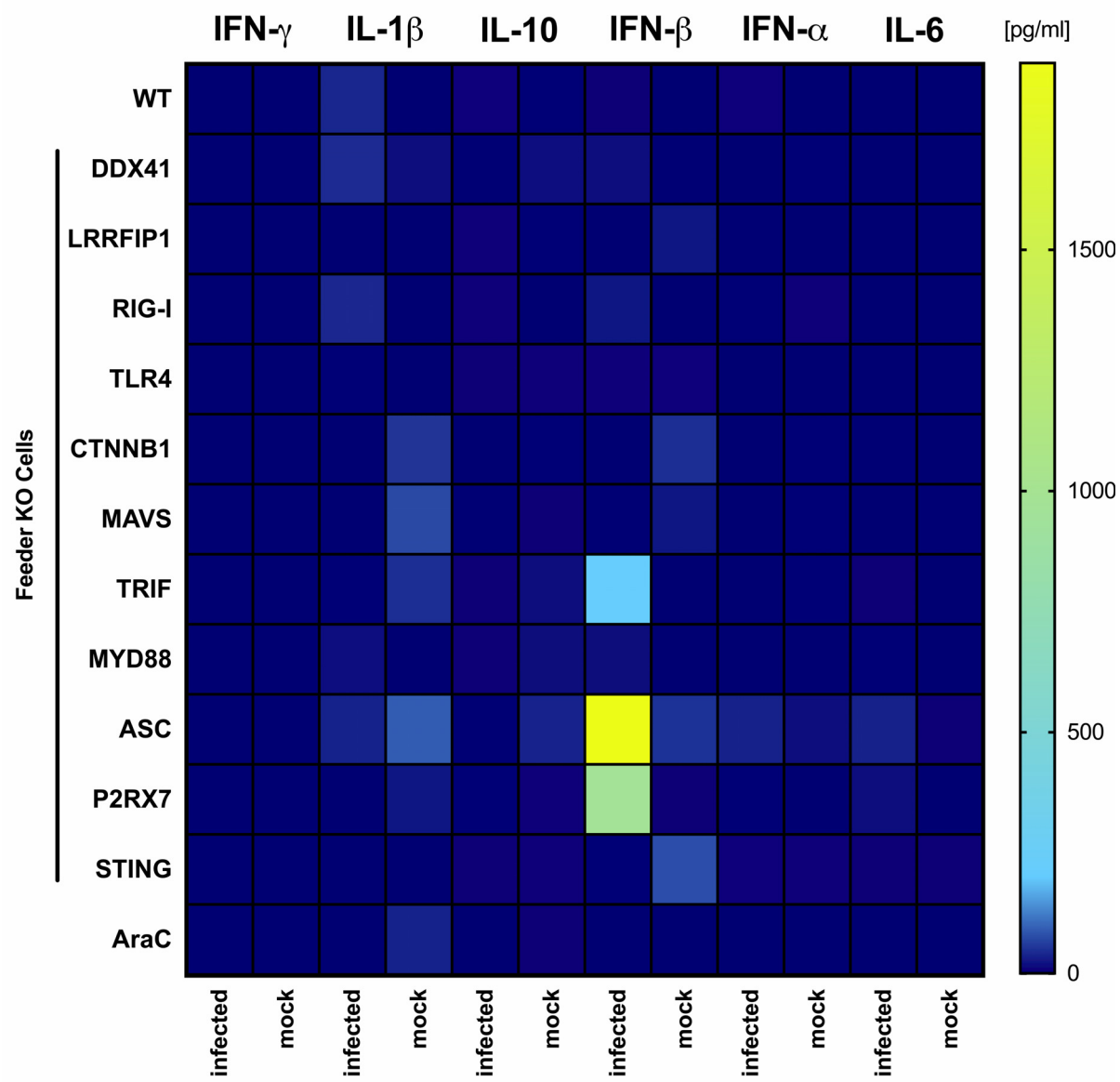

Figure 26: Cytokine response in gene-edited feeder cells. Feeder cells deficient for the indicated proteins and feeder WT cells were infected with MVA-PK1L-OVA at MOI 1, or mock-infected. Feeder WT cells were additionally treated with 40 µg/ml AraC during the infection. 16 h post infection supernatants were collected and the concentrations of IFN-γ, IL-1β, IL-10, IFN-β, IFN-α and IL-6 determined with LEGENDplex assays. Data represent the mean of two independent experiments.

IFN-β, respectively, than infected wildtype feeder cells. In addition to IFN-β, supernatants from ASC-deficient feeder cells contained three times more IFN-α than control cells, even though IFN-α levels remained at relatively low levels (Figure 26). Moreover, concentrations of the chemokines CCL5, CXCL1, MCP-1, IP-10, MIP-1α, and MIP-1β were determined using a bead-based immunoassay. The results of this immunoassay indicated that IP-10 was the only one of the tested chemokines produced by MVA-infected wildtype feeder cells (Figure 27). Surprisingly, only ASC- and P2RX7-deficient feeder cells produced IP-10 at higher levels than infected

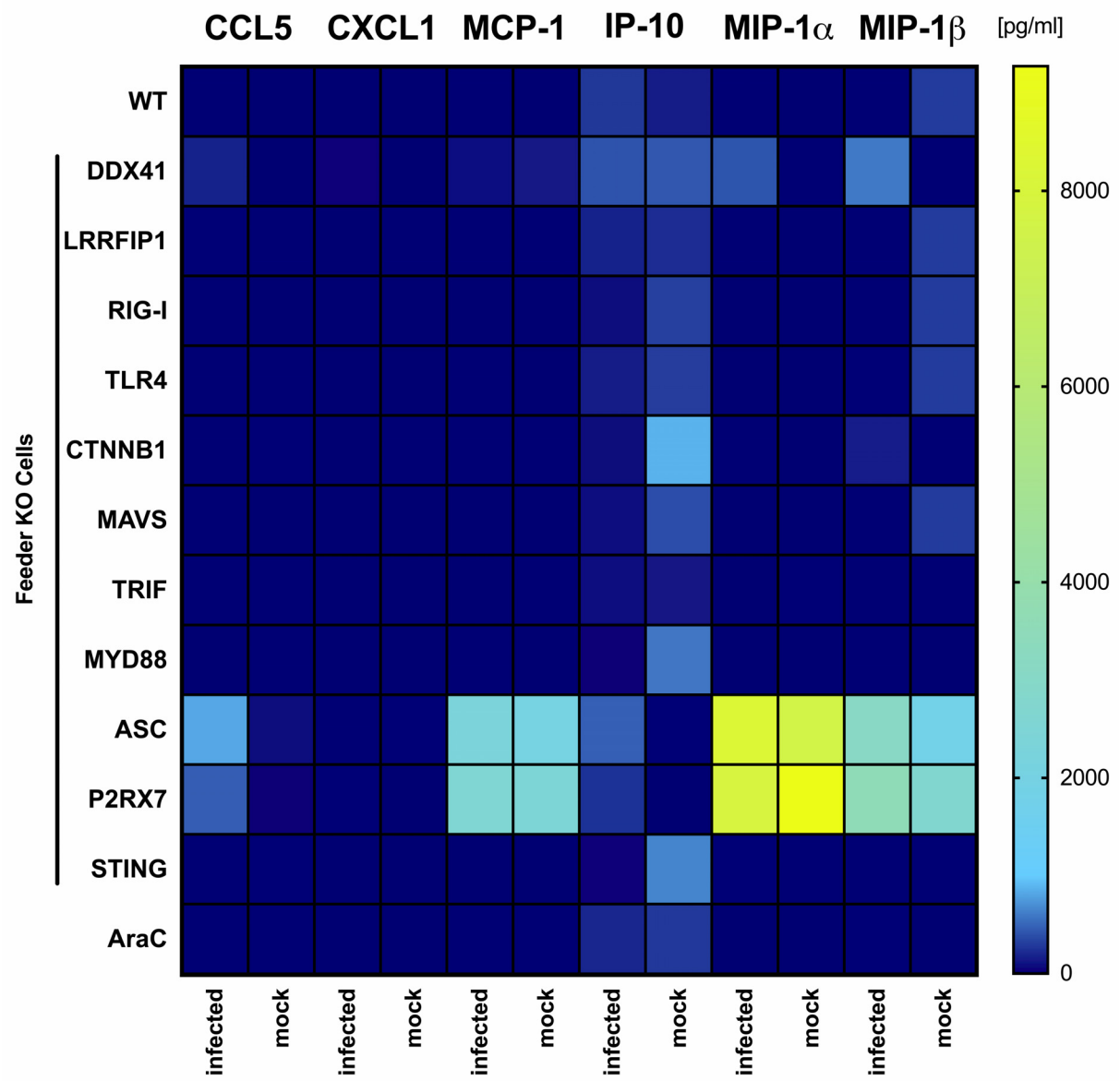

Figure 27: Chemokine response in gene-edited feeder cells. Feeder cells deficient for the indicated proteins and feeder WT cells were infected with MVA-PK1L-OVA at MOI 1, or mock-infected. Feeder WT cells were additionally treated with 40 µg/ml AraC during the infection. 16 h post infection supernatants were collected and the concentrations of CCL5, CXCL1, MCP-1, IP-10, MIP-1α and MIP-1β determined with LEGENDplex assays. Data represent the mean of two independent experiments.

wildtype cells after infection with MVA. In contrast, IP-10 was also produced by other gene-edited feeder cells but was probably not associated with MVA-infection, as I also observed elevated levels of IP-10 in mock-infected controls. Notably, supernatants from infected P2RX7-, ASC-, and DDX41-deficient feeder cells showed elevated CCL5 levels. Furthermore, in the absence of DDX41, I observed slightly increased concentrations of MIP-1α as well as MIP-1β in feeder cells. MIP-1β was also detected in supernatants from infected CTNNB1 KO feeder cells, but at lower levels. In contrast, infected and AraC-treated feeder cells were unable to produce any of the tested

chemokines at higher levels than were detected in mock-infected and AraC-treated feeder cells (Figure 27, Supplementary Figure 10). Taken together, these results suggest that my gene-edited feeder cell lines have the ability to produce several cytokines as well as chemokines in response to MVA-infection, although these are only produced at low level. Infected wildtype feeder cells in particular were able to produce only IP-10 at higher levels, whereas I IFNs were only found to be produced at marginal concentrations. Interestingly, gene-editing of different molecules involved in important innate immune signaling pathways resulted in the production of additional cytokines like IFN-α in TRIF-, ASC-, and P2RX7-deficient feeder cells, and of additional chemokines like CCL5 in the absence of DDX41, ASC, and P2RX7. Considering that MVA-infection mainly resulted in the production of I IFNs by directly infected but also cross-presenting BMDCs, only the absence of TRIF and ASC in infected feeder cells resulted in significantly decreased IFN-β levels, and in a non-significant reduction in the production of IFN-α in cross-presenting BMDCs (Figure 28A, B). In agreement with the results illustrated in Figure 15B, I observed an abrogated IFN-α and -β response in cross-presenting BMDCs, which had been cocultured with MVA-infected and AraC-treated feeder cells (Figure 28A, B). Concentrations of IL-6, IFN-γ and IL-1β were also determined in supernatants from feeder-BMDC-cocultures. Similarly, to the observed I IFN response in cross-presenting BMDCs, IL-6 production was impaired in BMDCs cocultured with MVA-infected feeder cells deficient in TRIF and ASC. In line with the abrogated ability of cross-presenting BMDCs to produce I IFNs after coculture with MVA-infected and AraC-treated feeder cells, IL-6 production was abolished (Figure 29A). Elevated IL-1β levels were observed compared to the control, especially in supernatants from infected DDX58-, TLR4-, CTNNB1-, MAVS- and TRIF-deficient feeder-BMDC-cocultures (Figure 29B). Surprisingly, AraC-treated and infected feeder cells activated cross-presenting BMDCs to produce IL-1β, although at lower levels than infected wildtype feeder-BMDC-cocultures (Figure 29B, Supplementary Figure 11).

In addition to IFN-α and -β, I analyzed the expression of IFN-α subtype 13 (Ifna13) during infection with MVA because my transcriptomic data suggested that Ifna13 was the only IFN-α subtype highly expressed by infected feeder cells. Interestingly, Ifna13 was differentially expressed in infected feeder cells in the presence or absence of AraC, as revealed by RNA sequencing and verified using semi-quantitative qRT-PCR analysis (Figure 30). In fact, during the course of the experiment, the highest expression levels of Ifna13 in MVA-infected cells were observed 6-8 h post-infection,

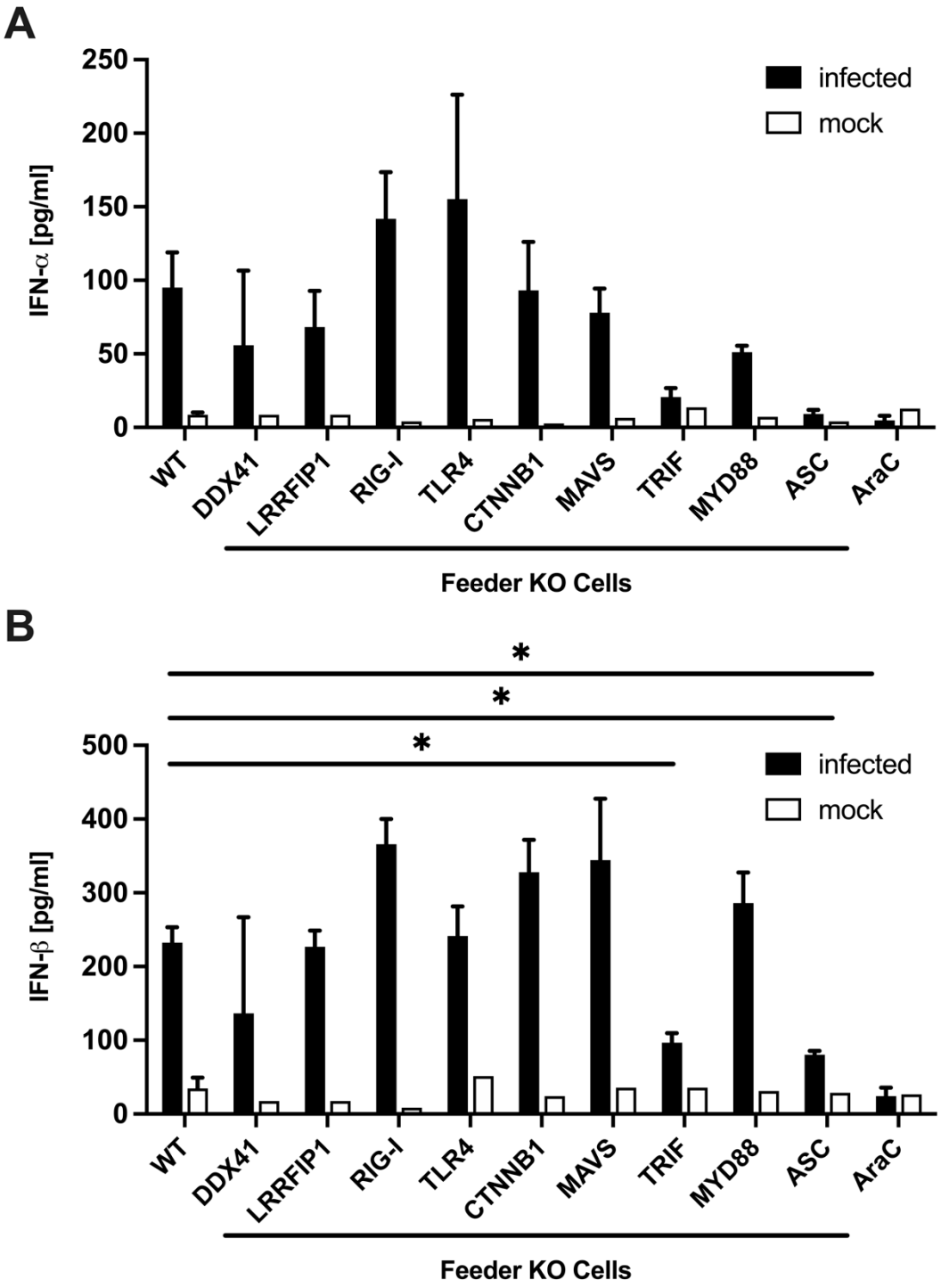

Figure 28: BMDCs cocultured with TRIF-, ASC-deficient feeder cells or AraC-treated wildtype feeder cells show significantly reduced production of type I interferons. Feeder cells deficient for the indicated protein and WT feeder cells were infected with MVA-PK1L-OVA at MOI 1, or mock-infected for 16 h. Additionally, WT feeder cells were used as control and infected with MVA in the presence of 40 µg/ml AraC. After PUVA-treatment and washing, feeder cells were cocultured with C57BL/6 GM-CSF-BMDCs for 20 h. Supernatants were collected and concentrations of IFN-α (A) and -β (B) determined with LEGENDplex assays. Data represent the mean ± SD of two independent experiments. Statistical significance (P); * = $p \leq 0{,}05$; two-way ANOVA with Fisher's LSD multiple comparison post-hoc test.

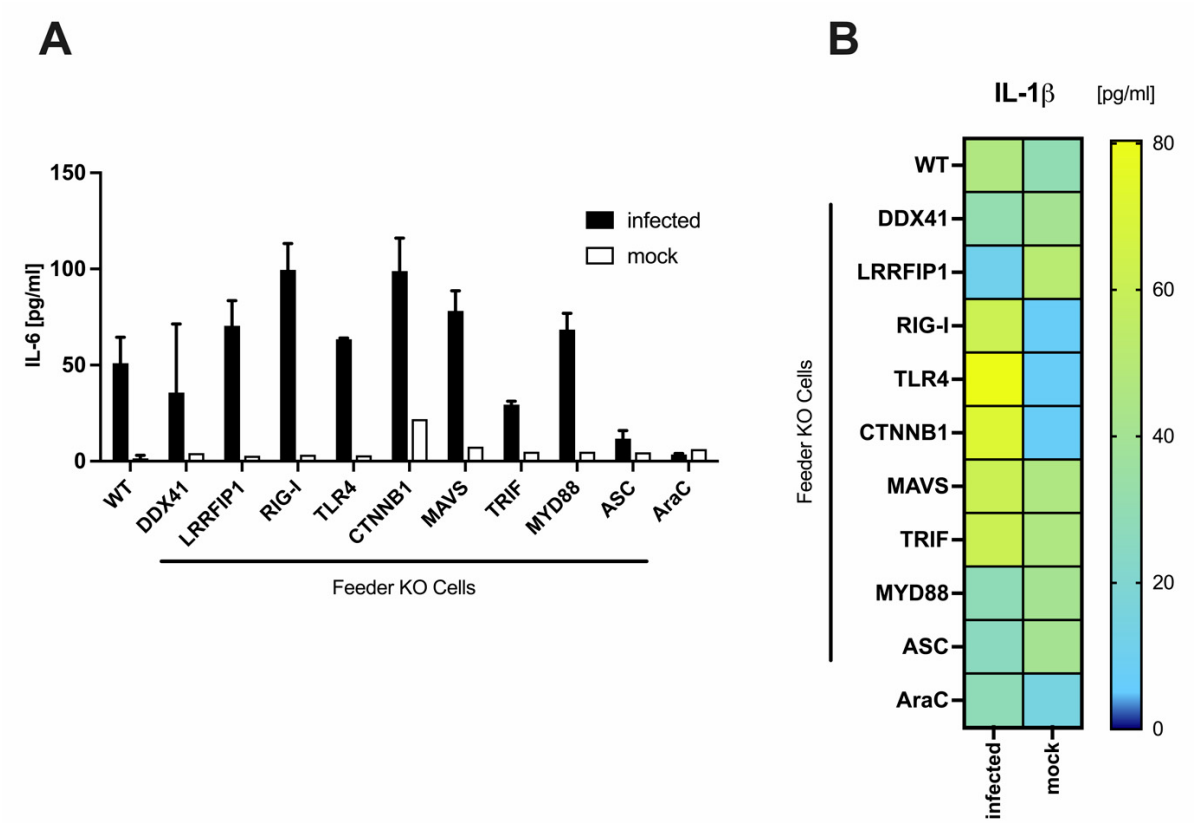

Figure 29: BMDCs cocultured with TRIF-, ASC-deficient feeder cells or AraC-treated wildtype feeder cells show a reduced IL-6 response, while DDX58, TLR4, CTNNB1, MAVS and TRIF KO feeder-BMDC-cocultures exhibit elevated IL-1β levels. Feeder cells deficient for the indicated protein and WT feeder cells were infected with MVA-PK1L-OVA at MOI 1, or mock-infected for 16 h. Additionally, feeder WT cells were used as control and infected with MVA in the presence of 40 µg/ml AraC. After PUVA-treatment and washing, feeder cells were cocultured with C57BL/6 GM-CSF-BMDCs for 20 h. Supernatants were collected and concentrations of IL-6 (A) as well as IL-1β (B) determined with LEGENDplex assays. Data represent the mean of two independent experiments.

while AraC-treatment completely abrogated the expression of Ifna13. To determine whether P2RX7 and ASC were involved in the induction of Ifna13-expression, feeder cells deficient in P2RX7 and ASC were infected with MVA and analyzed for Ifna13 expression. Feeder STING KO cells were used as controls due to the observed opposite effects of both cell death and antigen-presentation by cross-presenting BMDCs in feeder STING KO-BMDC-cocultures. Interestingly, infected P2RX7-deficient feeder cells failed to express Ifna13 until 16 h post-infection (Figure 30). In contrast, at 6-16 h post-infection, Ifna13 was expressed in the absence of ASC at significantly lower levels than in MVA-infected control feeder cells. In fact, Ifna13 was expressed in MVA-infected P2RX7-deficient feeder cells at levels comparable to those in feeder cells infected with MVA in the presence of AraC. Surprisingly, deficiency of STING in infected feeder cells resulted in a significantly enhanced Ifna13-expression compared to that in infected wildtype feeder cells (Figure 30). Taken together, these

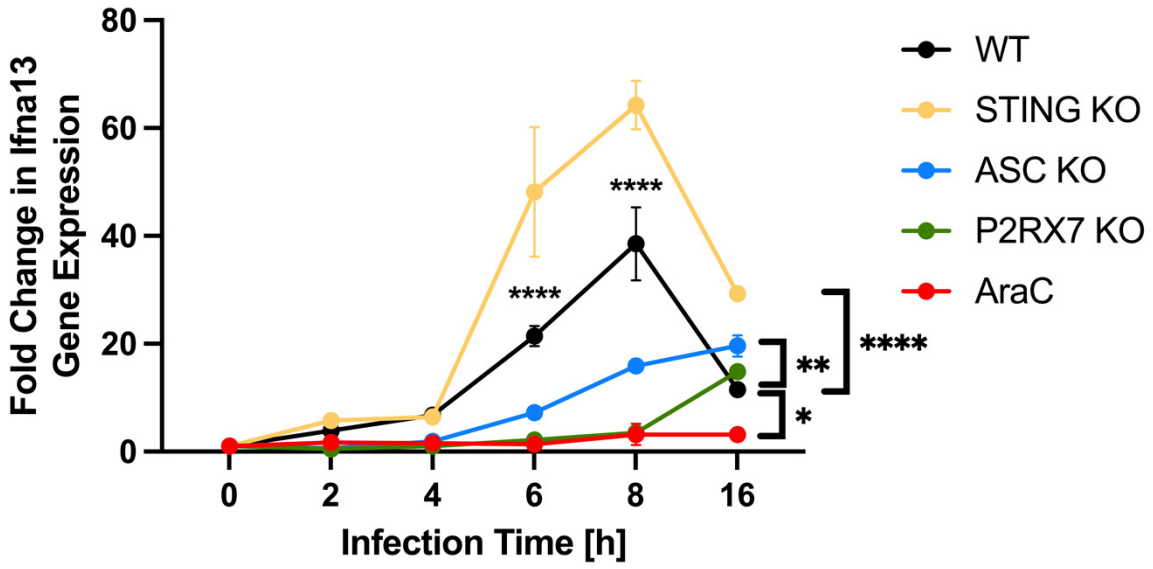

Figure 30: STING KO feeder cells show an increased Ifna13 expression. STING KO, ASC KO, P2RX7 KO and wildtype feeder cells were infected with MVA-PK1L-OVA at MOI 1, or mock-infected for the indicated time (0-8 h) or overnight (16 h). Additionally, feeder WT cells were infected with MVA in the presence of 40 µg/ml AraC as control. Cells were harvested, RNA isolated and Ifna13 expression determined by qRT-PCR. Data were normalized to the corresponding mock controls and are depicted as mean ± SD of two to three independent experiments. Statistical significance (P); * = $p \leq 0,05$; ** = $p \leq 0,01$; **** = $p \leq 0,0001$; two-way ANOVA with Fisher's LSD multiple comparison post-hoc test.

results indicate that wildtype feeder cells were able to express Ifna13 after infection with MVA. However, other IFN-α subtypes (1, 2, 4, 5, and 6) were not detectable in supernatants from infected wildtype feeder cells, and were absent after AraC-treatment, as tested with ELISA or a bead-based immunoassay (Figure 16A, Figure 26, Figure 30). Moreover, ASC seemed to support Ifna13-expression, while P2RX7 appeared to be crucial for the expression of Ifna13. In line with the data previously described in this study, the absence of STING seemed to be beneficial not only for antigen presentation by cross-presenting BMDCs, but also for Ifna13 expression in MVA-infected feeder cells.

Impaired antigen presentation by cross-presenting BMDCs after coculture with infected gene-edited or with AraC-treated feeder cells might be attributed to a reduction in the phagocytic activity of BMDCs. Therefore, I labeled my gene-edited or AraC-treated feeder cells with a cell tracer and determined the frequency and MFI of cell tracer$^+$ BMDCs after cocultivation. To investigate whether STING deficiency in both presenter and feeder cells impacts the phagocytic activity of cross-presenting BMDCs, either STING-deficient or wildtype feeder cells were infected with MVA, and cocultured with STING KO or wildtype BMDCs. However, I observed equal cell frequencies and

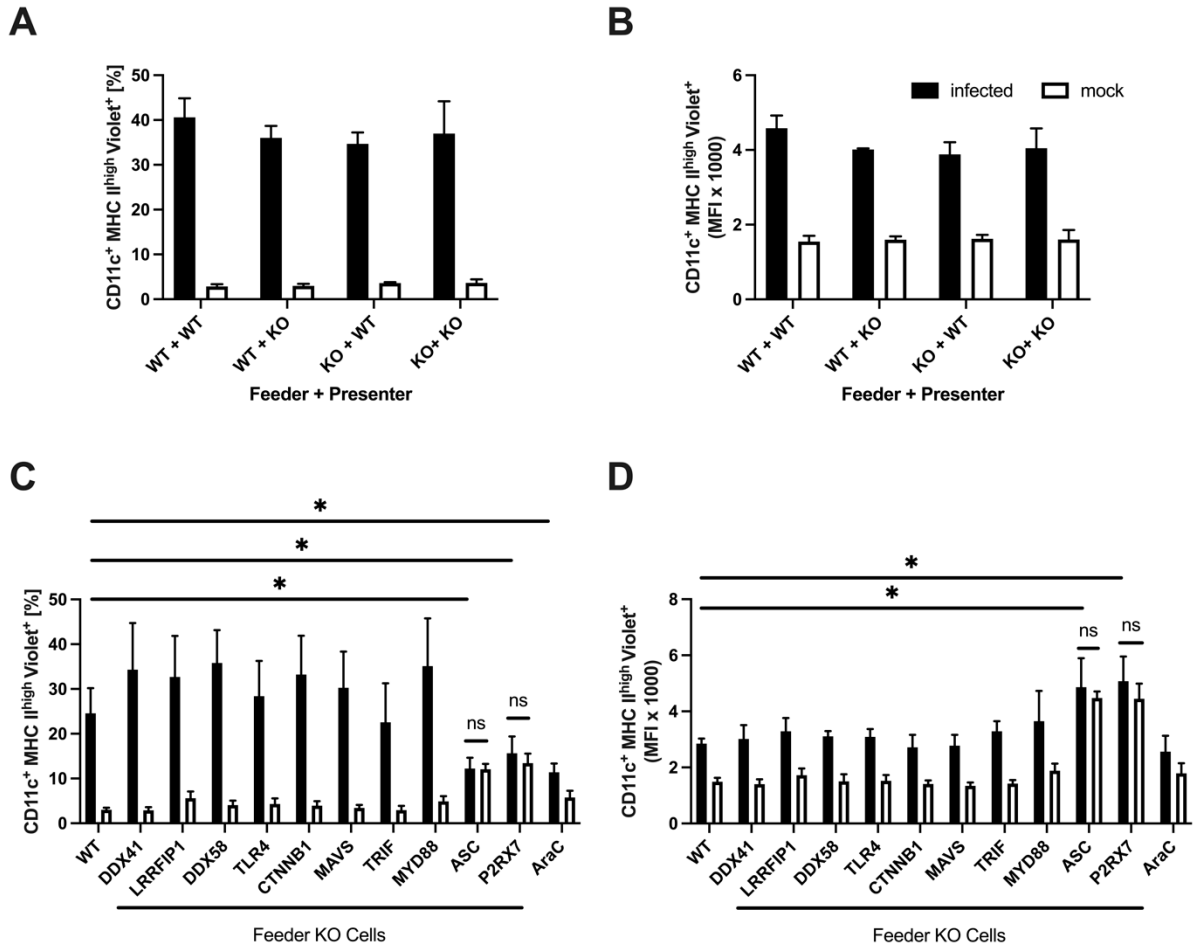

Figure 31: ASC- and P2RX7-deficient feeder cells as well as AraC-treated wildtype feeder cells appear to be less attractive for phagocytosis by BMDCs. STING KO and WT feeder cells were labeled using the cell tracer (Tag-it Violet™ Proliferation and Cell Tracking Dye from Biolegend) and infected with MVA-PK1L-OVA at MOI 1, or mock-infected for 16 h. After washing, cells were cocultured with GM-CSF-BMDCs generated from STING KO or WT-littermates for 20 h (A, B). Feeder cells deficient for the indicated protein and wildtype feeder cells were labeled with the cell tracer, infected with MVA-PK1L-OVA at MOI 1, or mock-infected for 16 h. Additionally, labeled WT feeder cells were infected with MVA in the presence of 40 µg/ml AraC as control. After washing, cells were cocultured with GM-CSF-BMDCs generated from C57BL/6 mice for 20 h (C, D). The phagocytic activity of $CD11c^+$ MHC II^{high} expressing DCs was analyzed using flow cytometry by determining the frequencies (A, C) and MFIs (B, D) of $Violet^+$ cells. Data are represented as mean ± SD of two (A, B) to three (C, D) independent experiments. Statistical significance (P); * = $p \leq 0{,}05$; two-way ANOVA with Fisher's LSD multiple comparison post-hoc test.

MFIs for $tracer^+$ cells in all combinations tested (Figure 31A, B). These results suggest that STING had relevance for phagocytosis of cross-presenting BMDCs neither in feeder nor in presenter cells. However, I observed significantly reduced numbers of phagocytosing BMDCs in cocultures of BMDCs with feeder cells deficient in ASC or P2RX7 (Figure 31C). Even though a significantly lower percentage of BMDCs was able or activated to recognize and phagocytose infected feeder cells deficient in ASC or P2RX7, increased MFIs in these cocultures suggest that BMDCs which have

encountered antigen from ASC- or P2RX7-deficient feeder cells showed an enhanced phagocytic efficiency in comparison to MVA-infected control feeder cells (Figure 31C, D). Similarly, cocultures of BMDCs with infected and AraC-treated feeder cells showed a significant drop in cell frequencies of $CD11c^+$ MHC-II^{high} $Violet^+$ cells (Figure 31C). In addition, TRIF-deficient feeder cells tended to reduce the phagocytic activity by cross-presenting BMDCs, which could be observed in the reduced numbers of $Violet^+$ cells in BMDC-feeder TRIF KO cell-cocultures, although this was not statistically significant (Figure 31C). However, AraC-treated, as well as TRIF-deficient, infected feeder cells, showed MFIs equivalent to infected control feeder cells, suggesting unaltered phagocytic activity (Figure 31D). Surprisingly, in contrast to AraC-treated feeder cells, mock-infected ASC and P2RX7 KO feeder cells were also phagocytosed at comparable numbers and efficiencies (Figure 31C, D). These results collectively indicate that ASC and P2RX7 were the only targets investigated in this study which had an impact on the phagocytic activity of cross-presenting BMDCs. Surprisingly, the reduced phagocytic activity in cocultures of BMDCs with infected ASC or P2RX7 KO feeder cells was attended by increases in the phagocytic efficiency by these BMDCs. Interestingly, this phenomenon was comparable for both MVA- infected and mock-infected feeder cells and resulted in higher numbers of phagocytosing BMDCs than wildtype feeder-BMDC cocultures without infection.

5.7. MAVS and MYD88 signaling in cross-presenting BMDCs

Considering that membrane-associated and cytosolic PRRs could influence the activation of the BMDC itself, I investigated the abilities of cross-presenting MYD88- and MAVS-deficient BMDCs to present antigens and stimulate $CD8^+$ T cells. MYD88 mediates signal transduction for all TLRs except TLR3, and MAVS is activated by the cytosolic sensors RIG-I and MDA-5, leading to the activation of the NF-κB and IRF pathways and the subsequent expression of inflammatory cytokines and I IFNs (Figure 1). I studied the impact of MYD88- and MAVS-deficiency on the cross-presentation and direct presentation of poxviral or recombinant antigens, using IFN-γ and TNF-α expression by OVA- or B8-specific $CD8^+$ T cells as a read-out for T cell activation, as well as a fluorochrome-labeled antibody recognizing SIINFEKL/MHC-I-complexes to monitor the loading of SIINFEKL on MHC-I. The absence of MYD88 or MAVS had no impact on activation of IFN-γ expression in OVA- or B8-specific T cells by cross-presenting and directly presenting BMDCs (Figure 32A, B). In addition, MYD88 and

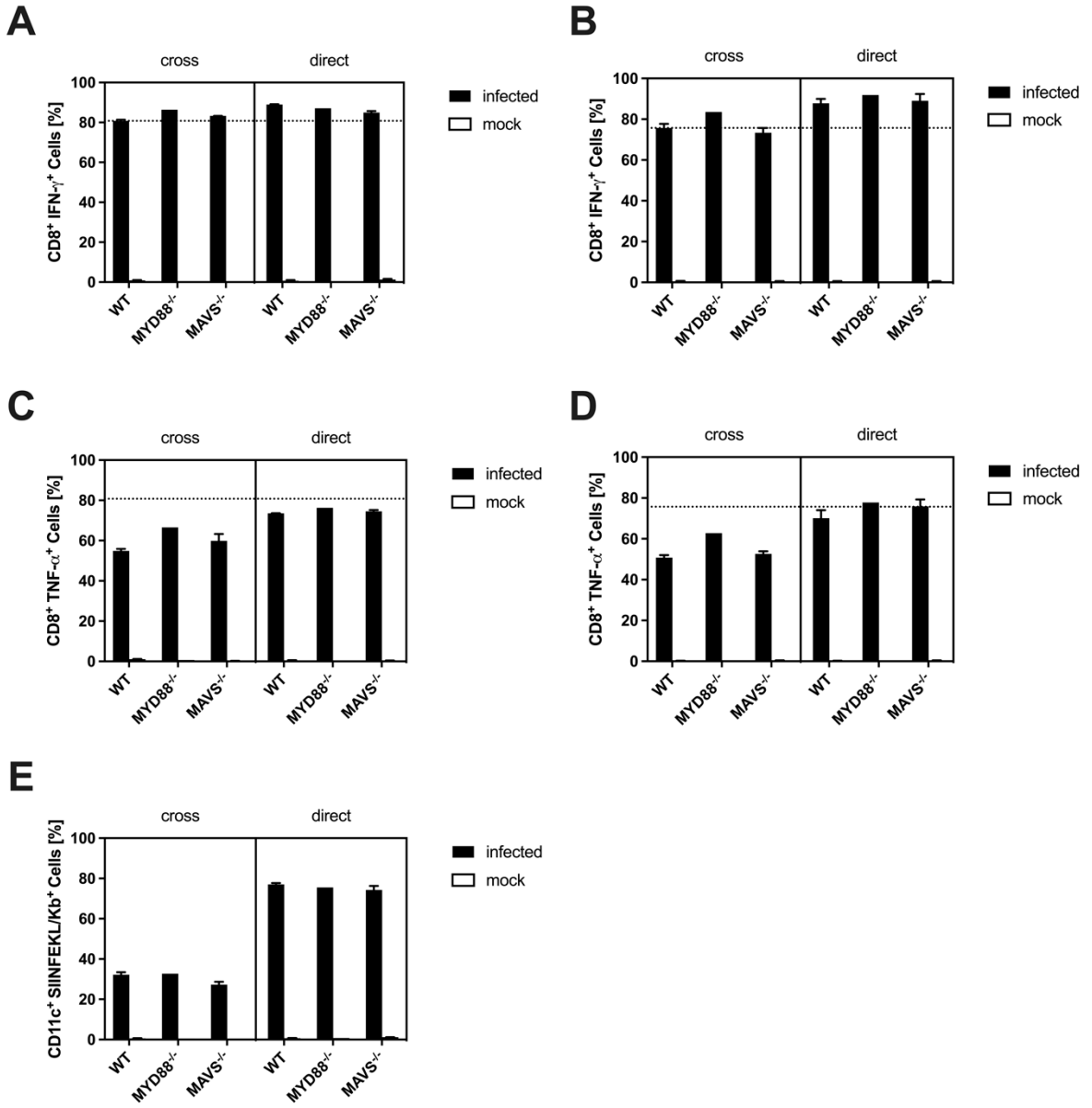

Figure 32: The ability to cross-present antigens or to present antigens directly is not impaired in MYD88- or MAVS-deficient BMDCs. MHC-I mismatched wildtype feeder cells (murine Cloudman S91 melanoma cells) and GM-CSF-BMDCs generated from wildtype, MYD88- or MAVS-deficient C57BL/6 mice were infected with MVA-PK1L-OVA at MOI 1, or mock-infected for 16 h. For the analysis of the ability to cross-present antigens, infected and mock-infected feeder cells were treated with PUVA, washed and cocultured with uninfected MYD88$^{-/-}$ or MAVS$^{-/-}$ BMDCs for 20 h. Feeder-BMDC-cocultures (cross) and directly infected BMDCs (direct) were incubated with CD8$^+$ T cells specific for the recombinant antigen OVA (A, C) or the viral antigen B8 (B, D). The ability to activate T cells was analyzed by flow cytometry and determined as frequency of IFN-γ (A, B) or TNF-α (C, D) expressing CD8$^+$ T cells. In addition, the ability of cross-presenting and directly infected CD11c$^+$ MHC II^{high} expressing BMDCs to process and present the SIINFEKL epitope of OVA at the cell surface on MHC-I was analyzed by flow cytometry. Data are presented as frequency (E). Data represent one experiment with two biological replicates.

MAVS deficiency in BMDCs resulted in comparable numbers of TNF-α$^+$ OVA- as well as B8-specific T cells following coculture with directly infected BMDCs or cross-presenting BMDCs (Figure 32C, D). Indeed, TNF-α represents a more sensitive

marker for T cell activation than IFN-γ and therefore may support the discovery of more subtle effects on the ability of infected BMDCs to activate $CD8^+$ T cells. Furthermore, MYD88- and MAVS-deficient cross-presenting and directly infected BMDCs showed an equivalent SIINFEKL/Kb-loading ability compared to control BMDCs (Figure 32E). In summary, these results indicate that MYD88 and MAVS signaling in presenter cells was not crucial for the ability to either directly present or cross-present antigens during infection with MVA.

6. DISCUSSION

Since MVA is a highly attenuated virus strain, is replication-incompetent in most mammalian cells and can induce robust immune responses, it is currently under investigation as a promising vaccine vector against infectious diseases and various cancers (36, 37, 155). The induction of $CD8^+$ T cell responses during primary infection with MVA is mastered by directly and cross-presenting DCs (51, 58). However, the time available for $CD8^+$ T cell priming by directly infected DCs is limited because infection with MVA results in massive apoptosis shortly after infection. Subsequent $CD8^+$ T cell responses can only be induced by DCs, which cross-present viral antigens from dying or dead cells on MHC-I molecules to activate $CD8^+$ T cells (51, 156). To date, only a few studies have looked at the underlying mechanisms that favor the induction of $CD8^+$ T cell responses by cross-presentation of antigens using MVA as a vaccine vector (58). However, knowledge of the precise mechanisms which license DCs to induce efficient cytotoxic T cell responses may advance the development of MVA-based vaccines. Hence, this thesis aims to investigate one or more particular innate immune triggers which activate DCs for the cross-presentation of antigens to stimulate poxvirus-specific $CD8^+$ T cell responses.

6.1. AraC-treatment of MVA-infected feeder cells impairs the activation of BMDCs for antigen cross-presentation

AraC is an antimetabolite analog of cytidine. It inhibits viral replication and therefore impairs the synthesis of late and intermediate transcribed genes (144). In line with the inhibitory effect of AraC on the expression of late and intermediate gene transcripts, MVA-infected BMDCs showed an impaired activation of $CD8^+$ T cells specific for late expressed viral or recombinant antigens (Figure 4A). Using AraC to study viral replication, I observed that AraC had a striking effect on cross-presented antigens. Astonishingly, AraC treatment of MVA-infected feeder cells abolished, in addition to intermediate and late expressed antigens, cross-presentation of early expressed antigens, and subsequent T cell activation by BMDCs (Figure 4B). Even though early gene transcription and protein synthesis of early expressed antigens were not impaired by AraC, cross-presenting BMDCs lost the ability to cross-present early antigens and, consequently, the capacity to activate antigen specific T cells (Supplementary Figure 1). In contrast to directly infected and AraC-treated BMDCs, cross-presenting BMDCs

only encountered AraC-treated cells but had no direct contact with AraC. In accordance with the hampered T cell activation after AraC-treatment of infected feeder cells, cross-presentation of the Kb-restricted SIINFEKL-epitope of OVA on MHC-I by BMDCs was utterly abolished (Figure 4C, D). As well as proper antigen presentation, costimulation mediated by CD40 and CD86 is necessary for the efficient activation of T cell responses (157, 158). Furthermore, it was shown that mannose receptors and CD40 are crucial for the activation of cross-presentation because they target engulfed antigens to early endosomes via CD40-dependent activation of NIK (159, 160). NIK is crucial for activating signaling through NF-κB, which seems to be important for $CD8^+$ T cell cross-priming by $CD8^+$ splenic DCs (161). Moreover, it has been shown that I IFNs are able to promote the expression of costimulatory molecules by APCs (162-164). Since neither AraC-treated nor untreated infected feeder cells produced IFN-β, it is unlikely that the striking reduction in CD40 and CD86 expression in AraC-feeder-BMDC-cocultures can be attributed to the missing I IFN response in feeder cells (Figure 5A, B, D; Figure 15B; Figure 16B). Pascutti and colleagues demonstrated that during infection with MVA, I IFNs rather contribute to the induction of IP-10 than to the phenotypic maturation of bystander cells (50). Nevertheless, I IFNs trigger not only paracrine but also autocrine IFNAR signaling to activate a positive feedback loop for the augmentation of I IFN signaling (165). Indeed, IFNAR signaling has been shown to be crucial for the induction of IFN-α and IFN-β during infection with MVA (1, 42). Therefore, the missing I IFNs might indeed contribute to the reduced phenotypic maturation of cross-presenting BMDCs in AraC-feeder-BMDC-cocultures. However, it is more likely that another trigger, which is present in feeder cells following infection with MVA, is more important to stimulate the functional activation of cross-presenting BMDCs.

Previous research has shown that many murine and human melanoma cells exhibit a defective I IFN signaling pathway, which could explain the inability of my feeder cells to produce any cytokines apart from IP-10 in response to MVA infection ((148); Figure 16B). Because AraC inhibits the transcription of intermediate and late genes, and only early mRNA is transcribed in the presence of AraC, dsRNA levels are reduced by about a third (144). Considering that dsRNA is sensed by PKR during vaccinia virus infection, particularly in the absence of the viral inhibitor E3L, this innate immune pathway might gain importance in melanoma cells (166). E3 has been shown to inhibit I IFN production by sequestering dsRNA during infection with vaccinia virus or MVA, thereby

circumventing PKR activation (21). Moreover, E3 is known to be essential for intact late protein synthesis by MVA in certain cell types, due to its ability to inhibit apoptosis (23). Besides the inhibition of I IFN production, in the presence of AraC, MVA-infection induced significantly higher levels of early apoptosis and necrosis in feeder cells (Figure 6A). In line with these results, I observed increased levels of cleaved CASP-8 in protein lysates from infected and AraC-treated feeder cells, indicating apoptotic cell death (Figure 6B). Interestingly, Zhang and colleagues showed that AraC abrogated the PKR-dependent phosphorylation of IRF3 during infection with an ΔE3 vaccinia virus (166). Hence, PKR activation during infection with MVA in Cloudman S91 melanoma cells might be crucial to activate a particular signaling pathway, which triggers the activation of BMDCs for cross-presentation of antigens. To elucidate the role of PKR in the ability of feeder cells to trigger the functional activation of cross-presentation competent BMDCs, further studies using ΔE3-MVA for the infection of feeder cells in the presence or absence of AraC would be required. Considering the importance of E3L for the inhibition of dsRNA sensing by PKR during vaccinia virus infection, this innate immune pathway might gain relevance in certain cell lines. For instance, Cloudman S91 melanoma cells might not only exhibit a defective I IFN pathway but might also fail to activate proper cGAS-STING signaling, which has been shown to be the main pathway for the sensing of MVA (1, 148, 167).

As the licensing of BMDCs for efficient cross-presentation of antigen may be influenced either directly in the cross-presenting BMDC in terms of PRR activation or indirectly at the level of phagocytosis, I labeled AraC-treated feeder cells with a cell tracer and determined the phagocytic activity of BMDCs in feeder-BMDC-cocultures. Since MVA infection in the presence of AraC resulted in a significant decline in the phagocytic activity of cross-presenting BMDCs, it seems that feeder cells failed to activate BMDCs for phagocytosis (Figure 31C). This missing activation after MVA infection could result in the induction of an aberrant cytokine/chemokine pattern or the release and exposure of different molecules by feeder cells, which renders these cells less attractive for phagocytosis by BMDCs in the presence of AraC. In accordance with the notion that AraC might alter the cytokine/chemokine pattern of MVA-infected feeder cells, I observed lower IL-1β and IP-10 levels in supernatants from AraC-treated and infected feeder cells compared with those of infected control cells (Figure 26; Figure 27).

6.2. The AraC effect on cross-presenting BMDCs is cell type dependent

To elucidate whether the effect of AraC observed on cross-presenting BMDCs is dependent on the feeder cell type, I conducted a cross-presentation assay using Cloudman S91 melanoma cells, MHC-I mismatched BMDCs and other cell types, including immune and non-immune cells. In general, AraC did not have any impact on the ability to license cross-presenting BMDCs for the activation of $CD8^+$ T cells by immune cells such as MHC-I mismatched BMDCs, J774, or WEHI3 (Figure 7-8). Surprisingly, efficient stimulation of cross-presentation and subsequent $CD8^+$ T cell activation by BMDCs was similarly impaired by AraC in Cloudman S91 melanoma cells, DF1 and HeLa cells (Figure 9). In contrast to these non-immune cells (fibroblasts and epithelial cells), professional APCs and immune cells may be less sensitive to AraC because these cells feature a greater diversity in PRRs for the efficient detection of pathogens. However, the non-immune MEF cells were also non-susceptible to AraC (Figure 9). As discussed in section 6.1, the phenotype induced in cross-presenting BMDCs after coculture with infected AraC-treated feeder cells showed a notable similarity to the role of PKR-inhibition by E3L for the sensing of dsRNA during MVA as well as vaccinia virus infection. In line with the missing susceptibility of MEF cells to AraC, Smith and colleagues found that MEF cells do not depend on PRK signaling during infection with vaccinia virus (21). To gain insight into the phenotype of AraC-treated Cloudman S91 melanoma cells as feeder cells, I sequenced RNA from MVA-infected or mock-infected cells with or without AraC-treatment. As the volcano plot in Figure 11A illustrates, several genes exhibited both high significance and high FC. Among these genes, I identified several target genes involved in important innate immune signaling pathways, such as P2RX7 and PYCARD (protein name: ASC). Since MVA replicates exclusively in the cytoplasm, I also selected genes involved in DNA sensing, like LRRFIP1 and XCCR6 (protein name: Ku70), for further analysis. The comparison of “MVA-infected” with “AraC-treated and MVA-infected feeder cells” showed the upregulation of many genes. Most of these upregulated genes were listed with GO-terms assigned to the biological processes antigen processing and presentation, innate immune response, and cell death. Since MVA does not directly interfere with antigen presentation pathways, AraC not only seemed to impair the ability of infected feeder cells to stimulate cross-presentation of antigen by BMDCs but might also affect the processing and presentation of antigen on MHC-I by the infected feeder cell itself (55). Since the latter has not been tested in this study, it remains to be

confirmed whether AraC affects antigen presentation by MVA-infected feeder cells at the transcription level only, or also the actual presentation of peptide/MHC-I complexes. However, aberrant MHC-I presentation by infected feeder cells should not interfere with antigen cross-presentation by BMDCs. In fact, the trigger that determines whether antigen will be cross-presented probably depends more on the release/exposure of molecules by feeder cells to stimulate BMDCs for efficient phagocytosis and proper coordination of antigen processing and presentation. My finding that cell death was listed among the GO-terms, and that these genes were frequently upregulated in AraC-treated and MVA-infected feeder cells is in accordance with the high numbers of early apoptotic cells as well as increased cleaved CASP-8 levels observed in the presence of AraC in both MVA-infected and mock-infected feeder cells (Figure 6; Figure 11B, C). The reason for the significantly higher cell death in mock-infected AraC-treated feeder cells might be attributed to the fact that AraC, as a cytostatic drug, induces an apoptotic cell death by interrupting DNA replication (168, 169). That some of the upregulated genes were listed with GO-terms assigned to “innate immune response” might support the idea that AraC functions in susceptible feeder cells by blocking a particular PRR. At this point, it is tempting to speculate that this PRR may be PKR, given its role in dsRNA sensing during MVA and vaccinia virus infection and the associated type I interferon production. Considering that the RNA sequencing results showed several other regulated genes in feeder cells infected in the presence of AraC, other PRRs, such as P2RX7 and PYCARD (protein name: ASC), could be involved in the recognition and subsequent activation of BMDCs for cross-presentation by my feeder cells. In addition to the RNA sequencing of feeder cells, I further analyzed the impact of AraC on the gene expression patterns in cross-presenting BMDCs following incubation with AraC-treated/-untreated and either MVA-infected or mock-infected feeder cells. Interestingly, after excluding data with a fold change lower than 2 and higher than -2 as well as data with unspecific p-values ($p > 0.05$), the analysis revealed that the comparison “CD11c MVA AraC vs. CD11c MVA” only comprised data with positive FC, indicating that in comparison to “CD11c MVA AraC”, “CD11c MVA” samples exhibited solely upregulated genes (Figure 12A). Usually, NGS-data exhibit a more balanced distribution pattern and show, as in the comparison “CD11c Mock vs. CD11c MVA”, a huge number of down- as well as upregulated genes (Figure 12B). This finding supports my hypothesis that AraC in feeder cells blocks a crucial innate immune signaling pathway, resulting in the lack of

PRR activation in cross-presenting BMDCs. Furthermore, analysis of gene expression in cross-presenting BMDCs showed that AraC seems to mostly affect signaling pathways involved in recognition and processing exogenous dsRNA rather than I and II IFN signaling (Figure 13C, D). Since I IFN expression by BMDCs was differentially regulated in dependence of MVA-infection rather than AraC-treatment, the I IFN signaling pathway might not be affected, at least not directly, by AraC in cross-presenting BMDCs. However, these results are in contrast to the observed impaired IFN-β response by cross-presenting BMDCs in AraC-treated feeder-BMDC-cocultures (Figure 15B). When interpreting these findings, one has to consider that the "$CD11c^+$ MVA" group is heterogeneous and comprises cross-presenting BMDCs and other BMDCs, which have not encountered and phagocytosed MVA-infected feeder cells. Interestingly, BMDCs cocultured with infected feeder cells showed a comparable SIINFEKL/Kb-loading ability and phagocytic activity, suggesting that BMDCs that phagocytosed material from infected feeder cells also appear to be able to present SIINFEKL/Kb-complexes at the cell surface (Figure 22A; Figure 31C). In contrast, the SIINFEKL/Kb^- population showed a higher expression of I and II IFN related genes than SIINFEKL/Kb^+ cells, while the latter showed a higher expression of genes linked to exogenous dsRNA signaling pathway components (Figure 13B-D). Since I ensured that MVA-infected feeder cells could not transmit the virus to cocultured BMDCs during my cross-presentation assays by including several washing steps and PUVA-treatment, these results suggest that in addition to cross-presenting BMDCs, there might be another BMDC population that produced I IFNs. As Pascutti *et al.* reported, bystander DCs show an elevated maturation phenotype, increased IP-10 production, and increased capacity to activate autologous peripheral blood lymphocytes for IFN-γ expression compared to directly infected DCs. Although the authors demonstrated that I IFNs have a supportive role in this setting, the extent of the contribution of the bystander cells to I IFNs production remains elusive (50). However, these findings need to be interpreted cautiously until more research is conducted to confirm this NGS analysis. In conclusion, my data suggest that dsRNA sensing might be important not only in the feeder but also in the cross-presentation competent BMDC. As reviewed by Mittelbrunn & Sánchez-Madrid, genetic material can be transferred from cell to cell via exosomes, ectosomes and apoptotic bodies. Exosomes are derived from late endosomes and are released after fusion of the endosomal membrane with the plasma membrane. Ectosomes contain cytosolic material of the donor cell. Both exosomes

and ectosomes can be either constitutively released or their release can be enhanced due to activation of the donor cell or stress (170). As described in section 2.3, endosomal and cytosolic dsRNA can be recognized via different mechanisms. The potential mechanisms that could play an important role in MVA recognition were investigated using different genetically modified feeder cells and will be discussed in more detail in section 6.5. Extracellular vesicles can be taken up by the target cell via phagocytosis, fusion of the vesicle membrane with the plasma membrane, and endocytosis. In accordance with the notion that MVA-infection might induce or increase the release of extracellular vesicles, I observed a higher expression of genes related to exogenous dsRNA signaling pathway components in the SIINFEKL/Kb+ population (Figure 13D). Therefore, the missing activation of BMDCs for cross-presentation in cocultures with AraC-treated and infected feeder cells may be attributed to an altered activity for the release of extracellular vesicles by infected feeder cells. However, it remains to be shown whether these extracellular vesicles are produced by my feeder cells and whether these vesicles are involved in the activation of BMDCs for cross-presentation.

Another way to transfer genetic material from cell to cell is to engulf apoptotic cells. Since I observed increased cell death in infected and AraC-treated feeder cells compared to infected control cells, there should be more apoptotic cells that could release apoptotic bodies, which in turn could be taken up by APCs (Figure 6). Despite the increased cell death in AraC-treated and infected feeder cells, these cells fail to activate BMDCs for antigen cross-presentation (Figure 4B-D). I speculate that the altered exposure or composition of molecules by feeder cells in the presence of AraC likely makes these infected cells less attractive for phagocytosis. Considering that the cGAS-STING pathway is essential for the sensing of MVA due to its cytoplasmic replication (1), STING and the induced I IFNs might nevertheless have even greater relevance for the activation of cross-presenting BMDCs by infected feeder cells.

6.3. IFNAR is crucial for the activation of cross-presenting BMDCs

In contrast to vaccinia virus, MVA lacks many immunomodulatory genes and is well-known to induce a robust I IFN response (42). Due to the important role of I IFNs during infection with MVA, I investigated the role of IFNAR and IFN-β in the activation of MVA-specific $CD8^+$ T cells as well as antigen presentation by cross-presenting BMDCs. Using two different recombinant MVA expressing OVA either early (PK1L) or late (P11)

during viral gene transcription, I observed that, in the absence of IFNAR, cross-presenting BMDCs demonstrated a significantly reduced ability to activate $CD8^+$ T cells specific for late expressed antigens (OVA, A3, A19) (Figure 14B). These results suggest that autocrine signaling, which maintains a positive feedback loop to multiply the immune response initiated by I IFNs, was particularly important for the activation of T cells specific for late expressed antigens. During the replication cycle of MVA, early and late transcription differs not only in timing but also in the site of transcription. While early gene transcription begins as soon as the viral core has been released into the cytoplasm, late genes are transcribed in viral factories, a special organelle for viral DNA replication (171, 172). Despite normal protein synthesis, late antigens only induce poor $CD8^+$ T cell responses (173, 174). This phenomenon is attributed to an immune evasion strategy adopted by vaccinia virus and MVA, in which late antigens are trapped in viral factories to inhibit efficient processing of these antigens for direct presentation or cross-presentation by DCs (53, 54). Furthermore, several studies have shown that signaling of I IFNs via IFNAR during infection with MVA is crucial for the induction of IFN-α and -β (1, 42). Therefore, the induction of $CD8^+$ T cells specific for late antigens might rely even more on the IFNAR-mediated positive feedback loop for the amplification of the already poor $CD8^+$ T cell responses against late antigens. Moreover, Waibler and colleagues reported that, unlike IFNAR signaling, IFN-β expression in Flt3-L-derived-BM-pDCs is dispensable for the production of IFN-α (42). In line with the negligible role of IFN-β, my data show that IFN-β expression in cross-presenting as well as directly infected BMDCs was dispensable for the *in vitro* activation of $CD8^+$ T cell lines (Figure 14C, D). Surprisingly, I observed a significantly reduced efficiency in antigen presentation by cross-presenting as well as directly presenting BMDCs in the absence of IFN-β (Figure 14F). These results indicate that IFN-β expression in both cross-presenting and directly infected BMDC supports efficient antigen presentation on MHC-I. To date, most research into the role of I IFNs has focused on IFNAR or the production of IFN-α and -β during viral infections, emphasizing a supportive function during the differentiation and maturation of DCs (162, 163, 175). In addition, I IFNs have been shown to promote antigen presentation and cross-priming by increasing TAP and MHC-I expression (176-178). In fact, I IFNs are also able to stimulate cross-presentation via regulating the pH to prevent antigen degradation and cellular trafficking (179, 180). As described by Lorenzi and colleagues I IFNs even enhance the survival of cross-presenting DCs through upregulation of

antiapoptotic gene expression (181). On top of the common roles of IFN-α and -β in the generation of innate and adaptive immune responses, Rudd *et al.* reported that solely IFN-β, and not IFN-α, contributes to cytokine production of IP-10 and MCP-1 as well as TLR expression during infection with RSV (164). For this reason, the positive feedback loop mediated by IFNAR may well have had a stronger impact on efficient cross-presentation and subsequent T cell activation during infection with MVA compared to the expression of IFN-β alone, due to its binding of both IFN-α and -β. Since IFN-β was obviously produced at higher levels than IFN-α by both directly infected and cross-presenting wildtype BMDCs, IFN-β might be more important for IFNAR activation (Figure 20). Nevertheless, it would be interesting to investigate whether IFN-α has a different role to IFN-β in antigen presentation by directly and cross-presenting BMDCs during infection with MVA.

In addition, the cytokine analysis of supernatants from cocultured IFNAR-deficient BMDCs with MVA-infected feeder cells revealed reduced expression of several cytokines, including IFN-β (Figure 15A). As IFN-β is one of the primary interferons that are produced upon stimulation of PRR and DAMPs, which triggers positive feedback signaling mediated by IFNAR, it is not surprising that IFNAR deficiency reduced the overall IFN-β production (182-184). In line with my data, previous research found that following RSV infection and PolyI:C treatment, levels of IL-6, IL-1α, and TNF-α were reduced in the absence of IFNAR (185, 186). Interestingly, BMDCs cocultured with MVA-infected and AraC-treated feeder cells showed an impaired production of IL-1α, IFN-β, MCP-1 and IL-6, which are exactly the same cytokines which showed reduced levels in the absence of IFNAR in cross-presenting BMDCs (Figure 15B). These results suggest that AraC might inhibit a molecule that is either part of the IFNAR-JAK-STAT signaling pathway or is important for the expression of I IFNs. The similar cytokine pattern in IFNAR-deficient cross-presenting BMDCs and AraC-feeder-BMDC-cocultures suggest that AraC might function downstream of IFNAR. However, since AraC-treated cells completely failed to activate BMDCs for the production of IFN-β, it is more likely that AraC blocks a signaling pathway which is important for the induction of I IFNs, for instance downstream of PRRs required for the sensing of MVA. In general, my findings imply that I IFNs support the activation of cross-presenting BMDCs but are not required for T cell activation nor for the induction of SIINFEKL/Kb^+ cells. Nevertheless, the absence of IFN-β results in a significantly decreased antigen presentation efficiency, suggesting its complementary role in the surface expression

of SIINFEKL/Kb-complexes. Furthermore, the unaffected stimulation of $CD8^+$ T cells specific for early antigens by IFNAR-deficient cross-presenting BMDCs is consistent with a supportive role for IFNAR in cross-presenting BMDCs. Thus, because of the abolished I IFN response and the loss of the ability to cross-present antigen, I hypothesize that AraC inhibits a PRR or innate immune signaling pathway important for MVA sensing in certain feeder cells, as discussed in sections 6.1 and 6.2. Considering the importance of the cGAS-STING pathway for the induction of I IFNs as well as the generation of $CD8^+$ T cell responses during infection with MVA, I speculate that STING might either be a direct or indirect target for AraC (1, 143).

6.4. STING is essential for the induction of type I interferons, but is dispensable for the stimulation of cross-presentation

My work, and that of other researchers, has shown that STING is crucial for the induction of I IFNs as well as the generation of primary $CD8^+$ T cell responses *in vivo* during infection with MVA. Therefore, I investigated the role of STING in feeder as well as presenter cells for the licensing of BMDCs to enable cross-presentation of antigen and the stimulation of $CD8^+$ T cells *in vitro* (1, 47, 143). To elucidate the impact of STING in feeder cells, STING was silenced in murine Cloudman S91 melanoma cells using CRISPR/Cas9 (Supplementary Figure 7). Unfortunately, STING had no impact on the activation of cross-presenting BMDCs for the stimulation of $CD8^+$ T cells, either in the feeder or in the presenter cells (Figure 17). However, I observed a significant drop in the antigen presentation ability (from SIINFEKL/Kb^+ cell numbers) as well as antigen presentation efficiency of STING-deficient cross-presenting and directly infected BMDCs (Figure 18). Because my $CD8^+$ T cell lines represent antigen-specific effector cells, which acquire effector functions already after the recognition of low epitope densities presented by APCs, even significant differences in SIINFEKL/Kb-complexes at the cell surface might result in a comparable T cell activation, as shown in Figure 17. In fact, STING deficiency in the feeder cell revealed that STING had no major impact on the amount of SIINFEKL/Kb-complexes presented at the surface of cross-presenting BMDCs (Figure 18D). On the other hand, STING-deficient feeder cells induced significantly higher numbers of SIINFEKL/Kb^+ BMDCs, suggesting that the lack of STING was beneficial for feeder cells in the activation of BMDCs for cross-presentation (Figure 18C). Considering the promoting effect of IFN-α on antigen presentation, the significantly elevated expression of Ifna13 mRNA in infected STING-

deficient feeder cells might account for the improved cross-presentation by BMDCs in cocultures with infected STING-deficient feeder cells (Figure 30; (179, 187)). Consistent with these results, the absence of STING in the feeder cell also favored MHC-II expression on the cell surface of cross-presenting BMDCs (Figure 19F). As described by Spadaro *et al.* BMDCs are able to upregulate cross-presentation via distinct strategies in the presence of IFN-α. They showed that IFN-α was able to enhance antigen cross-presentation in BMDCs by preserving antigens from degradation, increasing trafficking of MHC-I molecules to antigen-containing endosomes, and targeting antigens to recycling $Rab11^+$ endosomes (179). It appears that IFN-α expression in my feeder cells was activated via a different signaling pathway in the absence of STING. I speculate that this signaling pathway could be actively inhibited by STING in wildtype feeder cells. As shown by Wang and colleagues, the β-transcript isoform of STING dominantly inhibits the recognition of nucleic acids by the original STING-α isoform (188). Since this isoform also contains the functional C-terminal domain but lacks the transmembrane domain, it is likely that I could not distinguish between both isoforms in my experiments. Therefore, it would be interesting to analyze which STING isoform is predominantly present in my feeder cells. Another theory for the elevated IFN-α expression in STING KO feeder cells could be that TBK1 can be recruited by other molecules in the absence of STING, thus contributing to the activation of additional signaling pathways. These pathways could play a minor role in the presence of STING and might even be indirectly or directly inhibited by STING. However, I was unable to confirm whether the Ifna13 mRNA detected by qRT-PCR was translated (see section 6.5.2 for a more detailed discussion). For this reason, IFN-α production cannot reliably explain the improved antigen presentation and the expression of costimulatory molecules in cocultures of BMDCs with STING-deficient feeder cells. Since the phagocytic activity of STING-deficient cross-presenting BMDCs could affect the efficiency of antigen presentation, I investigated the impact of STING in the infected feeder cell as well as the cross-presenting BMDC on phagocytosis. However, I was unable to detect any effect of STING on phagocytosis, indicating that STING-deficient BMDCs engulfed comparable quantities of dead cell material and were equally able to process and present the encountered antigens on MHC-I molecules (Figure 31B).

Furthermore, by studying the impact of STING in feeder as well as presenter cells for the maturation of cross-presenting BMDCs, my data revealed that STING signaling

had an impact predominantly on the maturation phenotype of cross-presenting BMDCs regarding the expression of CD86 and MHC-II (Figure 19B-C, E-F). In line with the well-known positive effect of I IFNs on the expression of costimulatory molecules, I confirmed that the STING-mediated I IFN response during infection with MVA facilitates CD86 and MHC-II expression by cross-presenting BMDCs (163, 189). On top of the supportive role of STING for DC maturation, my work, and that of other researchers, has shown that STING is essential for the induction of I IFNs during infection with MVA by directly infected DCs *in vitro* as well as *in vivo* (Figure 20A-B; (1, 143)). Here I demonstrate that STING signaling is not only crucial in directly infected BMDCs, but also of remarkable importance in cross-presenting BMDCs that have never been infected with MVA. Even in the cross-presentation scenario, STING in the presenter cell was crucial for the expression of costimulatory molecules and, indeed, essential for the induction of I IFNs. Since it has been shown that MVA infection of DCs results in massive apoptosis, there are only limited possibilities to stimulate $CD8^+$ T cell responses by directly infected BMDCs (190, 191). As reported by Pascutti and colleagues, non-infected bystander DCs express higher levels of costimulatory molecules and are able to activate antigen specific $CD4^+$ and $CD8^+$ T cells. The authors also showed that I IFNs were not responsible for the phenotypic maturation of bystander DCs, yet induced IP-10 production (50). Considering that cross-presenting BMDCs in my setting resemble non-infected bystander cells, it is surprising that the induced I IFN response was still STING-dependent. Because of the essential function of STING in the induction of I IFN and the rather supportive role in cross-presentation of antigen, STING signaling in cross-presenting BMDCs might not be activated as result of intrinsic DNA sensing. My findings are in line with the study performed by Ahn *et al.*, who reported that in phagocytes, extrinsic STING activation by tumor cell derived cGAMP, which is synthesized by cGAS from ATP and GTP after binding to DNA, is crucial for the induction of an inflammatory immune response (109, 192). As Ablasser and colleagues have demonstrated, cGAMP can be transferred extracellularly to neighboring cells to activate STING functions (46). Recently, several studies have found that cGAMP can be transported by different mechanisms through the plasma membrane using the SLC19A1 transporter, LRRC8 volume-regulated anion channels and connexins (193-196). Furthermore, it has been shown that cGAMP can be incorporated into viral particles and transferred to neighboring cells to propagate STING signaling (197, 198). However, the activation of STING signaling through viral

particles containing cGAMP is not likely to occur during infection with MVA, due to the inability of MVA to complete its replication cycle in most mammalian cells. In fact, extracellular transfer of cGAMP from infected feeder cells to cross-presenting BMDCs might provide a potential mechanism underlying the improved ability to cross-present antigen as well as the enhanced MHC-II expression in BMDCs cocultured with infected STING-deficient feeder cells (Figure 18C; Figure 19F). Since I did not observe higher I IFN production by STING KO feeder-BMDC-cocultures compared to control cocultures, the extracellular transfer of cGAMP appears to be rather unlikely (Figure 20C-D). However, it is necessary to take into account the fact that both STING-deficient and wildtype feeder cells might exhibit a comparable cGAMP production during infection with MVA, due to their inability to produce type I interferons (Figure 26). Assuming a comparable cGAMP production, STING-deficient as well as wildtype feeder cells should induce comparable I IFN responses in cross-presenting wildtype BMDCs. Yet it remains unclear whether Cloudman S91 melanoma cells are able to produce cGAMP during MVA-infection, and, whether the produced cGAMP is extracellularly transferred to cross-presenting BMDCs in my settings. To answer this question, a more detailed analysis would be required, for instance by using cGAS-deficient feeder cells. Furthermore, phagocytosed material might contain DNA, which can be sensed by endosomal TLRs. However, there is more and more evidence that bacterial and mitochondrial tumor DNA is able to escape by an unknown mechanism from the endosomal compartment into the cytosol, which results in the activation of the cGAS-STING pathway (97, 199). Therefore, it would be also necessary to exclude the possibility that viral DNA might be sensed by cGAS in the cytosol of cross-presenting BMDCs.

In conclusion and in accordance with previous research, I have demonstrated that STING is essential for the sensing of MVA in directly infected BMDCs, as well as for the activation of BMDCs for cross-presentation, and the subsequent induction of I IFNs. Despite the contribution of STING to antigen presentation by BMDCs in both the direct infection and cross-presentation contexts, it is likely that other mechanisms are more important, because the SIINFEKL/Kb-loading ability remains intact in the absence of STING. In line with the role of IFNAR and IFN-β in BMDCs, the results described above suggest that another pathway might trigger efficient antigen presentation during infection with MVA.

6.5. TRIF-, P2RX7- and ASC-deficient feeder cells fail to activate cross-presenting BMDCs

To elucidate how the sensing of MVA is accomplished in infected feeder cells and whether the contributing innate immune pathways are responsible for the activation of cross-presenting BMDCs, the target genes listed in Table 8 were silenced individually in feeder cells using CRISPR/Cas9 as a gene-editing approach. T cell activation and DC maturation were assessed in these feeder cell lines, to characterize them by their ability to induce cross-presentation, and they were also analyzed for their susceptibility to apoptosis, the release of cytokines and chemokines, and their impact on the phagocytic activity of cross-presenting BMDCs.

6.5.1. Do TRIF-, P2RX7- and ASC-deficient feeder cells represent a spoiled meal?

Of all the tested gene-edited feeder cells, cells deficient in TRIF and MAVS showed the strongest impairment of both the ability to activate cross-presenting BMDCs for the activation of $CD8^+$ T cells and the processing and presentation of the Kb-restricted SIINFEKL epitope derived from OVA on MHC-I (Figure 21-22). However, the cocultivation of MVA-infected TRIF-deficient feeder cells with BMDCs had only a marginal impact on the BMDC maturation phenotype. Despite a high background expression of CD86 and MHC-II, I observed that cross-presenting BMDCs cocultured with MVA-infected TRIF-deficient feeder cells showed reduced tendencies for the expression of CD40 as well as CD86 (Figure 23). It is possible that the observed elevated background expression of CD86 and MHC-II by BMDCs cocultured with mock-infected feeder cells were caused by the use of GM-CSF for the differentiation of bone marrow cells into BMDCs (146, 147). An even greater impairment of T cell activation and SIINFEKL/Kb-loading was observed only in P2RX7- and ASC-deficient feeder-BMDC-cocultures, which were generated and characterized as part of a masters thesis project (data not shown). Furthermore, the absence of P2RX7 and ASC in MVA-infected feeder cells resulted in an impaired BMDC maturation phenotype, characterized by significantly decreased CD40 and CD86 expression (data not shown). TRIF- and ASC-deficiency in feeder cells not only resulted in impaired activation of BMDCs in the cross-presentation setting, but also in decreased I IFN and IL-6 production in cross-presenting BMDCs (Figure 28-29). In line with the previous results, the phagocytic activity of cross-presenting BMDCs in cocultures with either infected P2RX7- or ASC-deficient feeder cells was significantly diminished. Despite the lower

percentage of BMDCs able to recognize and phagocytose infected feeder cells in the absence of ASC or P2RX7, increased MFIs in these cocultures suggest that BMDCs that have already encountered antigens from ASC- or P2RX7-deficient feeder cells showed an enhanced phagocytic efficiency compared to MVA-infected control feeder cells (Figure 31). Surprisingly, the activation of BMDCs for phagocytosis by P2RX7- and ASC-deficient feeder cells was independent of MVA-infection, because mock-infected and infected KO feeder cells showed similar phagocytic activities (Figure 31C). In addition, these KO feeder cells showed a significantly higher basal phagocytic activity compared to control feeder cells (Figure 31D). These results imply that during infection with MVA, intact P2RX7 and ASC signaling in feeder cells might be associated with the ability to attract BMDCs by releasing “find-me” and/or “eat-me” signals. As reviewed by Ravichandran, “find-me” signals are released by dying cells to attract phagocytes to their proximity. These “find-me” signals represent soluble molecules that mediate the migration of phagocytes along a gradient to the site of apoptosis by binding to specific receptors on the cell surface of the phagocyte (200). “Find-me” signals comprise lipids and proteins, but also nucleotides (201). Elliott and coworkers identified ATP and UTP released by apoptotic cells and bound to the ATP/UTP receptor $P2Y_2$ of phagocytes as a crucial “find-me” signal (202). Since MVA-infection of DCs results, at least 12 h post-infection, in massive apoptosis, it is likely that my feeder cells also underwent apoptotic cell death after infection with MVA (51). As reported by Tappe and colleagues, MVA-infection causes both an immunogenic cell death and the release of ATP (156). Therefore, in my setting, ATP might be a crucial trigger for the attraction of DCs for phagocytosis. Consequently, an inhibited release of “find-me” signals by MVA-infected feeder cells would result in an impaired attraction of BMDCs and reduced phagocytosis. Considering the decreased phagocytic activity in the absence of P2RX7 and ASC in feeder cells, P2RX7 and ASC, as part of the inflammasome signaling pathway, might be involved in the release of find-me signals, in particular ATP. Consistent with this hypothesis, previous research has reported that P2RX7 mediates Pannexin-1 (PANX1) activation for the passage of large molecules, including IL-1β and ATP (203, 204). However, the nature of the relationship between PANX-1 and the inflammasome remains controversial. While Pelegrin and colleagues demonstrated that the release of IL-1β is dependent on PANX-1 as well as CASP-1 and ASC, a growing body of literature suggests that PANX-1 is dispensable for inflammasome activation (205-208).This discrepancy might

arise from the use of different cell types and stimuli for priming of the inflammasome. For instance, Parzych and coworkers reported that TLR2- and TLR4-triggered activation of the NLRP3 inflammasome in monocytes is accomplished by completely different signaling pathways. While the inflammasome assembly following TLR2 activation was PANX-1-dependent, PANX-1 was not necessary for the activation of the inflammasome after stimulation of TLR4 (209). Since my data showed that ASC-deficient feeder cells, comparable to P2RX7-deficient feeder cells, lacked the ability to activate BMDCs for efficient phagocytosis, I speculate that ASC and subsequent inflammasome activation might be crucial for the release of ATP as a “find-me” signal via PANX-1 (Figure 31).

Several studies have reported that ASC can also serve as a “find-me” signal, due to its extracellular function as a second messenger in addition to its intracellular role as part of the inflammasome (132, 210). ASC has been found in the extracellular space in the form of ASC specks, which can be released together with other inflammasome components by inflammasome-activated cells (153, 211). ASC specks can be incorporated by other cells to propagate inflammatory or apoptotic signaling following their release from endosomes and the recruitment of either CASP-1 or CASP-8 (153, 212, 213). However, the detailed mechanism behind ASC speck release, and whether the liberation of ASC specks into the extracellular space is a passive or active mechanism, remains unknown (210). In a recent study, Sagoo and coworkers demonstrated that MVA infection of macrophages results in inflammasome activation, rapid cell death, and subsequent release of ASC specks (214). In accordance with the notion that ASC might represent an essential “find-me” signal, I observed that MVA-infected feeder cells are a poor target as cargo for phagocytic BMDCs in the absence of ASC (Figure 31). Previous research has established that TRIF and P2RX7 mediate crucial signaling pathways for the activation of several inflammasomes, including the NLRP3 inflammasome. In fact, TLR-signaling, including TRIF activation, was shown to be an important step in the priming of inflammasomes (215-217). In contrast, P2RX7 signaling is well known to mediate the second signal for inflammasome activation (134, 204). For this reason, TRIF and P2RX7 signaling in MVA-infected feeder cells, and ASC as an inflammasome component, may represent signaling pathways crucial for the full activation of inflammasome signaling. Considering that ASC specks are only released in the extracellular space by inflammasome-activated cells, TRIF- and P2RX7-deficient feeder cells probably lack an active inflammasome, and therefore

“find-me” signal ASC specks are not released to attract phagocytic BMDCs. Since I also characterized all gene-edited feeder cells without coculture with BMDCs, gene-edited feeder cells were assessed for their susceptibility to apoptosis after MVA-infection, and for the production of cytokines and chemokines. I hypothesized that MVA-infected wildtype feeder cells exhibit an active inflammasome due to the produced IL-1β at 16 h post-infection (Figure 26; Supplementary Figure 9). Interestingly, IL-1β production in supernatants from infected ASC-, TRIF- and P2RX7-deficient feeder cells was absent, suggesting that inflammasome activation was abolished in these feeder cells. However, only low IL-1β levels could be detected in supernatants from infected wildtype feeder and feeder-BMDC-cocultures. Some supernatants from mock-infected knockout feeder cells showed elevated background levels of IL-1β and IFN-β, suggesting a steady-state activation of these cells. These knockout cells produced and secreted inflammatory cytokines as well as chemokines independently of an innate immune trigger. As discussed in the following section, steady-state cytokine production might support the idea of the activation of a negative regulator following MVA-infection. In general, I was not surprised to find a poor IL-1β response following MVA-infection of wildtype feeder cells because my feeder cells represent melanoma cells instead of immune cells, which are prone to express a greater set of pro- and anti-inflammatory cytokines in response to a viral infection. Moreover, the low IL-1β production in MVA-infected wildtype feeder cells may be caused by MVA immune evasion mechanisms. Since MVA exhibits a viroceptor that can capture IL-1β produced by the infected cell, IL-1β concentrations might be detectable in MVA-infected cells at limited levels (5, 10). In line with the extracellular function of ASC specks, I observed impaired IL-1β secretion by cross-presenting BMDCs in supernatants from BMDC-feeder ASC KO cell-cocultures, which would support the theory that there is ineffective transfer of ASC specks to presenter cells from infected feeder cells lacking active inflammasome signaling (Figure 29B; Supplementary Figure 9).

In addition to “find-me” signals, phagocytes are activated by “eat-me” signals to engulf apoptotic cells. “Eat-me” signals are only recognized by phagocytes in close proximity to the apoptotic cell, and involve newly exposed or modified surface molecules as well as alteration of the cell surface charge (200). Among these molecules exposed as “eat-me” signals is for instance, phosphatidylserine (PS), which is displayed on the cell surface during early apoptosis (218). Even though several MVA-infected gene-edited

feeder cells displayed more frequent early as well as late apoptosis, only TRIF-, P2RX7- and ASC-deficient feeder cells also showed significantly increased necrosis after infection with MVA (Figure 24). According to Mackenzie *et al.*, the exposure of PS following short P2RX7 activation can be transient and will not necessarily result in apoptosis (219). As reviewed by Nagata *et al.*, apoptosis is not only associated with PS exposure but also requires caspase activation. Considering that the phospholipid translocase Flippase, which regulates PS exposure, is inactivated during apoptosis and that some Flippases exhibit a CASP-3 recognition site, it was hypothesized that Flippase might be a target for caspases (220). In line with the increased necrosis observed in MVA-infected P2RX7-deficient feeder cells compared to infected wildtype cells or mock-infected control cells, the absence of P2RX7 resulted in elevated levels of cleaved CASP-8 (Figure 25A). Infected TRIF-deficient feeder cells showed significantly elevated numbers of early apoptotic cells. However, the numbers of late apoptotic and necrotic cells were significantly increased for both MVA- and mock-infected feeder cells in comparison to MVA- and mock-infected wildtype feeder cells, suggesting that TRIF-knockout feeder cells showed less MVA-dependent apoptosis than P2RX7- or ASC-deficient cells (Figure 24A-C). In accordance with the exposure of PS and the plasma membrane integrity, cell lysates of infected TRIF-deficient feeder cells contained cleaved CASP-8 levels comparable to those in infected control cells (Figure 25B). Based on these results, TRIF-deficient and wildtype feeder cells definitely showed signs of apoptosis, doubtlessly caused by infection with MVA, yet PS exposure appears to be considerably lower than in P2RX7- and ASC-deficient feeder cells. These results suggest that deficiency in P2RX7 and ASC might hamper the release of “find-me” signals, leading to impaired attraction of phagocytes to the apoptotic cells. However, phagocytes that stumble across apoptotic P2RX7- and ASC-deficient cells, can identify and engulf these cells due to the exposure of “eat-me” signals on the cell surface at sufficient levels, or levels that are possibly even higher than those on control cells. In summary, the activation of BMDCs for phagocytosis by P2RX7- and ASC-deficient feeder cells was independent of MVA-infection, as mock-infected and infected KO feeder cells showed a very similar phagocytic activity (Figure 31C). Furthermore, these particular KO cells showed a significantly higher basal phagocytic activity than control feeder cells (Figure 31D). Considering that BMDCs in cocultures with P2RX7- and ASC-deficient feeder cells could only internalize a limited amount of antigen due to the reduced phagocytic activity, antigen presentation and

subsequent activation of antigen-specific $CD8^+$ T cells were impaired (data not shown), as antigen internalization correlates with antigen presentation in an inflammatory environment (221).

Moreover, the missing activation of cross-presenting cells for antigen presentation, T cell activation, and DC maturation by TRIF-, P2RX7- and ASC-deficient feeder cells during infection with MVA could result from the activation of different cell death pathways in the absence of P2RX7, ASC, and TRIF. Since apoptosis has been described as an immunologically silent form of cell death, in contrast to pyroptosis or necroptosis, representing two types of programmed necrosis, the absence of P2RX7 and ASC might shift the MVA-triggered cell death from pyroptosis/necroptosis to apoptosis (222). Because, in contrast to infected wildtype feeder cells, infected feeder cells lack IL-1β production in the absence of P2RX7, ASC, and TRIF, pyroptotic cell death seems unlikely. Furthermore, high levels of cleaved CASP-8 in supernatants from infected P2RX7- and ASC-deficient feeder cells support the idea of apoptotic cell death. Necroptosis constitutes a further inflammatory cell death pathway. Necroptotic cell death is accompanied by cytoplasm swelling and membrane rupture and the subsequent release of DAMPs, for instance, ATP (223). As TRIF signaling has been shown to trigger the formation of the necrosome, the absence of TRIF in infected feeder cells could have abolished necroptotic cell death following MVA-infection (224, 225). Indeed, necroptosis should be inhibited in the absence of P2RX7 and ASC in infected feeder cells due to the observed elevated levels of active CASP-8, which has been described to inhibit RIPK3 and therefore necrosome formation (226, 227). Furthermore, Zhou and colleagues have recently emphasized the role of MER proto-oncogene tyrosine kinase (MerTK) in the induction of immune responses by phagocytes. In fact, they showed that apoptotic tumor cells, which are phagocytosed following PS exposure, activate phagocytes for the induction of immune tolerance. However, when MerTK is inhibited, ATP and cGAMP, released by the tumor cell, stimulate phagocytes via the extracellular transfer of cGAMP to induce an inflammatory immune response (228). Considering that deficiencies in TRIF, P2RX7, and ASC result in enhanced PS exposure, elevated levels of active CASP-8 and the absence of IL-1β, MVA-induced cell death in these gene-edited feeder cells possibly endorse the induction of immune tolerance by the phagocyte, as well as apoptotic, rather than pyroptotic or necroptotic, cell death. However, a tolerogenic immune response might be rather unlikely due to the production of inflammatory cytokines like type I interferon

or IL-1β by these cells. To confirm or refute this hypothesis, the cell death in my feeder cells during infection with MVA, and how exactly TRIF, P2RX7 and ASC are involved in this, should be addressed in further studies. The impact of different cell death pathways during MVA-infection could be studied by analyzing the expression and oligomerization of the gasdermin D (GSDMD) or mixed lineage kinase domain-like (MLKL) in infected and mock-infected feeder cells during pyroptosis/necroptosis.

6.5.2. TRIF, P2RX7 and ASC deficiency in feeder cells rescues type I interferon production

On top of the differentially regulated IL-1β production by MVA-infected TRIF-, P2RX7- and ASC-deficient feeder cells, the cytokine and chemokine analysis of several genetically modified cells revealed striking differences in IFN-β, CCL5, and IP-10 expression compared to infected wildtype feeder cells. Although MVA is known to induce a robust STING-dependent I IFN response in cDCs, MVA-infected wildtype feeder cells barely showed any IFN-β production (Figure 26; (1)). The lack of IFN-β in supernatants from infected wildtype feeder cells suggests that Cloudman S91 melanoma cells could not produce I IFN, most likely due to well-known defects in the STING and JAK-STAT signaling pathways in melanoma cells (1, 167, 229, 230). Surprisingly, feeder cells infected with MVA mounted a robust IFN-β response in the absence of TRIF, P2RX7, and ASC, ranging from around 200 pg/ml for TRIF-deficient feeder cells to almost 1900 pg/ml for ASC-deficient feeder cells (Figure 26). However, I was unable to detect more than negligible IFN-α levels in supernatants from MVA- or mock-infected gene-edited or control feeder cells. Despite the lack of IFN-α production at the protein level, semi-quantitative RT-PCR analysis revealed that Ifna13 was expressed in MVA-infected wildtype and STING-deficient feeder cells. Because the detection of secreted IFN-α proteins by ELISA is mostly limited to a few IFN-α subtypes, the absence of IFN-α in the supernatants does not necessarily mean that IFN-α is not produced. Consistent with the prominent role of IFN-α in the innate and adaptive immune responses, limited activation of BMDCs for antigen presentation and T cell activation by infected P2RX7- and ASC-deficient feeder cells was accompanied by significantly reduced levels of Ifna13 expression in these feeder cells (data not shown; Figure 30). Previous research has shown that IFN-α facilitates the expression of MHC-I and -II on APCs, promotes cross-presentation of viral antigen to $CD8^+$ T cells, and supports the optimal clonal expansion of virus-specific T cells (176, 231, 232). In

addition, P2RX7 and ASC KO feeder cells showed delayed Ifna13 expression compared to infected wildtype feeder cells (Figure 30). Even though in the absence of P2RX7 and ASC, feeder cells exhibited an elevated IFN-β response, the transcription of additional genes coding for IFN-α subtypes (Ifna4 or Ifna13) apparently was not stimulated via an autocrine positive feedback loop (182-184). However, according to the company BioLegend, the subtype IFN-α1 should be detected by the IFN-α capture bead B7 of the LEGENDplex assay. Since Ifna1 and Ifna13 were reported to encode identical proteins, no further conclusions regarding translated protein levels should be drawn from levels of Ifna13 mRNA (233).

My findings raise the question of how TRIF, P2RX7, and ASC, which are crucial components for signaling for most inflammasomes, might be associated with the induction of I IFN. Due to the lack of intact viral IFN-binding proteins, MVA-infection results in a robust I IFN response, in contrast to vaccinia virus infection (5). Dai and colleagues demonstrated that the sensing of MVA and the subsequent induction of I IFNs in conventional DCs is solely accomplished via the cGAS-STING signaling pathway (1, 47). However, it has been demonstrated that melanoma cells in particular show varying expression levels of cGAS and STING (167). Therefore, in my feeder cells, the STING-dependent induction of I IFNs might be hampered due to low expression levels of cGAS (Supplementary Figure 12). As well as low levels of cGAS expression, I observed detectable STING expression in wildtype feeder cells, indicating that cGAS-STING signaling in my feeder cells might be compromised at the cGAS level (Supplementary Figure 7). In addition to the STING-dependent I IFN response, Delaloye and coworkers proposed that in murine and human macrophages, the sensing of MVA is mediated via four additional pathways. First, it was hypothesized that the TLR2-TLR6 heterodimer activates the transcription of pro-IL-1β and IFN-β-independent chemokines via MYD88. The NLRP3 inflammasome further processes pro-IL-1β to mature IL-1β. Simultaneously, viral RNA is sensed by MDA5, which activates MAVS signaling and the expression of IFN-β. IFN-β in turn binds to IFNAR, via STAT signaling, and mediates the expression of IFN-β-dependent chemokines such as IP-10 (41). In line with the signaling cascade described above, supernatants from MVA-infected P2RX7- and ASC-deficient feeder cells showed elevated IFN-β and IP-10 levels (Figure 26; Figure 27). Despite the observed increases in IFN-β production in TRIF-deficient feeder cells, I was unable to detect elevated IP-10 levels (Figure 27). Because IFN-β levels in supernatants from infected TRIF-deficient feeder cells were

almost 5 to 10 times lower compared to P2RX7- or ASC-deficient feeder cells, I speculate that the IFN-β concentration might be too low to trigger IFNAR-dependent IP-10 expression. Because infected wildtype feeder cells were able to mount an IP-10 response even in the absence of IFN-β production, it is tempting to speculate that IP-10 is stimulated in Cloudman S91 melanoma cells following IFNAR-dependent activation. In fact, Brownell and colleagues showed that IRF3 and NFκB are recruited to the IP-10 promoter following HCV infection, sensed by TLR3 and RIG-I (234). In accordance with this notion, I observed decreased IP-10 levels in infected feeder cells deficient in RIG-I. However, mock-infected RIG-I KO feeder cells also showed elevated IP-10 production, indicating high levels of background expression. Therefore, these results need to be treated as tentative until more research is conducted to identify whether RIG-I and TLR3 might also be crucial for innate signaling in my feeder cells during infection with MVA.

Furthermore, Waibler *et al.* reported that IFN-α in pDCs was mainly produced independently of TLR or PKR signaling in response to MVA-infection, even though a combined knockout of MYD88 and TRIF resulted in a significantly reduced IFN-α response (42). Indeed, it is not only different cell types but also different APCs that use distinct PRRs and are therefore capable of inducing various distinct immune responses. These results suggest that another PRR might be involved in the production of IFN-α. Although PKR was dispensable for the induction of IFN-α, PKR and OAS have been shown to be targets of the viral immunomodulatory gene E3L, which is functional in MVA and which limits the production of I IFNs as well as the induction of apoptosis (235). Because the effect of the viral protein E3 in infected cells shares some phenotypic features with my observations in infected TRIF-, P2RX7- and ASC-deficient feeder cells, I speculate that in the absence of TRIF, P2RX7, and ASC, a potential target of E3 might not be activated. As a result, E3 would be able to block neither the induction of I IFNs nor the initiation of apoptosis in TRIF-, P2RX7- and ASC-deficient feeder cells. In particular, E3 inhibits the induction of I IFNs by blocking the phosphorylation of IRF3 and IRF7 (23). Indeed, I observed higher levels of phosphorylated IRF3 in cell lysates of P2RX7- and ASC-deficient MVA-infected feeder cells compared to those of TRIF-deficient feeder cells or wildtype feeder cells, supporting the theory that E3 counteracts the activation of IRF3 in wildtype but not in P2RX7- and ASC-deficient feeder cells (data not shown). However, the detailed mechanisms by which the deficiency in P2RX7 and ASC might hamper the activation

of a potential molecule which is concomitantly an E3 target remain unclear, and whether there is an interaction between inflammasome signaling and the missing activation of this particular E3-targeted molecule should be addressed in further studies. Interestingly, Zhang and colleagues reported for vaccinia virus that PKR mediated the sensing of dsRNA in the absence of E3. The PKR-dependent phosphorylation of IRF3 and the nuclear translocation of phosphorylated IRF3, which has been shown to depend on MAVS signaling after activation by both RIG-I and MDA-5, are important for the induction of I IFNs during infection with ΔE3 vaccinia virus (236). However, I found that Cloudman S91 melanoma cells lack MDA-5 at the protein level and that RIG-I deficiency had no impact on the activation of cross-presenting BMDCs (data not shown; Figure 21-22). Although I observed a significantly reduced ability to license BMDCs for activating $CD8^+$ T cells and antigen cross-presentation for MAVS-deficient feeder cells, other genetically modified cell lines lacking TRIF, P2RX7, or ASC showed a more significant reduction in the ability to activate BMDC functions (Figure 21-22). Additionally, Delaloye and coworkers identified in macrophages MDA-5 as a crucial sensor for the induction of I IFNs during infection with MVA (41). As my feeder cells lack MDA-5, other signaling pathways for dsRNA sensing, for instance, PKR or TLR3-TRIF signaling, might gain importance. In particular, PKR was reported to be involved in inflammasome activation and HMGB1 release, which is considered to be a DAMP with its various extracellular forms and functions (237-239). As Lu and colleagues demonstrated, PKR is able to interact directly with NLRP3, NLR family pyrin domain containing 1 (NLRP1), absent in melanoma 2 (AIM2) and NLR family CARD domain containing 4 (NLRC4) (238). Furthermore, it was shown that HMGB1 secretion from macrophages requires inflammasome and caspase activation (240, 241). In addition, HMGB1 release was triggered by IFN-β and subsequent binding to IFNAR (237). Due to the involvement of PKR, the inflammasome, and I IFNs, I believe that HMGB1 could function as another “eat-me” signal to activate BMDCs for phagocytosis and cross-presentation of antigen.

Another theory explaining the lack of IFN-β in supernatants from infected wildtype feeder cells could be the activation of a negative regulator of the I IFN signaling pathway in Cloudman S91 melanoma cells. I speculate that the negatively regulated induction of I IFNs could directly or indirectly depend on TRIF, P2RX7, and ASC signaling. Because TRIF-, P2RX7-, and ASC-deficient infected feeder cells share a common phenotype, including the inability to activate cross-presenting BMDCs for

phagocytosis and subsequent antigen presentation, interference with inflammasome assembly and signaling is very likely to be involved in this process. As reviewed by Zheng *et al.*, several NLRs have been shown to regulate immune signaling negatively, yet not all NLRs contain a pyrin domain for the recruitment of ASC (132). NLRP12 and NLRP4 might be involved in suppressing I IFNs in infected wildtype feeder cells, assuming that a particular NLR negatively regulates the IFN-β response by forming an active inflammasome together with ASC and caspases. Previous research has shown that it is NLRP12 that is predominantly responsible for the negative regulation of the expression of inflammatory cytokines and I IFNs by inhibiting NF-κB phosphorylation and blocking RIG-I and IRAK signaling (206, 242-244). As well as NLRP12, NLRP4 has also been shown to inhibit the induction of I IFNs by targeting TBK1 for degradation (245). In contrast to pyrin-containing NLRs, NLR family member X1 (NLRX1), NLR family CARD domain containing 5 (NLRC5), and NLR family CARD domain containing 3 (NLRC3) lack the ability to assemble to inflammasomes. Furthermore, NLRX1 is the only member of the NLR family, which exhibits a mitochondrial localization sequence (246). In particular, NLRX1 inhibits the induction of I IFNs by binding to MAVS and blocking its interaction with RIG-I (247, 248). It has been suggested that NLRC5 is able to restrain the expression of I IFNs. However, other studies report opposing findings (249, 250). There is a substantial body of literature on the inhibitory role of NLRC3 in the induction of I IFNs. As well as inhibition of TRAF6 and NF-κB inhibition, NLRC3 also mediates the blocking of I IFN induction at the STING level (251, 252). Interestingly, using NGS analysis, I observed a differential NLRC3 gene expression in MVA-infected feeder cells with or without AraC treatment (data not shown). Because NLRC3 has been identified as an AraC-dependent regulated gene following MVA-infection, and because NLRC3 is able to inhibit the expression of I IFNs, additional research would be required to assess any potential connection of NLRC3 to the activation of BMDCs for cross-presentation in my setting.

IFI16 has been found to be an intracellular sensor for DNA, and is able to initiate the assembly of an inflammasome (253). Zheng and colleagues have shown that porcine IFI16 is able to restrict cGAS signaling by competitively binding to DNA (254). Unfortunately, I failed to silence IFI16 expression in my feeder cells using gene editing approaches. For this reason, whether or not IFI16 is involved in the sensing of MVA in Cloudman S91 melanoma cells still remains unclear.

In addition to the role of TRIF, P2RX7, and ASC in the activation of cross-presenting BMDCs in MVA-infected feeder cells, I observed a significant drop in T cell activation and antigen presentation in the absence of MAVS and LRRFIP1 in feeder cells (Figure 21-22; data not shown). Moreover, deficiencies in LRRFIP1 and MAVS resulted in decreased IL-1β secretion by infected feeder cells (Figure 26). As Yang and coworkers have reported, LRRFIP1 mediates the expression of IFN-β via β-catenin following sensing of dsRNA and dsDNA (131). Although LRRFIP1 has never been described to have an impact on the sensing of MVA, LRRFIP1-mediated signaling after dsDNA detection could be more important in melanoma cells than in other cells, because these cells exhibit a limited variety of PRRs for DNA and RNA sensing, and LRRFIP1 is able to detect both DNA and RNA. In contrast to LRRFIP1, MAVS has been shown to be involved in IFN-β expression during infection with MVA in macrophages (41). However, Dai *et al.* demonstrated that the cGAS-STING-IRF3 axis is crucial for the induction of I IFNs in response to MVA-infection of cDCs (1). For this reason, the impact of MAVS during infection with MVA might be cell type dependent. Beyond the role of MAVS for the induction of I IFNs, several studies have demonstrated the importance of MAVS for inflammasome activation (255). Nevertheless, LRRFIP1 and MAVS probably contribute to the activation of cross-presenting BMDCs by MVA-infected feeder cells, but beyond any doubt, TRIF, P2RX7, and ASC play a greater role in the licensing of BMDCs.

Taken together, my data clearly indicate the importance of TRIF-, and particularly P2RX7- and ASC-mediated signaling for the licensing of BMDCs for antigen cross-presentation by Cloudman S91 melanoma cells during infection with MVA, including the ability to stimulate virus-specific $CD8^+$ T cells *in vitro*. A tentative conclusion at this point is that, most probably, MVA-infection in the absence of TRIF, P2RX7, and ASC results in an immunologically silent cell death resulting in a restricted release of “find-me” signals. Of course, this conclusion is preliminary and requires further investigation of the cell death pathways and possibly also evidence of the liberation of DAMPs into the extracellular space. Moreover, my results suggest that the induced I IFN response during infection with MVA might be negatively regulated in Cloudman S91 melanoma cells. On the evidence presented, I cannot be certain whether the possible inhibition of I IFNs arises from viral immunomodulatory proteins or is suppressed by cellular proteins. Although the involvement of TRIF, P2RX7, and ASC may be most likely attributed to inflammasome signaling, I need to consider additional methods to find

evidence for active caspases which facilitate the release of mature IL-1β since I failed to detect cleaved CASP-1 in western blot analyses.

6.6. MYD88 and MAVS in presenter cells are dispensable for cross-presentation

Because of the important role of PRRs in the sensing of pathogens by professional APCs, I studied the impact of MYD88 and MAVS in presenter cells for the sensing and activation of cross-presentation by infected feeder cells. Using antigen-specific $CD8^+$ T cell lines and antigen loading of SIINFEKL on MHC-I as a readout for the ability to activate T cells and to present antigen, I investigated the impact of MYD88 and MAVS signaling for cross-presenting as well as directly infected BMDCs. However, I was unable to detect any impact of MYD88 and MAVS for T cell activation in either directly infected or cross-presenting BMDCs (Figure 32A-D). Even the surface expression of SIINFEKL/Kb-complexes by directly infected and cross-presenting BMDCs in the absence of MYD88 or MAVS was almost identical to that in infected control cells (Figure 32E). These results suggest that neither MYD88 nor MAVS were involved in activating BMDCs for cross-presentation of antigens. As discussed in section 6.5, the phenotype of the infected feeder cell might be more important for licensing of cross-presenting BMDCs than the composition of PRRs in the professional APC. However, previous research has shown that only antigens from phagosomes also containing TLR ligands were efficiently cross-presented and rescued from excessive antigen degradation (77, 78, 98). Since MYD88 mediates signaling from all TLRs except TLR3 and TLR4, further analysis using BMDCs from global TRIF knockout mice or the combined deletion of TRIF and MYD88 would be needed to access the role of TLR-signaling in cross-presenting DCs during infection with MVA. Interestingly, even in the direct infection setting, MYD88 and MAVS were not involved in antigen presentation or T cell stimulation following infection with MVA. My findings seem to contradict those of Delaloye *et al.*, who demonstrated that MAVS mediates signaling via MDA-5 to induce the expression of IFN-β in murine macrophages. However, innate signaling induced in response to MVA-infection might be different in macrophages than in directly infected BMDCs. Furthermore, they showed that MYD88 mediates signaling via the heterodimer TLR2/6 and results in both inflammasome priming and the induction of IFN-β-independent chemokines such as CCL3, CCL4, and IL-8 (41). However, it has to be taken into account that Delaloye and colleagues focused their

research on the induction of IFN-β by MVA-infected macrophages while I analyzed the impact of MYD88 and MAVS on the antigen presentation ability of directly as well as cross-presenting BMDCs. In accordance with Waibler *et al.*, who reported that the IFN-α response induced during infection with MVA is mostly independent of TLR or PKR signaling, I conclude that neither MYD88 nor MAVS in BMDCs are crucial for the licensing of BMDCs for antigen presentation *in vitro* (42). To elucidate whether MAVS or MYD88 in cross-presenting BMDCs might be crucial for inflammasome activation after extracellular transfer of ASC specks, as described earlier, coculture experiments with MVA-infected TRIF-, P2RX7- or ASC-deficient feeder cells would be required.

6.7. Conclusion

In conclusion, the results obtained in this study show a notable parallel between AraC-treated, TRIF-, P2RX7- or ASC-deficient feeder cells in the ability to stimulate cross-presenting BMDCs during infection with MVA. My data further support the idea that these feeder cells fail to attract phagocytes due to the impaired release of a “find-me” signal, which remains to be identified. Because phagocytosis of infected feeder cells is abrogated, cross-presenting BMDCs are not activated, and therefore subsequent poxviral $CD8^+$ T cell responses are not stimulated. There is evidence that AraC treatment, and the absence of TRIF, P2RX7 or ASC, in infected feeder cells fails to activate a shared PRR-dependent signaling pathway. Despite the essential role of STING for the induction of I IFNs by directly infected and cross-presenting BMDCs during infection with MVA, my findings suggest that feeder cell signaling might play a major role in the activation/licensing of cross-presentation in BMDCs to stimulate adaptive immune responses (1). Based on my data, I assume that upon infection with MVA, inflammasome activation following dsRNA sensing in certain cell lines which do not depend on the cGAS-STING signaling pathway may be relevant for the functional activation of cross-presenting BMDCs. Since my results suggest that most DNA sensing pathways are not involved in the recognition of MVA by my feeder cells, it is more likely that dsRNA could be the innate immune trigger, which licenses my feeder cells to activation BMDCs for antigen cross-presentation. In fact, the question of whether or how feeder cell signaling might affect antigen cross-presentation in general and especially during MVA infection has been underestimated by most prior research. MVA is currently under investigation as a promising vaccine vector. Therefore,

understanding the detailed mechanisms that stimulate DCs for the induction of efficient cytotoxic T cell responses may contribute to the optimization of MVA-based vaccines.

7. LIST OF ABBREVIATIONS

AIM2	Absent in melanoma 2
APC	Antigen-presenting cell
AraC	Cytarabine
ASC	Apoptosis-associated speck-like protein
BFA	Brefeldin A
BiP	Immunoglobulin binding protein
BIR	Baculovirus inhibitor of apoptosis repeat domain
BMDC	Bone marrow derived dendritic cell
CARD	Caspase recruitment and activation domain
CM cells	Cloudman S91 melanoma cells
COPII	Coat protein complex II
DAMP	Damage associated pattern
DC	Dendritic cell
DDX41	DEAD-box helicase 41
DNA-PK	DNA-dependent protein kinase
DNA-PKcs	DNA-dependent protein kinase catalytic subunit
dsDNA	Double stranded DNA
dsRNA	Double stranded RNA
eIF2α	Eukaryotic initiation factor 2 alpha
ER	Endoplasmic reticulum
FC	Fold change
GM-CSF	Granulocyte-macrophage colony-stimulating factor
GO-term	Gene ontology term
gRNA	Guide RNA
GSDMD	Gasdermin D
I IFNs	Type I interferons
IFNAR	Interferon-α/β receptor
IRAP	Insulin-regulated aminopeptidase
ISG	Interferon stimulated gene
Ku70	X-ray repair complementing defective repair in Chinese hamster cells 6
LRR	Leucin-rich repeat domain

LRRFIP1	Leucine rich repeat (in FLII) interacting protein 1
MAVS	Mitochondrial antiviral-signaling protein
MerTK	MER proto-oncogene tyrosine kinase
MFI	Mean fluorescence intensity
MHC	Major histocompatibility complex
MLKL	Mixed lineage kinase domain-like
MVA	Modified vaccinia virus Ankara
MYD88	Myeloid differentiation primary response 88
NGS	Next-generation sequencing
NLR	NOD-like receptors
NLRC4	NLR family CARD domain containing 4
NLRP1	NLR family pyrin domain containing 1
NLRP3	NLR family pyrin domain containing 4
NOD	Nucleotide-binding and oligomerization domain
ORF	Open reading frame
PAMP	Pattern recognition receptor
PI	propidium iodide
pDC	Plasmacytoid dendritic cell
PKR	Protein kinase double-stranded RNA-dependent
PLC	Peptide-loading complex
PRR	Pattern recognition receptor
PuroR	Puromycin resistance gene
PYD	Pyrin domain
RLR	RIG-I-like receptor
rMVA	Recombinant MVA
P2RX7	Purinergic receptor P2X, ligand-gated ion channel, 7
PS	Phosphatidylserine
RPKM	Reads per kilobase of transcript per million mapped reads
RIG-I	Retinoic acid inducible gene I
RNA Pol III	RNA-polymerase III
RT-PCR	Real-time PCR
SNAP23	Synaptosomal-associated protein 23
SNARE	Soluble N-ethylmaleimide-sensitive-factor attachment receptor
ssRNA	Single-stranded RNA

STAT	Signal transducers and activators of transcription
STING	Stimulator of interferon genes
TAP	Transporter associated with antigen processing
TLR	Toll-like receptor
TRIF	Toll-like receptor adaptor molecule 2
WHO	World health organization
β_2m	β_2-microglobulin

8. REFERENCES

1. Dai P WW, Cao H, Avogadri F, Dai L, Drexler I, Joyce JA, Li XD, Chen Z, Merghoub T, Shuman S, Deng L. 2014. Modified vaccinia virus Ankara triggers type I IFN production in murine conventional dendritic cells via a cGAS/STING-mediated cytosolic DNA-sensing pathway. *PLoS Pathogen* 10: e1003989

2. Smith GL. 2007. Genus Orthopoxvirus: vaccinia virus. In *Poxviruses*, pp. 1-45: Springer

3. Sánchez-Sampedro L, Perdiguero B, Mejías-Pérez E, García-Arriaza J, Di Pilato M, Esteban M. 2015. The evolution of poxvirus vaccines. *Viruses* 7: 1726-803

4. Antoine G, Scheiflinger F, Dorner F, Falkner F. 1998. The complete genomic sequence of the modified vaccinia Ankara strain: comparison with other orthopoxviruses. *Virology* 244: 365-96

5. Blanchard TJ, Alcami A, Andrea P, Smith GL. 1998. Modified vaccinia virus Ankara undergoes limited replication in human cells and lacks several immunomodulatory proteins: implications for use as a human vaccine. *Journal of General Virology* 79: 1159-67

6. Larocca C, Schlom J. 2011. Viral vector-based therapeutic cancer vaccines. *Cancer J* 17: 359-71

7. Yang Z, Reynolds SE, Martens CA, Bruno DP, Porcella SF, Moss B. 2011. Expression profiling of the intermediate and late stages of poxvirus replication. *Journal of virology* 85: 9899-908

8. Nash P, Barrett J, Cao JX, Hota-Mitchell S, Lalani AS, Everett H, Xu XM, Robichaud J, Hnatiuk S, Ainslie C. 1999. Immunomodulation by viruses: the myxoma virus story. *Immunological reviews* 168: 103-20

9. Johnston J, McFadden G. 2004. Technical knockout: understanding poxvirus pathogenesis by selectively deleting viral immunomodulatory genes. *Cellular microbiology* 6: 695-705

10. Zimmerling S, Waibler Z, Resch T, Sutter G, Schwantes A. 2013. Interleukin-1β receptor expressed by modified vaccinia virus Ankara interferes with interleukin-1β activity produced in various virus-infected antigen-presenting cells. *Virology journal* 10: 34

11. Falivene J, Zajac MPDM, Pascutti MF, Rodríguez AM, Maeto C, Perdiguero B, Gómez CE, Esteban M, Calamante G, Gherardi MM. 2012. Improving the MVA vaccine potential by deleting the viral gene coding for the IL-18 binding protein. *PloS one* 7: e32220

12. Drillien R, Koehren F, Kirn A. 1981. Host range deletion mutant of vaccinia virus defective in human cells. *Virology* 111: 488-99

13. Gillard S, Spehner D, Drillien R, Kirn A. 1986. Localization and sequence of a vaccinia virus gene required for multiplication in human cells. *Proceedings of the National Academy of Sciences* 83: 5573-7

14. Perkus ME, Goebel SJ, Davis SW, Johnson GP, Limbach K, Norton EK, Paoletti E. 1990. Vaccinia virus host range genes. *Virology* 179: 276-86

15. Backes S, Sperling KM, Zwilling J, Gasteiger G, Ludwig H, Kremmer E, Schwantes A, Staib C, Sutter G. 2010. Viral host-range factor C7 or K1 is essential for modified vaccinia virus Ankara late gene expression in human and murine cells, irrespective of their capacity to inhibit protein kinase R-mediated phosphorylation of eukaryotic translation initiation factor 2α. *Journal of general virology* 91: 470-82

16. Meyer H, Sutter G, Mayr A. 1991. Mapping of deletions in the genome of the highly attenuated vaccinia virus MVA and their influence on virulence. *Journal of general virology* 72: 1031-8

17. Sutter G, Wyatt LS, Foley PL, Bennink JR, Moss B. 1994. A recombinant vector derived from the host range-restricted and highly attenuated MVA strain of vaccinia virus stimulates protective immunity in mice to influenza virus. *Vaccine* 12: 1032-40

18. Davies M, Elroy-Stein O, Jagus R, Moss B, Kaufman R. 1992. The vaccinia virus K3L gene product potentiates translation by inhibiting double-stranded-

RNA-activated protein kinase and phosphorylation of the alpha subunit of eukaryotic initiation factor 2. *Journal of virology* 66: 1943-50

19. Chang H-W, Watson JC, Jacobs BL. 1992. The E3L gene of vaccinia virus encodes an inhibitor of the interferon-induced, double-stranded RNA-dependent protein kinase. *Proceedings of the National Academy of Sciences* 89: 4825-9

20. Beattie E, Tartaglia J, Paoletti E. 1991. Vaccinia virus-encoded eIF-2α homolog abrogates the antiviral effect of interferon. *Virology* 183: 419-22

21. Smith EJ, Marié I, Prakash A, García-Sastre A, Levy DE. 2001. IRF3 and IRF7 phosphorylation in virus-infected cells does not require double-stranded RNA-dependent protein kinase R or IκB kinase but is blocked by vaccinia virus E3L protein. *Journal of Biological Chemistry* 276: 8951-7

22. Xiang Y, Condit RC, Vijaysri S, Jacobs B, Williams BR, Silverman RH. 2002. Blockade of interferon induction and action by the E3L double-stranded RNA binding proteins of vaccinia virus. *Journal of virology* 76: 5251-9

23. Hornemann S, Harlin O, Staib C, Kisling S, Erfle V, Kaspers B, Häcker G, Sutter G. 2003. Replication of modified vaccinia virus Ankara in primary chicken embryo fibroblasts requires expression of the interferon resistance gene E3L. *Journal of virology* 77: 8394-407

24. Postigo A, Cross J, Downward J, Way M. 2006. Interaction of F1L with the BH3 domain of Bak is responsible for inhibiting vaccinia-induced apoptosis. *Cell Death & Differentiation* 13: 1651-62

25. Wasilenko ST, Stewart TL, Meyers AF, Barry M. 2003. Vaccinia virus encodes a previously uncharacterized mitochondrial-associated inhibitor of apoptosis. *Proceedings of the National Academy of Sciences* 100: 14345-50

26. Fischer S, Ludwig H, Holzapfel J, Kvansakul M, Chen L, Huang D, Sutter G, Knese M, Häcker G. 2006. Modified vaccinia virus Ankara protein F1L is a novel BH3-domain-binding protein and acts together with the early viral protein E3L to block virus-associated apoptosis. *Cell Death & Differentiation* 13: 109-18

27. Sperling KM, Schwantes A, Staib C, Schnierle BS, Sutter G. 2009. The orthopoxvirus 68-kilodalton ankyrin-like protein is essential for DNA replication and complete gene expression of modified vaccinia virus Ankara in nonpermissive human and murine cells. *Journal of virology* 83: 6029-38

28. Herbert MH, Squire CJ, Mercer AA. 2015. Poxviral ankyrin proteins. *Viruses* 7: 709-38

29. Mosavi LK, Cammett TJ, Desrosiers DC, Peng Zy. 2004. The ankyrin repeat as molecular architecture for protein recognition. *Protein science* 13: 1435-48

30. McCoy LE, Fahy AS, Chen RA-J, Smith GL. 2010. Mutations in modified virus Ankara protein 183 render it a non-functional counterpart of B14, an inhibitor of nuclear factor κB activation. *The Journal of general virology* 91: 2216

31. Lehmann MH, Kastenmuller W, Kandemir JD, Brandt F, Suezer Y, Sutter G. 2009. Modified vaccinia virus ankara triggers chemotaxis of monocytes and early respiratory immigration of leukocytes by induction of CCL2 expression. *Journal of virology* 83: 2540-52

32. Drexler I, Heller K, Wahren B, Erfle V, Sutter G. 1998. Highly attenuated modified vaccinia virus Ankara replicates in baby hamster kidney cells, a potential host for virus propagation, but not in various human transformed and primary cells. *Journal of General Virology* 79: 347-52

33. Carroll MW, Moss B. 1997. Host range and cytopathogenicity of the highly attenuated MVA strain of vaccinia virus: propagation and generation of recombinant viruses in a nonhuman mammalian cell line. *Virology* 238: 198-211

34. Sutter G, Moss B. 1992. Nonreplicating vaccinia vector efficiently expresses recombinant genes. *Proceedings of the National Academy of Sciences* 89: 10847-51

35. Drexler I, Staib C, Sutter G. 2004. Modified vaccinia virus Ankara as antigen delivery system: how can we best use its potential? *Current opinion in biotechnology* 15: 506-12

36. Hui EP, Taylor GS, Jia H, Ma BB, Chan SL, Ho R, Wong W-L, Wilson S, Johnson BF, Edwards C. 2013. Phase I trial of recombinant modified vaccinia ankara encoding Epstein–Barr viral tumor antigens in nasopharyngeal carcinoma patients. *Cancer research* 73: 1676-88

37. Calvo-Pinilla E, Marín-López A, Moreno S, Lorenzo G, Utrilla-Trigo S, Jiménez-Cabello L, Benavides J, Nogales A, Blasco R, Brun A. 2020. A protective bivalent vaccine against Rift Valley fever and bluetongue. *NPJ vaccines* 5: 1-12

38. Hayes P, Gilmour J, von Lieven A, Gill D, Clark L, Kopycinski J, Cheeseman H, Chung A, Alter G, Dally L. 2013. Safety and immunogenicity of DNA prime and modified vaccinia ankara virus-HIV subtype C vaccine boost in healthy adults. *Clinical and vaccine immunology* 20: 397-408

39. Verheust C, Goossens M, Pauwels K, Breyer D. 2012. Biosafety aspects of modified vaccinia virus Ankara (MVA)-based vectors used for gene therapy or vaccination. *Vaccine* 30: 2623-32

40. Volz A, Sutter G. 2017. Modified vaccinia virus Ankara: history, value in basic research, and current perspectives for vaccine development. *Advances in virus research* 97: 187-243

41. Delaloye J, Roger T, Steiner-Tardivel Q-G, Le Roy D, Knaup Reymond M, Akira S, Petrilli V, Gomez CE, Perdiguero B, Tschopp J. 2009. Innate immune sensing of modified vaccinia virus Ankara (MVA) is mediated by TLR2-TLR6, MDA-5 and the NALP3 inflammasome. *PLoS pathogens* 5: e1000480

42. Waibler Z, Anzaghe M, Ludwig H, Akira S, Weiss S, Sutter G, Kalinke U. 2007. Modified vaccinia virus Ankara induces Toll-like receptor-independent type I interferon responses. *J Virol* 81: 12102-10

43. Isaacs A, Lindenmann J. 1957. Virus interference. I. The interferon. *Proceedings of the Royal Society of London. Series B-Biological Sciences* 147: 258-67

44. Der SD, Zhou A, Williams BR, Silverman RH. 1998. Identification of genes differentially regulated by interferon α, β, or γ using oligonucleotide arrays. *Proceedings of the National Academy of Sciences* 95: 15623-8

45. Sadler AJ, Williams BR. 2008. Interferon-inducible antiviral effectors. *Nat Rev Immunol* 8: 559-68

46. Ablasser A, Schmid-Burgk JL, Hemmerling I, Horvath GL, Schmidt T, Latz E, Hornung V. 2013. Cell intrinsic immunity spreads to bystander cells via the intercellular transfer of cGAMP. *Nature* 503: 530-4

47. Dai P, Wang W, Yang N, Serna-Tamayo C, Ricca JM, Zamarin D, Shuman S, Merghoub T, Wolchok JD, Deng L. 2017. Intratumoral delivery of inactivated modified vaccinia virus Ankara (iMVA) induces systemic antitumor immunity via STING and Batf3-dependent dendritic cells. *Science immunology* 2

48. Woo S-R, Fuertes MB, Corrales L, Spranger S, Furdyna MJ, Leung MY, Duggan R, Wang Y, Barber GN, Fitzgerald KA. 2014. STING-dependent cytosolic DNA sensing mediates innate immune recognition of immunogenic tumors. *Immunity* 41: 830-42

49. Bhat P, Leggatt G, Waterhouse N, Frazer IH. 2017. Interferon-γ derived from cytotoxic lymphocytes directly enhances their motility and cytotoxicity. *Cell death & disease* 8: e2836-e

50. Pascutti MF, Rodríguez AM, Falivene J, Giavedoni L, Drexler I, Gherardi MM. 2011. Interplay between modified vaccinia virus Ankara and dendritic cells: phenotypic and functional maturation of bystander dendritic cells. *J Virol* 85: 5532-45

51. Liu L, Chavan R, Feinberg MB. 2008. Dendritic cells are preferentially targeted among hematolymphocytes by Modified Vaccinia Virus Ankara and play a key role in the induction of virus-specific T cell responses in vivo. *BMC immunology* 9: 1-14

52. Altenburg AF, van de Sandt CE, Li BW, MacLoughlin RJ, Fouchier RA, van Amerongen G, Volz A, Hendriks RW, de Swart RL, Sutter G. 2017. Modified vaccinia virus Ankara preferentially targets antigen presenting cells in vitro, ex vivo and in vivo. *Scientific reports* 7: 1-14

53. Tao S, Tao R, Busch DH, Widera M, Schaal H, Drexler I. 2019. Sequestration of late antigens within viral factories impairs MVA vector-induced protective memory CTL responses. *Frontiers in immunology* 10: 2850

54. Tewalt EF, Grant JM, Granger EL, Palmer DC, Heuss ND, Gregerson DS, Restifo NP, Norbury CC. 2009. Viral sequestration of antigen subverts cross presentation to CD8+ T cells. *PLoS pathogens* 5: e1000457

55. Becker PD, Nörder M, Weissmann S, Ljapoci R, Erfle V, Drexler I, Guzmán CA. 2014. Gene expression driven by a strong viral promoter in MVA increases vaccination efficiency by enhancing antibody responses and unmasking CD8+ T cell epitopes. *Vaccines* 2: 581-600

56. Brandler S, Lepelley A, Desdouits M, Guivel-Benhassine F, Ceccaldi P-E, Lévy Y, Schwartz O, Moris A. 2010. Preclinical studies of a modified vaccinia virus Ankara-based HIV candidate vaccine: antigen presentation and antiviral effect. *Journal of virology* 84: 5314-28

57. Eickhoff S, Brewitz A, Gerner MY, Klauschen F, Komander K, Hemmi H, Garbi N, Kaisho T, Germain RN, Kastenmüller W. 2015. Robust anti-viral immunity requires multiple distinct T cell-dendritic cell interactions. *Cell* 162: 1322-37

58. Gasteiger G, Kastenmuller W, Ljapoci R, Sutter G, Drexler I. 2007. Cross-priming of cytotoxic T cells dictates antigen requisites for modified vaccinia virus Ankara vector vaccines. *J Virol* 81: 11925-36

59. Lauron EJ, Yang L, Elliott JI, Gainey MD, Fremont DH, Yokoyama WM. 2018. Cross-priming induces immunodomination in the presence of viral MHC class I inhibition. *PLoS pathogens* 14: e1006883

60. Gros M, Amigorena S. 2019. Regulation of Antigen Export to the Cytosol During Cross-Presentation. *Front Immunol* 10: 41

61. Blum JS, Wearsch PA, Cresswell P. 2013. Pathways of antigen processing. *Annual review of immunology* 31: 443-73

62. Akira S, Uematsu S, Takeuchi O. 2006. Pathogen recognition and innate immunity. *Cell* 124: 783-801

63. Medzhitov R. 2001. Toll-like receptors and innate immunity. *Nature Reviews Immunology* 1: 135-45

64. Rogers GL, Shirley JL, Zolotukhin I, Kumar SR, Sherman A, Perrin GQ, Hoffman BE, Srivastava A, Basner-Tschakarjan E, Wallet MA. 2017. Plasmacytoid and conventional dendritic cells cooperate in crosspriming AAV capsid-specific CD8+ T cells. *Blood, The Journal of the American Society of Hematology* 129: 3184-95

65. Brewitz A, Eickhoff S, Dähling S, Quast T, Bedoui S, Kroczek RA, Kurts C, Garbi N, Barchet W, Iannacone M. 2017. CD8+ T cells orchestrate pDC-XCR1+ dendritic cell spatial and functional cooperativity to optimize priming. *Immunity* 46: 205-19

66. Bevan MJ. 1976. Minor H antigens introduced on H-2 different stimulating cells cross-react at the cytotoxic T cell level during in vivo priming. *The Journal of Immunology* 117: 2233-8

67. Blander JM. 2018. Regulation of the cell biology of antigen cross-presentation. *Annual review of immunology* 36: 717-53

68. Guilliams M, Ginhoux F, Jakubzick C, Naik SH, Onai N, Schraml BU, Segura E, Tussiwand R, Yona S. 2014. Dendritic cells, monocytes and macrophages: a unified nomenclature based on ontogeny. *Nature Reviews Immunology* 14: 571-8

69. Shen L, Sigal LJ, Boes M, Rock KL. 2004. Important role of cathepsin S in generating peptides for TAP-independent MHC class I crosspresentation in vivo. *Immunity* 21: 155-65

70. Joffre OP, Segura E, Savina A, Amigorena S. 2012. Cross-presentation by dendritic cells. *Nat Rev Immunol* 12: 557-69

71. Cresswell P. 2012. Intracellular events regulating cross-presentation. *Frontiers in immunology* 3: 138

72. Rock KL, Shen L. 2005. Cross-presentation: underlying mechanisms and role in immune surveillance. *Immunological reviews* 207: 166-83

73. Saveanu L, Carroll O, Weimershaus M, Guermonprez P, Firat E, Lindo V, Greer F, Davoust J, Kratzer R, Keller SR. 2009. IRAP identifies an endosomal compartment required for MHC class I cross-presentation. *Science* 325: 213-7

74. Weimershaus M, Evnouchidou I, Saveanu L, van Endert P. 2013. Peptidases trimming MHC class I ligands. *Current opinion in immunology* 25: 90-6

75. Di Pucchio T, Chatterjee B, Smed-Sörensen A, Clayton S, Palazzo A, Montes M, Xue Y, Mellman I, Banchereau J, Connolly JE. 2008. Direct proteasome-independent cross-presentation of viral antigen by plasmacytoid dendritic cells on major histocompatibility complex class I. *Nature immunology* 9: 551-7

76. Delamarre L, Pack M, Chang H, Mellman I, Trombetta ES. 2005. Differential lysosomal proteolysis in antigen-presenting cells determines antigen fate. *Science* 307: 1630-4

77. Burgdorf S, Schölz C, Kautz A, Tampé R, Kurts C. 2008. Spatial and mechanistic separation of cross-presentation and endogenous antigen presentation. *Nature immunology* 9: 558-66

78. Nair-Gupta P, Baccarini A, Tung N, Seyffer F, Florey O, Huang Y, Banerjee M, Overholtzer M, Roche PA, Tampé R. 2014. TLR signals induce phagosomal MHC-I delivery from the endosomal recycling compartment to allow cross-presentation. *Cell* 158: 506-21

79. Blander JM, Medzhitov R. 2006. Toll-dependent selection of microbial antigens for presentation by dendritic cells. *Nature* 440: 808-12

80. Hoffmann E, Kotsias F, Visentin G, Bruhns P, Savina A, Amigorena S. 2012. Autonomous phagosomal degradation and antigen presentation in dendritic cells. *Proceedings of the National Academy of Sciences* 109: 14556-61

81. Mantegazza AR, Zajac AL, Twelvetrees A, Holzbaur EL, Amigorena S, Marks MS. 2014. TLR-dependent phagosome tubulation in dendritic cells promotes phagosome cross-talk to optimize MHC-II antigen presentation. *Proceedings of the National Academy of Sciences* 111: 15508-13

82. Alloatti A, Kotsias F, Magalhaes JG, Amigorena S. 2016. Dendritic cell maturation and cross-presentation: timing matters! *Immunological reviews* 272: 97-108

83. Samie M, Cresswell P. 2015. The transcription factor TFEB acts as a molecular switch that regulates exogenous antigen-presentation pathways. *Nature immunology* 16: 729-36

84. Sardiello M, Palmieri M, Di Ronza A, Medina DL, Valenza M, Gennarino VA, Di Malta C, Donaudy F, Embrione V, Polishchuk RS. 2009. A gene network regulating lysosomal biogenesis and function. *Science* 325: 473-7

85. Settembre C, Fraldi A, Medina DL, Ballabio A. 2013. Signals from the lysosome: a control centre for cellular clearance and energy metabolism. *Nature reviews Molecular cell biology* 14: 283-96

86. Rybicka JM, Balce DR, Chaudhuri S, Allan ER, Yates RM. 2012. Phagosomal proteolysis in dendritic cells is modulated by NADPH oxidase in a pH-independent manner. *The EMBO journal* 31: 932-44

87. Jancic C, Savina A, Wasmeier C, Tolmachova T, El-Benna J, Dang PM-C, Pascolo S, Gougerot-Pocidalo M-A, Raposo G, Seabra MC. 2007. Rab27a regulates phagosomal pH and NADPH oxidase recruitment to dendritic cell phagosomes. *Nature cell biology* 9: 367-78

88. Hari A, Ganguly A, Mu L, Davis SP, Stenner MD, Lam R, Munro F, Namet I, Alghamdi E, Fürstenhaupt T. 2015. Redirecting soluble antigen for MHC class I cross-presentation during phagocytosis. *European journal of immunology* 45: 383-95

89. Kotsias F, Hoffmann E, Amigorena S, Savina A. 2013. Reactive oxygen species production in the phagosome: impact on antigen presentation in dendritic cells. *Antioxidants & redox signaling* 18: 714-29

90. Shen L, Sigal LJ, Boes M, Rock KL. 2004. Important role of cathepsin S in generating peptides for TAP-independent MHC class I crosspresentation in vivo. *Immunity* 21: 155-65

91. Zehner M, Chasan AI, Schuette V, Embgenbroich M, Quast T, Kolanus W, Burgdorf S. 2011. Mannose receptor polyubiquitination regulates endosomal recruitment of p97 and cytosolic antigen translocation for cross-presentation. *Proceedings of the National Academy of Sciences* 108: 9933-8

92. Zehner M, Burgdorf S. 2013. Regulation of antigen transport into the cytosol for cross-presentation by ubiquitination of the mannose receptor. *Molecular immunology* 55: 146-8

93. Dingjan I, Linders PT, van den Bekerom L, Baranov MV, Halder P, ter Beest M, van den Bogaart G. 2017. Oxidized phagosomal NOX2 complex is replenished from lysosomes. *Journal of Cell Science* 130: 1285-98

94. Snyder DA, Kelly ML, Woodbury DJ. 2006. SNARE complex regulation by phosphorylation. *Cell biochemistry and biophysics* 45: 111-23

95. Vargas P, Maiuri P, Bretou M, Sáez PJ, Pierobon P, Maurin M, Chabaud M, Lankar D, Obino D, Terriac E. 2016. Innate control of actin nucleation determines two distinct migration behaviours in dendritic cells. *Nature cell biology* 18: 43-53

96. Faure-André G, Vargas P, Yuseff M-I, Heuzé M, Diaz J, Lankar D, Steri V, Manry J, Hugues S, Vascotto F. 2008. Regulation of dendritic cell migration by CD74, the MHC class II-associated invariant chain. *Science* 322: 1705-10

97. Moretti J, Blander JM. 2014. Insights into phagocytosis-coupled activation of pattern recognition receptors and inflammasomes. *Current opinion in immunology* 26: 100-10

98. Alloatti A, Kotsias F, Pauwels A-M, Carpier J-M, Jouve M, Timmerman E, Pace L, Vargas P, Maurin M, Gehrmann U. 2015. Toll-like receptor 4 engagement on dendritic cells restrains phago-lysosome fusion and promotes cross-presentation of antigens. *Immunity* 43: 1087-100

99. Mant A, Chinnery F, Elliott T, Williams AP. 2012. The pathway of cross-presentation is influenced by the particle size of phagocytosed antigen. *Immunology* 136: 163-75

100. Rodriguez A, Regnault A, Kleijmeer M, Ricciardi-Castagnoli P, Amigorena S. 1999. Selective transport of internalized antigens to the cytosol for MHC class I presentation in dendritic cells. *Nature cell biology* 1: 362-8

101. Reis e Sousa C, Germain RN. 1995. Major histocompatibility complex class I presentation of peptides derived from soluble exogenous antigen by a subset of cells engaged in phagocytosis. *The Journal of experimental medicine* 182: 841-51

102. Yu L, Wang L, Chen S. 2010. Endogenous toll-like receptor ligands and their biological significance. *J Cell Mol Med* 14: 2592-603

103. Alexopoulou L, Holt AC, Medzhitov R, Flavell RA. 2001. Recognition of double-stranded RNA and activation of NF-κB by Toll-like receptor 3. *Nature* 413: 732-8

104. Kurt-Jones EA, Popova L, Kwinn L, Haynes LM, Jones LP, Tripp RA, Walsh EE, Freeman MW, Golenbock DT, Anderson LJ. 2000. Pattern recognition receptors TLR4 and CD14 mediate response to respiratory syncytial virus. *Nature immunology* 1: 398-401

105. Poltorak A, He X, Smirnova I, Liu M-Y, Van Huffel C, Du X, Birdwell D, Alejos E, Silva M, Galanos C. 1998. Defective LPS signaling in C3H/HeJ and C57BL/10ScCr mice: mutations in Tlr4 gene. *science* 282: 2085-8

106. Yu L, Wang L, Chen S. 2010. Endogenous toll-like receptor ligands and their biological significance. *Journal of cellular and molecular medicine* 14: 2592-603

107. Wu J, Sun L, Chen X, Du F, Shi H, Chen C, Chen ZJ. 2013. Cyclic GMP-AMP is an endogenous second messenger in innate immune signaling by cytosolic DNA. *Science* 339: 826-30

108. Li X, Shu C, Yi G, Chaton CT, Shelton CL, Diao J, Zuo X, Kao CC, Herr AB, Li P. 2013. Cyclic GMP-AMP synthase is activated by double-stranded DNA-induced oligomerization. *Immunity* 39: 1019-31

109. Chen Q, Sun L, Chen ZJ. 2016. Regulation and function of the cGAS–STING pathway of cytosolic DNA sensing. *Nature immunology* 17: 1142-9

110. Zhang Z, Yuan B, Bao M, Lu N, Kim T, Liu Y-J. 2011. The helicase DDX41 senses intracellular DNA mediated by the adaptor STING in dendritic cells. *Nature immunology* 12: 959-65

111. Perčulija V, Ouyang S. 2019. Diverse roles of DEAD/DEAH-Box helicases in innate immunity and diseases. In *Helicases from All Domains of Life*, pp. 141-71: Elsevier

112. Lee K-G, Kim SS-Y, Kui L, Voon DC-C, Mauduit M, Bist P, Bi X, Pereira NA, Liu C, Sukumaran B. 2015. Bruton's tyrosine kinase phosphorylates DDX41 and activates its binding of dsDNA and STING to initiate type 1 interferon response. *Cell reports* 10: 1055-65

113. Parvatiyar K, Zhang Z, Teles RM, Ouyang S, Jiang Y, Iyer SS, Zaver SA, Schenk M, Zeng S, Zhong W. 2012. The helicase DDX41 recognizes the bacterial secondary messengers cyclic di-GMP and cyclic di-AMP to activate a type I interferon immune response. *Nature immunology* 13: 1155-61

114. Sun L, Wu J, Du F, Chen X, Chen ZJ. 2013. Cyclic GMP-AMP synthase is a cytosolic DNA sensor that activates the type I interferon pathway. *Science* 339: 786-91

115. Abe T, Harashima A, Xia T, Konno H, Konno K, Morales A, Ahn J, Gutman D, Barber GN. 2013. STING recognition of cytoplasmic DNA instigates cellular defense. *Molecular cell* 50: 5-15

116. Ferguson BJ, Mansur DS, Peters NE, Ren H, Smith GL. 2012. DNA-PK is a DNA sensor for IRF-3-dependent innate immunity. *elife* 1: e00047

117. Sui H, Zhou M, Imamichi H, Jiao X, Sherman BT, Lane HC, Imamichi T. 2017. STING is an essential mediator of the Ku70-mediated production of IFN-λ1 in response to exogenous DNA. *Science signaling* 10

118. Cavlar T, Ablasser A, Hornung V. 2012. Induction of type I IFNs by intracellular DNA-sensing pathways. *Immunology and Cell Biology* 90: 474-82

119. Syedbasha M, Egli A. 2017. Interferon lambda: modulating immunity in infectious diseases. *Frontiers in immunology* 8: 119

120. Thompson MR, Kaminski JJ, Kurt-Jones EA, Fitzgerald KA. 2011. Pattern recognition receptors and the innate immune response to viral infection. *Viruses* 3: 920-40

121. Seth RB, Sun L, Ea C-K, Chen ZJ. 2005. Identification and characterization of MAVS, a mitochondrial antiviral signaling protein that activates NF-κB and IRF3. *Cell* 122: 669-82

122. Hornung V, Ellegast J, Kim S, Brzózka K, Jung A, Kato H, Poeck H, Akira S, Conzelmann K-K, Schlee M. 2006. 5'-Triphosphate RNA is the ligand for RIG-I. *science* 314: 994-7

123. Kato H, Takeuchi O, Sato S, Yoneyama M, Yamamoto M, Matsui K, Uematsu S, Jung A, Kawai T, Ishii KJ. 2006. Differential roles of MDA5 and RIG-I helicases in the recognition of RNA viruses. *Nature* 441: 101-5

124. Pichlmair A, Schulz O, Tan C-P, Rehwinkel J, Kato H, Takeuchi O, Akira S, Way M, Schiavo G, Reis e Sousa C. 2009. Activation of MDA5 requires higher-order RNA structures generated during virus infection. *Journal of virology* 83: 10761-9

125. Schlee M, Roth A, Hornung V, Hagmann CA, Wimmenauer V, Barchet W, Coch C, Janke M, Mihailovic A, Wardle G. 2009. Recognition of 5′ triphosphate by RIG-I helicase requires short blunt double-stranded RNA as contained in panhandle of negative-strand virus. *Immunity* 31: 25-34

126. Ablasser A, Bauernfeind F, Hartmann G, Latz E, Fitzgerald KA, Hornung V. 2009. RIG-I-dependent sensing of poly (dA: dT) through the induction of an RNA polymerase III–transcribed RNA intermediate. *Nature immunology* 10: 1065-72

127. Chiu Y-H, MacMillan JB, Chen ZJ. 2009. RNA polymerase III detects cytosolic DNA and induces type I interferons through the RIG-I pathway. *Cell* 138: 576-91

128. Roberts WK, Hovanessian A, Brown RE, Clemens MJ, Kerr IM. 1976. Interferon-mediated protein kinase and low-molecular-weight inhibitor of protein synthesis. *Nature* 264: 477-80

129. Kumar A, Haque J, Lacoste J, Hiscott J, Williams B. 1994. Double-stranded RNA-dependent protein kinase activates transcription factor NF-kappa B by phosphorylating I kappa B. *Proceedings of the National Academy of Sciences* 91: 6288-92

130. Garcia M, Gil J, Ventoso I, Guerra S, Domingo E, Rivas C, Esteban M. 2006. Impact of protein kinase PKR in cell biology: from antiviral to antiproliferative action. *Microbiology and Molecular Biology Reviews* 70: 1032-60

131. Yang P, An H, Liu X, Wen M, Zheng Y, Rui Y, Cao X. 2010. The cytosolic nucleic acid sensor LRRFIP1 mediates the production of type I interferon via a β-catenin-dependent pathway. *Nature immunology* 11: 487

132. Zheng D, Liwinski T, Elinav E. 2020. Inflammasome activation and regulation: toward a better understanding of complex mechanisms. *Cell discovery* 6: 1-22

133. Bryant C, Fitzgerald KA. 2009. Molecular mechanisms involved in inflammasome activation. *Trends in cell biology* 19: 455-64

134. Kahlenberg JM, Lundberg KC, Kertesy SB, Qu Y, Dubyak GR. 2005. Potentiation of caspase-1 activation by the P2X7 receptor is dependent on TLR signals and requires NF-κB-driven protein synthesis. *The Journal of Immunology* 175: 7611-22

135. Tuladhar S, Kanneganti T-D. 2020. NLRP12 in innate immunity and inflammation. *Molecular Aspects of Medicine*: 100887

136. van Diemen FR, Kruse EM, Hooykaas MJ, Bruggeling CE, Schürch AC, van Ham PM, Imhof SM, Nijhuis M, Wiertz EJ, Lebbink RJ. 2016. CRISPR/Cas9-mediated genome editing of herpesviruses limits productive and latent infections. *PLoS pathogens* 12: e1005701

137. Lebbink RJ, de Jong DC, Wolters F, Kruse EM, van Ham PM, Wiertz EJ, Nijhuis M. 2017. A combinational CRISPR/Cas9 gene-editing approach can halt HIV replication and prevent viral escape. *Scientific reports* 7: 1-10

138. Zhang J-P, Li X-L, Neises A, Chen W, Hu L-P, Ji G-Z, Yu J-Y, Xu J, Yuan W-P, Cheng T. 2016. Different effects of sgRNA length on CRISPR-mediated gene knockout efficiency. *Scientific reports* 6: 1-10

139. Concordet J-P, Haeussler M. 2018. CRISPOR: intuitive guide selection for CRISPR/Cas9 genome editing experiments and screens. *Nucleic Acids Research* 46: W242-W5

140. Kent WJ, Sugnet CW, Furey TS, Roskin KM, Pringle TH, Zahler AM, Haussler D. 2002. The human genome browser at UCSC. *Genome research* 12: 996-1006

141. Livak KJ, Schmittgen TD. 2001. Analysis of relative gene expression data using real-time quantitative PCR and the 2(-Delta Delta C(T)) Method. *Methods* 25: 402-8

142. Beeton C, Chandy KG. 2007. Preparing T cell growth factor from rat splenocytes. *J Vis Exp*: 402

143. Barnowski C, Ciupka G, Tao R, Jin L, Busch DH, Tao S, Drexler I. 2020. Efficient Induction of Cytotoxic T Cells by Viral Vector Vaccination Requires STING-Dependent DC Functions. *Front Immunol* 11: 1458

144. Colby C, Jurale C, Kates JR. 1971. Mechanism of synthesis of vaccinia virus double-stranded ribonucleic acid in vivo and in vitro. *Journal of virology* 7: 71-6

145. Bidgood S, Mercer J. 2015. Cloak and dagger: alternative immune evasion and modulation strategies of poxviruses. Viruses 7: 4800–4825.

146. Helft J, Böttcher J, Chakravarty P, Zelenay S, Huotari J, Schraml BU, Goubau D, e Sousa CR. 2015. GM-CSF mouse bone marrow cultures comprise a heterogeneous population of CD11c+ MHCII+ macrophages and dendritic cells. *Immunity* 42: 1197-211

147. Wang W, Li J, Wu K, Azhati B, Rexiati M. 2016. Culture and identification of mouse bone marrow-derived dendritic cells and their capability to induce T lymphocyte proliferation. *Medical science monitor: international medical journal of experimental and clinical research* 22: 244

148. Alavi S, Stewart AJ, Kefford RF, Lim SY, Shklovskaya E, Rizos H. 2018. Interferon signaling is frequently downregulated in melanoma. *Frontiers in immunology* 9: 1414

149. Domanski P, Fish E, Nadeau OW, Witte M, Platanias LC, Yan H, Krolewski J, Pitha P, Colamonici OR. 1997. A region of the β subunit of the interferon α receptor different from box 1 interacts with Jak1 and is sufficient to activate the Jak-Stat pathway and induce an antiviral state. *Journal of Biological Chemistry* 272: 26388-93

150. Colamonici O, Yan H, Domanski P, Handa R, Smalley D, Mullersman J, Witte M, Krishnan K, Krolewski J. 1994. Direct binding to and tyrosine phosphorylation of the alpha subunit of the type I interferon receptor by p135tyk2 tyrosine kinase. *Molecular and Cellular Biology* 14: 8133-42

151. Krogsgaard M, Davis MM. 2005. How T cells' see'antigen. *Nature immunology* 6: 239-45

152. González PA, Carreño LJ, Coombs D, Mora JE, Palmieri E, Goldstein B, Nathenson SG, Kalergis AM. 2005. T cell receptor binding kinetics required for T cell activation depend on the density of cognate ligand on the antigen-presenting cell. *Proceedings of the National Academy of Sciences* 102: 4824-9

153. Franklin BS, Bossaller L, De Nardo D, Ratter JM, Stutz A, Engels G, Brenker C, Nordhoff M, Mirandola SR, Al-Amoudi A. 2014. The adaptor ASC has extracellular and'prionoid'activities that propagate inflammation. *Nature immunology* 15: 727-37

154. Lucae S, Salyakina D, Barden N, Harvey M, Gagné B, Labbé M, Binder EB, Uhr M, Paez-Pereda M, Sillaber I. 2006. P2RX7, a gene coding for a purinergic ligand-gated ion channel, is associated with major depressive disorder. *Human molecular genetics* 15: 2438-45

155. Ahmed MI, Pollakis G, Rogers L, Hoffmann VS, Munseri P, Aboud S, Lyamuya EF, Bakari M, Robb ML, Wahren B. 2020. Induction of Identical IgG HIV-1 Envelope Epitope Recognition Patterns After Initial HIVIS-DNA/MVA-CMDR Immunization and a Late MVA-CMDR Boost. *Frontiers in immunology* 11: 719

156. Tappe KA, Budida R, Stankov MV, Frenz T, R. Shah H, Volz A, Sutter G, Kalinke U, Behrens GM. 2018. Immunogenic cell death of dendritic cells following modified vaccinia virus Ankara infection enhances CD8+ T cell proliferation. *European journal of immunology* 48: 2042-54

157. Elgueta R, Benson MJ, De Vries VC, Wasiuk A, Guo Y, Noelle RJ. 2009. Molecular mechanism and function of CD40/CD40L engagement in the immune system. *Immunological reviews* 229: 152-72

158. Thiel M, Wolfs MJ, Bauer S, Wenning AS, Burckhart T, Schwarz EC, Scott AM, Renner C, Hoth M. 2010. Efficiency of T-cell costimulation by CD80 and CD86 cross-linking correlates with calcium entry. *Immunology* 129: 28-40

159. Chatterjee B, Smed-Sörensen A, Cohn L, Chalouni C, Vandlen R, Lee B-C, Widger J, Keler T, Delamarre L, Mellman I. 2012. Internalization and endosomal degradation of receptor-bound antigens regulate the efficiency of cross presentation by human dendritic cells. *Blood* 120: 2011-20

160. Sun S-C. 2017. The non-canonical NF-κB pathway in immunity and inflammation. *Nature Reviews Immunology* 17: 545

161. Katakam AK, Brightbill H, Franci C, Kung C, Nunez V, Jones C, Peng I, Jeet S, Wu LC, Mellman I. 2015. Dendritic cells require NIK for CD40-dependent cross-priming of CD8+ T cells. *Proceedings of the National Academy of Sciences* 112: 14664-9

162. Luft T, Pang KC, Thomas E, Hertzog P, Hart DN, Trapani J, Cebon J. 1998. Type I IFNs enhance the terminal differentiation of dendritic cells. *The Journal of Immunology* 161: 1947-53

163. Montoya M, Schiavoni G, Mattei F, Gresser I, Belardelli F, Borrow P, Tough DF. 2002. Type I interferons produced by dendritic cells promote their phenotypic and functional activation. *Blood, The Journal of the American Society of Hematology* 99: 3263-71

164. Rudd BD, Luker GD, Luker KE, Peebles RS, Lukacs NW. 2007. Type I interferon regulates respiratory virus infected dendritic cell maturation and cytokine production. *Viral immunology* 20: 531-40

165. Ivashkiv LB, Donlin LT. 2014. Regulation of type I interferon responses. *Nature reviews Immunology* 14: 36-49

166. Zhang P, Jacobs BL, Samuel CE. 2008. Loss of protein kinase PKR expression in human HeLa cells complements the vaccinia virus E3L deletion mutant phenotype by restoration of viral protein synthesis. *Journal of virology* 82: 840-8

167. Falahat R, Perez-Villarroel P, Mailloux AW, Zhu G, Pilon-Thomas S, Barber GN, Mulé JJ. 2019. STING signaling in melanoma cells shapes antigenicity and can promote antitumor T-cell activity. *Cancer immunology research*

168. Heo S-K, Noh E-K, Yu H-M, Kim DK, Seo HJ, Lee YJ, Cheon J, Koh SJ, Min YJ, Choi Y. 2020. Radotinib enhances cytarabine (Ara-C)-induced acute myeloid leukemia cell death. *BMC cancer* 20: 1-15

169. Jimenez PC, Wilke DV, Costa-Lotufo LV. 2018. Marine drugs for cancer: Surfacing biotechnological innovations from the oceans. *Clinics* 73

170. Mittelbrunn M, Sánchez-Madrid F. 2012. Intercellular communication: diverse structures for exchange of genetic information. *Nature reviews Molecular cell biology* 13: 328-35

171. Katsafanas GC, Moss B. 2007. Colocalization of transcription and translation within cytoplasmic poxvirus factories coordinates viral expression and subjugates host functions. *Cell host & microbe* 2: 221-8

172. Broyles SS. 2003. Vaccinia virus transcription. *Journal of General Virology* 84: 2293-303

173. Bronte V, Carroll MW, Goletz TJ, Wang M, Overwijk WW, Marincola F, Rosenberg SA, Moss B, Restifo NP. 1997. Antigen expression by dendritic cells correlates with the therapeutic effectiveness of a model recombinant poxvirus tumor vaccine. *Proceedings of the National Academy of Sciences* 94: 3183-8

174. Coupar BE, Andrew ME, Both GW, Boyle DB. 1986. Temporal regulation of influenza hemagglutinin expression in vaccinia virus recombinants and effects on the immune response. *European journal of immunology* 16: 1479-87

175. Paquette RL, Hsu NC, Kiertscher SM, Park AN, Tran L, Roth MD, Glaspy JA. 1998. Interferon-α and granulocyte-macrophage colony-stimulating factor differentiate peripheral blood monocytes into potent antigen-presenting cells. *Journal of leukocyte biology* 64: 358-67

176. Le Bon A, Etchart N, Rossmann C, Ashton M, Hou S, Gewert D, Borrow P, Tough DF. 2003. Cross-priming of CD8+ T cells stimulated by virus-induced type I interferon. *Nature immunology* 4: 1009-15

177. Lapenta C, Santini SM, Spada M, Donati S, Urbani F, Accapezzato D, Franceschini D, Andreotti M, Barnaba V, Belardelli F. 2006. IFN-α-conditioned dendritic cells are highly efficient in inducing cross-priming CD8+ T cells against exogenous viral antigens. *European journal of immunology* 36: 2046-60

178. Cho HJ, Hayashi T, Datta SK, Takabayashi K, Van Uden JH, Horner A, Corr M, Raz E. 2002. IFN-αβ promote priming of antigen-specific CD8+ and CD4+ T lymphocytes by immunostimulatory DNA-based vaccines. *The Journal of Immunology* 168: 4907-13

179. Spadaro F, Lapenta C, Donati S, Abalsamo L, Barnaba V, Belardelli F, Santini SM, Ferrantini M. 2012. IFN-α enhances cross-presentation in human dendritic cells by modulating antigen survival, endocytic routing, and processing. *Blood, The Journal of the American Society of Hematology* 119: 1407-17

180. Janssen EM, Thacker RI. 2012. Cross-presentation of cell-associated antigens by mouse splenic dendritic cell populations. *Frontiers in immunology* 3: 41

181. Lorenzi S, Mattei F, Sistigu A, Bracci L, Spadaro F, Sanchez M, Spada M, Belardelli F, Gabriele L, Schiavoni G. 2011. Type I IFNs control antigen retention and survival of CD8α+ dendritic cells after uptake of tumor apoptotic cells leading to cross-priming. *The Journal of Immunology* 186: 5142-50

182. Sato M, Hata N, Asagiri M, Nakaya T, Taniguchi T, Tanaka N. 1998. Positive feedback regulation of type I IFN genes by the IFN-inducible transcription factor IRF-7. *FEBS letters* 441: 106-10

183. Marié I, Durbin JE, Levy DE. 1998. Differential viral induction of distinct interferon-α genes by positive feedback through interferon regulatory factor-7. *The EMBO journal* 17: 6660-9

184. Erlandsson L, Blumenthal R, Eloranta M-L, Engel H, Alm G, Weiss S, Leanderson T. 1998. Interferon-β is required for interferon-α production in mouse fibroblasts. *Current Biology* 8: 223-6

185. Murray C, Griffin ÉW, O'Loughlin E, Lyons A, Sherwin E, Ahmed S, Stevenson NJ, Harkin A, Cunningham C. 2015. Interdependent and independent roles of type I interferons and IL-6 in innate immune, neuroinflammatory and sickness behaviour responses to systemic poly I: C. *Brain, behavior, and immunity* 48: 274-86

186. Goritzka M, Durant LR, Pereira C, Salek-Ardakani S, Openshaw PJ, Johansson C. 2014. Alpha/beta interferon receptor signaling amplifies early proinflammatory cytokine production in the lung during respiratory syncytial virus infection. *Journal of virology* 88: 6128-36

187. Thacker RI, Janssen EM. 2012. Cross-presentation of cell-associated antigens by mouse splenic dendritic cell populations. *Front Immunol* 3: 41

188. Wang P-H, Fung S-Y, Gao W-W, Deng J-J, Cheng Y, Chaudhary V, Yuen K-S, Ho T-H, Chan C-P, Zhang Y. 2018. A novel transcript isoform of STING that sequesters cGAMP and dominantly inhibits innate nucleic acid sensing. *Nucleic acids research* 46: 4054-71

189. Parlato S, Santini SM, Lapenta C, Di Pucchio T, Logozzi M, Spada M, Giammarioli AM, Malorni W, Fais S, Belardelli F. 2001. Expression of CCR-7, MIP-3β, and Th-1 chemokines in type I IFN-induced monocyte-derived dendritic cells: importance for the rapid acquisition of potent migratory and functional activities. *Blood, The Journal of the American Society of Hematology* 98: 3022-9

190. Kastenmuller W, Drexler I, Ludwig H, Erfle V, Peschel C, Bernhard H, Sutter G. 2006. Infection of human dendritic cells with recombinant vaccinia virus MVA

reveals general persistence of viral early transcription but distinct maturation-dependent cytopathogenicity. *Virology* 350: 276-88

191. Chahroudi A, Garber DA, Reeves P, Liu L, Kalman D, Feinberg MB. 2006. Differences and similarities in viral life cycle progression and host cell physiology after infection of human dendritic cells with modified vaccinia virus Ankara and vaccinia virus. *Journal of virology* 80: 8469-81

192. Ahn J, Xia T, Capote AR, Betancourt D, Barber GN. 2018. Extrinsic phagocyte-dependent STING signaling dictates the immunogenicity of dying cells. *Cancer cell* 33: 862-73. e5

193. Zhou C, Chen X, Planells-Cases R, Chu J, Wang L, Cao L, Li Z, López-Cayuqueo KI, Xie Y, Ye S. 2020. Transfer of cGAMP into bystander cells via LRRC8 volume-regulated anion channels augments STING-mediated interferon responses and anti-viral immunity. *Immunity* 52: 767-81. e6

194. Pépin G, De Nardo D, Rootes CL, Ullah TR, Al-Asmari SS, Balka KR, Li H-M, Quinn KM, Moghaddas F, Chappaz S. 2020. Connexin-dependent transfer of cGAMP to phagocytes modulates antiviral responses. *MBio* 11: e03187-19

195. Luteijn RD, Zaver SA, Gowen BG, Wyman SK, Garelis NE, Onia L, McWhirter SM, Katibah GE, Corn JE, Woodward JJ. 2019. SLC19A1 transports immunoreactive cyclic dinucleotides. *Nature* 573: 434-8

196. Ritchie C, Cordova AF, Hess GT, Bassik MC, Li L. 2019. SLC19A1 is an importer of the immunotransmitter cGAMP. *Molecular cell* 75: 372-81. e5

197. Gentili M, Kowal J, Tkach M, Satoh T, Lahaye X, Conrad C, Boyron M, Lombard B, Durand S, Kroemer G. 2015. Transmission of innate immune signaling by packaging of cGAMP in viral particles. *Science* 349: 1232-6

198. Bridgeman A, Maelfait J, Davenne T, Partridge T, Peng Y, Mayer A, Dong T, Kaever V, Borrow P, Rehwinkel J. 2015. Viruses transfer the antiviral second messenger cGAMP between cells. *Science* 349: 1228-32

199. Xu MM, Pu Y, Han D, Shi Y, Cao X, Liang H, Chen X, Li X-D, Deng L, Chen ZJ. 2017. Dendritic cells but not macrophages sense tumor mitochondrial DNA for

cross-priming through signal regulatory protein α signaling. *Immunity* 47: 363-73. e5

200. Ravichandran KS. 2011. Beginnings of a good apoptotic meal: the find-me and eat-me signaling pathways. *Immunity* 35: 445-55

201. Ravichandran KS. 2010. Find-me and eat-me signals in apoptotic cell clearance: progress and conundrums. *J Exp Med* 207: 1807-17

202. Elliott MR, Chekeni FB, Trampont PC, Lazarowski ER, Kadl A, Walk SF, Park D, Woodson RI, Ostankovich M, Sharma P. 2009. Nucleotides released by apoptotic cells act as a find-me signal to promote phagocytic clearance. *Nature* 461: 282-6

203. Chekeni FB, Elliott MR, Sandilos JK, Walk SF, Kinchen JM, Lazarowski ER, Armstrong AJ, Penuela S, Laird DW, Salvesen GS. 2010. Pannexin 1 channels mediate 'find-me'signal release and membrane permeability during apoptosis. *Nature* 467: 863-7

204. Pelegrin P, Surprenant A. 2006. Pannexin-1 mediates large pore formation and interleukin-1β release by the ATP-gated P2X7 receptor. *The EMBO journal* 25: 5071-82

205. Pelegrin P, Barroso-Gutierrez C, Surprenant A. 2008. P2X7 receptor differentially couples to distinct release pathways for IL-1β in mouse macrophage. *The Journal of Immunology* 180: 7147-57

206. Chen KW, Demarco B, Broz P. 2020. Pannexin-1 promotes NLRP3 activation during apoptosis but is dispensable for canonical or noncanonical inflammasome activation. *European journal of immunology* 50: 170-7

207. Silverman WR, de Rivero Vaccari JP, Locovei S, Qiu F, Carlsson SK, Scemes E, Keane RW, Dahl G. 2009. The pannexin 1 channel activates the inflammasome in neurons and astrocytes. *Journal of Biological Chemistry* 284: 18143-51

208. Qu Y, Misaghi S, Newton K, Gilmour LL, Louie S, Cupp JE, Dubyak GR, Hackos D, Dixit VM. 2011. Pannexin-1 is required for ATP release during apoptosis but not for inflammasome activation. *The Journal of Immunology* 186: 6553-61

209. Parzych K, Zetterqvist AV, Wright WR, Kirkby NS, Mitchell JA, Paul-Clark MJ. 2017. Differential role of pannexin-1/ATP/P2X7 axis in IL-1β release by human monocytes. *The FASEB Journal* 31: 2439-45

210. Franklin BS, Latz E, Schmidt FI. 2018. The intra-and extracellular functions of ASC specks. *Immunological reviews* 281: 74-87

211. Baroja-Mazo A, Martín-Sánchez F, Gomez AI, Martínez CM, Amores-Iniesta J, Compan V, Barberà-Cremades M, Yagüe J, Ruiz-Ortiz E, Antón J. 2014. The NLRP3 inflammasome is released as a particulate danger signal that amplifies the inflammatory response. *Nature immunology* 15: 738-48

212. Pierini R, Juruj C, Perret M, Jones C, Mangeot P, Weiss D, Henry T. 2012. AIM2/ASC triggers caspase-8-dependent apoptosis in Francisella-infected caspase-1-deficient macrophages. *Cell Death & Differentiation* 19: 1709-21

213. Vajjhala PR, Lu A, Brown DL, Pang SW, Sagulenko V, Sester DP, Cridland SO, Hill JM, Schroder K, Stow JL. 2015. The inflammasome adaptor ASC induces procaspase-8 death effector domain filaments. *Journal of Biological Chemistry* 290: 29217-30

214. Sagoo P, Garcia Z, Breart B, Lemaître F, Michonneau D, Albert ML, Levy Y, Bousso P. 2016. In vivo imaging of inflammasome activation reveals a subcapsular macrophage burst response that mobilizes innate and adaptive immunity. *Nature medicine* 22: 64-71

215. Meylan E, Tschopp J, Karin M. 2006. Intracellular pattern recognition receptors in the host response. *Nature* 442: 39-44

216. Bauernfeind FG, Horvath G, Stutz A, Alnemri ES, MacDonald K, Speert D, Fernandes-Alnemri T, Wu J, Monks BG, Fitzgerald KA. 2009. Cutting edge: NF-κB activating pattern recognition and cytokine receptors license NLRP3 inflammasome activation by regulating NLRP3 expression. *The Journal of Immunology* 183: 787-91

217. Zhong Z, Liang S, Sanchez-Lopez E, He F, Shalapour S, Lin X-j, Wong J, Ding S, Seki E, Schnabl B. 2018. New mitochondrial DNA synthesis enables NLRP3 inflammasome activation. *Nature* 560: 198-203

218. Grimsley C, Ravichandran KS. 2003. Cues for apoptotic cell engulfment: eat-me, don't eat-me and come-get-me signals. *Trends Cell Biol* 13: 648-56

219. Mackenzie AB, Young MT, Adinolfi E, Surprenant A. 2005. Pseudoapoptosis induced by brief activation of ATP-gated P2X7 receptors. *J Biol Chem* 280: 33968-76

220. Nagata S, Suzuki J, Segawa K, Fujii T. 2016. Exposure of phosphatidylserine on the cell surface. *Cell Death Differ* 23: 952-61

221. Singer DF, Linderman JJ. 1990. The relationship between antigen concentration, antigen internalization, and antigenic complexes: modeling insights into antigen processing and presentation. *J Cell Biol* 111: 55-68

222. Green DR, Ferguson T, Zitvogel L, Kroemer G. 2009. Immunogenic and tolerogenic cell death. *Nat Rev Immunol* 9: 353-63

223. Imre G. 2020. Cell death signalling in virus infection. *Cell Signal* 76: 109772

224. Kaiser WJ, Sridharan H, Huang C, Mandal P, Upton JW, Gough PJ, Sehon CA, Marquis RW, Bertin J, Mocarski ES. 2013. Toll-like receptor 3-mediated necrosis via TRIF, RIP3, and MLKL. *Journal of Biological Chemistry* 288: 31268-79

225. He S, Liang Y, Shao F, Wang X. 2011. Toll-like receptors activate programmed necrosis in macrophages through a receptor-interacting kinase-3–mediated pathway. *Proceedings of the National Academy of Sciences* 108: 20054-9

226. O'Donnell MA, Perez-Jimenez E, Oberst A, Ng A, Massoumi R, Xavier R, Green DR, Ting AT. 2011. Caspase 8 inhibits programmed necrosis by processing CYLD. *Nature cell biology* 13: 1437-42

227. Fritsch M, Günther SD, Schwarzer R, Albert M-C, Schorn F, Werthenbach JP, Schiffmann LM, Stair N, Stocks H, Seeger JM. 2019. Caspase-8 is the molecular switch for apoptosis, necroptosis and pyroptosis. *Nature* 575: 683-7

228. Zhou Y, Fei M, Zhang G, Liang W-C, Lin W, Wu Y, Piskol R, Ridgway J, McNamara E, Huang H. 2020. Blockade of the phagocytic receptor MerTK on tumor-associated macrophages enhances P2X7R-dependent STING activation by tumor-derived cGAMP. *Immunity* 52: 357-73. e9

229. Osborn JL, Greer SF. 2015. Metastatic melanoma cells evade immune detection by silencing STAT1. *International journal of molecular sciences* 16: 4343-61

230. Pansky A, Hildebrand P, Fasler-Kan E, Baselgia L, Ketterer S, Beglinger C, Heim MH. 2000. Defective Jak-STAT signal transduction pathway in melanoma cells resistant to growth inhibition by interferon-α. *International journal of cancer* 85: 720-5

231. Hermann P, Rubio M, Nakajima T, Delespesse G, Sarfati M. 1998. IFN-α priming of human monocytes differentially regulates gram-positive and gram-negative bacteria-induced IL-10 release and selectively enhances IL-12p70, CD80, and MHC class I expression. *The Journal of Immunology* 161: 2011-8

232. Kolumam GA, Thomas S, Thompson LJ, Sprent J, Murali-Krishna K. 2005. Type I interferons act directly on CD8 T cells to allow clonal expansion and memory formation in response to viral infection. *The Journal of experimental medicine* 202: 637-50

233. Pestka S, Krause CD, Walter MR. 2004. Interferons, interferon-like cytokines, and their receptors. *Immunol Rev* 202: 8-32

234. Brownell J, Bruckner J, Wagoner J, Thomas E, Loo Y-M, Gale Jr M, Liang TJ, Polyak SJ. 2014. Direct, interferon-independent activation of the CXCL10 promoter by NF-κB and interferon regulatory factor 3 during hepatitis C virus infection. *Journal of virology* 88: 1582-90

235. McFadden G. 2005. Poxvirus tropism. *Nat Rev Microbiol* 3: 201-13

236. Zhang P, Samuel CE. 2008. Induction of protein kinase PKR-dependent activation of interferon regulatory factor 3 by vaccinia virus occurs through adapter IPS-1 signaling. *J Biol Chem* 283: 34580-7

237. Bianchi ME, Crippa MP, Manfredi AA, Mezzapelle R, Rovere Querini P, Venereau E. 2017. High-mobility group box 1 protein orchestrates responses to tissue damage via inflammation, innate and adaptive immunity, and tissue repair. *Immunol Rev* 280: 74-82

238. Lu B, Nakamura T, Inouye K, Li J, Tang Y, Lundbäck P, Valdes-Ferrer SI, Olofsson PS, Kalb T, Roth J. 2012. Novel role of PKR in inflammasome activation and HMGB1 release. *Nature* 488: 670-4

239. Scaffidi P, Misteli T, Bianchi ME. 2002. Release of chromatin protein HMGB1 by necrotic cells triggers inflammation. *Nature* 418: 191-5

240. Willingham SB, Allen IC, Bergstralh DT, Brickey WJ, Huang MT-H, Taxman DJ, Duncan JA, Ting JP-Y. 2009. NLRP3 (NALP3, Cryopyrin) facilitates in vivo caspase-1 activation, necrosis, and HMGB1 release via inflammasome-dependent and-independent pathways. *The Journal of Immunology* 183: 2008-15

241. Lamkanfi M, Sarkar A, Walle LV, Vitari AC, Amer AO, Wewers MD, Tracey KJ, Kanneganti T-D, Dixit VM. 2010. Inflammasome-dependent release of the alarmin HMGB1 in endotoxemia. *The Journal of immunology* 185: 4385-92

242. Lich JD, Williams KL, Moore CB, Arthur JC, Davis BK, Taxman DJ, Ting JP. 2007. Cutting edge: Monarch-1 suppresses non-canonical NF-κB activation and p52-dependent chemokine expression in monocytes. *The Journal of Immunology* 178: 1256-60

243. Williams KL, Lich JD, Duncan JA, Reed W, Rallabhandi P, Moore C, Kurtz S, Coffield VM, Accavitti-Loper MA, Su L. 2005. The CATERPILLER protein Monarch-1 is an antagonist of Toll-like receptor-, tumor necrosis factor α-, and Mycobacterium tuberculosis-induced pro-inflammatory signals. *Journal of Biological Chemistry* 280: 39914-24

244. Zaki MH, Vogel P, Malireddi RS, Body-Malapel M, Anand PK, Bertin J, Green DR, Lamkanfi M, Kanneganti T-D. 2011. The NOD-like receptor NLRP12 attenuates colon inflammation and tumorigenesis. *Cancer cell* 20: 649-60

245. Cui J, Li Y, Zhu L, Liu D, Songyang Z, Wang HY, Wang R-F. 2012. NLRP4 negatively regulates type I interferon signaling by targeting the kinase TBK1 for degradation via the ubiquitin ligase DTX4. *Nature immunology* 13: 387-95

246. Shaw PJ, Lamkanfi M, Kanneganti TD. 2010. NOD-like receptor (NLR) signaling beyond the inflammasome. *Eur J Immunol* 40: 624-7

247. Allen IC, Moore CB, Schneider M, Lei Y, Davis BK, Scull MA, Gris D, Roney KE, Zimmermann AG, Bowzard JB. 2011. NLRX1 protein attenuates inflammatory responses to infection by interfering with the RIG-I-MAVS and TRAF6-NF-κB signaling pathways. *Immunity* 34: 854-65

248. Moore CB, Bergstralh DT, Duncan JA, Lei Y, Morrison TE, Zimmermann AG, Accavitti-Loper MA, Madden VJ, Sun L, Ye Z. 2008. NLRX1 is a regulator of mitochondrial antiviral immunity. *Nature* 451: 573-7

249. Cui J, Zhu L, Xia X, Wang HY, Legras X, Hong J, Ji J, Shen P, Zheng S, Chen ZJ. 2010. NLRC5 negatively regulates the NF-κB and type I interferon signaling pathways. *Cell* 141: 483-96

250. Benkő S, Kovács EG, Hezel F, Kufer TA. 2017. NLRC5 functions beyond MHC I regulation—what do we know so far? *Frontiers in immunology* 8: 150

251. Li X, Deng M, Petrucelli AS, Zhu C, Mo J, Zhang L, Tam JW, Ariel P, Zhao B, Zhang S. 2019. Viral DNA binding to NLRC3, an inhibitory nucleic acid sensor, unleashes STING, a cyclic dinucleotide receptor that activates type I interferon. *Immunity* 50: 591-9. e6

252. Schneider M, Zimmermann AG, Roberts RA, Zhang L, Swanson KV, Wen H, Davis BK, Allen IC, Holl EK, Ye Z. 2012. The innate immune sensor NLRC3 attenuates Toll-like receptor signaling via modification of the signaling adaptor TRAF6 and transcription factor NF-κB. *Nature immunology* 13: 823-31

253. Kerur N, Veettil MV, Sharma-Walia N, Bottero V, Sadagopan S, Otageri P, Chandran B. 2011. IFI16 acts as a nuclear pathogen sensor to induce the inflammasome in response to Kaposi Sarcoma-associated herpesvirus infection. *Cell Host Microbe* 9: 363-75

254. Zheng W, Zhou R, Li S, He S, Luo J, Zhu M, Chen N, Chen H, Meurens F, Zhu J. 2020. Porcine IFI16 Negatively Regulates cGAS Signaling Through the Restriction of DNA Binding and Stimulation. *Front Immunol* 11: 1669

255. Guan K, Wei C, Zheng Z, Song T, Wu F, Zhang Y, Cao Y, Ma S, Chen W, Xu Q. 2015. MAVS promotes inflammasome activation by targeting ASC for K63-linked ubiquitination via the E3 ligase TRAF3. *The Journal of Immunology* 194: 4880-90

9. APPENDIX

9.1. Supplementary material

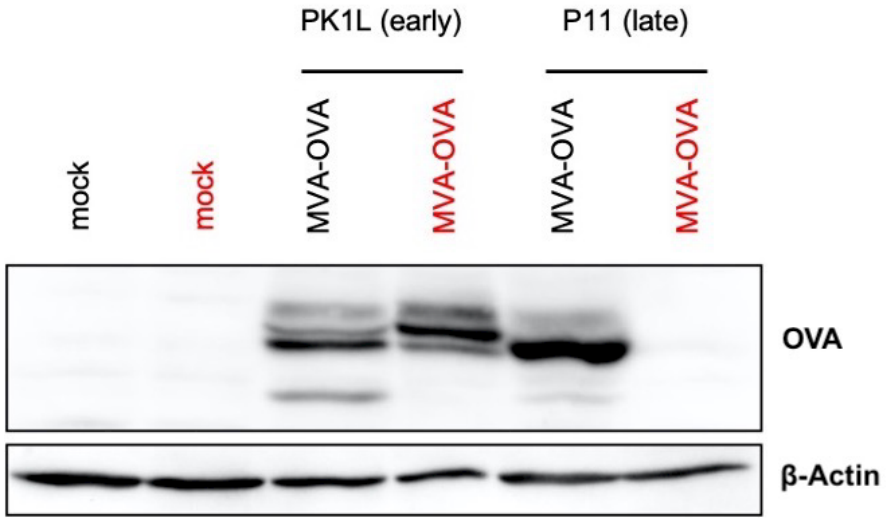

Supplementary Figure 1: In contrast to early antigens, late antigens are not expressed in the presence of AraC. Feeder cells (murine Cloudman S91 melanoma cells) were infected with MVA-PK1L-OVA (early) or MVA-P11-OVA (late) at MOI 1, or mock-infected for 24 h either in the presence or absence of 40 µg/ml AraC. The samples treated with AraC are indicated by red letters. Protein levels of the recombinant antigen OVA were determined using western blot analysis of feeder cell lysates. Data represent one blot representative of two experiments.

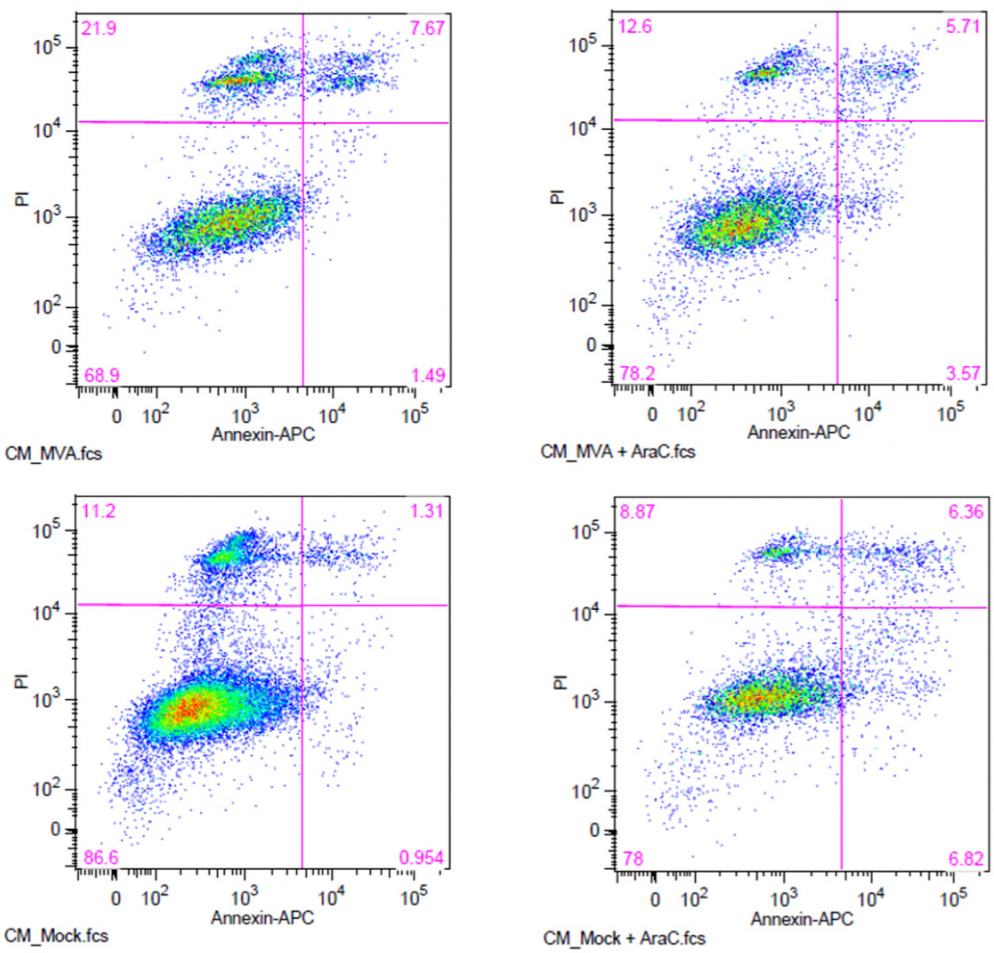

Supplementary Figure 2: Example for flow cytometric analysis (plot) after annexin V and PI staining of MVA-infected cells. Feeder cells (murine Cloudman S91 melanoma cells) were infected with MVA-PK1L-OVA at MOI 1 or mock-infected for either 16 h in the presence or absence of 40 µg/ml AraC. The induced cell death was determined using flow cytometry. Plasma membrane integrity and permeability were determined using annexin V (Annexin-APC) and propidium iodide (PI), and frequencies of healthy, early and late apoptotic as well as necrotic cells were determined. Data are representative of one of two independent experiments.

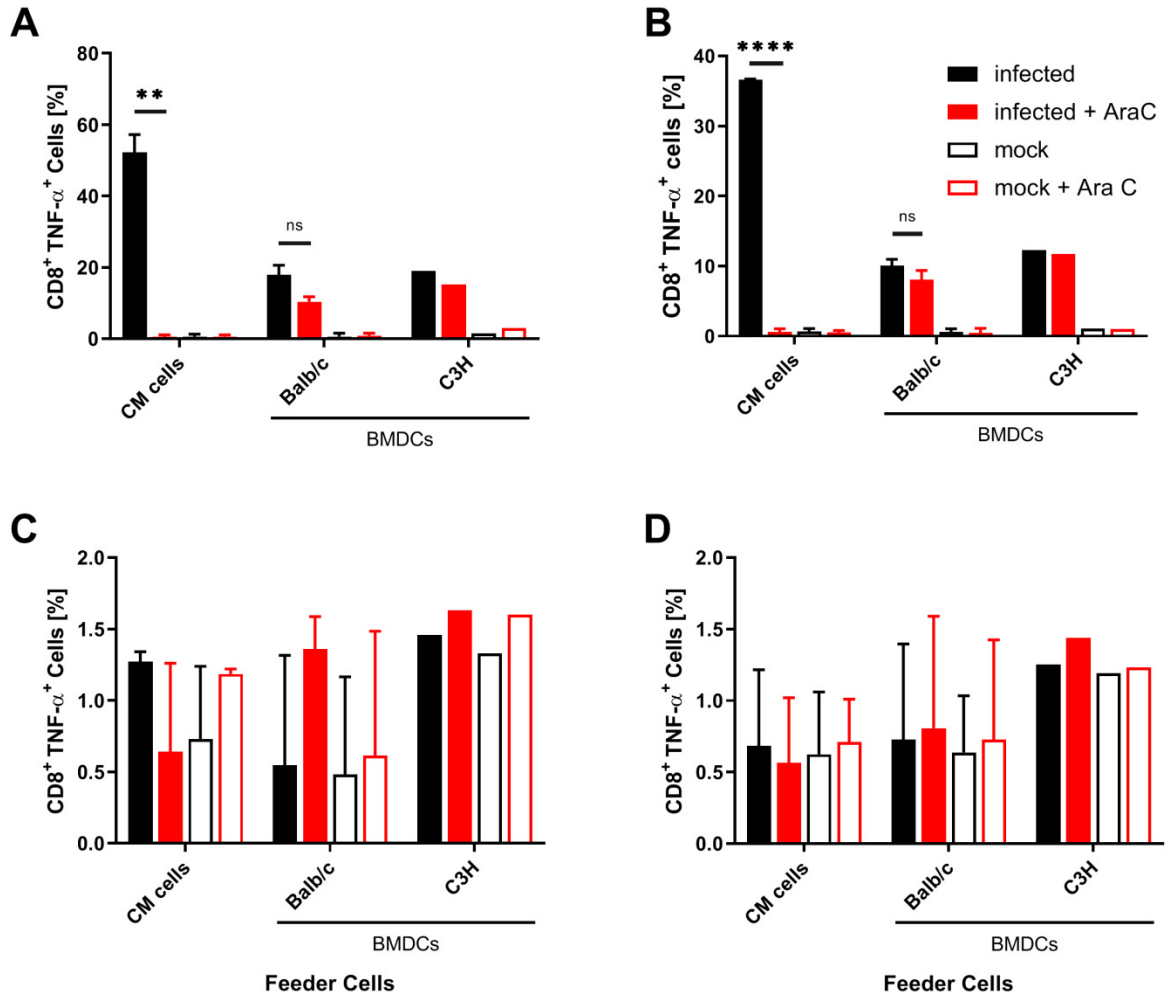

Supplementary Figure 3: TNF-α expression of activated CD8 T cells confirms that AraC has a non-significant effect on BMDCs compared to CM cells. Murine Cloudman S91 melanoma cells (CM) as well as GM-CSF-BMDCs derived from Balb/c and C3H mice, both MHC-I mismatched, were infected with MVA-PK1L-OVA at MOI 1, or mock-infected for 10 h in the presence or absence of 40 µg/ml AraC. After PUVA treatment and washing, feeder cells were cocultured with cross-presentation competent BMDCs generated from C57BL/6 mice. The ability to license cross-presenting BMDCs for the activation of $CD8^+$ T cells specific for the recombinant antigen OVA (A) and the viral antigens B8 (B), D13 (C) and A19 (D) was determined using flow cytometry as frequency of TNF-α expressing T cells. Data are depicted as mean ± SD of one (C3H) or two (CM & Balb/c) independent experiments. **** = $p < 0{,}0001$; ** = $p < 0{,}01$; ns = not significant; unpaired, two-tailed Student's t-test.

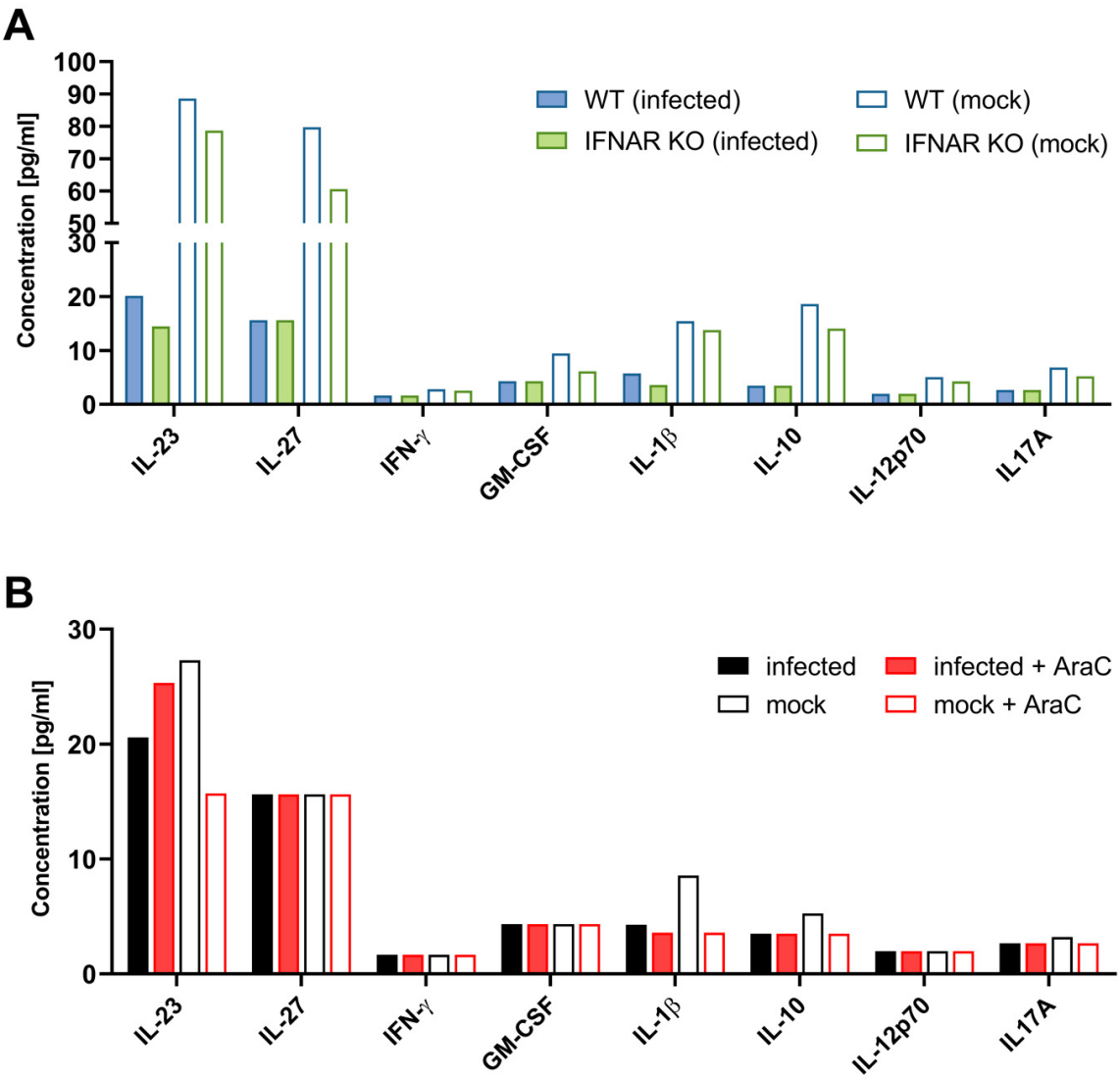

Supplementary Figure 4: The cytokine expression patterns derived from cocultures of infected feeder cells with IFNAR KO BMDCs resemble the cytokine responses of infected and AraC treated feeder plus BMDC cocultures. Supernatants from cocultures of feeder cells infected with MVA-PK1L-OVA at MOI 1, or mock-infected feeder cells with IFNAR KO or WT BMDCs (A) or supernatants from cocultures of AraC treated and infected feeder cells with WT BMDCs (B) were collected at 16 h post infection. Cytokines were determined with LEGENDplex assays and the concentrations calculated. Data are derived from one experiment.

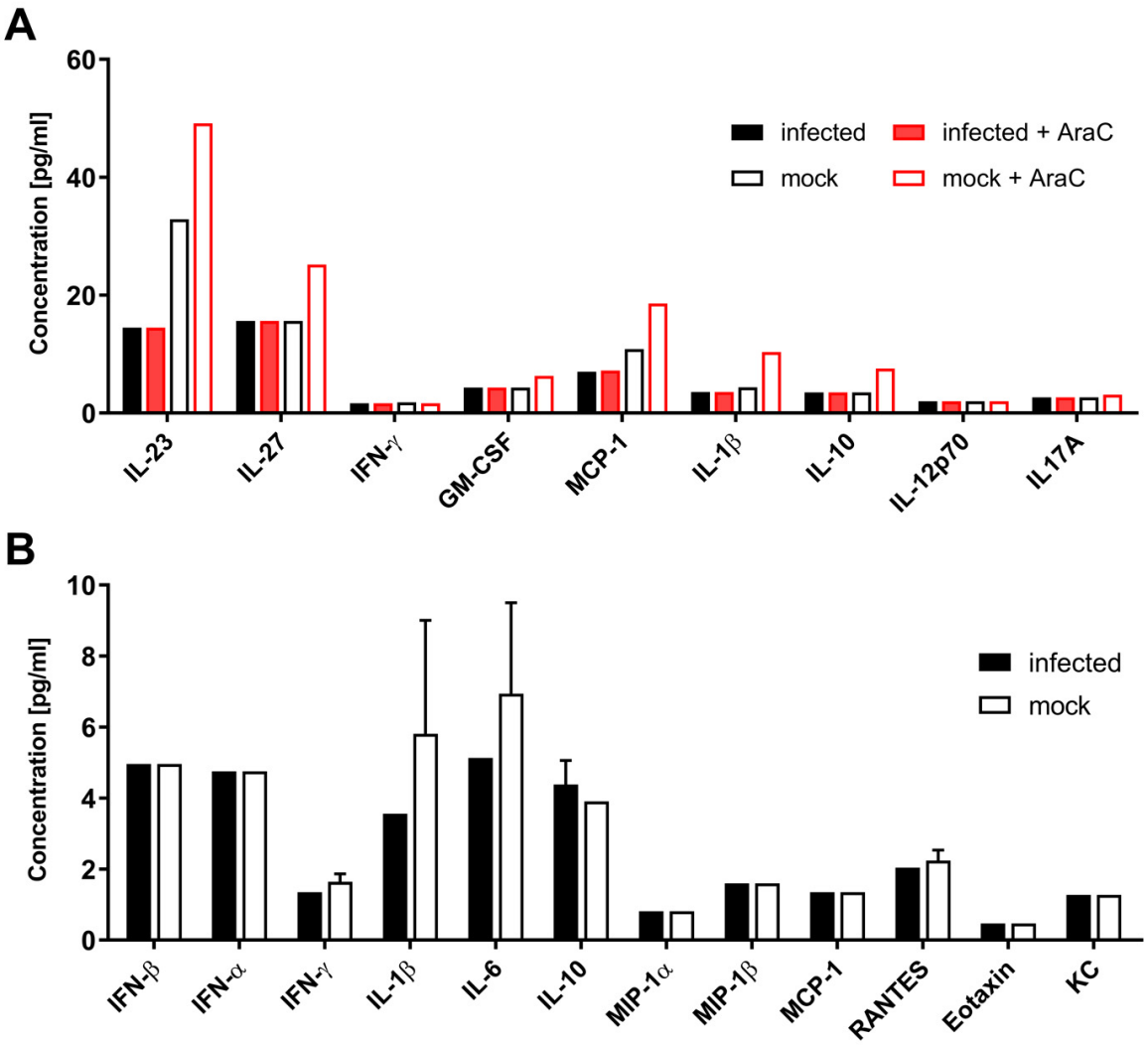

Supplementary Figure 5: Cytokine responses in directly infected cells. Supernatants from GM-CSF-BMDCs (A) or feeder cells (murine Cloudman S91 melanoma cells) (B), infected with MVA-PK1L-OVA at MOI 1, were collected at 16 h post infection. Cytokines were determined with LEGENDplex assays and the concentrations calculated. Data are derived from one experiment.

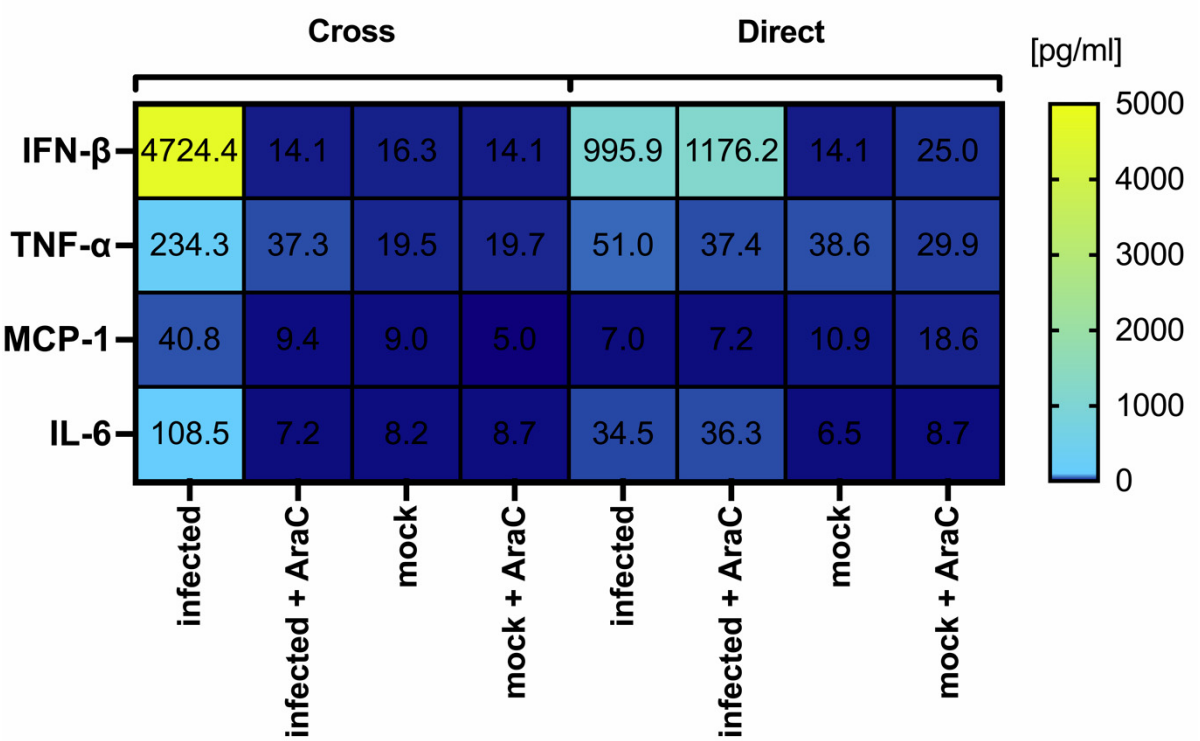

Supplementary Figure 6: Supernatants from cocultures of MVA-infected feeder cells with BMDCs showed higher IFN-β levels than directly infected BMDCs. Supernatants from cocultures of AraC-treated and infected feeder cells with WT BMDCs were collected at 16 h post infection and cytokines were determined with LEGENDplex assays (cross). Supernatants from GM-CSF-BMDCs infected with MVA-PK1L-OVA at MOI 1 or mock-infected, were collected at 16 h post infection and cytokine concentrations were determined with Cytoplex assays (direct).

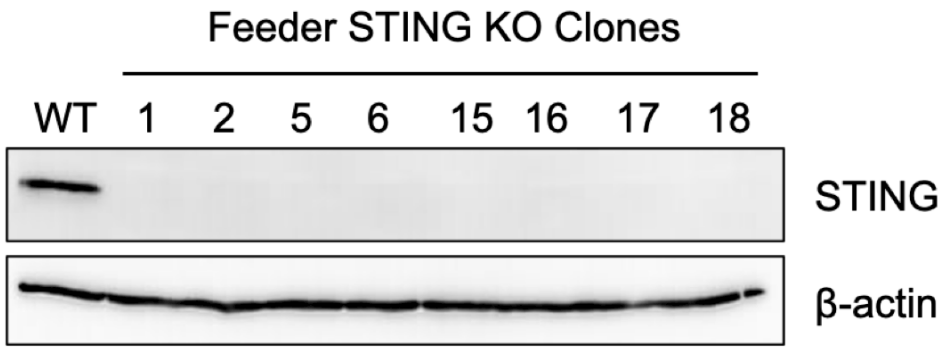

Supplementary Figure 7: Confirmation of the STING knockout in feeder cells using western blot analysis. STING expression in wildtype feeder cells (Cloudman S91 melanoma cells) was silenced by gene-editing using CRISPR/Cas9. After puromycin selection, the bulk population was separated into single-cell clones. After expansion of clones, the absence of STING was confirmed with western blot analysis. All feeder STING KO clones (clones 1, 2, 5, 6, 15, 16, 17 and 18) showed deficient STING expression in comparison to control feeder cells. Clone 15 was used for further experiments. β-actin levels in STING KO and WT feeder cell clones served as a loading control.

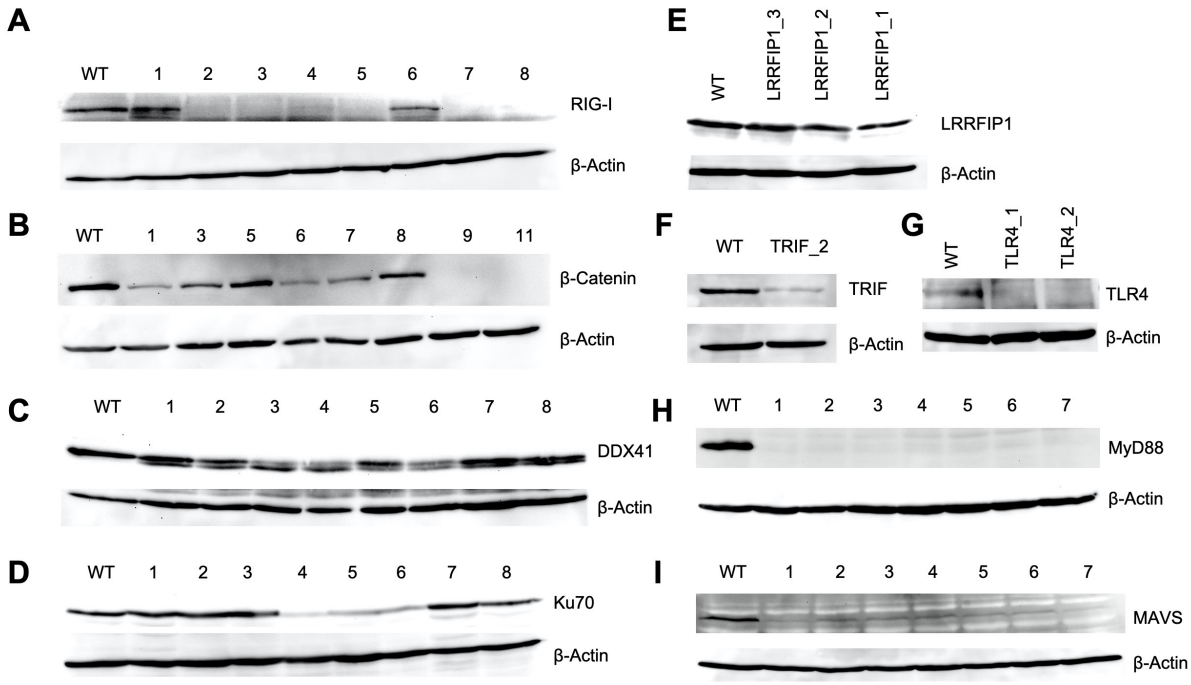

Supplementary Figure 8: Confirmation of diverse genetic knockouts in feeder cells using western blot analysis. Genes were silenced by gene-editing using CRISPR/Cas9. After puromycin selection, the bulk population was separated into single-cell clones, indicated by different numbers (A, B, C, D, H and I), or used as bulk population for further experiments (E, F and G). Single cell clones were characterized from RIG-I (clone 2) (A), β-catenin (clone 9) (B), DDX41 (clone 3) (C), Ku70 (clone 4) (D), MYD88 (clone 3) (H) and MAVS (clone 1) (I), while the bulk population was used for the analysis of LRRFIP1 (LRRFIP_1) (E), TRIF (TRIF_2) (F) and TLR4 (TLR4_2) (G). β-Actin levels in KO and WT feeder cell clones served as a loading control.

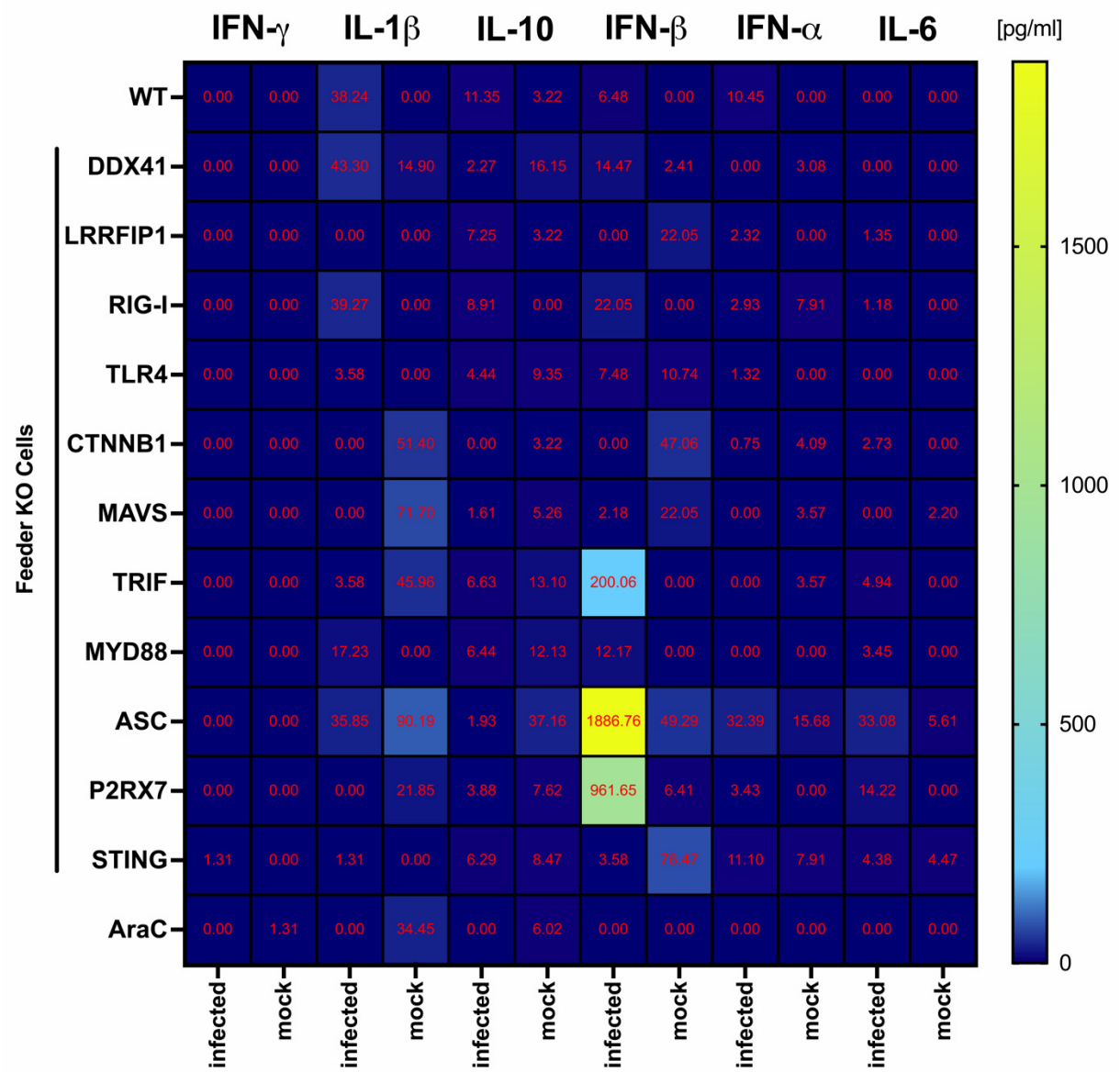

Supplementary Figure 9: Cytokine responses in gene-edited feeder cells. Feeder cells deficient in the indicated proteins and WT feeder cells were infected with MVA-PK1L-OVA at MOI 1, or mock infected. Feeder WT cells were additionally treated with 40 µg/ml AraC during the infection. 16 h post infection supernatants were collected and the concentrations of IFN-γ, IL-1β, IL-10, IFN-β, IFN-α and IL-6 determined with LEGENDplex assays. Data represent the mean of two independent experiments.

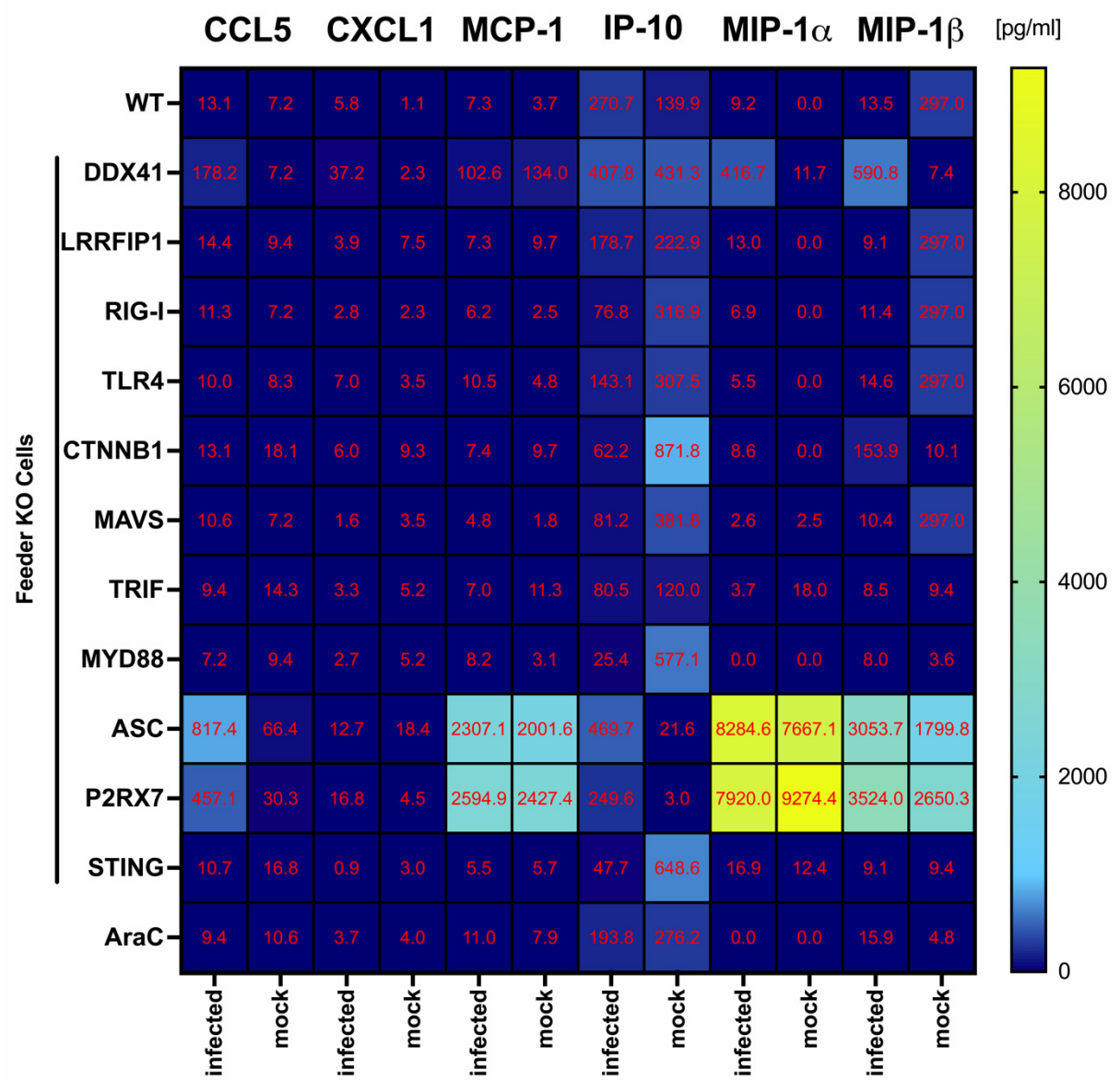

Supplementary Figure 10: Chemokine responses of in gene-edited feeder cells. Feeder cells deficient for the indicated proteins and WT feeder cells were infected with MVA-PK1L-OVA at MOI 1, or mock infected. WT feeder cells were additionally treated with 40 µg/ml AraC during the infection. 16 h post infection supernatants were collected and the concentrations of CCL5, CXCL1, MCP-1, IP-10, MIP-1α and MIP-1β determined with LEGENDplex assays. Data represent the mean of two independent experiments.

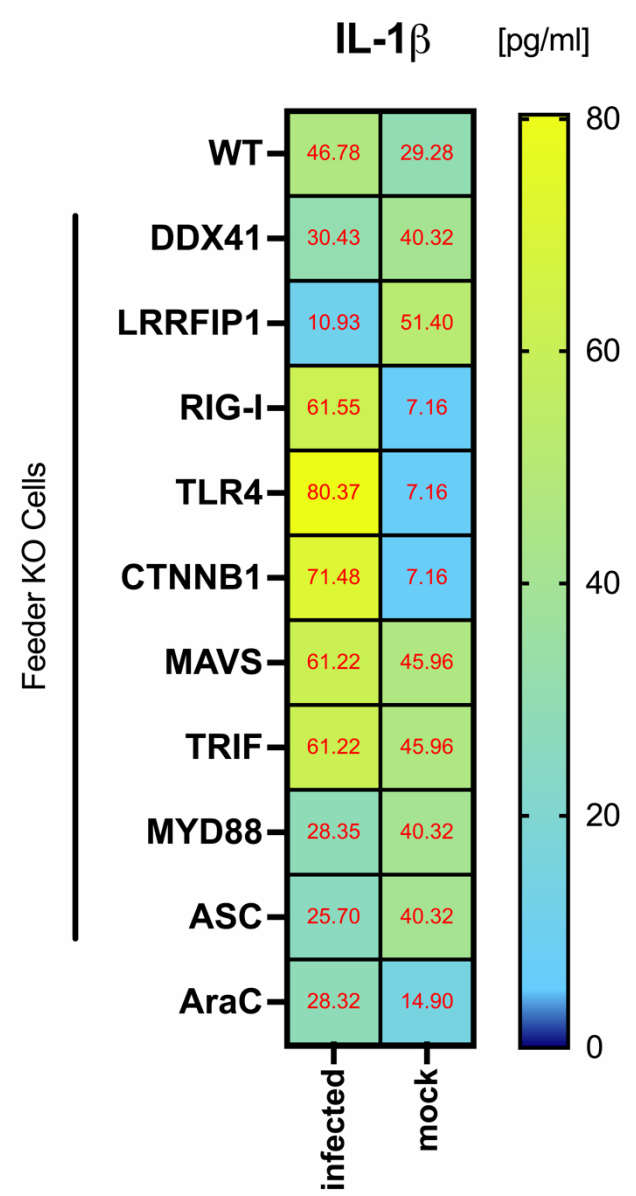

Supplementary Figure 11: BMDCs cocultured with Trif- or ASC-deficient feeder cells or AraC-treated wildtype feeder cells show a reduced IL-1β response. Feeder cells deficient in the indicated protein and WT feeder cells were infected with MVA-PK1L-OVA at MOI 1, or mock-infected for 16 h. Additionally, WT feeder cells were infected with MVA in the presence of 40 µg/ml AraC. After PUVA-treatment and washing, feeder cells were cocultured with C57BL/6 GM-CSF-BMDCs for 20 h. Supernatants were collected and concentrations of IFN-γ and IL-1β determined with LEGENDplex assays. Data represent the mean of two independent experiments.

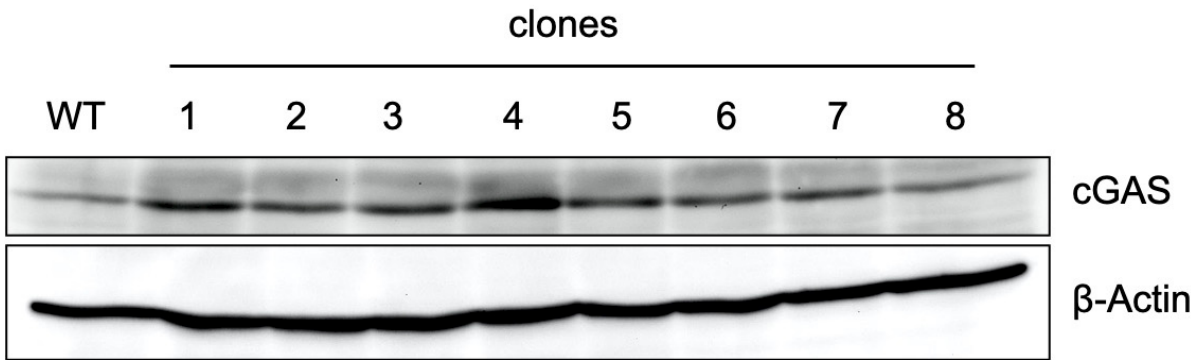

Supplementary Figure 12: Cloudman S91 melanoma cells express low levels of cGAS. This western blot shows an attempt to silence cGAS in wildtype feeder cells (Cloudman S91 melanoma cells) by gene-editing using CRISPR/Cas9. After puromycin selection, the bulk population was separated into single-cell clones and cGAS protein levels were determined by western blot analysis. β-Actin levels in STING KO and WT feeder cell clones served as a loading control.

9.2. List of figures

9.3. List of tables

Acknowledgments

This work was performed at the Institute of Virology in the group of Prof. Dr. Ingo Drexler and was funded as well as supported by the Research Training Group (RTG) 1949.

First of all, I would like to express my gratitude to my supervisor, Prof. Dr. Ingo Drexler, for giving me the opportunity to be part of a great project, to prepare my doctoral thesis in his lab and for his support and guidance. During this exciting time, I have learned to think outside the box, ask critical questions and to solve problems independently. I also thank Ingo for giving me the chance to visit the Lab of Prof. Dr. Emmanuel Wiertz at the UMC Utrecht to learn and apply CRISPR/Cas9 as the gene-editing technique for my project. Special thanks also to Dr. Robert-Jan Lebbink, who introduced me to the CRISPR/Cas9 system.

I am also thankful to the RTG1949 for their support and training, and for the possibility to extend my knowledge, as well as for the experience of presenting my project at several conferences.

Furthermore, I would like to thank Prof. Dr. Henike Heise for mentoring my second project.

Special thanks go to Noémi, who supported me with many inspiring conversations, advice, motivation, and her critical opinion. I also would like to thank Gregor for his help, especially at the beginning of my project. Thanks to Ylenia for her contribution with her master thesis to this project as well as for her help during this time. I would also like to thank to Ronny, Sha and all the former and current lab members.

However, most of all I would like to thank my family: my parents, who always supported me and believed in me. A special thank you also goes to my fiancé who always motivated me, provided emotional support and gave me good advice.

“The role of the infinitely small in nature is infinitely great.”

Louis Pasteur (1822-1895)

DECLARATION

I hereby declare that this thesis, submitted for the degree of Dr. rer. nat. at the Heinrich-Heine-University Düsseldorf, has been entirely written by me in consideration of “Good Scientific Practice”.

Düsseldorf, 20.01.22 Cornelia Barnowski